The electrical activity of the pulmonary vein and its potential role in cardiac arrhythmia

Amonrat Khayungarnnawee

A thesis submitted in the fulfilment of the requirements for

the degree of Doctor of Philosophy

Strathclyde Institute of Pharmacy and Biomedical Science

University of Strathclyde

March 2017

Declaration of Author's Rights

This thesis is the result of the author's original research. It has been composed by the author and has not been previously submitted for examination, which has led to the award of a degree.

The copyright of this thesis belongs to the author under the terms of the United Kingdom Copyright Acts as qualified by University of Strathclyde Regulation 3.50. Due acknowledgement must always be made of the use of any material contained in, or derived from, this thesis.

Signed:

Date:

Acknowledgements

Firstly, I am grateful to my supervisor Dr. Edward Rowan, Dr. John Dempster, and Dr. Robert Drummond for their support, advice and encouragement throughout the course of this study and I sincerely appreciate their guidance and tireless enthusiasm, which enabled me to complete this work in its present form.

I would also like to take this opportunity to thank the members of technical staff in both the lab and the BPU, as well as a number of lecturers for their assistance, advice and timely help during this the course of this project.

My sincere thanks to my friends Laura, Ali, Sukrut, Noel, Artiom, Danny, Pupae, Ple, P'Ann, Amy, P'Koy, Kanit, Thai friends and ThaiSiam staff for making life in Glasgow more enjoyable. I am extremely thankful to Dr Jamie, my wee boy for the encouragement, laughs and mostly keeping me sane throughout the PhD.

I would like to acknowledge the Royal Thai Government, Ministry of Science and Technology and Thailand Institute of Scientific Technological Research (TISTR) for funding this PhD.

Lastly, I would like to thank the most important people in my life, my family, for supporting me for absolutely everything

This thesis is dedicated to my parents and teachers

To my dad, I hope I have done you proud

Communications

Khayungarnnawee, A. and Rowan, E.G. The effect of stretch on noradrenaline induced activity of rat pulmonary veins: an electrophysiological study. In Proceedings of The Physiological Society. 29th – 31st July 2016.

Khayungarnnawee, A. and Rowan, E.G., 2014 Noradrenaline evokes ectopic activity in the rat pulmonary vein. In Proceedings of The Scottish Cardiovascular Forum, 22nd February 2014

Abstract

Atrial fibrillation (AF) is the most common sustained cardiac arrhythmia, which is strongly correlated with patients who go on to develop a stroke. AF is thought to be originated in the myocardial sleeve of the pulmonary vein (PV) extending from left atrium (LA). Some studies have shown automaticity activity in PV cardiomyocytes generated by pacemaker-like cells, which can lead to the generation of ectopic activity that initiates AF. Sympathetic and parasympathetic nervous systems play an important role in promoting AF as both a trigger and a substrate. Atrial arrhythmogenic remodelling, defined as any change in atrial structure e.g. mechanical stretch, is considered a critical factor in AF studies. However, the underlying mechanisms for this ectopic activity remain unclear. Thus, the aims of this thesis were to examine the characteristic of cardiomyocytes and nodal cells in the rat PV using Masson's trichrome staining and immunohistochemistry. The role of adrenergic receptors in the PV was investigated with the application of noradrenaline (NA) in a contraction (twitch-tension) study. Moreover, mechanical stretch was also investigated, which changes the electrical activity of the PV potentially leading to the genesis of AF.

Histological studies revealed cardiomyocytes extend from LA into the PV, which forms a myocardial sleeve, within which a non-uniform alignment of myocardial fibres was found**.** Sinoatrial node (SAN) cells were observed in right atrium (RA); however, they were not observed in any area of the rat PV section. Immunohistochemistry was used to identify the expression of HCN4, which is observed in SAN of the RA section but not in the rat PV section. In contractile studies, NA induced ectopic activity in the rat PVs at 37°C, although this ectopic activity decreased when temperature was

reduced to 25°C. Increasing extracellular Ca^{2+} also increased the frequency and the duration of ectopic contractions in the rat PVs. NA-induced ectopic activity in the rat PV was decreased by prazosin, propranolol, carbachol, and verapamil. Mechanical stretch increased the incidence of spontaneous activity but had no effect on the action potential characteristics in rat PV cardiomyocytes. The application of NA increases the incidence of ectopic action potentials, prolongs APD and induces EADs in rat PV cardiomyocytes under a stretch condition. These ectopic action potentials induced by the combination of stretch and NA were inhibited by gadolinium, ORM-10103, verapamil, prazosin and propranolol in the rat PV myocardium.

In conclusion, the PV contains a myocardial sleeve extending from the LA, which is thought to be the source of ectopic electrical activity underlying AF. NA-induced ectopic activity in rat PVs was mediated via α-β-adrenergic receptors, indicating that increased catecholaminergic activity is an important mediator of enhanced automaticity in rat PV cardiomyocytes. Mechanical stretch also induces changes in electrical characteristics, leading to ectopic action potentials in the rat PVs. Stretch-activated channels (SACs) may therefore be an important link between stretch and ectopic activity in the PV, potentially acting as a main factor in the development of AF. Thus, autonomic nervous system and structural remodelling in the rat PVs may be considered as an influence on the genesis of arrhythmogenic activity in the development of AF.

Table of Contents

Declaration of Author's Rights i
Acknowledgements ii
Communications iv
Abstract v
Table of Contents vii
List of Figures xi
List of Tables xiv
List of Abbreviations and Symbols xv
Chapter 1. Introduction 20
1.1 Atrial fibrillation (AF) 21
1.2 Basic mechanisms of AF 23
1.2.1 Focal ectopic activity 24
1.2.2 Re-entry 25
1.3 Clinical management of AF 27
1.3.1 Pharmacological treatment of AF 27
1.3.2 Radiofrequency ablation of AF 29
1.4 Atrial fibrillation and the PVs 30
1.4.1 The structure of the PV 31
1.5 Electrophysiology mechanism of AF initiation and maintenance in PVs 35
1.5.1 The role of action potentials and ionic currents 35
1.5.2 Enhanced automaticity and triggered activity 36
1.5.3 Re-entry 37
1.5.4 The relationship between AF and the general structure of the myocardial sleeve 38
1.6 Autonomic nervous system innervation of the PVs 39
1.6.1 The cardiac adrenergic system 39
1.6.2 The autonomic nerves and the PVs in arrhythmogenesis 43
1.7 Stretch-induced arrhythmia 45
1.7.1 The cardiac response to stretch 45

1.7.2 Stretch-activated ion channels in the heart 47
1.7.3 Stretch-induced calcium entry via L-type Ca^{2+} channels 55
1.7.4 Stretched-induced changes in electrical activity of the heart 55
1.7.5 Atrial fibrillation and the stretch of atrium 57
1.7.6 Mechanical stretch regulates the arrhythmogenic activity of PVs 59
1.7.7 Stretch activated channel modulators 60
1.8 Aims 65
Chapter 2. Morphological comparison of cardiomyocytes in the rat pulmonary vein and atria 67
2.1 Introduction 68
2.1.1 The PV muscular sleeve 68
2.1.2 The atria 70
2.1.3 Nodal cells in sinoatrial node (SAN) and node-like cells in myocardial layer of PV 71
2.1.4 The expression of HCN4 in sinoatrial node 72
2.2 Methods 74
2.2.1 Animals and dissection 74
2.2.2 Histology of cardiac sections 76
2.2.3 Immunohistochemistry 78
2.3 Results 80
2.3.1 Histological examination of rat atria and PVs 80
2.3.2 Nodal cells in SAN and PVs 85
2.3.3 Immunofluorescence staining of HCN4 in the rat SAN and PVs 87
2.4 Discussion 89
2.4.1 The arrangement of cardiomyocytes in LA and PV sections 89
2.4.2 Identification of node-cell in SAN and PV sections 90
2.4.3 Expression of HCN4 in SAN and PV sections 92
Chapter 3. The generation of noradrenaline (NA) induced ectopic activity in the rat pulmonary vein 95
3.1 Introduction 96
3.1.1 Contractile function and ectopic activity in the rat PV 96
3.1.2 Pharmacological modulators on the contractility in the rat PV 98

3.2 Methods 101
3.2.1 Animals and dissection 101
3.2.2 Preparation of the PVs 101
3.2.3 Experiment protocols 101
3.3 Results 107
3.3.1 NA induced spontaneous ectopic activity in the rat PVs 107
3.3.2 The temperature modulates ectopic contractions in the rat PV induced by NA 111
3.3.3 The effect of α and β adrenoceptor antagonist on ectopic contractions in the PV induced by NA 114
3.3.4 The effect of cholinergic agonist on ectopic contractions in the PV induced by NA 120
3.3.5 The effect of an increase in extracellular Ca^{2+} on the generation of NA induced ectopic contractions of rat PVs. 124
3.3.6 The effect of calcium-channel blocker on ectopic contractions in the PV induced by NA 128
3.4 Discussion 132
Chapter 4. The effect of stretch and pharmacological agents on electrical activity and mechanical activity of the rat pulmonary veins 138
4.1 Introduction 139
4.1.1 Stretch induced changes in electrical and mechanical properties of cardiac muscle 139
4.1.2 Pharmacological modulators of stretch-induced ectopic action potentials 142
4.1.3 Aims 145
4.2 Methods 146
4.2.1 Animals, dissection, and, preparation of the rat PVs 146
4.2.2 Experiment protocols 146
4.2.3 Statistics 153
4.3 Results 154
4.3.1 Stretch-induced spontaneous activity in the rat PV cardiomyocytes 154

4.3.2 Effect of NA on stretch-induced spontaneous activity in the rat PV cardiomyocytes 159
4.3.3 Effect of non-cumulative administration of NA on stretch-induced activity in the rat PV cardiomyocytes 164
4.3.4 Effect of gadolinium on the combined stretch and NA induced ectopic activity of the rat PV cardiomyocytes 170
4.3.5 Effect of verapamil on the combined stretch and NA induced ectopic activity of the rat PV cardiomyocytes 174
4.3.6 Effect of ORM-10103 on the combined stretch and NA induced ectopic activity of the rat PV cardiomyocytes 178
4.3.7 Effect of prazosin on the combination of stretch and NA induced ectopic activity of the rat PV cardiomyocytes 182
4.3.8 Effect of propranolol on the combination of stretch and NA induced ectopic activity of the rat PV cardiomyocytes 186
4.4 Discussion 190
4.4.1 Effect of stretch-induced spontaneous activity in the rat PV cardiomyocytes 190
4.4.2 Effect of NA on stretch-induced spontaneous activity in rat PV cardiomyocytes 191
4.4.3 Effect of pharmacological agents on stretch-induced spontaneous activity in rat PV cardiomyocytes 192
Chapter 5. General Discussion 197
5.1 Characteristics of cardiomyocytes in the rat PV and atria 198
5.2 Identification of the SAN and the expression HCN4 channel of the rat PV and atria 199
5.3 NA induced ectopic activity in the rat PVs 201
5.4 Stretch induced changes in PV cardiomyocytes 203
5.5 Summary 206
References 208

List of Figures

Figure 1-1 Basic mechanisms underlying atrial fibrilation (AF). 23
Figure 1-2 Focal ectopic and triggered activity. 25
Figure 1-3 Re-entry. 26
Figure 1-4 The anatomy of left atrium (LA) and pulmonary veins (PVs). 31
Figure 1-5 β_1-Adrenergic receptor (AR) signalling in cardiomyocytes. 40
Figure 1-6 α_1-Adrenergic receptor (AR) signalling in cardiomyocytes. 42
Figure 1-7 Mechanisms of stretch-induced atrial fibrillation (AF). 49
Figure 2-1 An example of myocardial sleeves from pulmonary vein section using Masson's trichrome staining. 69
Figure 2-2 Digital photographic images of the rat heart and lungs, pulmonary veins and right atrium. 75
Figure 2-3 Diagram indicating the histology cutting section of the rat pulmonary vein tissue. 77
Figure 2-4 Histological evaluation of Formalin fixed rat LA. 82
Figure 2-5 Histological evaluation of Formalin fixed rat PV longitudinal sections. . 83
Figure 2-6 Histological evaluation of Formalin fixed rat PV transverse sections. 84
Figure 2-7 Histological evaluation of Formalin fixed rat RA. 86
Figure 2-8 HCN4 expression in the rat atria. 88
Figure 3-1 The isolated- tissue organ bath set up. 102
Figure 3-2 Representative traces showing the NA-induced ectopic contractions in the rat PV. 108
Figure 3-3 An example of NA-induced ectopic contractions in the rat PV. 109
Figure 3-4 Analysis of the ectopic beats, recorded following addition of NA in the rat PVs 110
Figure 3-5 The effect of temperature on ectopic activity induced by NA in the rat PVs. 112
Figure 3-6 The effect of temperature on ectopic contractions induced by NA in the rat PVs at temperature 37°C and hypothermia at 25°C. 113
Figure 3-7 The effect of α and β adrenoceptor antagonists on ectopic contractions induced by NA. 115

Figure 3-8 The effect of prazosin on ectopic contractions induced by NA in the rat PVs. 116
Figure 3-9 The effect of propranolol on ectopic contractions induced by NA in the rat PVs. 118
Figure 3-10 The effect of carbachol on ectopic contractions induced by NA in the rat PV preparations. 121
Figure 3-11 The effect of carbachol on ectopic contractions induced by NA. 122
Figure 3-12 An example of the changes in ectopic activity following increases in extracellular Ca^{2+} on NA-induced ectopic contractions of rat PVs..... 125
Figure 3-13 Effect of the increases in extracellular [Ca^{2+}] on ectopic activity in the rat PVs. 126
Figure 3-14 The effect of calcium channel blocker (verapamil) on ectopic contraction induced by NA. 129
Figure 3-15 The effect of verapamil on ectopic contractions induced by NA. 130
Figure 4-1 Photographs illustrating the experimental set-up used for intracellular recordings under stretch. 147
Figure 4-2 Illustration of electrically evoked action potential in PV cardiomyocyte 150
Figure 4-3 Simultaneous twitch tension and action potential recordings in the rat PV cardiomyocytes at different tensions. 155
Figure 4-4 The action potential properties and contractile activity of the rat PV cardiomyocytes before (0 g) and after stretch (0.5 g, and 1 g). 156
Figure 4-5 Simultaneous twitch tension and action potential recordings in the rat PV cardiomyocytes at different tensions in the presence of NA 10 µM... 160
Figure 4-6 The action potential properties and contractile response during combined stretch and NA in the rat PV cardiomyocytes. 161
Figure 4-7 Simultaneous twitch tension and action potential recordings following non-cumulative administration of NA in the rat PV cardiomyocytes under 1 g stretch. 165
Figure 4-8 Examples showing the application of NA 100 µM induced the genesis of early after-depolarisations (EADs) in the rat PV cardiomyocytes under 1 g stretch. 166

Figure 4-9 The action potential properties and contraction activity of non-cumulative administration of NA in the rat PV cardiomyocytes under 1g stretch 167
Figure 4-10 Effect of gadolinium on the combination of stretch and NA induced ectopic activity in the rat PV cardiomyocytes. 171
Figure 4-11 Effect of gadolinium on the action potential parameters of the PVs with the combination of stretch and NA. 172
Figure 4-12 Effect of verapamil on the combination of stretch and NA induced ectopic activity of the rat PV cardiomyocytes. 175
Figure 4-13 Effect of verapamil on the action potential parameters of the PVs with the combination of stretch and NA. 176
Figure 4-14 Effect of ORM-10103 on the combination of stretch and NA induced ectopic activity in the rat PV cardiomyocytes. 179
Figure 4-15 Effect of ORM-10103 on the action potential parameters of the PVs with the combination of stretch and NA. 180
Figure 4-16 Effect of prazosin on the combination of stretch and NA induced ectopic activity in the rat PV cardiomyocytes. 183
Figure 4-17 Effect of prazosin on the action potential parameters of the PVs with the combination of stretch and NA. 184
Figure 4-18 Effect of propranolol on the combination of stretch and NA induced ectopic activity of the rat PV cardiomyocytes. 187
Figure 4-19 Effect of propranolol on the action potential parameters of the PVs with the combination of stretch and NA. 188

List of Tables

Table 1-1 Classification of atrial fibrillation 21
Table 3-1 Effect of prazosin on NA-induced ectopic activity in the rat PVs 117
Table 3-2 Effect of propranolol on NA-induced ectopic activity in the rat PVs 119
Table 3-3 Effect of carbachol on NA-induced ectopic activity in the rat PVs 123
Table 3-4 Effect of the increase in extracellular Ca^{2+} on NA-induced ectopic activity in the rat PVs 127
Table 3-5 Effects of verapamil on NA-induced ectopic activity in rat PVs 131
Table 4-1 Action potential parameters illustrating the effects of stretch on electrical activity of the rat PV cardiomyocytes 158
Table 4-2 Action potential parameters during combined stretch and NA in the rat PV cardiomyocytes 163
Table 4-3 Effect of non-cumulative administration of NA on action potentials in the rat PV cardiomyocytes under stretch 169
Table 4-4 The effect of gadolinium on action potential parameters of ectopic activity induced by combined stretch and NA in the rat PV cardiomyocytes .. 173
Table 4-5 The effect of verapamil on action potential parameters of ectopic activity induced by combined stretch and NA in the rat PV cardiomyocytes .. 177
Table 4-6 The effect of ORM-10103 on action potential parameters of ectopic activity induced by combined stretch and NA in the rat PV cardiomyocytes .. 181
Table 4-7 The effect of prazosin on action potential parameters of ectopic activity induced by combined stretch and NA in the rat PV cardiomyocytes .. 185
Table 4-8 The effect of propranolol on action potential parameters of ectopic activity induced by combined stretch and NA in the rat PV cardiomyocytes .. 189

List of Abbreviations and Symbols

AC- adenylyl cyclase

Ach-Acetylcholine

AF-Atrial fibrillation (AF)

APD_{20}-Action potential duration at 20% repolarisation

APD_{50}-Action potential duration at 50% repolarisation

APD_{90}-Action potential duration at 90% repolarisation

APD-Action potential duration

ATP-Adenosine triphosphate

AV node- Atrioventricular Node

Ca^{2+}-Calcium

cAMP-Cyclic-adenosine monophosphate

CV-Conduction velocity

DADs-Delayed afterdepolarisation

DAG-Diacylglycerol

EADs-Early afterdepolarisation

EC_{50}- Half maximal effective concentration

ET-1-Endothelin-1

Gi-protein-Inhibitory-G-protein

Gs-protein-Stimulatory-G-protein

GYG-Glycine tyrosine glycine

HCN- Hyperpolarisation-activated cyclic nucleotide-gated channel

IC_{50}- Half maximal inhibitory concentration

I_{CaL}-L-type calcium current

$I_{Cl\text{-}stretch}$-Stretch-activate chloride current

$I_{Cl\text{-}swell}$-Swelling-activate chloride current

I_f – Funny pacemaker current

IFR-Immediate force receptor

I_{Ki}-Inward rectifier potassium current

I_{Kr}-Rapidly activating delayed rectifier potassium channels.

I_{Ks}-Slowly activating delayed rectifier potassium channels.

$I_{NS\text{-}stretch}$-Stretch-activated nonselective cationic current

$I_{NS\text{-}swell}$-Swelling-induced nonselective cationic current

IP_3-Inositol trisphosphate

IPV-Inferior pulmonary vein

I_{SAC}-Stretch-activated current

IVC-Inferior vena cava

LA-Left atrium

L-Left

LPV-Left pulmonary vein

LSPV-Left superior pulmonary vein

LTCC-L-type calcium channel

LV-Left ventricle

mAChR-Muscarinic acetylcholine receptor

MEF-Mechanoelectric feedback

NA-Noradrenaline

NCX-Sodium-calcium exchanger

PAF-Paroxysmal atrial fibrillation

PAS-Periodic-acid-Schiff

PIP_2-Phosphtidylinositol bisphosphate

PKA-Protein kinase A

PLC-phospholipase C

PR-Posterior right

PV-Pulmonary vein

RFA-Radiofrequency ablation

RMP-Resting membrane potential

RPPV-Right posterior pulmonary vein

RP-Refractory period

RSPV-Right superior pulmonary vein

RT-PCR-Reverse transcription polymerase chain reaction

RyR-Ryanodine receptor

SAC_K-Stretch-activated potassium channels

SAC_{NS}-Non-selective cation channels

SACs-Stretch-activated channels

SADs-Stretch-activated depolarisation

SAN-Sinoatrial node

SPV-Superior pulmonary vein

SVC-Superior vena cava

T_{50}-Time taken for 50% repolarisation

T_{90}-Time taken for 90% repolarisation

TRC-Transient receptor potential channel

TRPA-Transient receptor potential channel, ankyrin

TRPC-Transient receptor potential channel, canonical

TRPML-Transient receptor potential channel, mucolipin

TRPM-Transient receptor potential channel, melastatin

TRPP- Transient receptor potential channel, polycystin

TRPV-Transient receptor potential channel, vanilloid

Vmax-Maximum phase 0 upstroke velocity

WL-Wavelength

Chapter 1. Introduction

1.1 Atrial fibrillation (AF)

Atrial fibrillation (AF) is a form of cardiac arrhythmia in which the normal sinus rhythm is converted into rapid irregular activity due to altered atrial depolarisation (Dang et al., 2002). The rate of atrium depolarisation can be elevated to 400-600 times per minute in humans during an arrhythmic episode (Nattel, 2003, Khan, 2004).

According to the Cardiac Pacing of the European Society of Cardiology and the North American Society of Pacing and Electrophysiology, AF is classified into four types: initial event, paroxysmal, persistent and permanent; details provided in Table 1-1.

Table 1-1 Classification of atrial fibrillation

Terminology	**Clinical features**
First diagnosed AF	Patients who experience AF for the first time
Paroxysmal AF	Spontaneous termination < 7days and most often < 48 hours
Persistent AF	Not self-terminating Lasting > 7days
Permanent AF (Accepted)	Not terminated Terminated but relapsed No cardioversion attempt

(Adapted from Lévy et al. (2003))

In England and Wales, AF affects about 1.3% of the population (Wallentin et al., 2010). In Northumberland, a study in which 4843 people aged 65 years and older were screened for AF found an approximate prevalence of 4.7 % (Sudlow et al., 1998). The Renfrew–Paisley study, with a population cohort of 15,406 aged 45–64 years living in the West of Scotland, showed the prevalence of AF was 6.5 cases in 1000 assessments (0.65%). The detection of AF was found to increase with age, and there were slightly more cases detected in men (53 of 7052, or 0.75%) than women (47 of 8354, or 0.56%) (Stewart et al., 2001). AF is a major public health problem, resulting in substantial morbidity and mortality, disability, and high health care costs.

Increased risk of stroke associated with AF is related to the upper chambers of the heart. If blood is not pumped properly into the lower chambers, it may pool in the upper chambers and form a blood clot. This clot may then be pumped out of the heart, which can travel to the brain causing a stroke (Ruff, 2012). The risk of stroke varies depending on the age of the patient and the presence of other medical conditions such as hypertension, diabetes mellitus, heart failure, and whether the patient has already suffered a prior stroke. The Framingham Study by Lin et al. (1996) showed that approximately 20% of stroke patients (n=501) had AF, and stroke severity in co-morbid patients was greater than in patients without AF.

1.2 Basic mechanisms of AF

The basic electrophysiological mechanisms leading to AF (Figure 1-1) are termed focal ectopic activity and re-entry (Schmidt et al., 2011, Nattel and Dobrev, 2012). Focal ectopic activity is produced by localized discharges from electrical pacemakers originating from a source other than the sinus node; e.g. pulmonary vein (PV) (Schmidt et al., 2011). Alternatively, re-entry, in which abnormal electrical circuits are formed in the heart, may be caused by shortening of the effective refractory period of cardiac tissue leading to anomalous electrophysiological activity (Schmidt et al., 2011).

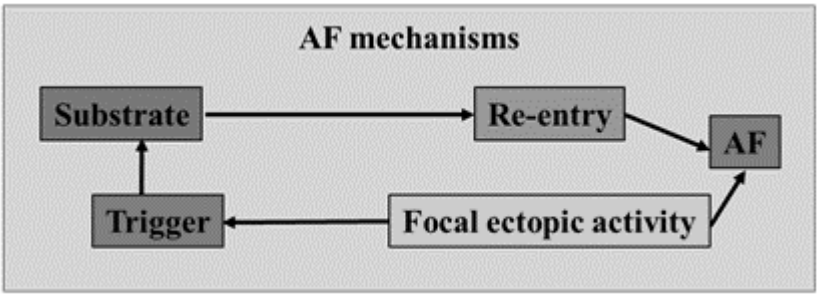

Figure 1-1 Basic mechanisms underlying atrial fibrilation (AF). AF can be generated by focal ectopic activity (e.g. from the PV) or re-entry. Re-entrant circuits require a trigger (e.g. an ectopic beat), which can promote AF (Nattel et al., 2008, Schmidt et al., 2011).

1.2.1 Focal ectopic activity

As noted above, focal ectopic activity is produced by local discharges of electrophysiological activity from irregular sources such as the PV (Schmidt et al., 2011). Ectopic impulses can arise from enhanced normal automaticity or from triggered activity, leading to early afterdepolarisations (EADs) preceding full repolarisation and delayed afterdepolarisations (DADs) occurring after full repolarisation (Nattel, 2003, Schmidt et al., 2011). These are illustrated in Figure 1-2.

EADs occur during the action potential plateau (phase 2 EADs) or during the late repolarisation (phase 3 EADs) (Nattel and Dobrev, 2012). The main consequence of EADs is the prolongation of APD; e.g. by increasing inward L-type calcium current (I_{CaL}), or reducing K^+ currents, allowing the I_{CaL} to recover from inactivation, leading to depolarisation of cardiac cells by allowing intracellular Ca^{2+} influx (Iwasaki et al., 2011, Nattel and Dobrev, 2012).

DADs are membrane potential oscillations, which occur after full repolarisation of the action potential. These result from abnormal diastolic Ca^{2+} leakage through ryanodine receptors (RyR2 is the cardiac form) from the sarcoplasmic reticulum (SR) into the cytoplasm (Dobrev et al., 2011). In addition, excess diastolic Ca^{2+} ions are handled by sodium-calcium exchanger (NCX), which transport three Na^+ ions into the cell per each single Ca^{2+} ion extruded from the cell, generating a net depolarising current which induces DADs (Wakili et al., 2011, Nattel and Dobrev, 2012).

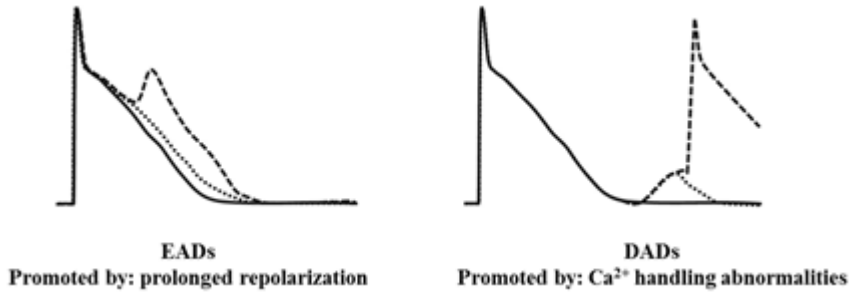

Figure 1-2 Focal ectopic and triggered activity. Early afterdepolarisations (EADs) can occur during phase 2 or phase 3 of the action potential and delayed afterdepolarisations (DADs) can occur after full repolarisation (Heijman et al., 2014).

1.2.2 Re-entry

Re-entry refers to a situation where electrical impulses flow through the heart in abnormal pathways. Normally when excited cardiomyocytes produce an action potential, which is transmitted to neighbouring cells before entering a refractory state, only adjacent cells that are not refractory can be excited by this mechanism, thus controlling the normal flow of electricity through the heart musculature (Klabunde, 2011). Re-entry occurs when either conduction velocity is too slow or the refractory period is too short. This can lead to the development of AF when occurring in the atria, although re-entry generally requires a trigger such as ectopic beats (Nattel et al., 2008, Nattel and Dobrev, 2012). The substrate for re-entry can be produced by atrial remodelling such as atrial fibrosis and atrial enlargement, which can create the appropriate conditions to allow re-entry to be initiated, and sustained AF (Arora and Koduri, 2014, Namdar et al., 2014, Nattel and Harada, 2014). Re-entry results from an ectopic impulse being blocked by refractory tissue when propagating in one direction,

whereas it is able to conduct in faster-recovering tissue in other direction, referred to as a unidirectional block. (Nattel and Dobrev, 2012).

As mentioned, this is determined by refractoriness and conduction conditions. The minimum sized circuit for re-entry to be established is given by the wavelength (WL), or distance travelled by the impulse in one refractory period (RP): WL = RP x CV, where CV is conduction velocity. If the number of circuits in atria is small, the re-entry circuits may be unstable and can terminate by themselves. When the WL is decreased, e.g. RP decreases, the circuits are smaller and more numerous; simultaneous termination of many circuits is less likely to happen and AF may remain, as illustrated in Figure 1-3 (Nattel and Dobrev, 2012, Nattel and Harada, 2014).

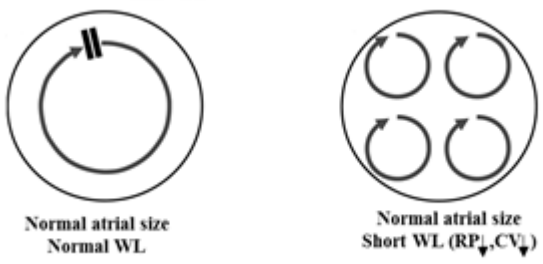

Figure 1-3 Re-entry. Determinats of AF maintenance by re-entry circuits depends on the impulse wavelength (WL). When WL is shortened by decreasing refractory period (RP) or conduction velocity (CV), re-entry circuits are smaller and can be sustained, promoting AF (Iwasaki et al., 2011).

1.3 Clinical management of AF

1.3.1 Pharmacological treatment of AF

Antiarrhythmic drugs have been used as a first line therapy for AF. Rate control and rhythm control are two principal goals to control the heart rate, or to maintain normal sinus rhythm (Baranchuk et al., 2008). Decreasing the ventricular response rate to achieve a rate of less than 100 beats per minute is generally the first step in managing AF, known as rate control (Iwasaki et al., 2011). Rhythm control is another strategy, which focuses on the pattern of heartbeats, and may involve using pharmacological or electrical cardioversion to restore the sinus rhythm for patients in persistent AF (Markides and Schilling, 2003). Rhythm or rate control can be achieved by pharmacological treatment in the form of antiarrhythmic drugs. Vaughan Williams, (1984) classified antiarrhythmic drugs according to their effects on the action potential of cardiac cells and their presumed mechanism of action. The classification of antiarrhythmic drugs is as follows: class I - sodium channel blockers, class II - β-blockers, class III - potassium channel blockers, and class IV - calcium channel blockers (Williams, 1984). The drugs commonly used for rate control are β-blockers, calcium channel blockers and digoxin (Markides and Schilling, 2003). β-blockers such as propranolol and atenolol, which reduce sympathetic influences that may inhibit ectopic pacemaker sites, resulting in decreased rate of automaticity, slow conduction velocity and prolong the refractory period (Cullington et al., 2008, Rang et al., 2014). calcium channel blockers are used for rate control in AF, and achieve this by blocking voltage-sensitive Ca^{2+} channels (Markides and Schilling, 2003). calcium channel blockers (e.g. verapamil) act on L-type calcium channel (LTCC), resulting in

shortening the plateau phase of action potentials, reducing after depolarisation, which supresses premature ectopic beats and decreases the contraction force in the heart (Abernethy and Schwartz 1999, Rang et al., 2014).

Rhythm control involves the use of pharmacological cardioversion to convert the arrhythmia associated with AF into a normal sinus rhythm (Sulke et al., 2007). Clinical practice commonly uses Vaughan–Williams' class I and III antiarrhythmic drugs for pharmacological cardioversion (Sulke et al., 2007). Class I drugs act on sodium channels, which reduce the maximum rate of rise in phase 0 of the action potential without changing the resting potential; however, they have different effects on APD. For example, class Ia; quinidine, which prolongs APD, class Ib; lidocaine, which decreases APD, and class Ic; flecainide, which does not have a significant effect on APD (Murakami and Kurachi, 2008, Rang et al., 2014).

Moreover, antiarrhythmic drugs class III; potassium channel blockers can also be used for rhythm control, by blocking potassium channels, which leads to prolonged repolarisation, APD, and the refractory period (Murakami and Kurachi, 2008, Sulke et al., 2007). Amiodarone is generally classified as a class III drug and APD prolongation is thought to be one of its major effects for effective antiarrhythmic action, due to blockade of the potassium channel (Murakami and Kurachi, 2008, Rang et al., 2014). Sotalol is both a non-cardioselective β-blocker as well as a class III; potassium channel blocker, which inhibits rapid delayed rectifier K^+ current, and increases APD and refractory period (Anderson and Prystowsky, 1999, Zimetbaum, 2012).

The Atrial Fibrillation Follow-up Investigation of Rhythm Management (AFFIRM) study showed a comparison of rhythm and rate control strategies in patients with AF

who were ≥ 65 years of age and at high risk of stroke or death. The antiarrhythmic drug was selected by the physician, which followed the rate control strategy using β-blockers, calcium-channel blockers, digoxin or a combination of these drugs; or the rhythm control strategy using the following antiarrhythmic drugs class I and III (see Section 1.3.1) alone or in combination. Cardioversion could be used if necessary (Wyse et al., 2002). Moreover, the anticoagulant; warfarin was used in both approaches applied in the AFFIRM study. The study reported that both strategies had similar effects on mortality and cardiovascular morbidity in patients with AF. The majority of strokes occurred after warfarin had been discontinued. Therefore, the outcomes of this study suggest that an anticoagulant should be used continuously high-risk patients (Wyse et al., 2002, Corley et al., 2004).

1.3.2 Radiofrequency ablation of AF

Since Haissaguerre et al. (1998) discovered that the ectopic foci associated with AF can originate in PVs after ablation with local radio-frequency energy and consequently, radiofrequency ablation (RFA) has become an established treatment in symptomatic AF patients (Schmidt et al., 2011). As a result of these findings by Haissaguerre et al. (1998), the catheter ablation technique called segmental PV isolation was created. Haïssaguerre and his colleagues used radiofrequency energy to ablate the PV ostium, the opening to the PVs, preventing the PVs from being a trigger source of AF; this technique is reportedly able to eliminate AF in 62% of paroxysmal AF patients (Haissaguerre et al., 1998). Moreover, circumferential ablation, which involves creating circumferential lesions that encircle the PVs, is also shown to

improve outcomes in patients with both paroxysmal and persistent AF (Yoshida and Aonuma, 2012). Circumferential ablation may extinguish areas that can be the source of a trigger or re-entry site for AF (Schmidt et al., 2011, Yoshida and Aonuma, 2012). Moreover, circumferential ablation near the PV ostia may cause an effect to sympathetic and parasympathetic innervation from the autonomic ganglia, which have been known as potential triggers for AF (Lemola et al., 2008). Radiofrequency catheter ablation for AF is a modern technique that effectively prevents arrhythmia recurrences; however, this is a complex procedure, which can increase the risk of various complications including pericardial tamponade, pericarditis, thromboembolic events, and pulmonary stenosis that can occur during or after the treatment (Aldhoon and Kautzner, 2012, Yoshida and Aonuma, 2012). Further understanding of the pathophysiology of AF may help to decrease the risk of these complications, specifically by refining the area of arrhythmogenic tissue treated.

1.4 Atrial fibrillation and the PVs

There are 4 main PVs in human anatomy; superior and inferior branch from the right and left lung, and one of which is connected to the left atrium (LA) of the heart (Seol et al., 2011). Nathan and Eliakim (1966) demonstrated that myocardial sleeves are found at the junction between the LA and PV, as seen in Figure 1-4. The PVs are suggested to be an important source of ectopic activity for the initiation of paroxysmal AF (Haissaguerre et al., 1998). Cheung (1981a) demonstrated that the action potential can be generated within PV myocardial sleeves. Thus, the anatomical and electrical properties of the PV may relate to the origination and the development of AF.

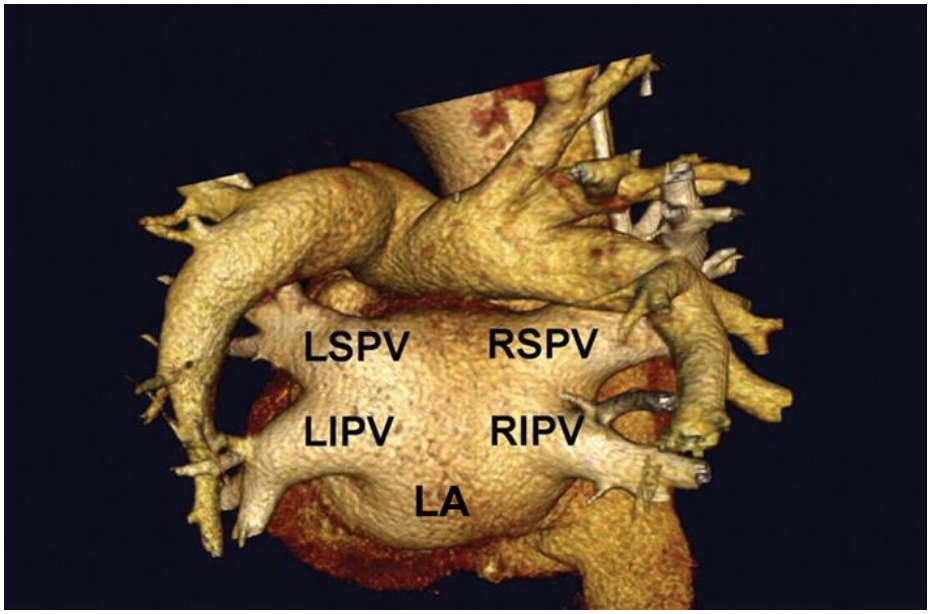

Figure 1-4 The anatomy of left atrium (LA) and pulmonary veins (PVs). The PVs are labelled as Right superior pulmonary vein (RSPV), Left superior pulmonary vein (LSPV), Right inferior pulmonary vein (RIPV), and Left inferior pulmonary vein (LIPV) (Adapted from Tops et al. (2010).

1.4.1 The structure of the PV

1.4.1.1 Anatomy of the PV

Previous studies identified myocardial sleeves formed by an extension of myocardial cells in the junction between LA and PV in the human heart (Nathan and Eliakim, 1966). These myocardial sleeves commonly extend up to 97% into the length of the PV (Nathan and Eliakim, 1966, Saito et al., 2000). Myocardial fibres within the sleeve of the human heart display various patterns in one or more layers; these are formed in circular, longitudinal, oblique and spiral directions (Nathan and Eliakim, 1966, Roux et al., 2004). Nathan and Eliakim (1966) also demonstrated that the myocardial sleeves are longer and thicker in the superior PV (SPV) than inferior PV (IPV). The longest

sleeves are in the left superior pulmonary vein (LSPV, 18 mm), the second longest are in the right superior pulmonary vein (RSPV, 13 mm), the third are in the left inferior pulmonary vein (LIPV, 10mm), and the shortest sleeve is the right inferior pulmonary vein (RIPV, 8 mm). The sleeves are thickest at the veno-atrial junction (1.1 mm) in the LSPV.

1.4.1.2 Anatomy of the PV

Histological study of the human heart has revealed that the structure of the PV comprises an internal tunica intima of endothelium, a tunica media of smooth muscle, and a thick outer layer of fibrous adventitia (Ho et al., 1999). The myocardium from the LA extends continuously along the outer aspect of the PV wall to form the myocardial sleeve (Calkins et al., 2008). This is also similar to histological studies in animals, which showed that myocardial sleeves are located between the media and adventitial layers of the PV wall in canine (Chen et al., 2000, Hocini et al., 2002, Ehrlich et al., 2003), guinea pig (Namekata et al., 2010, Takahara et al., 2011), rat (Mueller-Hoecker et al., 2008), and mouse (Tsuneoka et al., 2012).

1.4.1.3 Pacemaking cells in the PVs

The sinoatrial node (SAN) is located in the right atrium (RA), which is bound on two sides by the superior vena cava (SVC) and the inferior vena cava (IVC). (Boyett et al., 2000, Satoh, 2003). Histological studies of the SAN have identified specific cell types, which include nodal cells, transitional cells, and atrial muscle cells. Nodal cells (P-cells) are thought to generate the pacemaker activity of the heart (Waller et al., 1993, Nabipour, 2012). Node cells are small (3-10 μm), ovoid, pale-staining, and poorly striated compared with myocardial cells, and they are located around the sinus node artery (Davies and Anderson, 1983, Waller et al., 1993).

Masani (1986) discovered nodal-like cells, which are present in the myocardial layer in the rat PVs, using electron microscopy. The node-like cells are distributed in the intrapulmonary vein and they appear in single and in small groups among the general myocardial cells. These node-like cells may have the potential of generating pacemaker-like activity and represent a possible source of ectopic beats in the PVs.

Perez-Lugones et al. (2003) showed that nodal-like cells are present in human PVs. In the same study, some myocardial cells with pale cytoplasm were found using light microscopy. The presence of P cells, transitional cells, and Purkinje cells in the PVs was confirmed using electron microscopy (Perez-Lugones et al., 2003). Moreover, a study in canines showed that Periodic acid–Schiff (PAS) stain identified large cells with pale cytoplasm along the endocardial side of the PV muscle sleeve (Chou et al., 2005). The presence of PAS-positive cells is similar to specialised conduction cells found in human patients with AF (Perez-Lugones et al., 2003). In contrast the study by Nguyen et al. (2009), showed that PAS-positive cells are located in PV muscle

sleeve layers in both AF and sinus rhythm patients. This indicates that PAS-positive cardiomyocytes might have a potential pacemaking function.

1.4.1.4 The expression of the HCN4 channel in the PVs

Hyperpolarisation-activated cyclic nucleotide (HCN) -gated channels are responsible for the funny pacemaker current (I_f), which plays an important role in pacemaking activity in heart (Yamamoto et al., 2006, Scicchitano et al., 2012). HCNs are highly expressed in humans and in animals such as rabbit, rat and mouse (Dobrzynski et al., 2007, Liu et al., 2007, Yanni et al., 2010). Four different isoforms (HCN1-4) are expressed in the heart. HCN1 and HCN2 are found throughout the heart, although HCN2 is mainly expressed in the ventricles. The HCN4 is highly expressed in SAN, but not in the surrounding atrial muscle cells (Scicchitano et al., 2012). In human study, immunohistochemistry has been used to identify HCN4 in cardiomyocytes of the PV-LA junction in sinus rhythm and chronic AF patients (Nguyen et al., 2009). The same study showed the expression of HCN4, which is located the subendocardial layer in both sinus rhythm and AF patients, suggested to play a potential role in pacemaking activity (Nguyen et al., 2009).

A previous study in rat using immunolabelling showed the presence of HCN4-positive small node-like cells extending downwards from the SVC in the interatrial groove; however, HCN4 was not expressed in the PVs (Yamamoto et al., 2006). Likewise, another study in rat by Xiao et al. (2013) showed that the nodal maker HCN4 was only expressed in the SAN and atrioventricular node (AV node); however, it was not expressed in any area of myocardial sleeves of the rat PV or its branches.

1.5 Electrophysiology mechanism of AF initiation and maintenance in PVs

1.5.1 The role of action potentials and ionic currents

The first electrophysiological study of the PV was performed by Tasaki (1969) using striated muscle fibres of the extrapulmonary vein of the guinea pig. This study showed that action potentials in the PVs were similar to action potentials in the atrium. In a canine model of AF, LA cardiomyocytes were found to have a longer APD than PV cardiomyocytes (Melnyk et al., 2005). In studies of isolated PV cardiomyocytes from rabbit and dog, transient inward currents can induce DADs (Chen et al., 2001, Chen et al., 2002b). Also a rise in intracellular Ca^{2+} concentration can activate transient inward current, thought to be responsible for generating triggered cardiac arrhythmias (Berlin et al., 1989). Furthermore, transient inward currents and DADs through increasing NCX currents, altering the activity of the SR Ca^{2+} ATPase pump and causing leakage of intracellular Ca^{2+} all contribute to the generation of ectopic activity and AF (Chen and Chen, 2006).

Honjo et al. (2003) studied the effect of ryanodine in myocardial sleeves of PV in rabbit right atrial preparations. This study showed that ryanodine moved the pacemaker activity from the SAN to an ectopic focus near the right PV-atrium junction, which induced phase-4 depolarisation in the PV. These were not present in LA or RA. In addition, experiments on single cardiomyocytes isolated from rabbit PVs found that ryanodine receptors are associated with Ca^{2+} induced Ca^{2+} release, which can significantly alter cardiac electrical activity. This study also indicated that abnormal Ca^{2+} handling plays an important role in the PV arrhythmogenic activity

(Chen et al., 2002a). The properties involved in reducing maximum phase 0 upstroke velocity (Vmax) and decreasing resting membrane potential (RMP) are related to reducing inward-rectifier K^+ currents (I_{K1}). Decreasing APD then results from increasing rapid delayed-rectifier current (I_{Kr}) and slow delayed-rectifier current (I_{Ks}), and reducing I_{CaL} current. Therefore, previous investigations of the differences between PV and LA cardiomyocytes may suggest that distinct electrophysiological properties of the PV may cause ectopic foci and generate paroxysmal AF (Ehrlich et al., 2003).

1.5.2 Enhanced automaticity and triggered activity

There are a number of studies in PVs that have reported abnormal automaticity and/or triggered activity in patients with AF (Chard and Tabrizchi, 2009). In guinea pig PV cells, a study has shown that ectopic foci could affect cardiac activity and these cells could generate independent pace maker activity (Cheung, 1981a). Triggered activity can be generated by digitalis at concentrations of 0.5-2.5 μM in guinea pig PV tissues (Cheung, 1981b). (Chen et al. (2000), 2001) demonstrated that enhanced automaticity and induced triggered activity appear in isolated single cardiomyocytes in a canine model of AF. In addition, the study of PV sleeves in dogs showed spontaneous occurrences of EADs and bursts of high frequency irregular discharges that triggered activity. The same study found chronic rapid atrial pacing could induce AF and spontaneous impulses with characteristics of pacemaker cells (Chen et al., 2000). The rapid atrial pacing could lead to electrophysiological remodelling of single pulmonary cardiomyocytes in canines, increasing automaticity and triggered activity that could

maintain AF (Chen et al., 2001). Chen et al. (1999) showed that the β-blocker: propranolol, Ca^{2+} channel blocker: verapamil and sodium channel blocker: procainamide reduce ectopic activity in the PVs. However, a synthetic sympathomimetic amine: isoproterenol induces PV electrical activity. These findings suggest that abnormal automaticity and triggered activity play a role in the PV arrhythmogenic activity.

1.5.3 Re-entry

Fynn and Kalman (2004) have stated that "re-entry is responsible for the majority of clinical arrhythmias encountered by the cardiac electrophysiologist". Many studies have linked the PV with AF. A study of extracellular electrophysiology mapping and histology of the PV in isolated, blood-perfused dog heart showed that the structure of the myocardial sleeve could generate re-entry and arrhythmias related to ectopic activity (Hocini et al., 2002). The action potentials of PV cells displayed slower upstroke and duration compared with atrial cells, leading to shorter refractory periods and slower conduction velocity. PV cardiomyocytes demonstrated shorter action potentials than recorded from atrial tissue in canines (Hocini et al., 2002, Ehrlich et al., 2003). In addition, the re-entrant circuit in the PV–LA junction has been identified as an originating source of focal discharge in the PVs using a multi-electrode catheter (Kumagai et al., 2000). In another canine study re-entry was demonstrated to be due to PV tachycardia in the presence of acetylcholine that could be induced by activation of the parasympathetic nervous system (Po et al., 2005). This created a reduction in APD and refractory periods recorded from the PVs and as a consequence, promoting

re-entry. Based on a morphological study of the atrial myocardium in human PVs from patients with and without AF, severe discontinuity of the myocardium (separation of the atrial myocardial bands), hypertrophy and fibrosis were associated with AF (Hassink et al., 2003). Takahashi et al. (2003) studied re-entrant tachycardia in PVs of patients with paroxysmal AF and indicated that re-entrant tachycardia can occur in some isolated PVs with both decremental conduction properties and short refractory periods, which suggested that re-entry may be one of the mechanisms underlying PV arrhythmogenesis. Moreover, the PV-LA junction is suggested to be critical in encouraging re-entry formation and might play an important role as a substrate for the maintenance of AF (Kumagai et al., 2000).

1.5.4 The relationship between AF and the general structure of the myocardial sleeve

Haissaguerre et al. (1998) reported the links between AF and PVs and indicate that there is connection between physiology and pathology of PVs and the myocardium. The same study showed that spontaneous ectopic foci in the cardiac tissue can induce AF in patients with paroxysmal AF, and suggested that the PVs were responsible for up to 94% of the ectopic activity. Studies of human PVs have shown that the length of the cardiac sleeve may influence the generation of AF and other electrical abnormalities. In addition, longer sleeves are implicated in the generation of ectopic foci while shorter sleeves have abnormal conduction pathways (Nathan and Gloobe, 1970, Haissaguerre et al., 1998, Ho et al., 1999). Structural and morphological studies have shown that features of the myocardial sleeve such as variation of fibre length,

changes in thickness, disorganisation and irregularity of the myocardial fibre, fibrosis, gaps and abnormal distribution of gaps may predispose the vein to generate ectopic activity resulting in AF (Ho et al., 1999, Roux et al., 2004).

1.6 Autonomic nervous system innervation of the PVs

1.6.1 The cardiac adrenergic system

The autonomic nervous system has been shown to play a role in the initiation of AF. Preganglionic neurons enter the heart from the spinal cord, sympathetic trunk, cervical ganglia, and cardiac plexuses to synapse with postganglionic neurons (Kawashima, 2005). Those neurons penetrate the myocardium along coronary arterial pathways, terminating on cardiomyocytes and vessels of all of the chambers. Adrenergic stimulation involves neurotransmitter release from sympathetic nerves. These neurotransmitters are known as catecholamines, and include noradrenaline (NA), from postganglionic nerve terminals, and adrenaline from the adrenal medulla. In the human atrium, catecholamine binds to and activates cell surface adrenergic receptors, comprising α, β_1, β_2 and β_3 subtypes. (Hedberg et al., 1985, Chamberlain et al., 1999). In mice ventricular myocytes show the all 5 cardiac adrenergic receptors, encompassing β_1, β_2 and β_3, α_{1A}, and α_{1B} adrenoceptors. This study also showed the β_1 and α_{1B} adrenoceptors were expressed in all myocytes; however, β_2 and β_3 were detected in only about 5% of mice ventricular myocytes (Myagmar et al., 2017).

The β_1-adrenoceptor is the predominate receptor in the human heart. Studies have found β_1-adrenoceptors covering 70-80% of the ventricle tissue, and 60-70% of the

atrium; as reviewed by Wallukat (2002). The β_1 adrenergic receptors are coupled to Gs-proteins that activate adenylyl cyclase (AC), resulting in an elevation of the second messenger cyclic adenosine monophosphate (cAMP), which hydrolyses cAMP from adenosine triphosphate (ATP). The increase of intracellular cAMP can activate protein kinase A (PKA), which increases phosphorylation of the L-type Ca^{2+} channels, causing increased cellular influx of Ca^{2+} via Ca^{2+} channels and enhanced release of Ca^{2+} from the SR in the heart; as shown in Figure 1-5 (Mohrman and Heller, 2002, Wallukat, 2002, Klabunde, 2011).

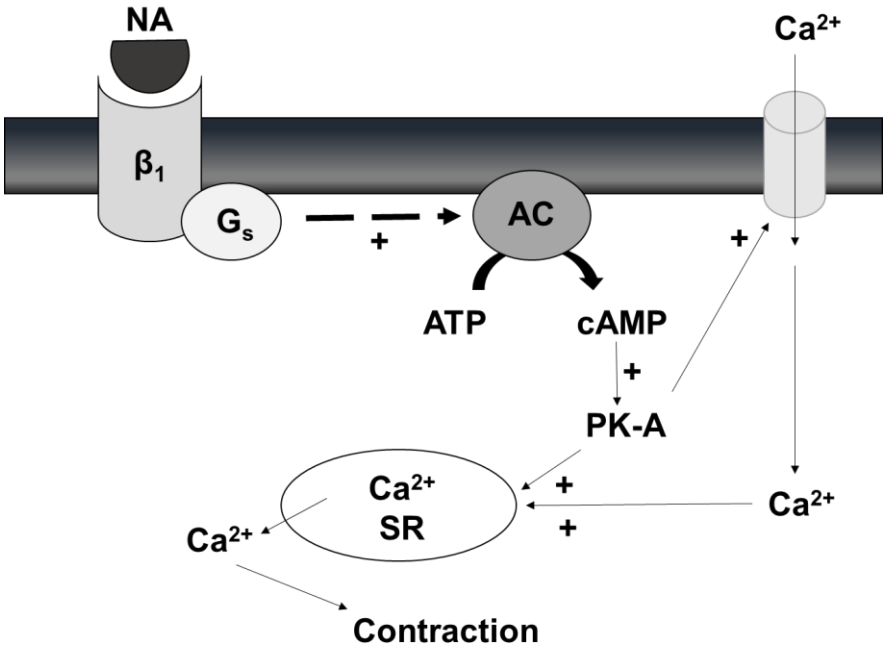

Figure 1-5 β_1-Adrenergic receptor (AR) signalling in cardiomyocytes. Noradrenaline (NA) binding to β_1- ARs stimulates adenylate cyclase (AC), which converts adenosine triphosphate (ATP) to cyclic monophosphate (cAMP). cAMP activates protein kinase A (PKA), which increases phosphorylation and causes increased cellular influx of Ca^{2+} via L-type calcium channels, and enhanced release of Ca^{2+} from the sarcoplasmic reticulum (SR) in the heart.

In addition, α_1-adrenoceptors are also found in the human heart. Expression in normal, non-failing hearts is approximately 11%, whereas that percentage increases to 25% in failing myocardium, suggesting that α_1 receptors are upregulated in certain pathological states (Jensen et al., 2011). The α_1-adrenoceptors are coupled to a phospholipase C (PLC)-coupled Gq-protein, which stimulates the formation of inositol trisphosphate (IP_3) from phosphatidylinositol biphosphate (PIP_2) and diacylglycerol (DAG). Increasing IP_3 induces Ca^{2+} release from the SR in the heart, thereby increasing inotropy. On the other hand, DAG acts as a second messenger to activate protein kinase C (PKC), which catalyses the phosphorylation of a protein that produces a response in the various of cellular protein substrates, including Ca^{2+} and K^+ channels, Na^+-H^+ exchanger, and Na^+-Ca^{2+} pump. The activation of PKC regulates gene-signalling pathway e.g. cell growth and cell proliferation and alters cardiac function such as ionotropic effects in cardiac muscle as seen in Figure 1-6 (Rosen et al., 1991, Finch et al., 2006, O'Connell et al., 2014).

Moreover, the inhibitory G-protein (Gi-protein) inhibits AC and reduces intracellular cAMP, thereby decreasing inotropy. Acetylcholine released by parasympathetic nerves within cardiac muscle bind to muscarinic receptors (M_2), which are coupled to Gi-proteins. Therefore, acetylcholine can be used as a negative inotropic agent to decrease cardiac contractility (Mohrman and Heller, 2002, Klabunde, 2011).

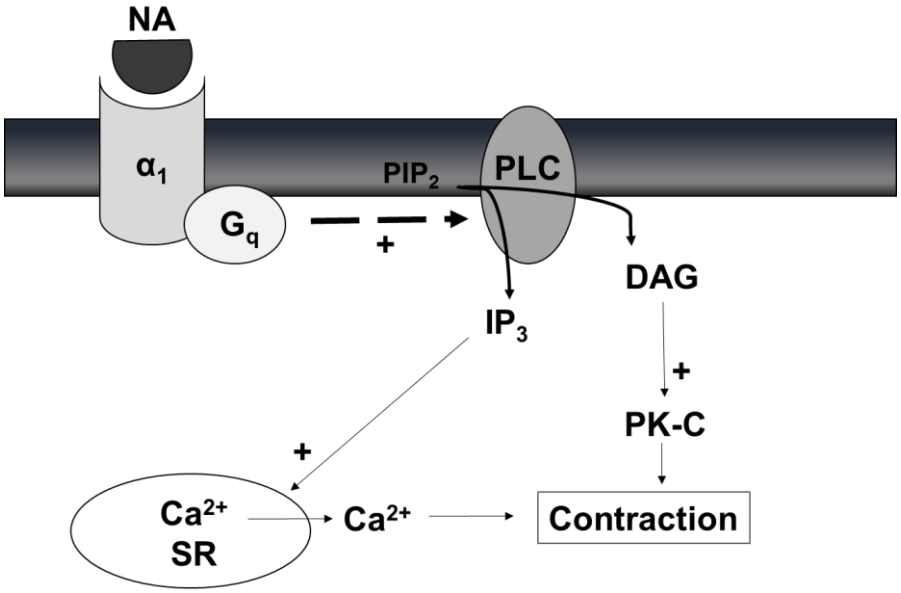

Figure 1-6 α_1-Adrenergic receptor (AR) signalling in cardiomyocytes. Noradrenaline (NA)-induced stimulation of α_1-ARs activates Gq and phospholipase C (PLC), resulting in hydrolysis of phosphatidylinositol bisphosphate (PIP_2), to generate inositol trisphosphate (IP_3) and diacylglycerol (DAG). IP_3 contributes to the regulation of intracellular Ca^{2+} responses, whereas DAG activates protein kinase C (PKC), which stimulates contraction.

1.6.2 The autonomic nerves and the PVs in arrhythmogenesis

The report by Patterson et al. (2006) indicated that there is a relationship between the atrial autonomic nerves and the PVs in arrhythmogenesis. There are seven ganglionated subplexuses and the superior left atrial ganglionated plexus is one of the collections of ganglia on the posterior surface of the LA between the human PVs. (Armour et al., 1997). The findings by Pauza et al. (2000) stated that three of the seven ganglionated plexuses are distributed in human PVs, found near the roots of the PVs: the dorsal right atrial, the left dorsal and the middle ganglia. The studies from Tan et al. (2006) and Chevalier et al. (2005) have shown the cardiac origin of the nerve plexus on the PVs. Immunostaining nerve densities along longitudinal and circumferential axes of the human PV-LA junction has indicated that adrenergic and cholinergic innervation are most densely located in the LA, closer to the junction than further away in the left atrium or the PVs (Tan et al., 2006). This study used anti-tyrosine hydroxylase antibodies to label adrenergic nerves and anti-choline acetyltransferase antibodies to label cholinergic nerves.

Atrial electrophysiology and AF generation are regulated by the autonomic nervous system (Zipes et al., 1974, Liu and Nattel, 1997). These studies in human PVs have identified different neurochemical types of nerve fibres, including the sensory, noradrenergic, cholinergic, and nitrergic systems that innervate the PVs. The adrenergic and cholinergic nerves may be located in and around the PVs. Moreover, found in the posterior sides of both inferior and the left superior PVs are the ganglion sites supplying intrinsic nerves to the human PVs. These locations may be considered

major targets for PV ablation in catheter-based therapy of AF (Vaitkevicius et al., 2008).

The cardiac muscle of PV function can be modulated by the autonomic influences, which may be of significance to the generation of AF (Sweeney et al., 2007, Maupoil et al., 2007). Sweeney et al. (2007) found that NA and acetylcholine (ACh) increase the cardiac contractility, which was inhibited by atenolol (a selective β_1 receptor antagonist) and atropine (a muscarinic ACh receptor antagonist). Thus, the PV cardiac muscle function may be modulated by the autonomic nervous system, which can potentially generate AF (Sweeney et al., 2007). Maupoil et al. (2007) also found nonselective adrenoceptor agonist; NA induces ectopic contractions in rat PVs, which may suggest that the induction of ectopic activity requires the activation of both α_1 and β_1- adrenergic receptors.

In an electrophysiological study, Cheung (1981a) observed electrical activity in guinea pig PVs, and showed that the application of NA initiated spontaneous action potentials in the distal end of the cardiac PVs and caused a slight change in the membrane potential of PV cardiomyocytes. Moreover, NA also generated automatic activity in mouse, rat, and guinea pig PV cardiomyocytes (Doisne et al., 2009, Namekata et al., 2010, Takahara et al., 2011, Tsuneoka et al., 2012, Okamoto et al., 2012). In mouse PV cardiomyocytes, it was shown that NA induces the generation of automatic electrical activity, which was preceded by depolarisation or hyperpolarisation of the RMP (Tsuneoka et al., 2012). Also, in guinea pig PV myocardium it was found that NA induces spontaneous activity and a slow depolarisation of the RMP in the PV preparations (Namekata et al., 2010, Takahara et al., 2011). However, in the rat PV,

NA was found to induce an initial hyperpolarisation and a subsequent depolarisation of RMP (Doisne et al., 2009, Namekata et al., 2010). In addition, NA also induces EADs in mouse PV myocardium (Tsuneoka et al., 2012), and DADs in guinea pig and rat PV cardiomyocytes (Takahara et al., 2011, Okamoto et al., 2012). In a canine study using intracellular electrodes, NA was found to prolong the APD and enhance formation of EADs and DADs (Patterson et al., 2006). Therefore, these results obtained from various species' PV myocardium indicate that the sympathetic nervous system influences the generation of automatic activity via activation of both α- and β-adrenergic receptors. These mechanisms may be related to the initiation and maintenance of AF and highlight the PVs as a source under autonomic nerve influence (Maupoil et al., 2007, Doisne et al., 2009).

1.7 Stretch-induced arrhythmia

1.7.1 The cardiac response to stretch

The heart adapts to changing volumes of entrant blood supply by the principal mechanism known as the Frank-Starling law of the heart (Zimmer, 2002). By using isolated frog hearts Frank (1895) demonstrated that increased filling pressure or increased initial tension is related to an increase in the peak pressure developed during systole. The study also showed that the stretching of cardiac muscle leads to changes in fibre length prior to contraction (Frank, 1895). In 1914, Ernest Starling and colleagues demonstrated the response of the heart to changes in venous return and arterial pressure using canine heart-lung preparations. The same study showed that greater venous return to the heart increased filling pressure of the ventricle, which can

in turn increase stroke volume (the blood volume pumped out of the left ventricle into the aorta) with each contraction (Patterson and Starling, 1914). Therefore, an increase in ventricular filling promotes an increase in developed tension, which leads to increased stroke volume; occurring in response to physical stress on cardiac tissue, e.g. from stretching (Frank, 1895, Patterson and Starling, 1914).

Mechanical stretch can lead to changes in intracellular Ca^{2+}, contraction force and electrical activity of cardiomyocytes (Tavi et al., 1998). The stretch-dependent change in cardiac contraction force has two components; an immediate force response (IFR), and a slow force response (SFR) (Parmley and Chuck, 1973). While cardiac muscle is stretched, the immediate increase in the force of contraction is referred to as IFR, and the secondary force known as SFR follows after stretching for 5-10 minutes (Calaghan and White, 1999, Ward and Allen, 2010).

Previous studies have shown atrial dilatation and atrial stretch may play an important role in AF. (Ravelli, 2003). Stretch changes the electrophysiological properties of the heart e.g. depolarisation of RMP in the left ventricle of rats (Kiseleva et al., 2000), prolongation of APD in rat atrial myocytes (Tavi et al., 1998). The electrophysiological response to stretch is a type of mechanoelectric feedback (MEF) (Lab, 1996). This MEF can be large enough to generate ectopic beats and trigger AF (Saint et al., 2014). The electrical activity of the myocardium in response to stretch can be measured at the tissue level and at the single-cell level, which may be due to the presence of mechanosensitive ion channels in myocytes (Saint, 2002).

1.7.2 Stretch-activated ion channels in the heart

Guharay and Sachs (1984) discovered stretch-activated channels (SACs) in chick skeletal muscles by applying negative pressure to the cell membrane with a patch pipette. SACs have also been found in many other cell types such as eukaryotic mechanosensitive channels (Árnadóttir and Chalfie, 2010), bacterial mechanosensitive channels (Martin et al., 1996), including ventricular myocytes (Craelius et al., 1988), and rat atrial myocytes (Zhang et al., 2000). The response to stretch involves at least two types of mechanosensitive ion channels; a non-selective cation channel (SAC_{NS}) and a potassium channel (SAC_K) (Saint, 2002, Reed et al., 2014). Ruknudin et al. (1993) demonstrated that SAC_{NS} and SAC_K channels are present in tissue-cultured embryonic chick cardiac myocytes, and found that SAC_{NS} have unitary conductance ranges from 21 to 25 pS, and SAC_K have unitary conductance ranges from 25 to 200 pS.

1.7.2.1 Stretch-activated nonspecific cation channels (SAC_{NS})

It has been shown that SAC_{NS} play an important role in the generation of arrhythmias during stretch (Bode et al., 2000). Craelius et al. (1988) demonstrated SAC_{NS} in ventricular myocyte of neonatal rat by using cell-attached patch-clamp techniques. SAC_{NS} have also been found in isolated embryonic chick heart cells (Hu and Sachs, 1996), ventricular myocytes in guinea pig (Sasaki et al., 1992), rat (Bett and Sachs, 2000), and mouse (Kamkin et al., 2003a), as well as atrial myocytes in rat (Zhang et al., 2000), and in human (Kamkin et al., 2003b). SAC_{NS} opening allows Na^+ or

possibly Ca^{2+} to entry into the cells, and subsequent Ca^{2+} increase through the NCX influx (Kim, 1993, Ward and Allen, 2010). The activation of SAC_{NS} in cardiomyocytes will depolarise the RMP (Kohl et al., 2006, Reed et al., 2014). In addition, some studies showed Ca^{2+} entry via SACs in embryonic chick cardiac myocytes (Sigurdson et al., 1992, Ruknudin et al., 1993), guinea pig ventricular myocytes (Gannier et al., 1996), and rat cardiomyocytes (Kim, 1993), which showed that the mechanical stretch can increase the amplitude of Ca^{2+} transients by activation of SACs in cardiomyocytes.

The rat atrial myocyte study showed the activation of SACs allows Na^{+} influx through SACs, which leads to the accumulation of Na^{+} in the cytosol and subsequent increase in intracellular Ca^{2+} by the activation of the reverse-mode NCX (Youm et al., 2006). Some studies also showed that stretch increases the intracellular Na^{+} concentration in human, mouse, and rat ventricular myocytes, leading to the activation of reverse-mode operation of NCX during the rising phase of the action potential. The increase in Ca^{2+} concentration via NCX can increase the Ca^{2+} transients during stretch as shown in Figure 1-7 (Alvarez et al., 1999, Pérez et al., 2001, Baartscheer et al., 2003b, Isenberg et al., 2003, Nishida et al., 2010).

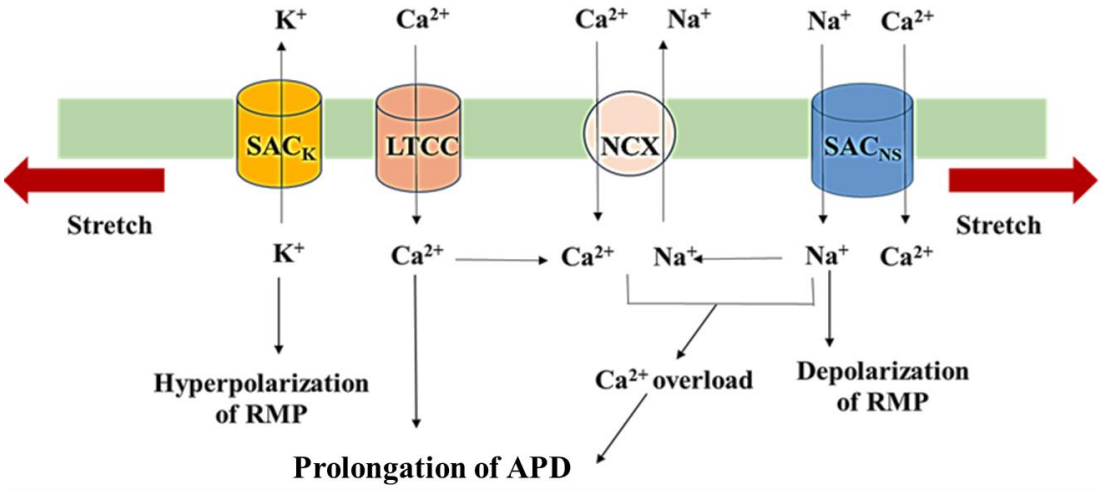

Figure 1-7 Mechanisms of stretch-induced atrial fibrillation (AF). Non-selective cation channel (SAC_{NS}) are permeant to Na^+, Ca^{2+} influx to the cells. The activation of SAC_{NS} will depolarise the plasma membrane. Increasing intracellular Na^+ also increase intracellular Ca^{2+} by the reverse mode of Na^+-Ca^{2+} exchanger (NCX), leading to prolongation of action potential duration (APD). Stretch in cardiac cells also can cause Ca^{2+} influx via L-type calcium channel (LTCC). The potassium-permeable stretch activated channel (SAC_K) allows K^+ to move out of the cell, which can cause hyperpolarisation of the resting membrane potential (RMP).

Recent studies suggest that transient receptor potential (TRP) channels can be the molecular candidates for SACs in cardiac myocytes (White, 2011, Reed et al., 2014). TRP channels were first discovered in Drosophila and now a total of 28 members of mammalian TRP subtypes have been reported (Takahashi et al., 2016). TRC membrane proteins has 6 transmembrane domains (TM1-6), cytoplasmic N- and C termini, and a pore region between TM5 and TM6 (Watanabe et al., 2009). TRP channels are divided into six related subfamilies, consisting of the canonical TRP (TRPC), vanilloid TRP (TRPV), melastatin TRP (TRPM), ankyrin TRP (TRPA), polycystic TRP (TRPP), and mucolipin TRP (TRPML) groups; as reviewed by Yue et al. (2015).

It has been reported that TRPC1, TRPC3, and TRPC6 channels are the main molecular candidates for stretch-activated ion channels (Inoue et al., 2012, Reed et al., 2014). In the cardiovascular system, studies using RT-PCR (reverse transcriptase polymerase chain reaction), Western blotting, immunostaining, and functional current recording have shown TRPC1 and TRPC3 in whole hearts, and TPRC6 in cardiac myocyte and in SAN cells (Maroto et al., 2005, Kuwahara et al., 2006, Spassova et al., 2006, Ju et al., 2007, Huang et al., 2009, Yue et al., 2015).

TRPC1 channels are activated by mechanical stretch (Maroto et al., 2005), and the expression of TRPC6 channels are activated by hypo-osmolarity and direct membrane stretch (Spassova et al., 2006). Ohba et al. (2007) reported that TRPC1 expression is significantly increased in rat hearts with abdominal aortic-banded compared to sham-operated rats. A study in hearts showed upregulation in TRPC6 when internal pressure was increased in mouse hearts in response to pressure overload, as well as in failing

human hearts (Kuwahara et al., 2006). (Bush et al. (2006)) also demonstrated that TRPC1, TRPC3, and TRPC6 expression is upregulated in a rat model using thoracic aortic banding to trigger pressure overload-induced hypertrophy of the left ventricle. The same study also showed the expression of TRPC channels in tissue culture from human heart failure, rat left ventricle and mouse left ventricle (Bush et al., 2006).

Seth et al. (2009) demonstrated that TRPC1 plays a key role in cardiac hypertrophy. This study showed that TRPC1-mediated Ca^{2+} entry into cardiomyocytes activates hypertrophic signalling during pressure overload in mouse myocardium; however, mouse cardiomyocytes lacking TRPC1 channels do not present TRPC currents during the pressure overload condition. Recent studies by Zhang et al. (2016) showed that TRPC1 channels are found in human atrial myocytes and activated by endothelin-1 (ET-1). This study also observed ET-1 activated TRPC1 currents in specimens of AF myocytes which were greater than specimens of sinus rhythm, and that ET-1-evoked TRPC1 current can be inhibited by BQ-123 and BQ788 (ETA and ETB receptor antagonists) or PKC inhibitor. Therefore, these findings may useful for understanding the role of TRPC1 channels in AF (Zhang et al., 2016).

Recent studies by Harada et al. (2012) demonstrated that TRPC3 regulates cardiac fibroblast function and suggested that this may be involved in the development of AF. This study in left atrial fibroblasts isolated from dogs showed TRPC3 protein expression, currents, extracellular signal-regulated kinase phosphorylation, and extracellular matrix gene expression were significantly increased after being kept in a state of AF by atrial tachypacing for 1 week (Harada et al., 2012). Harada et al. (2012) also showed pyazole-3 (TRPC3 blocker) suppressed AF while decreasing fibroblast

proliferation and extracellular matrix gene expression, resulting in prevention of the development of AF in the electrically maintained dog model of AF.

TRPC6 is reported as a SAC, which may contribute to stretch associated AF (Yue et al., 2015). Spassova et al. (2006) showed that TRPC6 is activated by hypo-osmolarity and direct membrane stretch, and that these responses can be inhibited by tarantula toxin GsMTx-4. A recent study by Nikolova-Krstevski et al. (2013) reported that TRPC6 activity may be evaluated by measuring extracellular Ca^{2+} influx through the TRPC6 channels in atrial endocardial endothelium cells, located between the myocardium and the circulating blood, under stretch conditions. Seo et al. (2014) demonstrated the effects of TRPC3/6 antagonists (GSK2332255B and GSK2833503A; against TRPC3 and TRPC6, respectively) in pathological cardiac hypertrophy. This study showed that combined TRPC3 and TRPC6 blockade dose-dependently inhibited cell hypertrophy signalling triggered by angiotensin II or endothelin-1 in HEK293T cells, derived from human embryonic kidney and neonatal and adult cardiac myocytes. Using mice with specific deletion of either TRPC3 or TRPC6, and a model with combined TRPC3/6 disruption, this group showed that individually these channels do not provide significant benefit, although when disrupted in combination they do, suggesting they act synergistically (Seo et al., 2014). These findings suggest TRPC channels may be useful targets for the future development of therapeutic agents for heart disease management.

1.7.2.1 Stretch-activated potassium channels (SAC_K)

SAC_K in the heart was first discovered by Kim (1992) in rat atrial myocardium. The cardiac response to stretch is related to SAC_K channels which have been found in many tissues, including atrial myocytes (Kim, 1992, 1993, Kamkin et al., 2003b) and ventricular myocytes (Kamkin et al., 2003a). In rat studies showed the expression of SAC_K in cardiac ventricular muscle by longitudinal stretch (Li et al., 2006). SAC_K in the heart was first discovered by Kim (1992) in rat atrial myocardium. The cardiac response to stretch is related to SAC_K channels which have been found in many tissues, including atrial myocytes (Kim, 1992, 1993, Kamkin et al., 2003b) and ventricular myocytes (Kamkin et al., 2003a). In rat studies showed the expression of SAC_K in cardiac ventricular muscle by longitudinal stretch (Li et al., 2006). As noted above, mechanical stretch of the resting myocardium causes depolarisation by the activation of SAC_{NS} (Kim, 1993, Ward and Allen, 2010). In contrast, SAC_K preferentially enables K^+ efflux over influx, with a reversal potential that is negative to the cardiac muscle resting potential, thus SAC_K opening leads to repolarisation or hyperpolarisation of the RMP (Ward and Allen, 2010, Reed et al., 2014, Peyronnet et al., 2016).

Recent studies have identified a new class of K^+ channels, characterized by four trans-membrane domains and two pore domains (K_{2P} channels): TREK-1, which is highly expressed in the heart; reviewed by Goonetilleke and Quayle (2012). TREK-1 channels have been found in rat atrial myocytes (Niu and Sachs, 2003, Terrenoire et al., 2001) and rat ventricular myocytes (Aimond et al., 2000, Tan et al., 2002). Li et al. (2006) demonstrated that the TREK-1 channel is found in longitudinal stripes at the external surface membrane of rat cardiomyocytes, and that K^+ currents flow through

SAC_K by applying moderate stretch across the longitudinal strip. In rat left ventricular myocardium, studies showed that TREK-1 mRNA is expressed in both endocardial and epicardial cells in the infarct area after myocardial infarction (Zhao et al., 2011).

In a porcine model, the expression of TREK-1 channels in the heart has been shown with predominance in the atrial tissue by using PCR and western blot during AF induced by atrial burst pacing. Moreover, down-regulation of TREK-1 mRNA has been observed in the RA during AF, which may result in shortening of APD and cardiac refractoriness. Through, these actions TREK-1 may be able to suppress re-entry induced AF, because re-entry depends partly on the refractory period of cardiac tissue. Overall, these findings suggest that human and porcine TREK-1 channels have similar structure and function, indicating that pigs might be useful for studying the physiological role of TREK-1 in preclinical studies (Schmidt et al., 2014).

Recent studies by Lugenbiel et al. (2016) have reported that the expression of atrial TREK-1 was reduced in chronic AF patients with concomitant severe HF. Moreover, down-regulation of repolarisation TREK-1 potassium channels prolonged atrial effective refractory periods. In the same study, mechanical stretch decreased TREK-1 mRNA expression in neonatal rat ventricular myocytes. In a preclinical therapeutic study, atrial Ad-TREK-1 gene therapy significantly increased TREK-1 protein levels and decreased atrial effective refractory periods in the porcine AF mode (Lugenbiel et al., 2016)l. Thus, the study of antiarrhythmic TREK-1 gene therapy can be useful for investigating future treatment strategies for AF.

1.7.3 Stretch-induced calcium entry via L-type Ca^{2+} channels

Increasing intracellular Ca^{2+} concentration results from Ca^{2+} influx through SACs during a stretch. Stretching in cardiomyocytes also modifies intracellular Ca^{2+} concentration by causing Ca^{2+} influx through LTCC, in addition to SACs, as reviewed by Calaghan et al. (2003) and Lammerding et al. (2004). A study in rabbit hearts showed that stretch can increase I_{CaL} by osmotic cell swelling and cell inflation; by applying a positive pressure of 10 to 15 cm H_2O via the patch pipette in single rabbit cardiac myocytes (Matsuda et al., 1996). Moreover, a study in mouse ventricular myocytes also suggested that mechanical stretching using a glass stylus induced depolarisation of the RMP and prolongation of the APD, augmenting Ca^{2+} influx through LTCC (Kamkin et al., 2003a). However, some studies demonstrated that an axial stretch does not affect I_{CaL} in an isolated preparation of guinea-pig ventricular myocytes (Sasaki et al., 1992, White et al., 1995, Hongo et al., 1996, Belus and White, 2003). Therefore, it may be summarised that mechanical stretch may induce extra Ca^{2+} to enter the cells via LTCC due to delayed voltage-dependent inactivation during prolonged depolarisation (Calaghan et al., 2003, Kamkin et al., 2003a, Youm et al., 2005, Youm et al., 2006, Rice and Bers, 2011).

1.7.4 Stretched-induced changes in electrical activity of the heart

Mechanical stretch is found to induce changes in the electrical activity of the heart; e.g. depolarisation of the RMP in rat (Zhang et al., 2000), guinea-pig (Nazir, 1996b), in mouse hearts (Kamkin et al., 2003a), and human hearts (Kamkin et al., 2003b). This

study in rat demonstrated that the application of longitudinal stretch prolonged the APD in isolated rat atrial myocytes using patch clamp techniques. This study also showed that stretch causes the opening of SAC_{NS} and SAC_K, increasing the stretch activated current (I_{SAC}), which depolarised the RMP (Zhang et al., 2000). The guinea pig study found a decrease of the action potential amplitude, an increase in the APD, and premature atria1 beats during stretch caused by intra-atrial pressure (Nazir, 1996b).

Moreover, Franz et al. (1989) found that stretch decreased the duration of action potentials measured at 20% repolarisation (APD_{20}); however, it increased the duration of action potential measured at 90% repolarisation (APD_{90}) during increasing ventricular volume and pressure in isolated canine hearts. Stretch has been found to induce the activation of $I_{SAC,}$ leading to increased membrane permeability for both Na^+ and Ca^{2+}, subsequent depolarisation of the RMP, and prolonged APD in both mouse ventricular myocytes and human atrial myocytes (Kim, 1993, Kamkin et al., 2003a, 2003b).

In addition, acute atrial stretch induced EADs and DADs, which may trigger premature action potentials (Ravelli, 2003). Production of stretch-activated depolarisations (SADs) leads to generation of atrial arrhythmias in human atrial myocytes and the isolated atrial myocytes from human hearts and mouse ventricular myocytes (Kamkin et al., 2003a, Kamkin et al., 2003b). Nazir (1996b) also demonstrated the incidence of EADs in isolated guinea pig hearts while the atrium was stretched by inflating a fluid-filled intra-atrial latex balloon catheter. In rat studies DADs have been shown in the isolated atria when increasing the intra-atrial pressure by a pressure generator (Tavi et

al., 1996). Isolated canine heart studies have shown premature ventricular extra-systole during increases in ventricular volume and pressure (Franz et al., 1989, 1992). Stacy Jr et al. (1992) also showed stretch-induced membrane depolarisations while increasing the pressure in isolated canine left ventricles.

1.7.5 Atrial fibrillation and the stretch of atrium

The pathophysiology of AF is mainly attributed to stretch caused by increased atrial pressure and volume (Savelieva and John Camm, 2003). Previous studies have shown increased atrial stretch leads to increase vulnerability in isolated guinea-pig heart and rabbit heart using increased atrial volume and increased atrial pressure, respectively (Nazir, 1996b, Bode et al., 2000). The study in the isolated Langendorff-perfused rabbit hearts also showed that of the ability to induce AF increased when increasing atrial pressure between 0-16.2 cm H_2O (Ravelli and Allessie, 1997). Rat studies have also shown increasing pressure inside the atrium (1 mmHg to 7 mmHg) may induce AF; analysed using intracellular voltage recordings from rat isolated atria (Tavi et al., 1996). In a study using dogs, spontaneous atrial tachycardia appeared during atrial balloon dilatation, which may relate to the pathogenesis of atrial arrhythmias (Solti et al., 1989). Henry et al. (1976) demonstrated the relationship between left atrial size and AF using echocardiography, finding only 3% of patients with the left atrial dimension below 40 mm showed AF; however, AF was more common (80 of 148 or 54%, $p < 0.01$) when patients' left atrial dimension exceeded 40 mm. In the human atrium, studies showed that acute atrial dilatation caused conduction slowing and a

significant increase in AF vulnerability, with 6 of 10 patients developing AF occurrences under stretch (Ravelli et al., 2011).

In pathological conditions, the stretch of cardiomyocytes may relate to arrhythmias (Seol et al., 2011). Several cardiac disorders such as hypertension, heart failure, and mitral value disease are thought to promote AF by increased intra atrial pressure, atrial dilation or increased stretch (Benjamin et al., 1994, De Jong et al., 2011, Seol et al., 2011). Another study in dogs has shown that chronic atrial dilatation increased the effective refractory period in dog mitral regurgitation, leading to an increased vulnerability to AF (Verheule et al., 2003). In a sheep study, myocytes were enlarged and showed repetitive atrial firing with moderate LA dilation (Deroubaix et al., 2004). Moreover, a goat model of chronic left atrial overload using bipolar electrodes found that 9 of 12 animals showed prolonged AF (>1 hour) during increased left atrial pressure, and six of them displayed persistent AF (>1 week) (Remes et al.). The study of feline hearts using electrocardiographic findings showed atrial tachycardia, atrial flutter and AF in cats with cardiomyopathy causing left atrial enlargement. In the same study, a significant reduction in RMP, maximum rate of phase 0 depolarisation, and action potential amplitude of excitable cells from the LA was found from the moderate and severe cardiomyopathy cats compared with the mild cardiomyopathy cats (Boyden et al., 1984). In a sheep model of chronic blood pressure elevation, a significant reduction of atrial conduction was shown in the elevated blood pressure group compared with controls, with conduction slowing at all atrial sites and shortened atrial wavelength in RA and LA of the hypertensive goat. Thus, this study suggested that these abnormalities can cause an increase in AF duration (Kistler et al., 2006). Furthermore, Lau et al. (2010b) demonstrated that hypertensive sheep showed higher

blood pressure, enlarged LA, reduced LA ejection fraction, uniformly higher mean effective refractory period, slower mean conduction velocity, higher conduction heterogeneity index, greater AF inducibility, and increased AF duration when compare with normal sheep. Another study by Lau et al. (2010a) also showed conduction abnormalities and AF caused by atrial remodelling in a sheep model of chronic hypertension.

1.7.6 Mechanical stretch regulates the arrhythmogenic activity of PVs

Stretch can cause an increase in ectopic activity measured from the PVs, which may relate to AF (Seol et al., 2011). Chang et al. (2007) demonstrated that stretch induces spontaneous activity, and the firing rate increases force dependently, in rabbit PV tissue preparations. In the same study, stretch was shown to decrease the amplitude and duration of action potentials; however, it increased membrane diastolic potential. This study also showed stretch induces EADs and DADs in the rabbit PVs. Another study by Seol et al. (2008) showed that membrane stretch induced currents in single isolated rabbit PVs by hypo-osmotic swelling and mechanical stretching. The hypo-osmotic swelling can activate swelling-activated Cl^- current ($I_{NS,swell}$). Thus, the atrial dilation may be a risk factor for the development of AF (Schotten et al., 2003, Seol et al., 2008). This study also showed that mechanical stretch by axial lengthening of PV cardiomyocytes with two electrodes activates stretch-induced currents ($I_{NSC,\ stretch}$), opening SAC_{NS} channels with higher permeability to K^+ than Na^+.

A recent study by Hamaguchi et al. (2016) also demonstrated mechanical stretch-induced electrical activity changes in guinea pig PV myocardium using microelectrode recordings. This study showed that stretch increases firing rate and the slope of phase 4 depolarisation; however, this study reported no effect on APD caused by stretch.

1.7.7 Stretch activated channel modulators

1.7.7.1 Gadolinium

Stretch-induced AF is blocked by the stretch-activated channel blocker; gadolinium (White, 2006, Nishida et al., 2010). Gadolinium was first discovered to inhibit SACs by Yang and Sachs (1989) in *Xenopus oocytes.* It has been widely used as a potent SAC blocker in a wide range of tissues including rat atrial myocytes (Tavi et al., 1996), rabbit atria (Bode et al., 2000), canine ventricles (Hansen et al., 1991), rat ventricles (Zeng et al., 2000), rabbit PVs (Chang et al., 2007, Seol et al., 2008), and guinea pig PVs (Hamaguchi et al., 2016). In cardiac muscle cells, gadolinium has been used for selective inhibition of SAC_{NS} and prevention of stretch-induced ectopic activity in cardiac muscle cells in the concentration range of 10-30 μM (Ruknudin et al., 1993, Hu and Sachs, 1997).

Using gadolinium as a SAC blocker may be useful for investigating stretch induced arrhythmias by inhibiting the activation of SACs (White, 2011). A previous study in the isolated rat atrium showed that gadolinium at 80 μM inhibited the stretch-induced changes in action potential parameters e.g. action potential amplitude, APD_{50}, and

APD_{90}. Moreover, the same study showed gadolinium suppresses atrial stretch-induced DADs and force contraction during increasing intra-atrial pressure (Tavi et al., 1996).

Another study in rat atrial myocytes by Zhang et al. (2000) demonstrated that gadolinium inhibits stretch activated currents in a concentration dependent manner (20 μM–1 mM) with an IC_{50} value of 46.2 μM. In the rabbit atria studies have shown spontaneous AF after increasing intra-atrial pressure, which increases the vulnerability to AF. Gadolinium decreases the duration of induced AF in rabbit hearts, suggesting that gadolinium reduces the vulnerability to AF caused by acute atrial dilatation (Bode et al., 2000). Another study in canine hearts has shown that gadolinium at concentrations of 1,3 and 10 μM significantly inhibited stretch-induced arrhythmias during left ventricular dilatation in a concentration dependent manner (Hansen et al., 1991). In isolated rat ventricular myocytes, longitudinal stretch has been shown to increase APD and depolarise the RMP; changes which were suppressed by gadolinium at a concentration of 100 μM (Zeng et al., 2000).

The pharmacological effects of gadolinium have also been examined in the PVs. Chang et al. (2007) demonstrated that stretch (100 and 300 mg) force dependently increased the incidence of spontaneous activity, firing rates of spontaneous activity, and incidence of EADs in the rabbit PV. The same study also showed that gadolinium (1, 3 and 10 μM) significantly decreased the incidence and firing rate of spontaneous activity in the PV cardiomyocytes. Hamaguchi et al. (2016) also showed that mechanical stretch increased the spontaneous automaticity of the guinea pig PV myocardium through the activation of SACs, which leads to phase 4 depolarisation; changes which were inhibited by gadolinium. Moreover, a study of stretch-activated

currents by Seol et al. (2008) showed that swelling induced stretch-activated nonselective cationic currents and Cl^- currents ($I_{NSC, swell}$ and $I_{Cl\ swell}$). In addition, axial mechanical stretching induced stretch-activated nonselective cationic currents ($I_{NSC, stretch.}$). Both $I_{NSC, swell}$ and $I_{NSC, stretch}$ were inhibited by gadolinium (100μM). Overall these findings in the PVs suggest that stretch-induced activation of SACs is suppressed by gadolinium; a SAC blocker, decreasing the genesis of AF by reducing the arrhythmogenic activity of the ectopic source (Chang et al., 2007, Seol et al., 2008, Seol et al., 2011, Hamaguchi et al., 2016).

Mechanical stretch can increase the amplitude of Ca^{2+} transients via the activation of SACs, LTCC, and NCX currents; as reviewed by Youm et al. (2006). Therefore, in addition to inhibiting activation of SACs, gadolinium has also been found to block I_{CaL} (Lacampagne et al., 1994) and NCX currents (Zhang and Hancox, 2000) in isolated ventricular myocytes of the guinea pig. (Lacampagne et al. (1994)) reported that gadolinium is a potent Ca^{2+} channel blocker that inhibits I_{CaL} in a dose-dependent manner with half-maximal effective concentration (EC_{50}) of 1.4 μM and complete inhibition at 10 μM. Moreover, another study in guinea pig showed that gadolinium inhibits both outward and inward NCX currents in isolated ventricular myocytes in a dose-dependent manner; with a half-maximal inhibition concentration (IC_{50}) of 30 ± 4.0 μM (Zhang and Hancox, 2000). These studies may suggest that the pharmacological effects of gadolinium are complex, potentially involving SACs, LTCC, and NCX.

1.7.7.2 Streptomycin

Streptomycin sulphate is another agent used to block mechanosensitive ion channels (Hamill and McBride, 1996, White, 2011). Streptomycin has been used to block SACs in a variety of tissues; e.g. rabbit ventricles (Eckardt et al., 2000, Dhein et al., 2014), guinea pig ventricles (Gannier et al., 1994, Belus and White, 2003, Iribe and Kohl, 2008), rat ventricles (Salmon et al., 1997), rabbit PVs (Chang et al., 2007, Seol et al., 2008), and guinea pig PVs (Hamaguchi et al., 2016). Streptomycin has been reported to block SACs in a range of concentrations ranging from 40-400 μM (Ward and Allen, 2010). Salmon et al. (1997) demonstrated that arrhythmias in rat hearts were induced by an increase of ventricular wall stress. Perfusion with streptomycin 200 μM caused a significant reduction in wall-stress-induced arrhythmias. A study in guinea pig also showed that stretch induced increases in resting Ca^{2+} in single ventricular myocytes, which were rapidly reversed by the effects of streptomycin (40 μM) (Gannier et al., 1994). Moreover, a study in rabbit showed that the application of streptomycin (200 μM) inhibits the number of ectopic beats during acute dilatation by balloon filling in the left ventricle (Eckardt et al., 2000). Another study in rabbit hearts showed that ventricular arrhythmias induced by inflating the left ventricular pressure balloon were blocked by streptomycin (100 μM) (Dhein et al., 2014)

In rabbit PV cardiomyocytes, streptomycin (10 and 40 μM) decreased the incidence of spontaneous activity under a 300-mg stretch while also decreasing action potential amplitude and prolonging APD (Chang et al., 2007). Another study in guinea pig PVs has shown that acute mechanical stretch increases the automaticity of PV cardiomyocytes through opening of SACs, leading to triggering of AF, which is

decreased by streptomycin (400 μM) (Hamaguchi et al., 2016). Furthermore, Seol et al. (2008) reported streptomycin (400 μM) blocks $I_{NSC,\ stretch}$ mechanical stretch-induced currents; however, streptomycin did not block swelling induced $I_{NSC,\ swell}$ in cardiomyocytes isolated from rabbit PV. Streptomycin has diverse biological effects, and this research suggests that it may play a role in attenuating electrophysiological changes induced by acute stretch, highlighting its anti-arrhythmia effects via SACs.

1.7.7.3 GsMTx4, a Peptide Blocker of SACs

It has been shown that GsMTx-4, a small peptide isolated from the venom of tarantula spider *Grammostola spatulata,* can be used to block mechanosensitive ion channels in cell membranes (Suchyna et al., 2000, Bode et al., 2001). Suchyna et al. (2000) demonstrated that GsMTx-4 inhibits SACs in astrocytes and ventricular cells from a rabbit dilated cardiomyopathy model. Bode et al. (2001) reported that GsMTx-4 (0.17 μM) suppresses the incidence and duration of AF during volume overload-dependency pacing-induced AF in isolated rabbit hearts. Moreover, GsMTx-4 (10 μM) significantly decreased the slow force response during stretch in the mouse left ventricular trabecular muscle (Ward et al., 2008). GsMTx-4 has been shown to inhibit the mechanical activation of TRPC1 and TRPC6, which are expressed in mouse ventricle (Ward et al., 2008) and in the cardiomyocytes of rat ventricles and atria (Huang et al., 2009). In addition, Spassova et al. (2006) demonstrated that TRPC6 is activated by hypo-osmolarity and direct membrane stretch, and that this stretch response is suppressed by the application of GsMTx-4 toxin. Preliminary in-vivo experiments have shown that injection of GsMTx4 into mice (at 4 times the K_d of

mechanosensitive channels in patch clamp) produces no behavioural change except for reduced water consumption over 24 hours, perhaps by acting on the thirst centre of the hypothalamus; as reviewed by Bowman et al. (2007). Therefore, GsMTx-4: spider-venom peptides can be useful for studying mechanosensitive channels with a view towards developing as a new antiarrhythmic drug.

Since autonomic nervous system activation and structural remodelling are thought to play a key role in the generation of arrhythmic activity in cardiomyocytes, this study hypothesised that adrenergic agonist and mechanical stretch could contribute to PV ectopic activity.

1.8 Aims

Animal and human histological studies on the junction between the LA and PV have shown the presence of myocardial sleeves, which extend from the LA into the PV and have been reported to influence arrhythmogenesis (Nathan and Eliakim, 1966, Nathan and Gloobe, 1970). Haissaguerre et al. (1998) demonstrated that PVs are an important source of ectopic beats, initiating frequent paroxysms of AF. Moreover, Masani (1986) showed that node-like cells are present in the myocardial sleeves of the rat PVs, which are similar in structure to SAN cells, may have potential pacemaking activity and generate ectopic activity in the PVs. Spontaneous electrical activity has been demonstrated in isolated PVs of guinea pig, which was enhanced by the application of NA (Cheung, 1981a).

Pathophysiological changes in the PVs are likely to be the result of autonomic nervous system responses; e.g. adrenergic stimulation, which may lead to automatic electrical activity in cardiac muscle in the PV (Doisne et al., 2009). Moreover, the cause of AF from structural alteration of myocardial sleeves such as stretching and remodelling of cardiac muscle tissue results in tissue damage, which may generate abnormal electrophysiological activity in cardiac cells (Chard and Tabrizchi, 2009). Therefore, this is thought to be an important factor associated with AF.

The aims of this study are to histologically evaluate and compare the arrangement of cardiomyocytes in the rat LA and PV. Moreover, this study investigates nodal cells in SAN in RA compared with the PV and the expression of HCN4 in the rat SAN and PV. In order to further understand, the role of adrenergic receptors in PVs, adrenergic stimulation (NA) was used to generate of ectopic activity in the rat PV. In addition, experiments examined a number of pharmacological agents; prazosin (α-adrenergic blockers), propranolol (β-adrenergic blockers), carbachol (cholinergic agonist) and verapamil (Ca^{2+} channel blocker) on the generation of NA-induced ectopic activity in the rat PV preparations. Lastly, the role of stretch, which changes the electrical activity of the PVs potentially leading to the genesis of AF was investigated. Furthermore, this study examines the effect of NA on stretch-induce ectopic action potential activity. These experiments were designed to examine how the electrical characteristics of PV cardiomyocytes are affected by pharmacological agents. Gadolinium (SAC blocker), ORM-10103 (NCX inhibitor), verapamil (Ca^{2+} channel blocker), prazosin (α-adrenergic blocker), and propranolol (β-adrenergic blocker) were investigated under the combination of stretch and adrenergic stimulation.

Chapter 2. Morphological comparison of cardiomyocytes in the rat pulmonary vein and atria

2.1 Introduction

2.1.1 The PV muscular sleeve

Nathan and Eliakim (1966) demonstrated the presence of myocardial sleeves extending from the LA into the PVs with a length of between 13-25 mm in humans. The superior PV are longer (left, 18 mm, right, 13 mm) and have better developed myocardial sleeves than the inferior PV (left, 10 mm, right, 8 mm). The histological studies by Ho et al. (2001) showed a thin endothelium, a media of smooth muscle, and a thick outer fibrous adventitial of the PV in the human. The muscular sleeve is thickest at the proximal end of the veins (1-1.5 mm) and it then gradually tapers distally. The sleeve is thickest at the inferior wall of the superior PVs and at the superior wall of the inferior PVs, although significant variations can be observed in individual PVs (Calkins et al., 2008).

Haissaguerre et al. (1998) demonstrated that the PVs are an important source of ectopic activity for the initiation of AF in the patients with paroxysmal AF (PAF). The myocardial sleeves within PVs specifically have been identified as a source of the ectopic beats that initiate AF (Chen et al., 1999, Waktare et al., 2001, Mueller-Hoecker et al., 2008). The myocardial sleeve is located on the adventitial side of the PV, separated from the smooth muscle layer by fibro-fatty tissue in human PVs (Saito et al., 2000, Moubarak et al., 2000, Steiner et al., 2006, Mueller-Hoecker et al., 2008). Myocardial cells located between the media and adventitial layers in the human PVs are similar to striated atrial myocytes in the myocardium, as seen in Figure 2-1. (Nathan and Eliakim, 1966, Ehrlich et al., 2003). The media was thin, consisting of

fibrous tissue, elastic tissue, and smooth muscle cells (Hocini et al., 2002, Sánchez-Quintana et al., 2012).

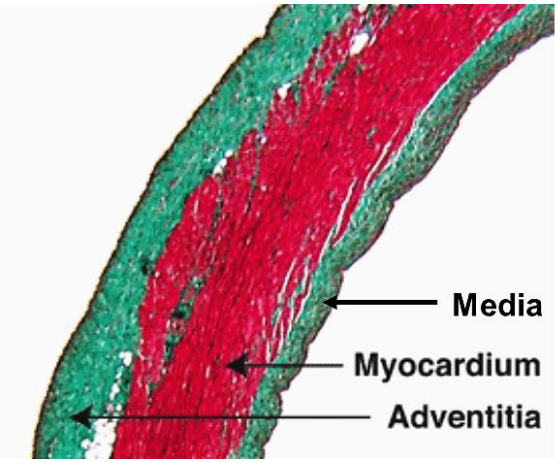

Figure 2-1 An example of myocardial sleeves from pulmonary vein section using Masson's trichrome staining. This section shows that the myocardial sleeves are the thickest layer, which is located between the media and adventitial layers of the PV (Adapted from Ehrlich et al. (2003).

Likewise, histological studies in canine, guinea pig, rat and mouse PVs have shown that myocardial sleeves exhibit the appearance of striated cardiac muscle, located in between the smooth muscle and adventitia layers, forming a major portion of the PV wall (Klavins, 1963, Ludatscher, 1968, Saito et al., 2000, Hocini et al., 2002, Hassink et al., 2003, Ehrlich et al., 2003, Mueller-Hoecker et al., 2008, Namekata et al., 2010, Takahara et al., 2011, Tsuneoka et al., 2012). Myocardial sleeves were found to be present in most, but not all PVs, which are found in up to 97% of PVs (Saito et al., 2000). The PV ultrastructure study by Ludatscher (1968) showed that the nucleus is round or ovoid and centrally located within the myocardium. Intercalated discs are

found at the end-to-end junctions of cardiomyocytes of the PVs (Ludatscher, 1968, Verheule et al., 2002, Kracklauer et al., 2013).

2.1.2 The atria

The LA has connections to the PVs and the left ventricle (LV). It also shares a septum with the RA and has an appendage for which the function is unknown (Ho et al., 2002). A study in humans showed that the LA wall is more uniform in thickness than the RA, which is thicker posteriorly and in the dome (Ho et al., 1999). In human LA, the superior wall is thickest (3.5-6.5 mm), while the anterior wall located behind the aorta is usually the thinnest (1.5-4.8 mm) (Ho et al., 2002, Calkins et al., 2008). Histological studies of human and rat atria have shown that the left atria wall generally consists of three layers: the outer epicardium (tunica adventitia), the middle myocardium (tunica media), and the inner endocardium (tunica intima) (Rhodin, 1975, Suckow et al., 2005, Young et al., 2013). Further histological studies have also shown that cardiomyocytes are essentially long cylindrical cells with a pattern of cross-striations, which is similar to that of skeletal muscle (Sobotta and Hammersen, 1980, Treuting and Dintzis, 2011, Young et al., 2013). The cardiac muscle cells contain one or at most two nuclei, which are located centrally within the cells (Young et al., 2013). In addition, individual cells are attached to each other end-to-end by specialised cell junctions referred to as intercalated discs (Sobotta and Hammersen, 1980, Gartner et al., 2002, Young et al., 2013).

2.1.3 Nodal cells in sinoatrial node (SAN) and node-like cells in myocardial layer of PV

The RA contains the SAN, the primary pacemaker of the heart, which can control the heart rhythm (Boyett et al., 2000). The SAN is located in the posterior wall of the RA near the SVC and appears as a translucent muscular region near the SAN artery (Boyett et al., 2000, Satoh, 2003, Klabunde, 2011). The SAN contains specific cell types including nodal cells, transitional cells, and atrial cells. Node cells or P cells are small (3-10 μm), ovoid, pale-staining and poorly striated compared with the general myocardium (James et al., 1966, Waller et al., 1993). P cells within the sinus node are thought to be the site of impulse formation (James, 1970, Waller et al., 1993, Boyett et al., 2000, Nabipour, 2012). Masani (1986) used electron microscopy to demonstrate node-like cells in the myocardial layer of rat PVs. These cells appeared individually or in small groups among the ordinary myocardium. The node-like cells are clear cells with structural characteristics similar to nodal cells in the sinus node (Masani, 1986). In some studies of normal human PVs, node-like cells were not seen in any area (Ho et al., 2001, Perez-Lugones et al., 2003); however, in PV of the patients with AF, myocardial cells with pale cytoplasm have been observed by haematoxylin and eosin staining. These pale cells were identified the presence of nodal cells by electron microscopy (Perez-Lugones et al., 2003). Chou et al. (2005) demonstrated positive Periodic acid–Schiff (PAS) staining in canine PVs. The PAS positive cells were pale cytoplasm along the endocardium of PV muscle sleeves. These cells are morphologically similar to the specialized conduction cells (P cells; the pacemaker cells of the heart) found in the PV from patients with AF (Perez-Lugones et al., 2003).

2.1.4 The expression of HCN4 in sinoatrial node

The SAN in the RA has been shown to generate pacemaker activity responsible for AF (Boyett et al., 2000). Previous studies by Ludwig et al. (1998) showed that the molecular cloning and functional expression of the gene encoding a hyperpolarisation-activated cyclic nucleotide–gated (HCN) channels that generate pacemaker current (I_f), which is essential for initiating and controlling heart rate (Scicchitano et al., 2012). HCN are tetramers, which are similar to voltage-gated potassium channels (Kv) and these channels are modulated by cyclic nucleotides; e.g. cAMP and cyclic guanosine monophosphate (cGMP) (DiFrancesco, 1993, Boyett et al., 2000, Bois et al., 2011).

There are four main HCN isoforms, named HCN1 to HCN4. Each isoform is contained by six transmembrane segments (S1-S6), voltage sensing located in S4 and pore region between S5 and S6 segments. HCN channels are permeable to sodium and potassium, and the pore region is characterized by a glycine-tyrosine-glycine (GYG) sequence, which is a specific requirement for K^+ channel selectivity (Bois et al., 2011, Scicchitano et al., 2012).

HCN1 is expressed in different areas of central nervous system and peripheral nervous system. HCN2, HCN3 and HCN4 are present in brain regions, e.g. the olfactory bulb, thalamus, and brain stem (Bois et al., 2011). In addition, the expression of HCN1, HCN2, and HCN4 has been found in the adult heart. HCN4 is the most highly expressed isoform in the SAN of humans and other mammals, followed by HCN1 then HCN2, whereas HCN2 is mainly expressed in the ventricle (Shi et al., 1999, Altomare et al., 2003, Nof et al., 2010, Scicchitano et al., 2012). However, HCN4 could not be identified in the surrounding atrial tissue in a review by Scicchitano et al. (2012). In

addition, the HCN4 isoform accounts for approximately 80% of total HCN mRNA in the rabbit SAN (Shi et al., 1999).

Previous studies have shown that HCN4 is a specific maker for SAN cells, which are responsible for the hyperpolarisation-activated current, I_f, playing an important role in the pacemaker potential of SAN, which generates electrical impulses (Scicchitano et al., 2012, Xiao et al., 2016). Immunohistochemistry techniques have since identified the HCN4 protein in the SAN from humans (Li et al., 2015, Perde et al., 2015) and other animals; e.g. mice (Liu et al., 2007, Wen and Li, 2015), rats (Yamamoto et al., 2006, Huang et al., 2016, Xiao et al., 2016) and rabbits (Altomare et al., 2003, Brioschi et al., 2009).

Furthermore, rat studies using immunolabelling for HCN4 showed that the expression of HCN4 was observed in the section of junction of SVC and RA, showing nodal cells but not in the myocardial sleeve of the PVs (Yamamoto et al., 2006). In addition, HCN4 was highly expressed in the plasma membrane of SAN but not PVs; however, a very weak HCN4 signal was detected in the atria (Xiao et al., 2016). However, in human studied showed that HCN4 positive staining was observed in PV-LA junction of patient with chronic AF (Nguyen et al., 2009).

The aims of this chapter are to histologically evaluate and compare the arrangement of cardiomyocytes in the rat LA and PV. Moreover, this study investigates nodal cells in SAN in RA compared with the PV. Following this, immunohistochemistry was used to investigate HCN4 expression in the rat SAN and PV.

2.2 Methods

2.2.1 Animals and dissection

Animals used in this study were obtained from licensed breeders and housed in the Biological Procedures Unit within the University of Strathclyde. The rats were individually housed on a 12-hr light/12-hr dark cycle with ad libitum access to food and water, maintained at an environmental temperature of 22 ± 3°C, 50-60% relative humidity. The PVs and atria were isolated from Sprague Dawley rats (weight, 250-350 g), which were sacrificed by cervical dislocation, in accordance with UK Home Office Regulations. The PVs and atria were carefully excised and placed in ice cold physiological saline solution, that had been previously gassed with 100% medical grade O_2 , made of the following composition, until used (in mM); NaCl 150, KCl 5.4, HEPES 10, glucose 10, $MgCl_2$ 1.2, and $CaCl_2$ 1.8 (pH adjusted to 7.4 with 1 M NaOH). The tissues were pinned out on a Sylgard®184 (Dow Corning Corporation, Midland, USA) coated Petri dish containing bath solution. The PVs were dissected from the left and right superior PVs and cleared of all visible connective tissue with the aid of a Nikon SMZ645 stereomicroscope (Figure 2-2).

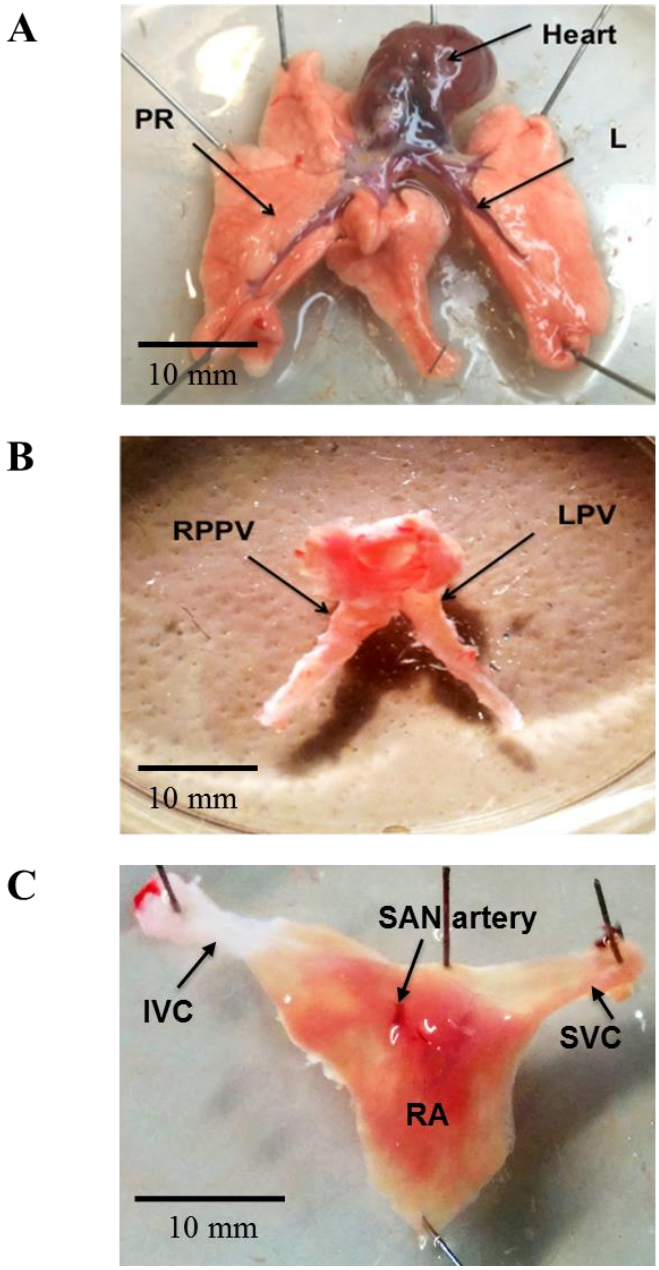

Figure 2-2 Digital photographic images of the rat heart and lungs, pulmonary veins and right atrium. (A) Dissected heart and lungs, showing the relative position of the PVs labelled as left pulmonary lobe (L) and posterior right lobe (PR). (B) Image showing the dissected PVs labelled as; right posterior pulmonary vein (RPPV) and left pulmonary vein (LPV). (C) Isolated right atrium (RA); labels indicate inferior vena cava (IVC), and superior vena cava (SVC).

2.2.2 Histology of cardiac sections

2.2.2.1 Preparation of tissue

After excision from the lung and heart, rat PVs were fixed in 10% paraformaldehyde for a minimum of 24 hours. Tissues were processed in a Citadel 1000 processor (Thermofisher, UK) in the following conditions: 3 hours in 70% ethanol (Sigma, UK); 3.5 hours 90% ethanol; 3 hours 100% ethanol; 1 hour in a mixture of 1:1 of ethanol and Histo-clear (National Diagnostics, USA), 1 hour; 3 hours in 100% Histo-Clear and 4 hours in paraffin wax. After that the tissues were then wax embedded using a Leica paraffin embedding station, model EG1140H. The wax blocks were cut in 4 μm thick sections (some transverse and longitudinal section tissue samples as seen in Figure 2-3 using a Leica RM2125RTF rotary microtome and floated onto polarised slides (Smith Scientific Limited, UK) which were washed with acetone (Sigma, UK) then 5% (v/v) (3-aminoproppyl) triethoxysaline (Sigma, UK) in acetone and then running tap water, covered and dried for 48 hours. The slides were placed in an oven set at 60-65°C for 30-40 minutes. Prior to staining, the tissue sections were rehydrated using a Varistain 24-4 autostainer (Thermo Shandon, UK) in the following conditions: 10 minutes wash in Histo-clear (3 times); 5 minutes wash in 100% ethanol (3 times); and 5 minutes wash with distilled water (1 time).

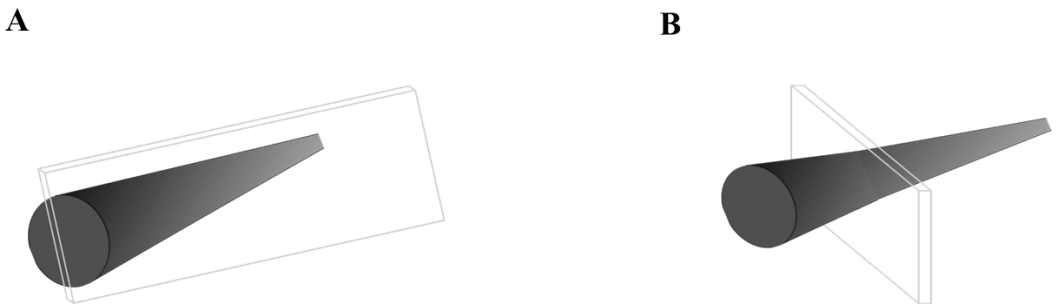

Figure 2-3 Diagram indicating the histology cutting section of the rat pulmonary vein tissue. The tissues were cut in 4 μm thick sections (A) Longitudinal section (B) transvers section .

2.2.2.2 Masson's trichrome stain

After rehydration, the tissue slides were stained with Masson's trichrome stain, which followed this procedure: staining for 10 minutes in Weigert′s iron haematoxylin solution (Sigma, UK); running for 10 minutes in warm tap water (30-32°C); staining for 15 minutes in Biebrich scarlet-acid fuchsin solution (Raymond A. Lamb, UK); quick washing in distilled water; differentiating 15 minutes in phosphomolybdic-phosphotungstic acid solution (Sigma, UK); transferring sections directly to aniline blue solution (Fisher Scientific, UK); staining for 10 minutes in aniline blue solution; rinsing 1 minute in distilled water; differentiating for 3 minutes in 1% acetic acid solution (Sigma, UK); washing in distilled water; dehydrating by a 2 second through 95% ethyl alcohol, absolute ethyl alcohol and clearing in Histo-clear. Then the slides were mounted with Histomount (Thermofisher, UK) and covered with coverslips 24x50 mm (VWR®, UK). The slides were placed on a benchtop to dry overnight before

viewing with a Leica DM LB2 microscope equipped with a Leica DFC 320 camera. Scale bars were added to the images using Image J software (version 4.8).

2.2.3 Immunohistochemistry

2.2.3.1 Antibodies

Guinea pig anti-HCN4 primary antibody and negative control antigen were obtained from Alomone Labs (Jerusalem, Israel). The secondary antibody, donkey anti-mouse Alexa 488 was obtained from Life Sciences (Invitrogen, UK).

2.2.3.2 Immunofluorescence

The rat atria and PV tissue slides were prepared and rehydrated as described in section 2.2.2.1. In the formalin fixed tissue, heat induced epitope retrieval was used in order to facilitate epitope unmasking. The slides were placed in pre-heated Tris/EDTA buffer (Sigma, UK) (10 mM Tris Base, 1.3 mM EDTA, pH 9.0) in a pressure cooker and microwaved for 10 minutes. Afterwards, the slides were washed in PBS (Sigma, UK) and tissue sections were circled with a hydrophobic barrier using a wax pen (Vector Laboratories, USA). The slides were incubated with blocking serum (10% donkey serum and 0.5 % Triton X-100 (Sigma, UK) in PBS) for decreasing non-specific antibody binding for 1 hour at room temperature. After which, the tissues were incubated with primary antibodies diluted to 1:100 with blocking serum overnight at 4^{o}C in the chamber with a moist paper towel which produced a humidifying effect. In the negative control, tissue slides were incubated with the negative control antigen,

which were diluted to 1:100 with blocking serum, overnight 4^{o}C at room temperature. After incubation, the tissues were washed with PBS five times (10 minutes each wash). The tissues were incubated with the secondary antibody, which was diluted to 1:200 with PBS, in the dark humidifying chamber at room temperature for 2.5 hours. After incubation with the secondary antibody, tissues were washed with PBS three times (10 minutes each wash). Tissues were mounted with VECTASHIELD® mounting medium with added DAPI (Vector Labs) the covered with coverslips and sealed the coverslip edges with nail varnish. The tissue slides were kept at 4^{o}C in a dark box until imaging. Presented images were taken by a TCS SP5 confocal microscope (Leica Microsystems, Mannheim, Germany). Scale bars were added with Image J software (Version 1.48).

2.3 Results

2.3.1 Histological examination of rat atria and PVs

The LA and the PVs from the rat were sectioned and Masson's trichrome stained to differentiate the musculature stained in red, connective tissue stained in blue and nuclei stained in black. The rectangular and striated appearance of the cardiomyocytes helped to differentiate these cells from smooth muscle cells, spindle-shaped cells, centrally located nucleus (Germann and Stanfield, 2005), present in the PV tissue. The cardiomyocytes-containing sleeve is separated from smooth muscle cells by connective tissue.

The longitudinal LA section cardiomyocytes are shown in Figure 2-4A, which displays a mix of uniform and non-uniform arrangements of cardiomyocytes. At high magnification (40x and 100x) it is clear that the cardiomyocytes comprise of one or two nuclei, centrally located within cardiac muscle cells and intercalated discs are found at the end-to-end junctions of cardiomyocytes in the LA (labelled with a black arrow in Figure 2-4B). Using a higher magnification (100x) view of the rat LA cardiomyocytes, the sections show the typical striated appearance of cells of cardiac origin and cardiomyocyte nuclei (Figure 2-4).

The longitudinal PV section in Figure 2-5A shows the extension of atrial myocardial cells from LA extend into the PVs to form a sleeve of cardiac muscle. All veins show the arrangement of the components of the PV wall i.e. endothelium, media, muscular sleeve and adventitia. The myocardial sleeves continuously covered the PV longitudinally, becoming gradually thinner towards the end of the PV. The magnified

PV cardiomyocytes section illustrates a mixture of uniform and non-uniform cell orientations in Figure 2-5B. The PV sections also showed that cardiac muscle cells are seen to contain nuclei, stained in black. The cardiomyocyte striations are visible at high magnification (100x) in Figure 2-5C.

The circumferential fibre arrangement on the endocardial side of the vessel wall was confirmed in transverse sections of PVs as illustrated in Figure 2-6A. The transverse section of the PV shows several layers of cardiomyocytes that encircle the lumen of the PV. These sections are displayed further in intermediate (40x) and high magnification (100x) in Figure 2-6B and Figure 2-6C, respectively.

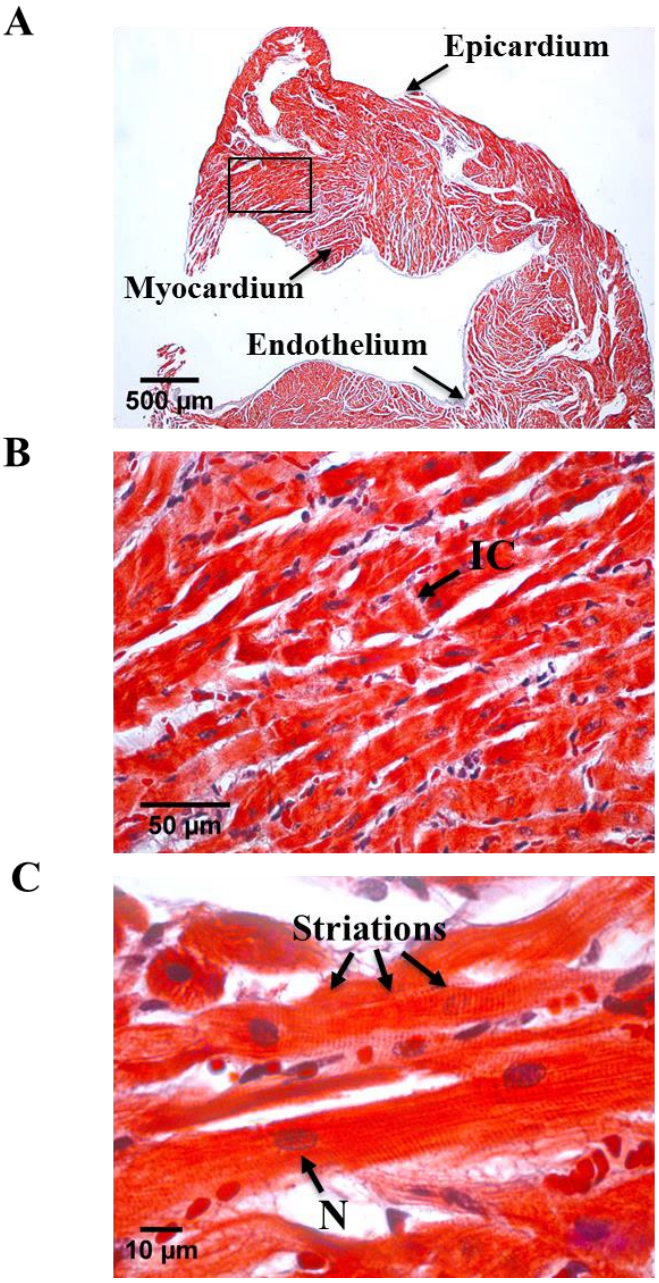

Figure 2-4 Histological evaluation of Formalin fixed rat LA. (A) Slices were sectioned longitudinally. Masson's Trichrome staining shown collagen is stained blue, muscle fibres red and nuclei black. LA section consists of endocardium, myocardium and epicardium. The boxed area in A is illustrated intermediate magnification (40x) in B and high magnification (100x) in C, respectively. Black arrow indicate intercalated discs (IC) in B. Nucleus (N) and striations illustrate in C.

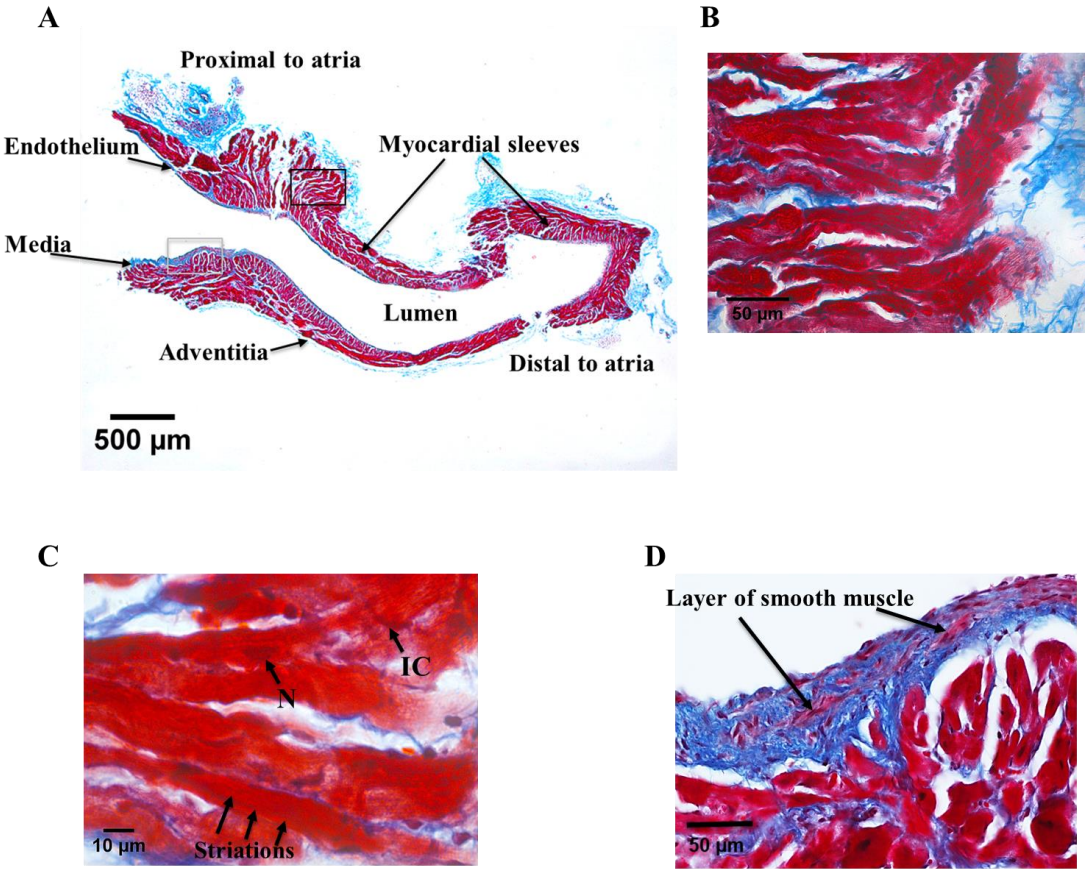

Figure 2-5 Histological evaluation of Formalin fixed rat PV longitudinal sections. **(**A) Slices were sectioned longitudinally. Myocardial sleeves were located between the media and adventitial layers of the PV. Masson's Trichrome staining shows collagen in blue, muscle fibres in red, and nuclei in black. The boxed area in A is illustrated in intermediate magnification (40x) in B and high magnification (100x) in C. Black arrows indicate intercalated discs (IC), nucleus (N) and striations illustrated in C. The white boxed area in A is illustrated intermediate magnification (40x) in D showing a media layer of smooth muscle next to endothelium.

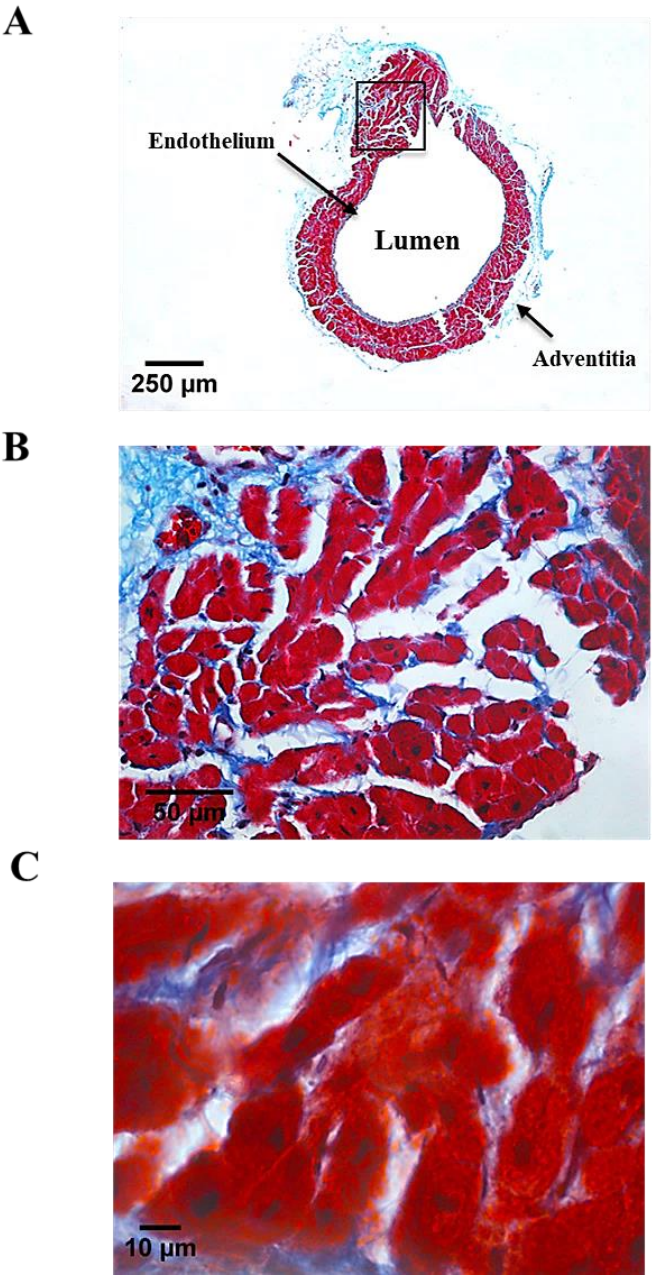

Figure 2-6 Histological evaluation of Formalin fixed rat PV transverse sections. (A) This PV section shows variations in the circumferential arrangement of the myocardial sleeves. Masson's Trichrome staining shows collagen in blue, muscle fibres in red, and nuclei in black. The boxed area in A is illustrated in intermediate magnification (40x) in B and high magnification (100x) in C, respectively.

2.3.2 Nodal cells in SAN and PVs

Sections of the RA showed the distribution of the different cell types including connective tissue, atrial muscle, the sinus node artery and nodal cells (Figure 2-7A). The SAN is shown by the black dashed line in Figure 2-7A; nodal cells were the compact groups within the SAN, which was separated from the atrial muscle (Figure 2-7C) on either side by connective tissue. The SAN cells are presented at higher magnification in Figure 2-7B, which are small, ovoid, pale staining and poorly striated compared with the cardiac muscle. Using the same Masson's Trichrome staining mentioned in section 2.3.1, nodal cells (small, ovoid, pale-staining, translucent cells) were not observed in the rat PVs in any sections.

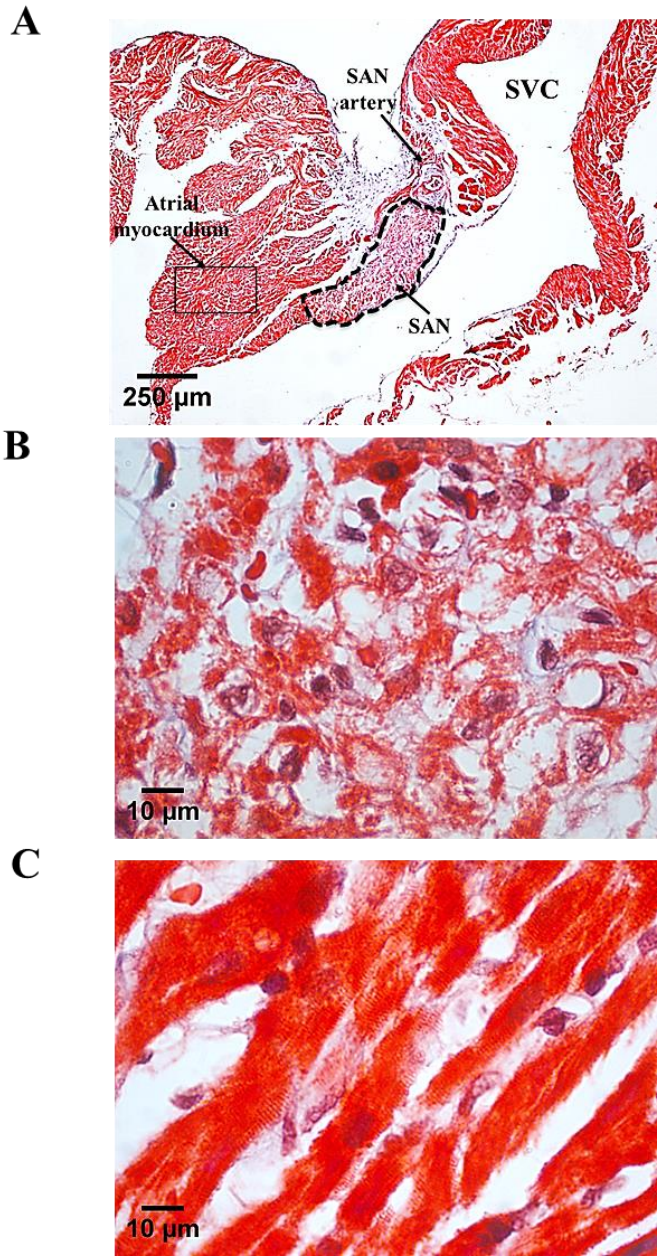

Figure 2-7 Histological evaluation of Formalin fixed rat RA. (A) This RA section shows the superior vena cava (SVC), sinoatrial node (SAN), SAN artery, atrial myocardium. Masson's Trichrome staining shows connective tissue in blue, myocytes in red, and nuclei in black. The SAN area with a dashed-line perimeter in A is presented at higher magnification (100x) in (B).The boxed area of atrial muscle in A is illustrated at higher magnification (100x) in (C).

2.3.3 Immunofluorescence staining of HCN4 in the rat SAN and PVs

This study also aimed to investigate the expression of HCN4 in the SAN and PV myocardium using immunofluorescence staining. It was observed that HCN4 is expressed in SAN cells (Figure 2-8A) but not in atrial muscle cells in the RA and PV myocardium in Figure 2-8B and Figure 2-8C, respectively. The negative control was carried out with using the appropriate antigen provided by the supplier; the resulting sample is illustrated in Figure 2-8D, which shows that HCN4 was not expressed in this section.

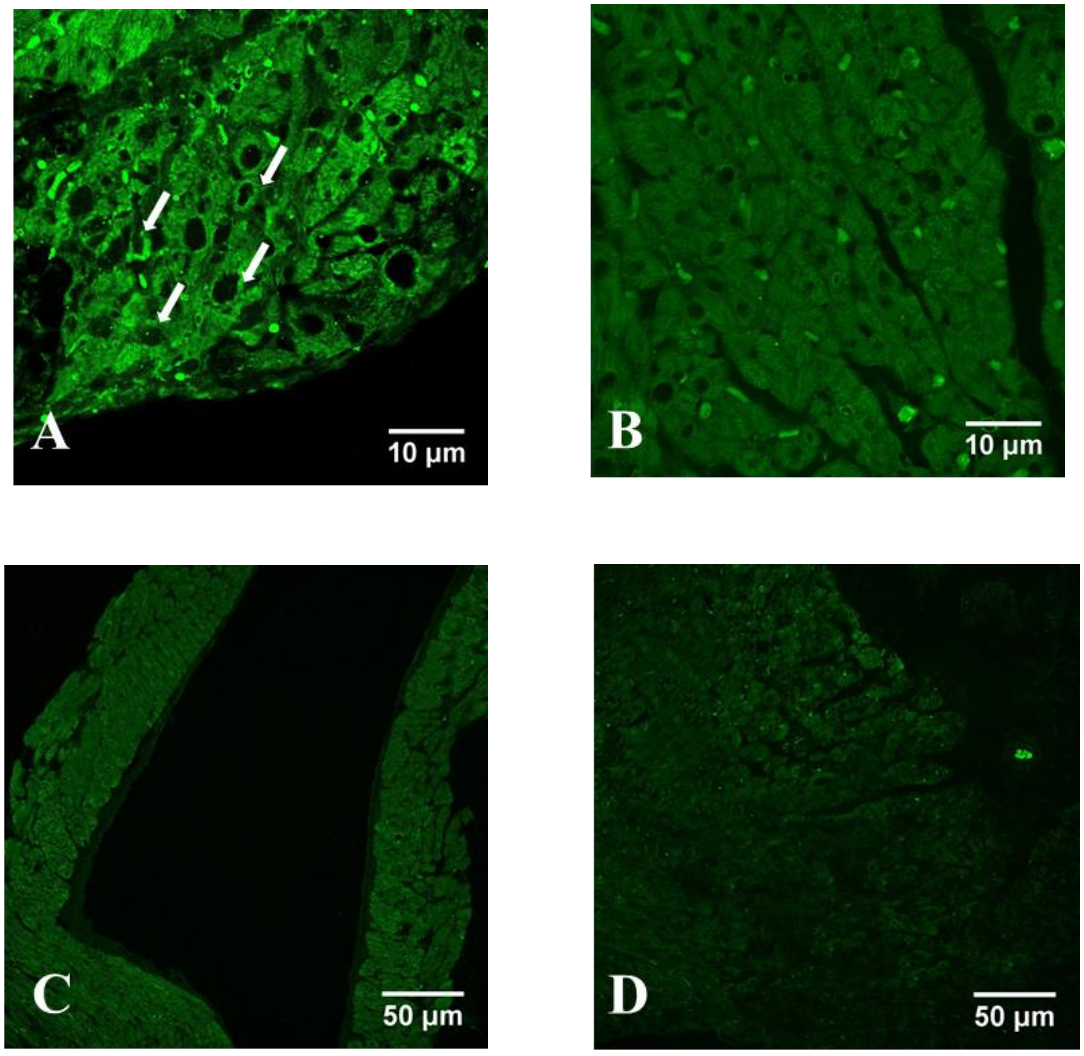

Figure 2-8 HCN4 expression in the rat atria. Immunofluorescence technique for HCN4 shown that this maker is presented in SAN (A) but not in atrial muscle cells in RA (B), and in PV (C), respectively. Arrows indicate SAN cells, and asterisks show atrial cardiomyocytes. (D) Negative control was obtained when the primary antibody was omitted from the incubation procedure.

2.4 Discussion

2.4.1 The arrangement of cardiomyocytes in LA and PV sections

This histological study has presented different sections of the rat PVs stained with Masson's trichrome staining. As noted, Masson's trichrome staining identifies collagen fibres (stained blue), nuclei (stained black) and muscle (stained red). In the longitudinal sections of the rat PV, all showed that cardiomyocytes extend from the left atrium into the intrapulmonary tissues of the vein. Moreover, transverse sections of rat PV revealed cardiomyocytes surrounding the lumen. The cardiomyocytes are located in between the media and adventitial layers in the PV, which are similar to the layers in the LA sections. In the LA and PV cardiomyocytes showed the rectangular and striated appearance of cardiac muscle fibres. The sections also revealed cardiomyocytes contain one or two nuclei, which are located in central region of the cells. Higher magnification of the rat LA cardiomyocytes showed intercalated discs, which were also seen in PV sections. This result indicates that the myocardial sleeve formed a main part at mid-layer of the of the PV tissue.

Histological studies in rodent and canine cardiac tissue have shown that the myocardial sleeve of the LA spreads into the PV at the proximal end (Chen et al., 2000, Ludatscher, 1968, Mueller-Hoecker et al., 2008). Most histological studies have shown that myocardial sleeves cover more than 80% of the area of the PVs (Saito et al., 2000, Hassink et al., 2003), however, the length and thickness of the myocardial sleeve inside of the PVs are also found to vary widely (Huang et al., 2006). Previous studies in mouse, rat, guinea pig, and human PV myocardium using Masson's trichrome staining have shown that the myocardial sleeve is observed at the mid-layer of the PV, while

vascular smooth muscle is detected on the luminal face of the PV (Calkins et al., 2008, Namekata et al., 2010, Takahara et al., 2011, Tsuneoka et al., 2012). Some studies of human PV showed the presence of myocardial muscle extensions, which spread from left atrium onto the proximal end of PVs, consisting of a complex arrangement of cardiomyocytes (Ho et al., 2001). Therefore, the results of the present histological study in rats confirm that cardiomyocytes extend from LA into the PV, which forms as myocardial sleeve, in agreement with previous findings in humans and other mammals.

2.4.2 Identification of node-cell in SAN and PV sections

The present study used Masson's trichrome staining to identify the location of SAN and SAN cells in the rat RA. The rat SAN was located between the SVC and the RA near the venous sinus. The shape of the rat SAN was ovoid or irregular in horizontal sections. The SAN was surrounded by connective tissue and cardiac atrial muscles. In addition, Masson's trichrome staining showed collagen fibres in the sinoatrial node and clearly indicated that nodal cells were positioned close to the sinus node artery. Therefore, as found by Berdajs et al. (2003) using human heart and Wen and Li (2015) using mice, the SAN artery may be used as a location marker of the SAN in the rat.

In the human heart, the SAN is located at the junction of the SVC with the RA and it is not thought to extend to the IVC (Monfredi et al., 2010). The location of the human SAN is similar in the dog, horse, and domestic cat; however, in rabbit and guinea pig, the SAN is located beneath the epicardium, near the junction between the SVC and the

RA (James, 1962, James, 1967, Bishop and Cole, 1967, Ghazi et al., 1998, Nabipour, 2012). A study of rabbit SAN cells showed that SAN cells contained large nuclei and a few myofilaments (Satoh, 2003). Moreover, the study of human and dog SAN histology showed that nodal cells are small, ovoid, pale-staining and poorly striated compare with the general cardiomyocytes (James et al., 1966).

The present study did not observe nodal cells in the Masson's trichrome staining of the rat PVs. This may be consistent with previous reports by Perez-Lugones et al. (2003), which demonstrated that nodal cells were not found in normal human PVs; however, the same study showed that the node-like cells with pale cytoplasm were only found in human PV with AF by using haematoxylin and eosin staining under light microscopy. This findings argue against the presence of node-like cells in the rat PV study using electron microscopy by Masani (1986) and in the canine study using Periodic acid-Schiff (PAS) staining by Chou et al. (2005). These studies in rat and human found clear cells with structural features similar to nodal cells SAN and the morphology of the cells were similar to the specialized conduction cells in human PVs with AF (Masani, 1986, Perez-Lugones et al., 2003).

2.4.3 Expression of HCN4 in SAN and PV sections

This present study showed expression of HCN4 in the rat SAN using an immunohistochemistry approach; however, HCN4 was not expressed in the atrial muscle of the rat. This is consistent with previous reports of the SAN in rats (Yanni et al., 2010, Ferreira et al., 2011, Huang et al., 2016) and mice (Liu et al., 2007, Wen and Li, 2015), in which immunofluorescence highlighted the expression of HCN4 in pacemaker cells of the SAN. Rabbit SAN myocytes also showed a high density of HCN4 channels (Brioschi et al., 2009). Likewise, a study from non-failing healthy hearts found HCN4 protein to be expressed in sinus node myocytes (Chandler et al., 2009). In this study, the nodal marker HCN4 was not expressed in the myocardial sleeves of the rat PVs, which is consistent with the reports by Xiao et al. (2016) where the expression of HCN4 was only found in the SAN but not in cardiomyocytes of the rat PVs. Likewise, Yamamoto et al. (2006) also demonstrated that the expression of HCN4 was observed from nodal cells in the interatrial groove and SAN; however, HCN4 was not expressed in the rat PVs. In contrast, the study in adult and aged dogs by Li et al. (2014) showed that there was a reversal in the local tissue distribution of HCN4 channel mRNA and protein, with low levels in the SAN but high levels in the LA and PVs correlated with aging. These finding may suggest that aging plays a role in HCN4 expression levels, perhaps explaining why the current study in rats (aged 8-10 weeks; i.e. young adults) did not reveal HCN4 markers in the PV or LA. This also coincides with AF incidence increasing with age in humans.

In conclusion, histological data has shown that the myocardial sleeve of the LA extends into the PVs. In the rat PVs, a mixture of cell arrangement of cardiomyocytes

with areas of non-uniformity, where cardiomyocytes were orientated in differing directions. Sections were stained with Masson's trichrome to show histology; connective tissue is stained blue, cardiac myocytes are stained red and nuclei are stained dark blue/black. This staining was successfully used to identify the SAN under light microscope, which was located in between the RA and SVC. The presence of collagenous connective tissue was found surrounding SAN cells, which is a characteristic of the SAN, thus these can be used to differentiate atrial muscle from SAN tissue. The nodal cells surround the sinus nodal artery, which may be used as the marker of the SAN. However, expression of node-like cells was not identified at any point in the myocardial sleeves of the rat PVs using Masson's trichrome staining. In further investigation of the SAN, immunohistochemical techniques were applied to detect HCN4 antibodies in both RA and PV sections. These were only expressed in nodal cells of the SAN; however, HCN4 was not expressed anywhere else in the myocardial sleeve of the rat PVs.

This study was investigated the PV section, showing myocardial sleeves extend from the LA into all the PVs. The muscular sleeve was thickest at the proximal to LA and it then gradually tapers distal to LA. However, the expression of pacemaker cells; which is generating electrical impulses of the heart were not observed in any area of the rat PV. Despite evidence that the PV may become spontaneously active in pathological states, potentially contributing to AF, the lack of HCN4 expression in this preparation may indicate the presence of a physiologically 'normal' specimen, as may be expected when using healthy rats. Therefore, further investigations may aim to actively examine tissue under a pathological condition, which may be more likely to display properties that could potentially contribute to ectopic beats and AF.

Furthermore, future studies may apply different imaging protocols using specific makers of cardiac ion channels.

Chapter 3. The generation of noradrenaline (NA) induced ectopic activity in the rat pulmonary vein

3.1 Introduction

3.1.1 Contractile function and ectopic activity in the rat PV

Cardiomyocytes from the LA extend into the PVs to form a sleeve of cardiac muscle and are thought to contribute to the generation of ectopic beats that initiate and sustain AF (Haissaguerre et al., 1998, Maupoil et al., 2007). Previous studies reported that PV morphology influences on arrhythmogenesis i.e. the superior PVs, which had longer muscular sleeves, were reported to be more arrhythmogenic than the inferior vein (Nathan and Eliakim, 1966). Autonomic nervous system activation can lead to changes of atrial electrophysiology and initiate AF by both re-entry and triggered activity, which may be caused by enhanced Ca^{2+} transient currents; as reviewed by Nattel (2005), Chen and Tan (2007). Tan et al. (2006), (2007) demonstrated the distribution of autonomic nerves at the PV-LA junction in human hearts. These reports also showed that the density of adrenergic and cholinergic nerve innervation was greatest within 5 mm of the PV-LA junctions (left and right, superior and inferior).

NA is an adrenergic receptor agonist, which stimulates both α and β adrenoceptors. (Klabunde, 2011). This produces distinct physiological responses associated with each adrenoceptor, such as increased heart rate and increased cardiac inotropy via β_1-adrenoceptor on the heart and vasoconstriction in arteries and veins through α_1-adrenoceptors (Mohrman and Heller, 2002, Klabunde, 2011).

The stimulatory β-adrenergic response is mediated via Gs-proteins, leading to the activation of adenylyl cyclase to form cAMP from ATP. Increased cAMP activates cAMP dependent PKA, resulting in PKA phosphorylating LTCC, which leads to

increased Ca^{2+} entry into the cells and subsequent SR release of Ca^{2+} in response to transmembrane Ca^{2+} entry (van der Heyden et al., 2005, Klabunde, 2011). Additionally, activation of α-adrenoceptor by NA stimulates Gq-protein coupled to PLC, which activates the formation of IP3 and DAG from PIP2. Increased IP3 in the cell stimulates Ca^{2+} release from the SR in the heart (Klabunde, 2011, Rang et al., 2014, O'Connell et al., 2014, Droual, 2015).

Previous studies by Sweeney et al. (2007) demonstrated that NA had a positive inotropic response upon the paced contractile activity in the rat PV which partly mediated by β_1-adrenoceptors. Thus, this study may involve autonomic influences which may be of significance to the generation of AF (Sweeney et al., 2007). Another study showed NA which activates both α and β adrenoceptors that induced ectopic contractions in the rat PVs (Maupoil et al., 2007). Moreover, the same study showed that the mixture of phenylephrine; α-adrenoceptor agonist and isoproterenol; β-adrenoceptor agonist induced ectopic activity while ectopic activity could not be generated by the phenylephrine or isoproterenol alone (Maupoil et al., 2007). This finding suggests that ectopic activity in the rat PVs requires activation of both α_1-and β_1-adrenoceptors (Maupoil et al., 2007).

Therefore, we may hypothesise that the generation of abnormal contractile activity may relate to the alteration of autonomic influences in the PV cardiac muscle involving both α_1-and β_1 receptors.

Previous studies have shown that temperature plays an important role in the modulation of contractile and electrophysiological activity of cardiomyocytes (Cavalié et al., 1985, Bjørnstad et al., 1993). In rabbit PV cardiomyocytes, changes from normal (38-39°C) to high (40-41°C) temperature have been shown to enhance automaticity, induce triggered activity and shorten the APD during increased temperatures (Chen et al., 2003). Another study by Bolter and Atkinson (1988) showed that an increase in temperature from 35.6 to 42.8°C induced spontaneous activity in rat SAN cells. Increasing the temperature from 34°C to 37°C stimulated the occurrence of triggered activity and generated DADs in a study of Purkinje fibres from sheep hearts (Mugelli et al., 1986). This enhanced triggered activity may be the result of a high arrhythmogenic state caused by higher temperatures. These studies certainly suggest that temperature is one of the main factors involved in the modulation of electrophysiological characteristics of myocytes in different cardiac preparations.

3.1.2 Pharmacological modulators on the contractility in the rat PV

Previous studies have shown that NA induces ectopic contractions in the rat PVs through stimulation of both α_1-and β_1-adrenoceptors as described above (Maupoil et al., 2007, Doisne et al., 2009). Prazosin is an α_1-adrenoceptor antagonist, considered selective for α_1-adrenergic receptors, which is usually used to treat high blood pressure (Rang et al., 2014). Previous studies in rat PVs showed that the ectopic contractions induced by NA were inhibited by the application of prazosin (Maupoil et al., 2007). Moreover, prazosin also decreased automatic activity induced by NA in cardiac muscle of the rat LA and PVs (Doisne et al., 2009, Okamoto et al., 2012).

Additionally, propranolol; a nonselective β-adrenoceptor antagonist is much more potent antagonist that blocks β_1- and β_2 adrenoceptors, which is widely used in the treatment or prevention of many disorders including acute myocardial infarction, hypertension and rate control in AF (Rang et al., 2014). Previous studies showed that propranolol inhibited the positive inotropic effect induced by isoproterenol, NA and adrenaline on inferior and SVC and PVs of the rats (MacLeod and Hunter, 1967). Tsuneoka et al. (2012) also showed NA-induced automaticity of the mouse PV myocardium was inhibited by propranolol. In a study using dogs, propranolol depressed the spontaneous activities induced by applying isoproterenol (Chen et al., 2000). Study of the human PV has shown that propranolol suppresses ectopic beats, which originate from patients with paroxysmal AF. (Chen et al., 1999).In the human heart studies, carbachol, an agonist of muscarinic acetylcholine receptors (mAchR), decreases in force of contraction stimulated by NA in isolated human RA (Wangemann et al., 2003). Carbachol produces dose-dependent negative inotropic responses in left atrial strips and the PVs in the presence of isoproterenol (MacLeod, 1986). In isolated left atria of rat and guinea pig studies showed that carbachol induces the negative inotropic effect and shortening of APD in LA cardiomyocytes (Ravens and Ziegler, 1980). Moreover, in guinea pig PV myocardium showed carbachol decreases the number of triggered activity in the PV preparation. In the same study, carbachol decreases the APD of the LA and PV cardiomyocytes and hyperpolarises RMP in the PV myocardium (Takahara et al., 2011).

Verapamil, a calcium channel antagonist, is a widely antidysrhythmic drug, which acts through blocking the LTCC (Rang et al., 2014). (Rang et al., 2014). The study in guinea pigs showed that verapamil produces negative inotropic effect in isolated

guinea pig RA preparations (Tanaka et al., 1996). Verapamil also inhibits the spontaneously beating induced by adrenaline in the atria of the guinea-pig (Zonta et al., 1986). Likewise, the studies in the isolated atria from rabbits, guinea pigs, and rats showed verapamil reduces the positive inotropic effect induced by isoproterenol (Sarantos-Laska et al., 1984). In guinea pig PV study showed verapamil inhibited the occurrence of triggered activity induced by a train of stimulation (Takahara et al., 2011). In rabbit study showed that verapamil reduced spontaneous activity in isolated single cardiomyocytes from the PVs (Chen et al., 2008). Chen et al. (1999) demonstrated that verapamil inhibits ectopic beats originating from PVs patients with paroxysmal AF.

Many studies have focused on pathological alterations to the electrophysiological activity in cardiomyocytes of the rat PV. There are a few studies of contractile function; however, it is unclear about the mechanisms generating focal activity in the PVs that might be controlled by adrenergic or cholinergic receptors. This study aims to investigate the role of adrenergic receptor stimulation (NA) in the genesis of ectopic activity in the rat PVs.

In addition, experiments in this chapter were examined a number of pharmacological agents; prazosin (α-adrenergic blockers), propranolol (β-adrenergic blockers), carbachol (cholinergic agonist) and verapamil (Ca^{2+} channel blocker) on the generation of NA-induced ectopic activity in the rat PV preparations.

3.2 Methods

3.2.1 Animals and dissection

The PV was isolated from the rat as described in section 2.2.1.

3.2.2 Preparation of the PVs

The PVs were dissected from left and right superior PVs and cleared of all visible connective tissue. The tissue preparations were mounted on stainless steel wire hooks in a 10 ml organ bath with a modified Krebs–Henseleit solution of the following composition (mM); NaCl 119, $NaHCO_3$ 25, KCl 4.7, KH_2PO_4 1.18, $MgSO_4$ 1.17, $CaCl_2$ 1.36 and glucose 5.5, gassed with 95% O_2 and 5% CO_2 at 37 °C. Contractions were generated by electrical field stimulation (FS: 0.1 Hz, 2ms duration, supramaximal voltage) applied via platinum electrodes connected to a Grass SSS stimulator and stimulus isolation unit (Grass Technologies, West Warwick, RI, USA).

3.2.3 Experiment protocols

A standard protocol was used in all of the experiments described in this chapter. Contractions were continuously recorded with a force–displacement transducer (Model FT03) connected to a Grass 79D EEG & Polygraph Data Recording system and a PC computer running Chart V5.0.7 software (Version 5.0.7, Dr. John Dempster, University of Strathclyde). The baseline tension of PVs was adjusted so that the maximal contraction amplitude evoked by electrical field stimulation under basal

conditions was 90% of the maximum, and if necessary this was readjusted during the experiment. Experiments began following at least 1 hour of equilibration and after ensuring that the FS contractures were stable within that time frame (Figure 3-1).

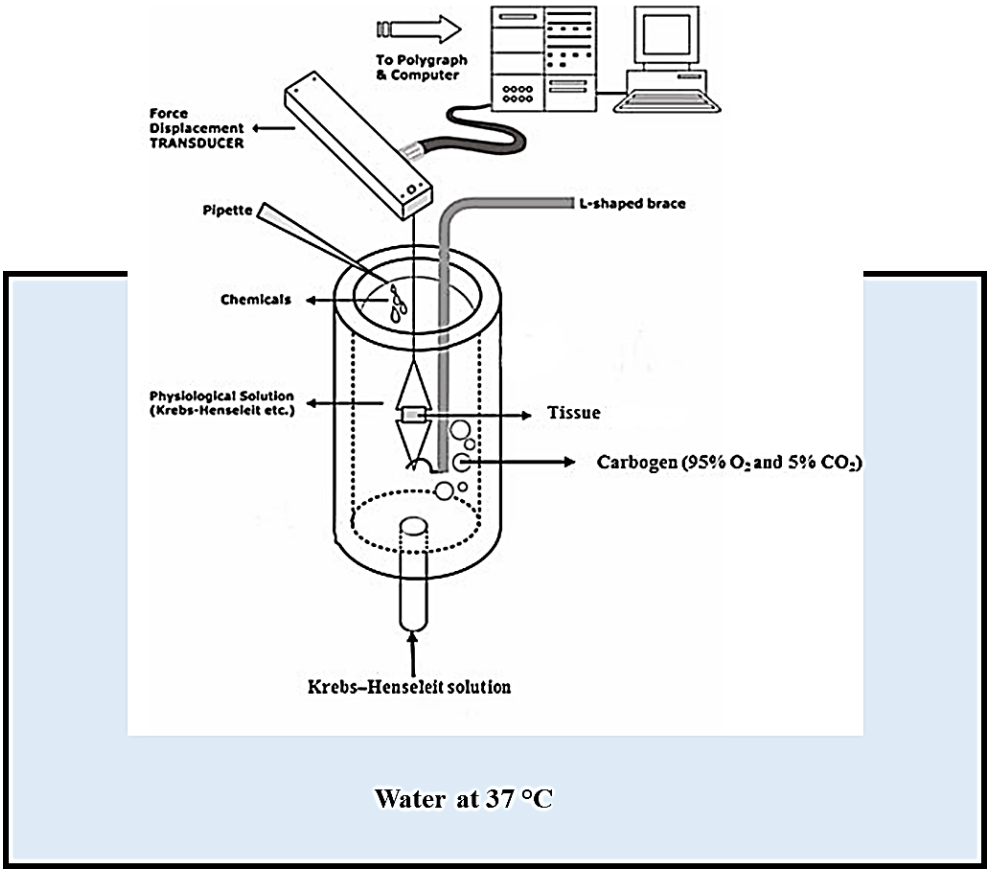

Figure 3-1 The isolated- tissue organ bath set up. The organ bath with the data acquisition equipment is shown above. In the insert, the PV is electrically stimulated when a voltage is applied via platinum electrodes, connected to a Grass SSS stimulator. The tissue is mounted in Krebs-Henseleit solution (KHS), with continuous carbogen gas being continuously supplied via a tube submerged in the KHS (Adapted from Yildiz et al. (2013)).

3.2.3.1 Noradrenaline (NA) evokes spontaneous ectopic activity in the PVs

This adrenergic receptor agonist has been shown to stimulate the electrical and contractile activity of the rat PVs (MacLeod and Hunter, 1967). NA, which stimulates α and β adrenoceptors can induce ectopic activity in the rat PVs (Maupoil et al., 2007). Testing the effect of NA on the activity of the PVs was conducted by adding non-cumulative concentrations of NA 10 µM, 30 µM and 100 µM, respectively into the organ bath for 30 minutes and then washing out (10 mL/min) with drug free physiological salt solution for 5 minutes prior to adding the subsequent concentration.

3.2.3.2 Temperature modulates the ectopic contractions in the PV induced by NA

The effect of cooling on ectopic contractions of the rat PVs was examined. In control conditions, PVs were recorded while the tissue was incubated in modified Krebs–Henseleit solution in the organ bath at 37 °C for 1 hour. Ectopic contractions were induced following application of NA 100 µM at 37 °C. Thereafter, temperature was decreased to hypothermic condition from 37 °C to 25 °C, the laboratory room temperature (Pharmacopoeia, 2016), and contractions of the rat PVs were recorded for 30 minutes to investigate the ectopic activity in rat PVs.

3.2.3.3 The effect of α and β adrenoceptor antagonist on ectopic contractions in the rat PV induced by NA

The effect of prazosin (α_1-blocker) and propranolol (non-selective β-blocker) on ectopic contractions of the rat PVs were investigated in separate experiments. After

obtaining control recordings, NA (100 µM) was added to the organ bath after tissues were stabilized for 1 hour in the modified Krebs–Henseleit solution and changes recorded for a 30 min period. Then prazosin/propranolol 1 µM was added into the bath, the recording continued for 10 minutes in the presence of the drug.

3.2.3.4 The effect of a cholinergic agonist on ectopic contractions in the PV induced by NA

The effect of carbachol (cholinergic agonist) was also examined. Control PVs were incubated in the modified Krebs–Henseleit solution for 1 hour then NA (100 µM) was added and changes recorded over a 30-minute period. Carbachol 1 µM and 10 µM were then applied into the bath following the addition of NA and the contractions were recorded for 10 minutes.

3.2.3.5 The effect of an increase in extracellular Ca^{2+} on the generation of NA induced ectopic contractions of rat PVs.

To test the effect of increasing extracellular Ca^{2+} in the rat PVs, NA (30µM) triggered ectopic contractions in the rat PVs was used as the control group The effect of increasing the extracellular Ca^{2+} concentration ($CaCl_2$ 1.86 mM and $CaCl_2$ 2.36 mM) on the generation of NA induced ectopic contractions of rat PVs was studied and the contractions were recorded for 10 minutes at each concentration of $CaCl_2$.

3.2.3.6 The effect of a calcium-channel blocker on ectopic contractions in the PV induced by NA

To record the effect of verapamil, a Ca^{2+} channel blocker, PVs were incubated in the modified Krebs–Henseleit solution for stabilizing for 1 hour. NA100 µM was then added into the bath and PV activity recorded for 30 minutes. Verapamil at concentrations of 0.01 µM, 0.1 µM and 1 µM were applied into the bath following the addition of NA and the contractions were recorded for 10 minutes at each concentration of verapamil.

3.2.3.7 Data analysis

Data was recorded using Chart software version 5.1.0 (Dr. John Dempster, University of Strathclyde) and converted into a text file using same software to enable analysis the contractions. The text file was opened with Chart5 software (AD Instruments, Dunedin, New Zealand) then analysis of evoked and ectopic contractions was performed. To calculate the ectopic contractions induced by NA, the height of ectopic contractions were detected using event markers in each ectopic event. The Chart5 software using cyclic measurements was used to analyse the amplitude, frequency and duration of ectopic contractions; with the average of these parameters in each ectopic event taken as the final measurement for each sample. Graphs were produced using Graph Prism (version 6.01, Graph PAD Software Inc., San Diego, CA, USA). Data are reported as mean ± sem., with values obtained from n different preparations. Prism was used to carry the differences between groups determined by using one-way

analysis of variance followed by Tukey's HSD Post-hoc test and $P<0.05$ was considered to be statistically significant.

3.3 Results

3.3.1 NA induced spontaneous ectopic activity in the rat PVs

In control preparations, there was no evidence of spontaneously generated ectopic contractions in the rat PV in the absence of NA. The application of NA at concentration 10 µM, 30 µM and 100 µM increased the amplitude of contraction in rat PVs by 42.0 ± 3.0 %, 46.9 ± 9.8 %, and 49.0 ± 3.3 % respectively.

The data shows that NA at concentration 10 µM, 30 µM and 100 µM generated ectopic contractions in rat PVs (Figure 3-2). This consisted of individual contractions that occurred out with the stimulus cycle that then developed into clearly defined bursts of contractions (Figure 3-3). NA at concentrations of 10 µM, 30 µM and 100 µM first induced ectopic event at 11.5 ± 0.7, 10.0 ± 1.8 and 5.8 ± 1.1 minutes, respectively. NA 100 µM was also significantly different from NA 10 µM ($n=6$, $p<0.05$) but not different from NA 30 µM in the time to first ectopic event (Figure 3-4A).

Moreover, NA increased the number of ectopic events in a dose-dependent manner (NA 10 µM 15.6 ± 3.4, NA 30 µM 24.5 ± 7.1 and NA 100 µM 36.5 ± 4.3 ectopic events within 30 minutes, respectively (Figure 3-4B). NA 100 µM was significantly different from NA 10 µM ($n=6$, $p<0.05$) in the amount of ectopic events elicited, but was not significantly different from NA 30 µM ($n=6$). There were no statistically significant differences between ectopic events in tissues treated with NA 10 µM and NA 30 µM.

However, NA at 10 µM, 30 µM and 100 µM did not produce statistically significant differences in frequency of ectopic activity and the duration of the ectopic contraction

(n=6); as shown in Figure 3-4D-E. In addition, this study shows that the amplitude of ectopic contractions is not significantly different following the addition of each concentration of NA (n=6, Figure 3-4C).

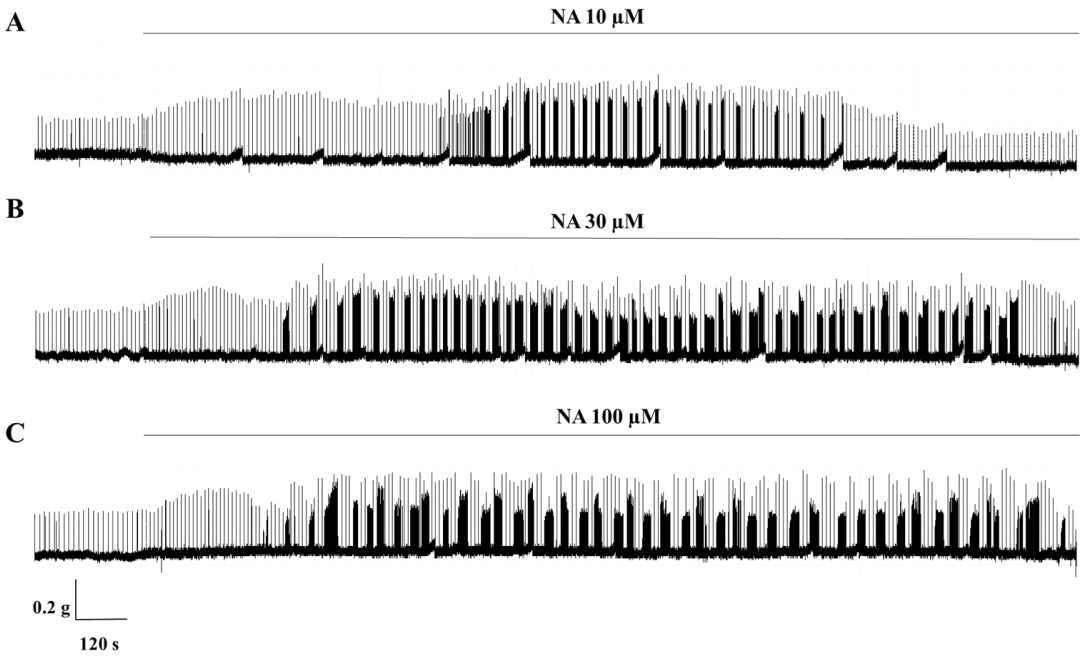

Figure 3-2 Representative traces showing the NA-induced ectopic contractions in the rat PV. NA 10 µM (A), NA 30 µM(B) and NA 100µM (C) indicated by the bar above the traces. Each preparation was stimulated at 0.1 Hz 2 ms and a supramaximal voltage in order to generate electrically evoked contractures at 37°C.

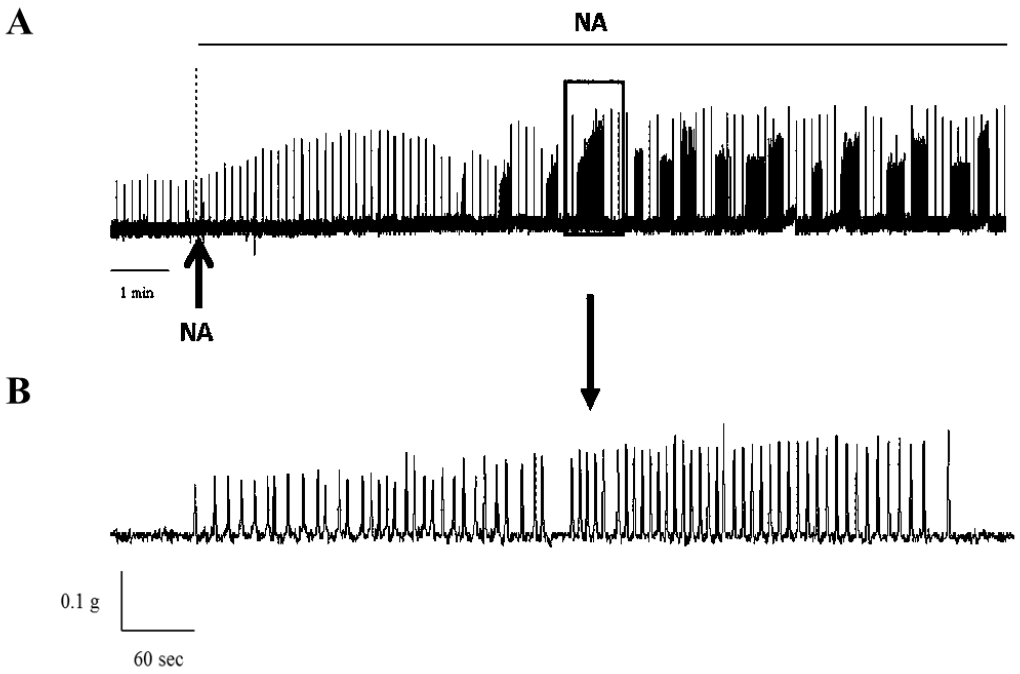

Figure 3-3 An example of NA-induced ectopic contractions in the rat PV. (A) The ectopic contraction consisted of the isolated individual contractions (B) The boxed area in A illustrates that ectopic contractions consist of isolated individual contractions.

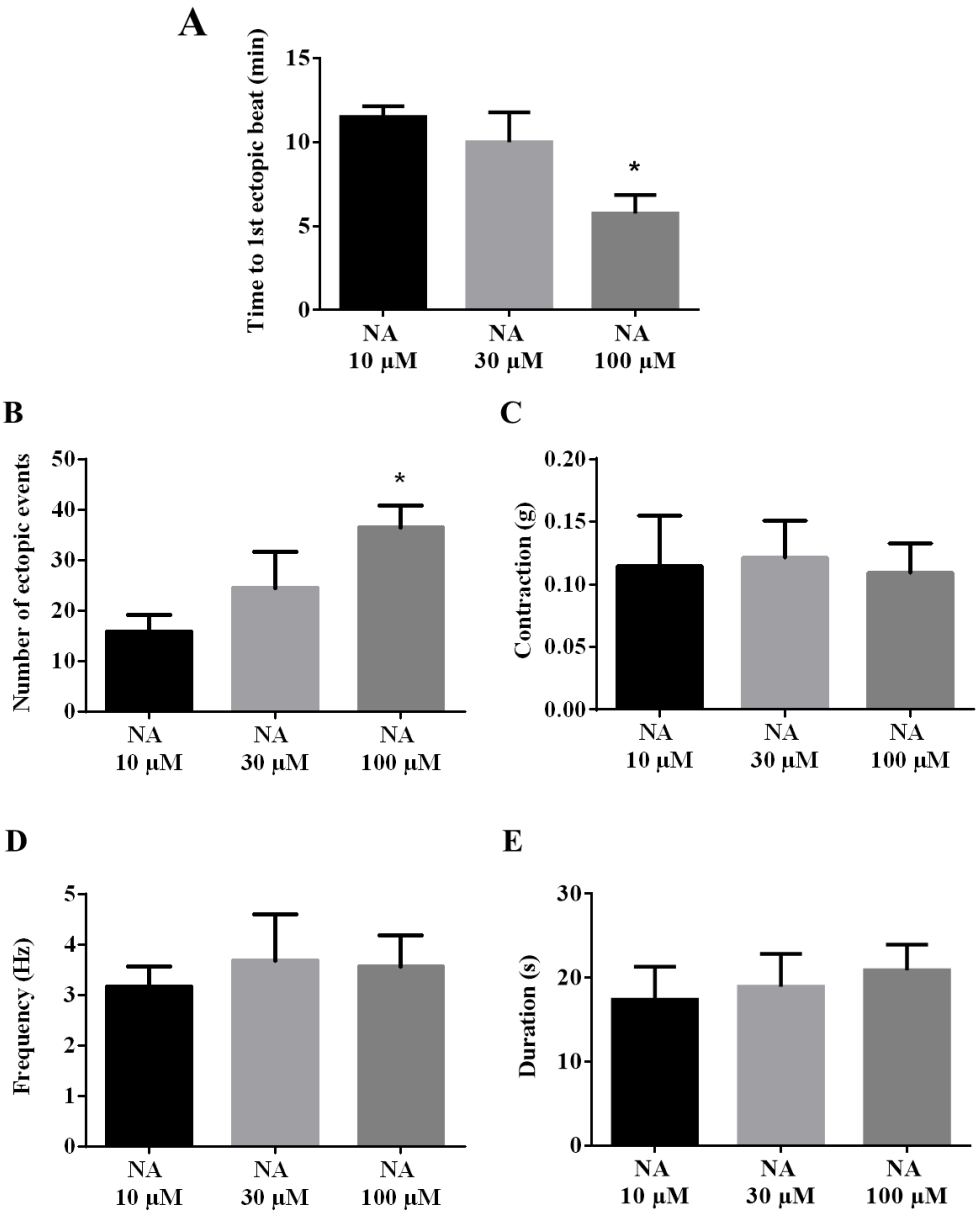

Figure 3-4 Analysis of the ectopic beats, recorded following addition of NA in the rat PVs (A) Time to first ectopic beat. (B) Number of ectopic events (C) Amplitude of ectopic contraction (D) Contraction frequency. (E) Duration of ectopic activity. All data are presented as mean ± s.e.m., *$p<0.05$ vs NA 10 µM, and n=6.

3.3.2 The temperature modulates ectopic contractions in the rat PV induced by NA

Under control conditions there was no evidence of ectopic contractions in the rat PVs at 37°C in absence of NA (Figure 3-5A). Ectopic contractions were induced by applying NA 100 µM at 37°C (Figure 3-5B). In the presence of NA 100 µM, the number of ectopic events gradually decreased to zero with reducing temperature from 37°C to 25°C. (Figure 3-5C). The amplitude of ectopic contractions in the rat PV plus NA 100 µM (0.1 ± 0.006 g) was not significantly different compared with the contraction in control PVs at 37°C (0.1 ± 0.02 g) and the contraction at low temperature at 25°C (0.1 ± 0.03 g) PV preparations (Figure 3-6A).

The frequency of ectopic contractions in the presence of NA at 37°C (3.1 ± 0.6 Hz) was significantly different compared with the frequency of contractions in the control condition at 37°C (0.2 ± 0.02 Hz, n=3, $p<0.05$). However the frequency of contractions at low temperature (25°C), (0.2 ± 0.04 Hz) in presence of NA was not significantly different compared with in the control group (n=3); as shown in Figure 3-6B.

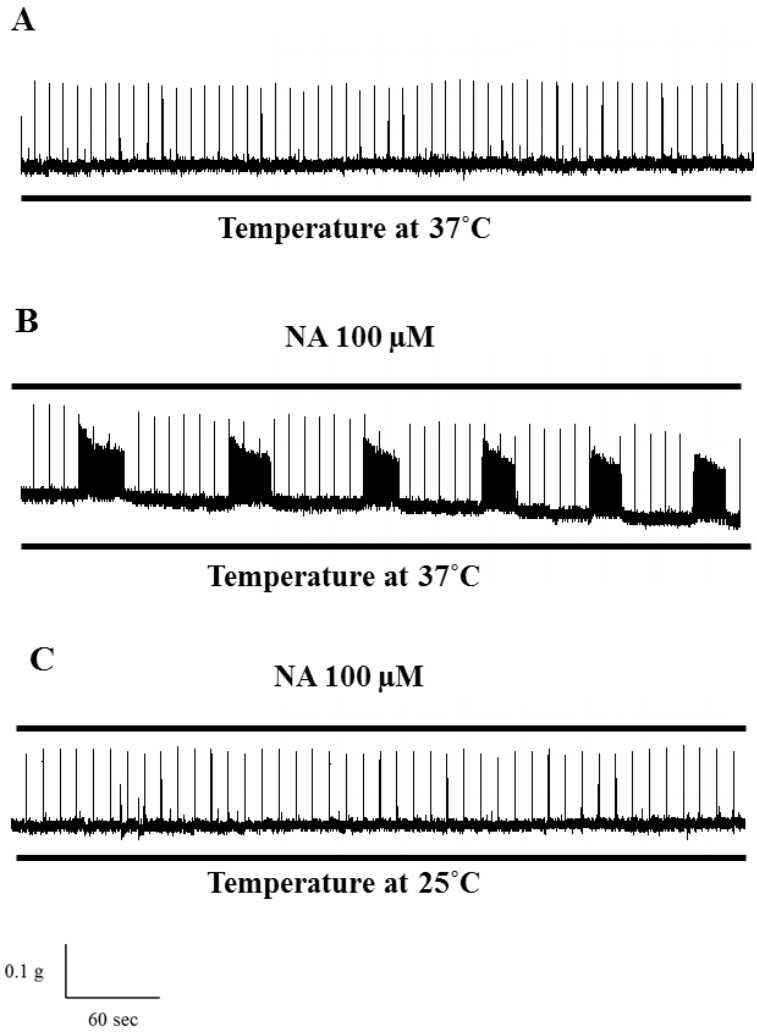

Figure 3-5 The effect of temperature on ectopic activity induced by NA in the rat PVs. (A) The PV contraction in the absence of NA at 37°C. (B) The ectopic contractions were induced by NA 100 µM in the rat PV at 37°C. (C) The PV ectopic contractions ceased after the temperature was decreased from 37°C to 25°C.

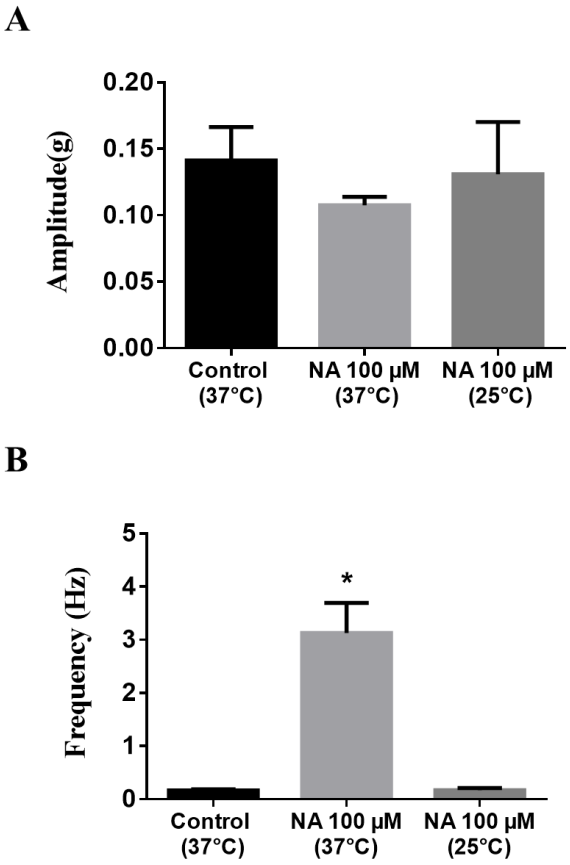

Figure 3-6 The effect of temperature on ectopic contractions induced by NA in the rat PVs at temperature 37°C and hypothermia at 25°C. (A) Amplitude of ectopic activity (B) Contraction frequency. All data are presented as mean ± s.e.m., *$p<0.05$ vs NA 10 µM, and n=3

3.3.3 The effect of α and β adrenoceptor antagonist on ectopic contractions in the PV induced by NA

In the control preparation, there was no evidence of spontaneously generated ectopic contractions in the rat PV in the absence of NA. Previous studies showed that prazosin; an α1- adrenoceptor antagonist (1 μM) inhibits ectopic activity induced by NA in the rat PVs (Maupoil et al., 2007, Doisne et al., 2009). In addition, the presence of propranolol (1 μM) decreased contractile responses in the rat LA (Doggrell, 1990). Figure 3-7A and Figure 3-7B illustrated that the number of ectopic contractions induced by NA 100 μM was significantly reduced ($n=4$, $p<0.05$) by the application of either prazosin 1 μM, from 18.0 ± 1.2 to 3.3 ± 0.9 ectopic events (Figure 3-8A), or propranolol 1 μM from 19.0 ± 3.0 to 10.8 ± 2.4 ectopic events (Figure 3-9A).

Prazosin 1 μM had no effect on the amplitude, frequency or duration of ectopic activity in the rat PVs ($n=4$, Figure 3-8B-D and Table 3-1). However, treatment with propranolol significantly decreased the frequency of ectopic activity from 3.4 ± 0.5 to 2.4 ± 0.5 Hz and the duration of ectopic activity from 18.6 ± 2.6 to 10.9 ± 2.0 seconds ($n=4$, $p<0.05$, Figure 3-9C-D). The application of propranolol 1 μM did not cause a significantly change in the amplitude of ectopic activity when compared with the NA control group (Figure 3-9B, and Table 3-2).

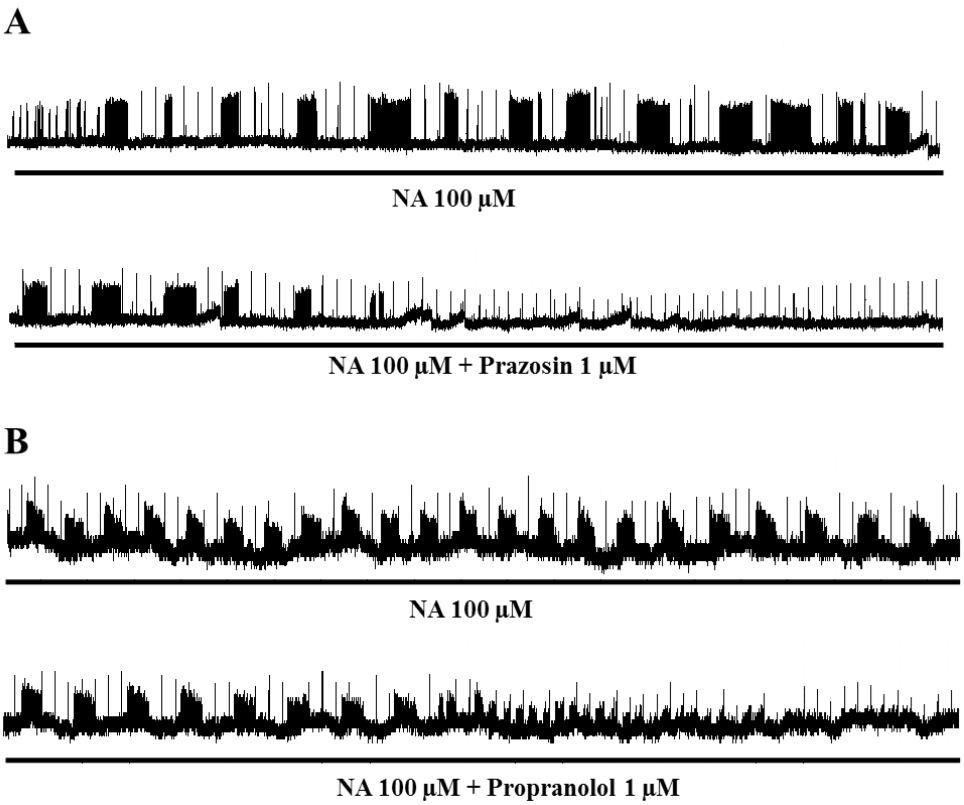

Figure 3-7 The effect of α and β adrenoceptor antagonists on ectopic contractions induced by NA. The ectopic contractions were induced by NA 100 µM in the rat PV. The PV preparation was stimulated at 0.1 Hz 2 ms and a supramaximal voltage in order to generate electrically evoked contractures at 37°C (A) Prazosin; α-adrenoceptor antagonist, (B) Propranolol; β-adrenoceptor antagonist.

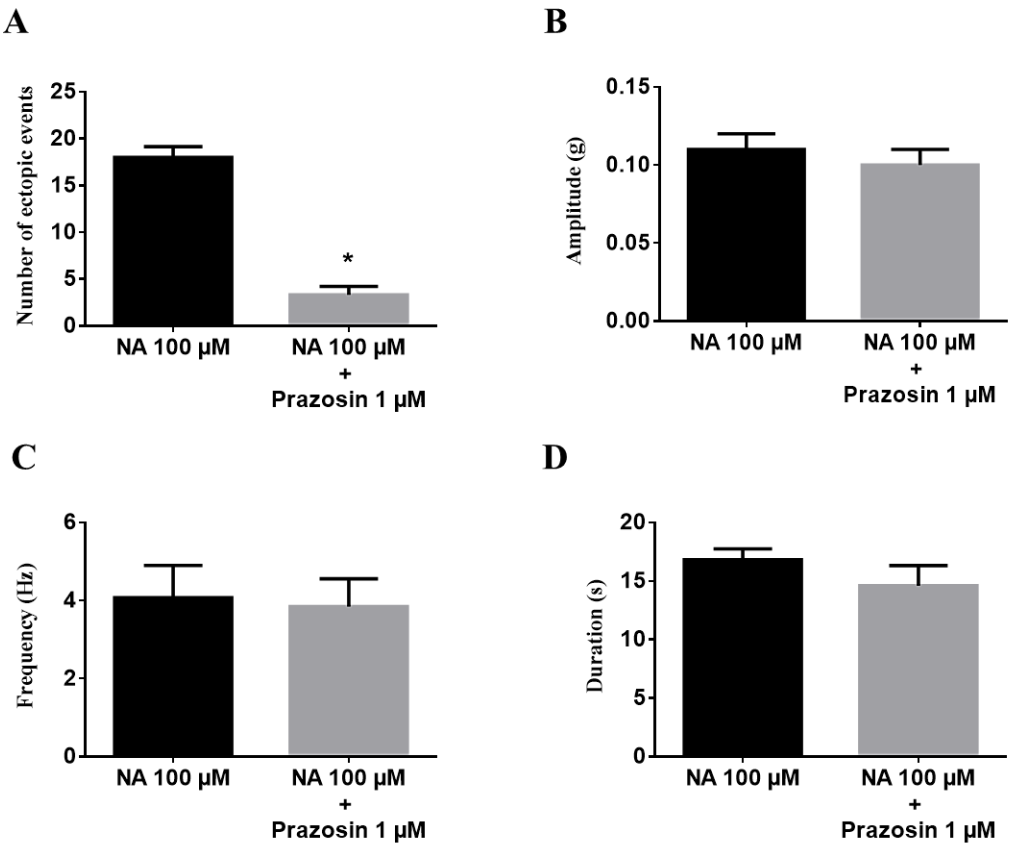

Figure 3-8 The effect of prazosin on ectopic contractions induced by NA in the rat PVs. (A) Number of ectopic beats (B) Amplitude of ectopic contraction (C) Contraction frequency (D) Duration of ectopic activity. All data are presented as mean ± s.e.m., *$p<0.05$ vs NA 10 µM, and n=4.

Table 3-1 Effect of prazosin on NA-induced ectopic activity in the rat PVs

Contraction parameters	NA 100 μM	Prazosin 1 μM
Number of ectopic activity	18.0 ± 1.2	3.3 ± 0.9*
Amplitude (g)	0.1 ± 0.01	0.1 ± 0.03
Frequency (Hz)	4.1 ± 0.8	3.9 ± 0.7
Duration (s)	16.8 ± 0.9	14.6 ± 1.7

All data are presented as mean ± s.e.m., and n=4**.**

*p<0.05 vs NA 100 μM

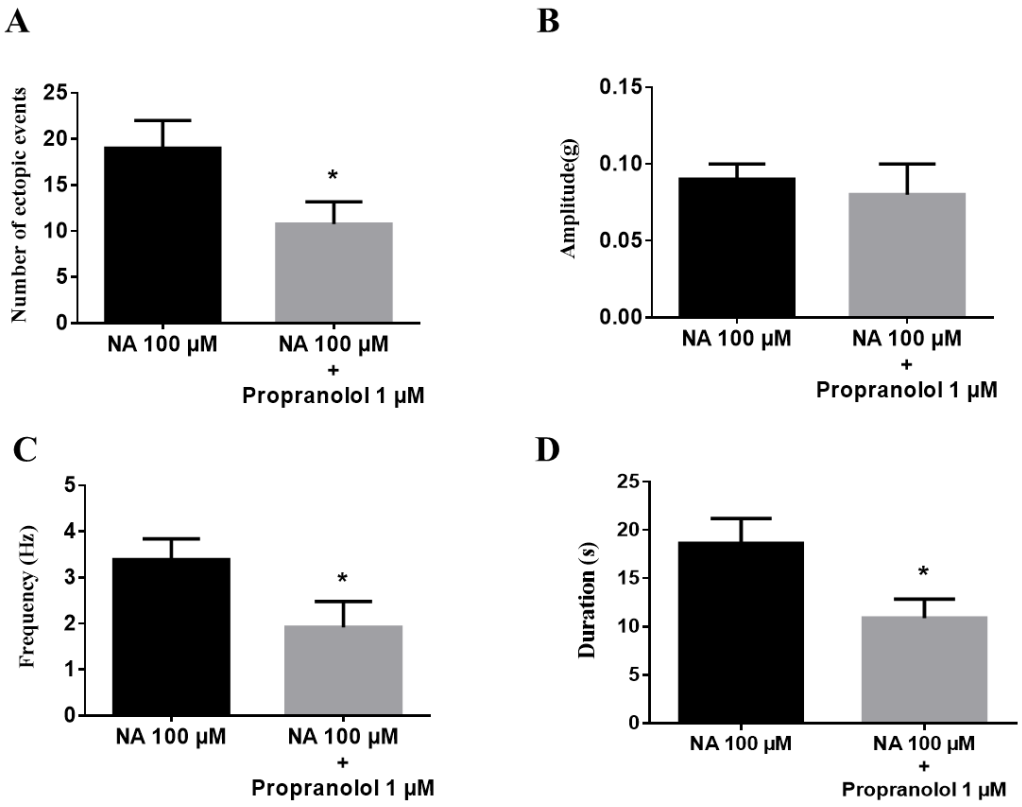

Figure 3-9 The effect of propranolol on ectopic contractions induced by NA in the rat PVs. (A) Number of ectopic beats (B) Amplitude of ectopic contraction (C) Contraction frequency (D) Duration of ectopic activity. All data are presented as mean ± s.e.m., *$p<0.05$ vs NA 10 µM, and n**=4.**

Table 3-2 Effect of propranolol on NA-induced ectopic activity in the rat PVs

Contraction parameters	NA 100 μM	Propranolol 1 μM
Number of ectopic activity	19.0 ± 3.0	10.8 ± 2.4*
Amplitude (g)	0.1 ± 0.01	0.1 ± 0.02
Frequency (Hz)	3.4 ± 0.5	2.4 ± 0.5*
Duration (s)	18.6 ± 2.6	10.9 ± 2.0*

All data are presented as mean ± s.e.m., and n=4**.**

*p<0.05 vs NA 100 μM.

3.3.4 The effect of cholinergic agonist on ectopic contractions in the PV induced by NA

In the absence of NA, there is no ectopic activity in the rat PVs. The ectopic activity appeared in PV tissues after application of NA 100 μM. This study showed carbachol 1 μM and 10 μM significantly reduced the number of ectopic activity in the rat PVs (4.2 ± 0.6 and 2.0 ± 0.6 ectopic events) when compared with the NA group (14.4 ± 1.7 ectopic events), ($n=5$, $p<0.05$); as presented in Figure 3-10, and Figure 3-11A, respectively. However, carbachol was not significantly different in amplitude, frequency duration of ectopic activity in the rat PVs when compared with the control group (Figure 3-11B-D and Table 3-3).

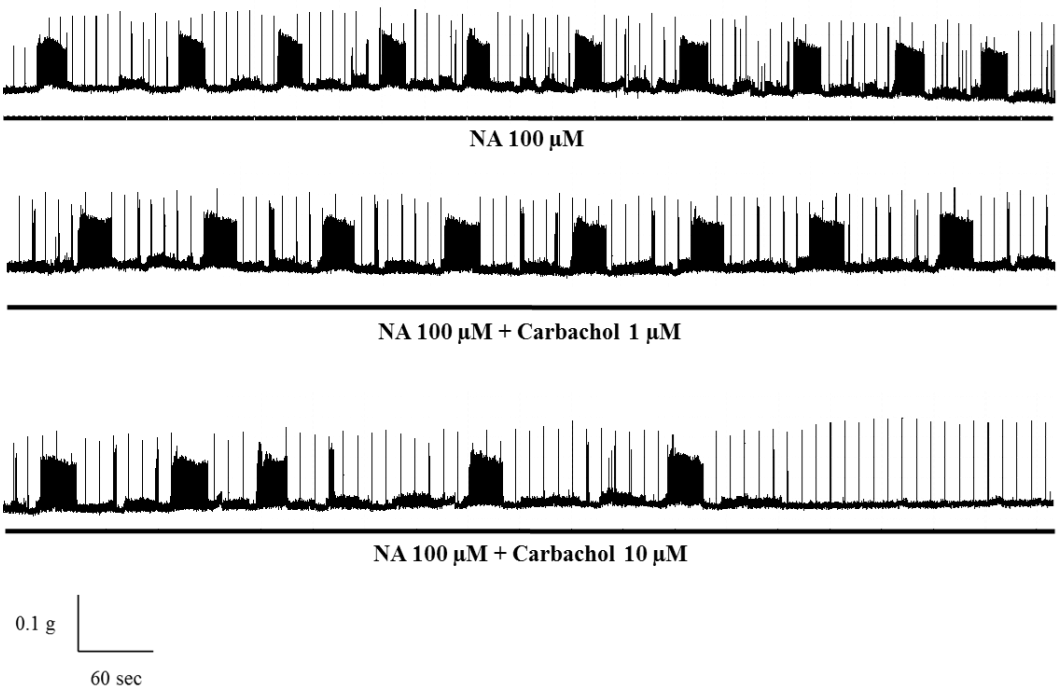

Figure 3-10 The effect of carbachol on ectopic contractions induced by NA in the rat PV preparations. Electrical stimulation was applied at 0.1 Hz for 2 ms, at a supramaximal voltage throughout the recording at 37°C. Ectopic contractions were induced by superfusion of 100 µM NA. Carbachol was added to the organ bath in accumulative-concentration (1 µM and 10 µM).

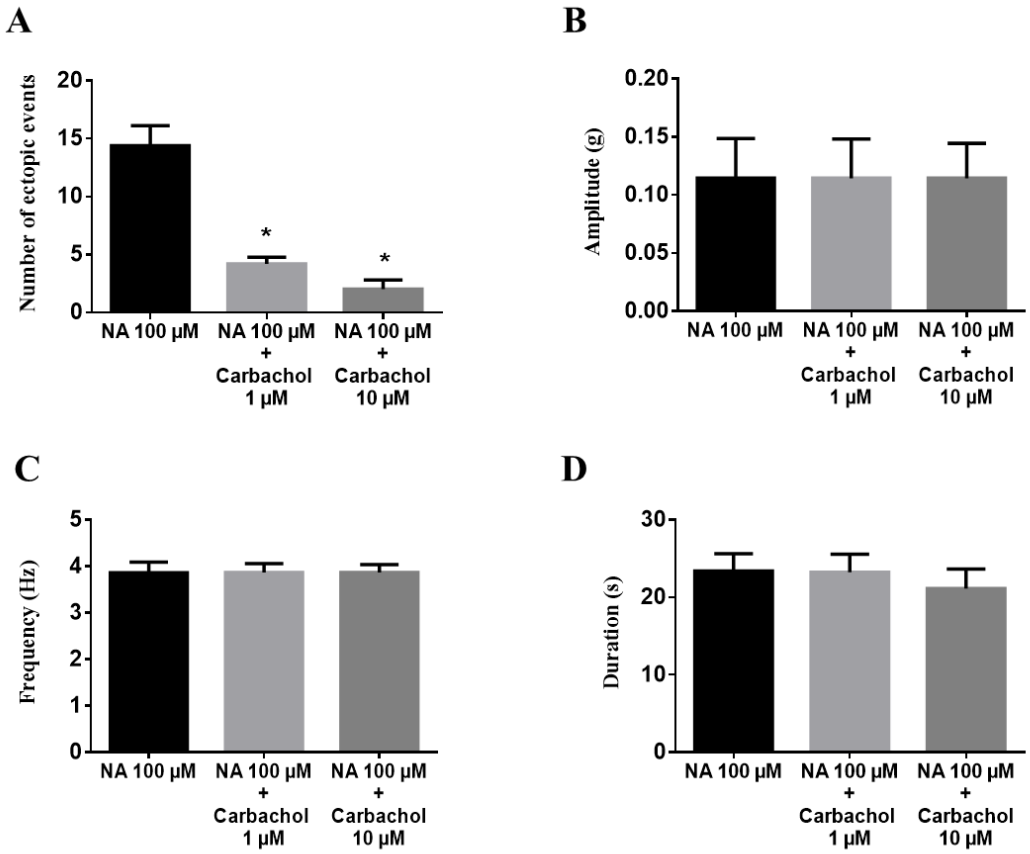

Figure 3-11 The effect of carbachol on ectopic contractions induced by NA. (A) Number of ectopic beats (B) Amplitude of ectopic contraction (C) Contraction frequency (D) Contraction duration. All data are presented as mean ± s.e.m., *$p<0.05$ vs NA 10 µM, and n=**5.**

Table 3-3 Effect of carbachol on NA-induced ectopic activity in the rat PVs

Contraction parameters	NA 100 μM	carbachol 1 μM	carbachol 10 μM
Number of ectopic activity	14.4 ± 1.7	4.2 ± 0.6*	2.0 ± 0.6*
Amplitude (g)	0.1 ± 0.03	0.1 ± 0.03	0.1 ± 0.03
Frequency (Hz)	3.9 ± 0.2	3.9 ± 0.2	3.9 ± 0.2
Duration (s)	23.0 ± 2.2	23.2 ± 2.3	21.1 ± 2.5

All data are presented as mean ± s.e.m., and n=5**.**

*p<0.05 vs NA 100 μM.

3.3.5 The effect of an increase in extracellular Ca^{2+} on the generation of NA induced ectopic contractions of rat PVs.

In control PVs, a submaximal concentration of NA 30 μM triggered bursts of ectopic contractions (16.0 ± 1.5 events), as shown in Figure 3-12. Increases in extracellular Ca^{2+} concentration via $CaCl_2$ up to 2.36 mM significantly decreased the number of ectopic activity induced by NA in the rat PVs (3.7 ± 1.2 events; n=3, $p<0.05$); as shown in Figure 3-13A. Rising concentration of $CaCl_2$ from 1.36 mM to 2.36 mM significantly increased the frequency of contractions within a burst (3.3 ± 0.2 Hz) compared with the NA control group (2.3 ± 0.2 Hz), (n=3, $p<0.05$); as seen in Figure 3-13C. Likewise, adding $CaCl_2$ up to 2.36 mM significantly increased the duration of the NA induced bursts of ectopic contractions from 9.0 ± 1.1 to 41.8 ± 11.8 seconds (n=3, $p<0.05$), as seen in Figure 3-13D. However, increasing extracellular Ca^{2+} from 1.36 to 1.86 mM had no effect on the amplitude, frequency and the duration of ectopic activity induced by NA in rat PVs. In some preparations, the amplitude of ectopic contractions at 1 mM $CaCl_2$ increased throughout the burst (Figure 3-12, and Table 3-4).

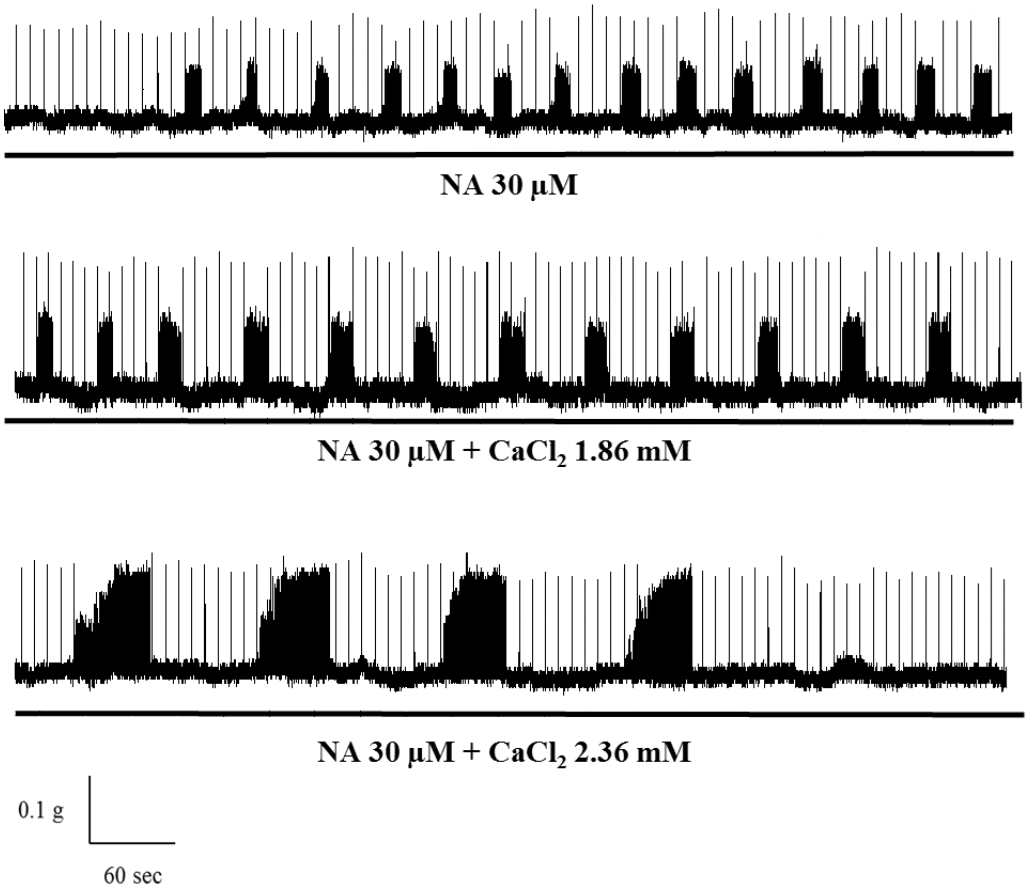

Figure 3-12 An example of the changes in ectopic activity following increases in extracellular Ca^{2+} on NA-induced ectopic contractions of rat PVs. Each preparation was stimulated at 0.1 Hz, 2 ms at a supramaximal voltage in order to generate electrically evoked contractions at 37°C. $CaCl_2$ was added in accumulative concentrations (1.86 mM and 2.36 mM) for the period indicated by the bars below the recording.

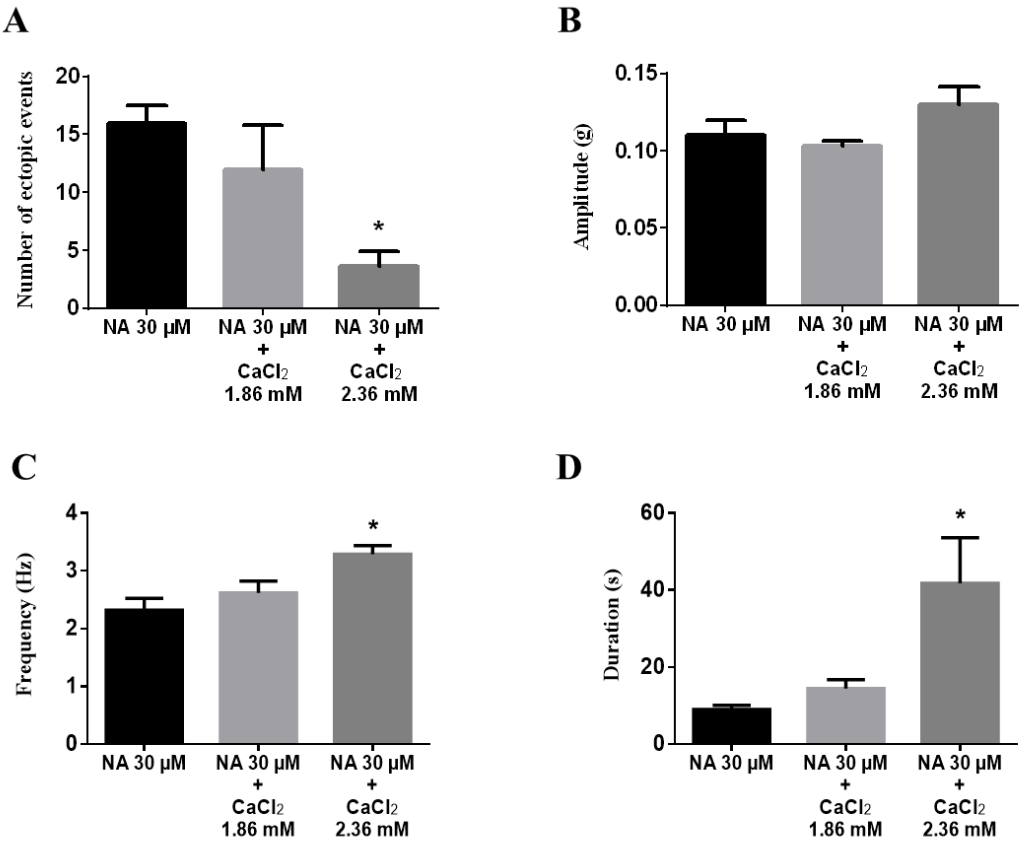

Figure 3-13 Effect of the increases in extracellular [Ca^{2+}] on ectopic activity in the rat PVs. (A) Number of ectopic beats (B) Amplitude of ectopic contraction (C) Contraction frequency (D) Contraction duration. All data are presented as mean ± s.e.m., *p<0.05 vs NA 10 µM, and n=**3.**

Table 3-4 Effect of the increase in extracellular Ca^{2+} on NA-induced ectopic activity in the rat PVs

Contraction parameters	NA 30 μM	$CaCl_2$ 1.86 mM	$CaCl_2$ 2.86 mM
Number of ectopic activity	16.0 ± 1.5	12.0 ± 3.8	3.7 ± 1.2*
Amplitude (g)	0.1 ± 0.01	0.1 ± 0.003	0.1 ± 0.01
Frequency (Hz)	2.3 ± 0.2	2.6 ± 0.2	3.3 ± 0.2*
Duration (s)	9.0 ± 1.1	14.4 ± 2.3	41.8 ± 11.8*

All data are presented as mean ± s.e.m., and n=3**.**

*p<0.05 vs NA 100 μM.

3.3.6 The effect of calcium-channel blocker on ectopic contractions in the PV induced by NA

Ectopic activity in rat PVs was induced by NA 100 µM (19.5 ± 1.7 ectopic events; Figure 3-14). There was a significantly decreased number of ectopic events in the presence of verapamil at concentration of 1 µM (4.3 ± 1.1 events, n=6, $p<0.05$, Figure 3-14 and Figure 3-15A); however, there were not significantly different at concentrations of 0.01 µM (16.7 ± 0.6 events) or 0.1 µM (16.0 ± 2.0 events), (n=6, Figure 3-14). Verapamil 1 µM significantly decreased the amplitude (0.07 ± 0.01 g), frequency (2.2 ± 0.2 Hz) and duration of ectopic activity (5.9 ± 1.9 sec) compared with the NA group (0.1 ± 0.01 g, 3.4 ± 0.1 Hz, and 13.2 ± 1.5 sec), (n=6, $p<0.05$) shown in Figure 3-15B, C, and D, respectively. Verapamil 0.1 µM also significantly decreased the duration of ectopic activity (10.7 ± 1.0 sec), (n=6, $p<0.05$). In addition, verapamil 0.01 µM had no effect on the amplitude of ectopic contractions and the duration of ectopic activity induced by NA in the rat PVs (Table 3-5).

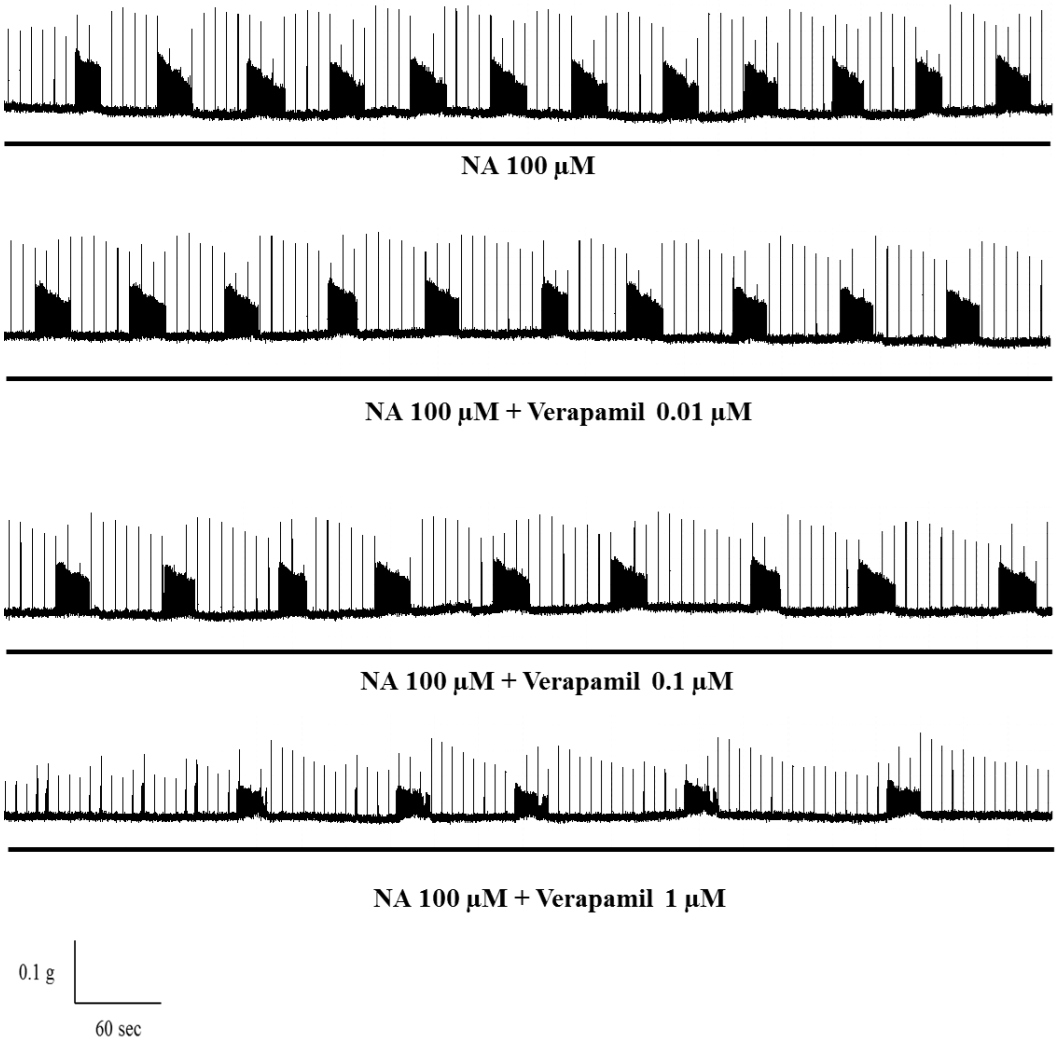

Figure 3-14 The effect of calcium channel blocker (verapamil) on ectopic contraction induced by NA. Each preparation was stimulated at 0.1 Hz, 2 ms at a supramaximal voltage in order to generate electrically evoked contractures at 37°C. Verapamil was added to the organ bath in accumulative-concentration (0.01 µM, 0.1 µM and 1 µM) as indicated below the trace.

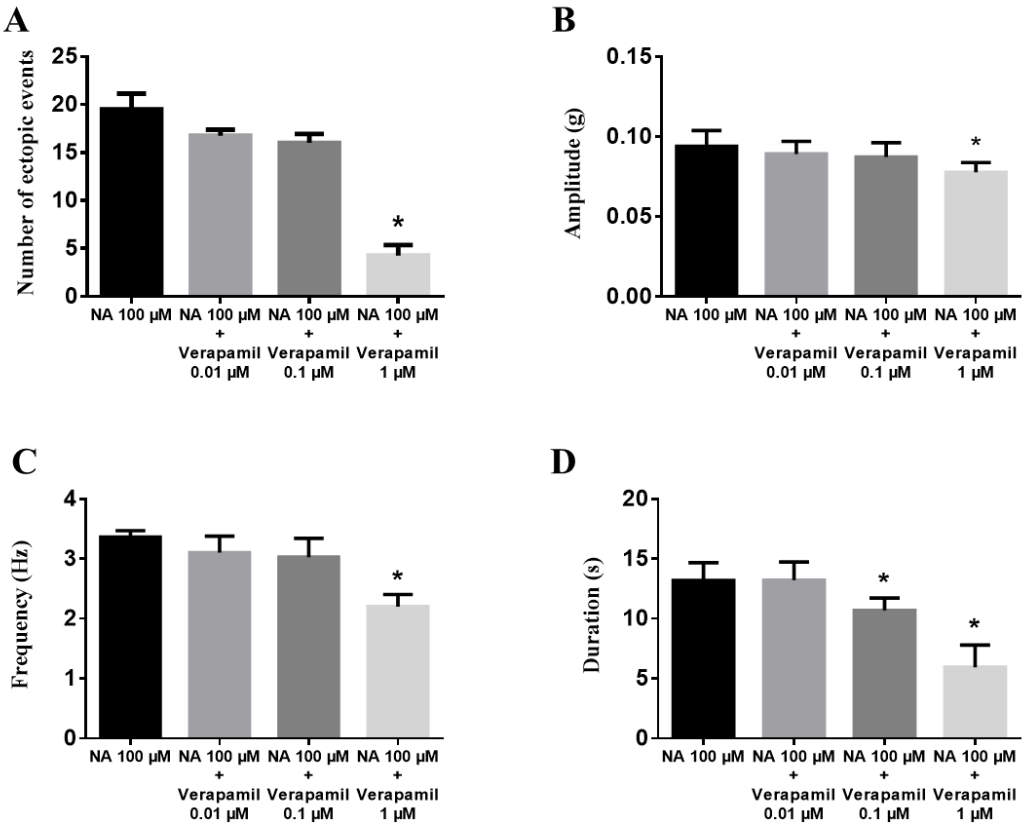

Figure 3-15 The effect of verapamil on ectopic contractions induced by NA. (A) Number of ectopic beats (B) Amplitude of ectopic contraction (C) Contraction frequency (D) Contraction duration. All data are presented as mean ± s.e.m., *$p<0.05$ vs NA 10 µM, and n=6.

Table 3-5 Effects of verapamil on NA-induced ectopic activity in rat PVs

Contraction parameters	NA 100 µM	Verapamil 0.01 µM	Verapamil 0.1 µM	Verapamil 1 µM
Number of ectopic activity	19.5± 1.7	16.7 ± 0.6*	16 ± 2.0*	4.3 ± 1.11*
Amplitude (g)	0.1 ± 0.01	0.1 ± 0.01	0.1 ± 0.01	0.07 ± 0.01*
Frequency (Hz)	3.4 ± 0.1	3.1 ± 0.3	3.03 ± 0.3	2.2 ± 0.2*
Duration (s)	13.2 ± 1.5	13.2 ± 2.5	10.7 ± 1.0*	5.9 ± 1.9*

All data are presented as mean ± s.e.m., and n=6**.**

*p<0.05 vs NA 100 µM.

3.4 Discussion

This study has shown that NA increases contraction responses in the rat PVs *in vitro*. This is consistent with the report of rat PVs under isometric conditions *in vitro* by Sweeney et al. (2007). The study found that NA increased the cardiac muscle contractile response in the rat PVs, which had a positive inotropic influence mediated by β-adrenoceptors (Sweeney et al., 2007). MacLeod and Hunter (1967) also demonstrated that NA has a positive inotropic effect on the rat PVs; indicating a role for β-adrenoceptor. NA (α/β agonist) which has a stimulant effect on the heart rate (chronotropic effect) and the force of contraction. Thus, the results may suggest that the sympathomimetic NA has a positive inotropic influence mediated via adrenergic receptors.

Moreover, the present study illustrates that NA, a non-selective adrenoceptor agonist, induces ectopic activity in the rat PVs in a concentration-dependent manner. This observation is consistent with an earlier study by Maupoil et al. (2007), which showed that ectopic activity in rat PVs requires activation of both α and β adrenergic receptors. Doisne et al. (2009) demonstrated that NA induced automatic activity of cardiac muscle in the rat PVs. Likewise, studies in rat and guinea pig have shown that PV cardiomyocytes generate automatic electrical activity under adrenergic stimulation with NA (Namekata et al., 2010, Okamoto et al., 2012). This ectopic activity generated by NA may relate to the activation of α and β adrenergic receptors, which causes increased Ca^{2+} entry into the cell via LTCC and subsequent Ca^{2+} release from the SR in cardiac muscle tissue (Mohrman and Heller, 2002, Maupoil et al., 2007, Klabunde, 2011).

In this study, temperature has been shown to change the number of ectopic events in the presence of NA. Ectopic contractions were induced by NA at 37°C; however, these gradually decreased and disappeared with falling temperature from 37°C to 25°C. This is somewhat similar to a study in rabbit PVs using the whole-cell clamp technique by Chen et al. (2003), which showed the incidence of DADs in normal (38–39°C) and high (40–41°C) temperatures but not at low temperatures (22–25°C). The same study also showed larger transient inward currents of PV cardiomyocytes at normal (38–39°C) and high (40–41°C) temperatures compared with the currents at low temperatures (22–25°C). These findings suggest that temperature is a considerable factor in modulating transient inward currents of PV cardiomyocytes, which may be associated with the genesis of DADs.

Likewise, a study in isolated rabbit atria showed that atrial arrhythmias were produced by electrical stimulation in the presence of acetylcholine at 37°C, and these were reduced on lowering the temperature to 29°C (Beaulnes and Day, 1957). In guinea pig hearts, prolonged APD at 95 % repolarisation in ventricular myocytes has been shown at low temperature (24-25 °C). The same study also showed low temperature decreased the Ca^{2+} current, the delayed rectifier potassium current (I_K) and the inwardly rectifying potassium current (I_{KI}) using whole-cell clamp experiments. Research in dog hearts has also shown that increasing temperature from 32°C to 38°C increased isometric magnitude, duration of force development and the duration of action potentials (Patterson et al., 2006). Rabbit hearts held in a cardiac hypothermia state present a relevant decrease in ventricular heart rate during AF (Mischke et al., 2011). In addition, the hypothermic condition produced by reducing temperature from 37°C to 34.9°C using an immersion technique in patients with heart diseases; e.g. AF, atrial

flutter, atrioventricular dissociation, and multiple ectopic ventricular beats. (Somerville, 1960). Overall, these findings suggest that temperature may be involved in modulating arrhythmogenic activity through its effects on transient inward currents, Ca^{2+} current and K^{+} current. Thus, this study suggests that the hyperthermia or high-temperature condition may result in increasing arrhythmogenic activity of the PV, while the hypothermic or low-temperature condition may reduce arrhythmogenic activity in the rat PVs.

Additionally, this study showed that ectopic contractions were inhibited by prazosin and propranolol, which are α_1 and β-adrenoreceptor antagonists, respectively. Prazosin is α_1-adrenoreceptor antagonist, which has the potency of prazosin (pA2=9.5); indicating the involvement of prazosin-sensitive functional α_1-adrenoceptors (Southan et al., 2015). In addition, propranolol is β-adrenoreceptor blocker (pA2=8.2-9.2) indicating that propranolol has high potency and specific antagonist to β-adrenoreceptor, which can inhibit sympathetic stimulation (Southan et al., 2015).

This present study is consistent with previous investigations in rat PVs by Maupoil et al. (2007), which showed that prazosin inhibits ectopic activity induced by NA. Likewise, Okamoto et al. (2012) demonstrated that NA induced automaticity was inhibited by prazosin in the rat PV cardiomyocytes. Moreover, the study in dogs with chronic (6–8 weeks) rapid atrial pacing showed that propranolol suppressed spontaneous activities induced by isoproterenol in the dog PVs (Chen et al., 2000). Chen et al. (1999) also demonstrated that propranolol suppresses ectopic beats that originated from human PV with frequent occurrences of paroxysmal AF. These findings are in agreement with the present study, and suggest that ectopic activity

induced by NA may relate to both α and β adrenergic receptors.

Furthermore, the present study shows that carbachol, a cholinomimetic drug that binds and activates the muscarinic receptor, inhibited NA-induced ectopic contractions in the rat PVs. A study of the muscle connections and autonomic nerve distribution in the human PV-LA junction showed that this area favoured the formation of re-entrant arrhythmias (Tan et al., 2006). Additionally, parasympathetic innervation of the PVs and posterior LA is thought to contribute to focal AF; the posterior LA is the most richly innervated region of the LA, with parasympathetic fibres comprising a majority of the nerves supplying this area (Arora et al., 2007, Arora et al., 2008). Arora et al. (2008) also reported muscarinic type 2 receptor (M_2) distribution in the posterior LA and PVs in healthy dog hearts. Moreover, the study in sheep PV using immunofluorescent techniques showed M_2 receptors distributed heterogeneously in the cardiomyocytes, with the highest density in the PV antrum (Liang et al., 2008). Another study by Sweeney et al. (2007) showed that acetylcholine had a muscarinic receptor-mediated negative inotropic effect which decreased the contractile response of the rat PV. In addition, findings from Takahara et al. (2011) showed that the application of carbachol as a muscarinic receptor agonist to the PV preparation hyperpolarised the RMP and suppressed triggered activity induced by a burst pacing of train stimulation in isolated guinea pig PVs. A previous study by Faria et al. (2009) also showed that carbachol decreased atrial tachyarrhythmia induced by electrical field stimulation in isolated rat atria. Thus, the decrease in ectopic activity caused by carbachol in the rat PV may be due to the suppression of cholinergic activity.

Previous studies have indicated that abnormal Ca^{2+} regulation increases PV arrhythmogenesis (Chen and Chen, 2006). This study showed that the extracellular Ca^{2+} concentration increased the amplitude, frequency and duration of ectopic activity induced by NA. This may be consistent with the earlier report by Luk et al. (2008), which demonstrated that elevation of extracellular Ca^{2+} (from 2.7 mM to 5.4 mM and then 8.1 mM) increased the contraction of rabbit PV sleeve preparations driven by electrical stimuli in a dose-dependent manner. In isolated rabbit papillary muscles an increase in extracellular Ca^{2+} of up to 3 mM resulted in an increase in frequency-dependent positive inotropy effect (Singal et al., 1985). Raising extracellular Ca^{2+} from 1.8 mM to 5.0 mM increased the amplitude of action potentials; however; it decreased the duration of action potentials in guinea pig ventricular tissue (Leitch and Brown, 1999). The same study also demonstrated a rise in extracellular Ca^{2+} increased peak inward Ca^{2+} current; however, it increased in the inactivation rate of I_{CaL}, which may be associated with shortening action potentials (Leitch and Brown, 1999). Therefore, this study may associated with the increase intracellular Ca^{2+}, facilitated by excessive availability of Ca^{2+} from the extracellular space, which induced changes in the ectopic activity generated by NA.

In addition, this study demonstrates that verapamil, which is the LTCC blocker with antiarrhythmic properties, can inhibit ectopic activity in rat PVs. Previous studies in guinea pigs have also shown that verapamil effectively inhibits the amount of triggered activity in the PV myocardium, suggesting that inhibition of Ca^{2+} influx through voltage-dependent channels that prevents Ca^{2+} accumulation in PV cardiomyocytes induced by train stimulation (Takahara et al., 2011). Chen et al. (2008) also demonstrated that isoproterenol induces the spontaneous activity in isolated single

cardiomyocytes from rabbit PVs, which suppressed by verapamil. In the study of rabbit PVs showed that oxidative stress can induce Ca^{2+} overload resulting in PV burst firing and EADs, which also inhibited by verapamil (Lin et al., 2010) Moreover, verapamil has been found to suppress ectopic beats originating from PVs in patients with paroxysmal AF (Chen et al., 1999). Thus, verapamil reduced the arrhythmogenic activity of PV cardiomyocytes, which the arrhythmogenicity induced by NA.

In conclusion, this study has found ectopic contractions of the isolated rat PV increase in response to activation by NA (non-specific adrenergic agonist) at 37°C but not at the lower temperature of 25°C. Moreover, the α-adrenoceptor antagonist prazosin and β-adrenoceptor antagonist propranolol reduced the number of ectopic events generated by NA. The cholinergic agonist, carbachol, also inhibited NA-induced ectopic contractions in the rat PVs. In addition, increasing extracellular Ca^{2+} concentration from 1.36 to 2.36 mM decreased the number of ectopic events induced by NA; however, it increased the frequency and duration of ectopic activity within each burst, which may be associated with increases in intracellular Ca^{2+} concentration. Verapamil, which is a Ca^{2+} channel blocker, inhibited ectopic activity generated by NA. Overall, these results suggest a role for catecholamine in the generation of AF and that decreasing organ bath temperature causes a decline in ectopic activity. Both adrenergic and cholinergic receptors may be associated with this ectopic activity, related to the sympathetic and parasympathetic nervous systems. These finding also suggested that Ca^{2+} plays an important role either directly or indirectly in the induced ectopic contractions of the rat PV myocardium, which may be the substrate to initiate and sustain AF.

Chapter 4. The effect of stretch and pharmacological agents on electrical activity and mechanical activity of the rat pulmonary veins

4.1 Introduction

4.1.1 Stretch induced changes in electrical and mechanical properties of cardiac muscle

The study by Frank (1895) using isolated frog hearts showed that the strength of ventricular contraction was increased following stretching prior to contraction. Patterson and Starling (1914) found that increasing venous return to the heart raises the filling pressure of the ventricle, leading to increased stroke volume, which is the amount of oxygenated blood pumped out of the left ventricle into the aorta. This increase in ventricular filling causes increased sarcomere length, which generates great wall tension, and hence pressure; referred to as the Frank-Starling Law of the heart; as reviewed by Klabunde (2011) and Gerilechaogetu (2014).

The myocardial stretch leads to significant electrophysiological changes; e.g. depolarisation in the left ventricle of rats (Kiseleva et al., 2000), prolongation of APD in rat atrial myocytes (Tavi et al., 1998). Stretch also increases the intracellular Ca^{2+} via stretch-activated channels (SACs), which allows Ca^{2+} entry to the cells during stretch; as reviewed by Calaghan and White (1999). These alterations in the electrophysiological properties of the heart may be caused by changes in myocardial segment length, a phenomena referred to as mechanoelectric feedback (Lab, 1996). Mechanoelectrical feedback can trigger cardiac arrhythmias (Hansen et al., 1990), which may arise by the activation of SACs in the cell membrane of cardiomyocytes (Saint, 2002, Kelly et al., 2006, Reed et al., 2014).

The SAC was first discovered in chick skeletal muscles by Guharay and Sachs (1984). SACs are found in many cardiomyocytes including those found in chick embryo ventricle (Ruknudin et al., 1993, Hu and Sachs, 1996), rat atrium (Kim, 1993, Van Wagoner, 1993) and ventricle (Craelius et al., 1988), and rabbit sinoatrial and atrial cells (Hagiwara et al., 1992). SACs are also found in human atria and ventricles (Kamkin et al., 2000, Kamkin et al., 2003b).

Two distinct types of stretch-sensitive ion channels have been found in cardiac tissue; a non-selective cation channel and a potassium channel (Kelly et al., 2006, Reed et al., 2014). The non-selective cation channel (stretch-activated channel: SAC_{NS}) was first discovered in cardiomyocytes by Craelius et al. (1988). The single channel conductance to cations through SAC_{NS} is approximately 21-25 pS; reviewed by Kelly et al. (2006) and Baumgarten (2013). The activation of SAC_{NS} leads to Na^+ or Ca^{2+} to entry into the cells that will depolarise resting cardiac muscle cells (Peyronnet et al., 2016, Reed et al., 2014). The potassium stretch-activated channel (SAC_K) was first discovered in snail heart ventricle muscle cells by Brezden et al. (1986). A study in rat atrial myocytes found that $SAC_{K,}$ has a single conductance of approximately 100 pS (Kim, 1992, Niu and Sachs, 2003). In contrast to the activation of SAC_{NS}, SAC_K opening leads to K^+ efflux, which produces hyperpolarisation or repolarisation (Kohl et al., 2006, Peyronnet et al., 2016).

Stretch-induced changes in intracellular Ca^{2+} modify the electrical activity of cardiac myocytes by opening SAC_{NS} channels, depolarising the cell, which then activates LTCC opening (Matsuda et al., 1996, Calaghan et al., 2003). Matsuda et al. (1996) demonstrated that the osmotic cell swelling and cell inflation by applying positive

pressure through patch pipette enhanced the I_{CaL} in rabbit cardiac myocytes. Kamkin et al. (2003a) also showed that stretch using a glass stylus increased Ca^{2+} influx through LTCC, which depolarised the cell and prolonged the APD in mouse ventricular myocytes. These may suggest that stretch increases Ca^{2+} currents via LTCC, which can change the electrophysiological characteristics of cardiac cells.

The myocardial sleeve, which extends from the left atria into the PV is considered to be a source that may initiate and sustain AF (Haissaguerre et al., 1998). Moreover, stretching in PVs may increase the incidence of ectopic activity by activating stretch-induced currents (Seol et al., 2011). Seol et al. (2008) demonstrated that membrane stretch using hypo-osmotic swelling and mechanical axial stretch induced currents in cardiomyocytes isolated from rabbit PVs. This study showed that swelling induced the activation of a stretch-activated nonselective cationic current ($I_{NSC,\ swell}$) and a Cl^- current ($I_{Cl,\ swell}$), including higher permeability to K^+ than Na^+ (permeability ratio: 2.84). Additionally, axial mechanical stretch also induced the activation of a stretch-activated nonselective cationic current ($I_{NSC,\ stretch}$), which was permeable to Na^+, K^+. Another study in rabbit PVs also showed that stretch increased incidence of spontaneous activity and firing rates increased force dependently in PV cardiomyocytes (Chang et al., 2007). The same study also showed the incidence of early after-depolarisations (EADs), and delayed after-depolarisation (DADs) by stretch, as well as shortening the duration and decreasing the amplitude of action potentials (Chang, 2007). Likewise, another study in guinea pig demonstrated that application of cumulative mechanical stretch to the isolated PV myocardium increased the firing rate of spontaneous electrical activity in the myocardial layer (Hamaguchi et al., 2016). Overall, this evidence is highly suggestive that modification of SACs in the

PV myocardial sleeve by stretching results in abnormal electrophysiological activity in the heart, which is a potential source of AF.

4.1.2 Pharmacological modulators of stretch-induced ectopic action potentials

Gadolinium is a trivalent lanthanide, which was first identified as a stretch-activated channels blocker (SAC blocker) in Xenopus oocytes (Yang and Sachs, 1989). Gadolinium has been widely used as a potent SAC blocker in a wide range of tissues such as rat atrial myocytes (Tavi et al., 1996), rabbit atria (Bode et al., 2000), canine ventricles (Hansen et al., 1991), rat ventricles (Zeng et al., 2000), rabbit PVs (Chang et al., 2007, Seol et al., 2008), and guinea pig PVs (Hamaguchi et al., 2016).

Gadolinium may be useful for investigating stretch induced arrhythmias by inhibiting the activation of SAC (White, 2011). It has been shown that gadolinium blocked cardiac ion channels in a range of concentrations (1-30 μM), effecting non-specific mechanosensitive channels (Ruknudin et al., 1993, Hu and Sachs, 1997, White, 2006). Moreover, gadolinium inhibited stretch activated currents in a concentration dependent manner in rat atrial myocytes, with an IC_{50} value of 46.2 μM (Zhang et al., 2000). The same study also showed that the application of gadolinium 100 μM caused hyperpolarisation of the RMP and shortened the APD (Zhang et al., 2000).

A study of intra-atrial pressure in isolated rat atria found that gadolinium (80μM) inhibited stretch-induced DADs, shortens APD during stretch, and decreases the force of the atrial contraction (Tavi et al., 1996). Additionally, a study in isolated Langendorff-perfused rabbit heart has shown that gadolinium (12.5, 25, and 50 mM) reduced stretch-induced vulnerability to AF in a dose dependent manner (Bode et al., 2000). Another study in canine ventricle showed stretch-induced arrhythmias by increasing the left ventricular volume, which were reduced by gadolinium (1-10 μM) from 95% to 5% (Hansen et al., 1991). Moreover, in isolated rat ventricular myocytes, a study showed longitudinal stretch increased APD and depolarising resting potential, which were blocked by gadolinium (100 μM) (Zeng et al., 2000).

Seol et al. (2008) demonstrated that swelling induced $I_{NSC,\ swell}$ and mechanical stretching induced $I_{NSC,\ stretch.}$ Both $I_{NSC,\ swell}$ and $I_{NSC,\ stretch}$ were blocked by gadolinium. (100 μM). Chang et al. (2007) demonstrated stretch produced spontaneous activity and increased firing rates in the rabbit PVs. The study also showed shortening of APD, decreasing the amplitude of action potentials and induction of EADs and DADs. These changes in rabbit PVs were all reportedly inhibited by gadolinium (1, 3 and 10 μM) in a dose-dependent manner. Additionally, gadolinium (10 μM) has been found to inhibit the effect of mechanical stretch on spontaneous electrical activity in isolated guinea pig PV cardiomyocytes (Hamaguchi et al., 2016). These studies suggested that mechanical stretch to the PVs increases the ectopic activity of PV cardiomyocytes through opening of SACs, which can be inhibited by gadolinium; a well-established SAC blocker (Chang et al., 2007, Seol et al., 2008, Hamaguchi et al., 2016).

In addition to inhibiting activation of SACs, gadolinium has also been found to block cardiac LTCC. Lacampagne et al. (1994) reported that gadolinium is a potent Ca^{2+} channel blocker that inhibits I_{CaL} in a concentration dependent manner; with EC_{50} of 1.4 μM and complete inhibition at 10 μM in guinea-pig isolated ventricular myocytes. Moreover, another study in guinea pig showed that gadolinium inhibited in NCX currents in isolated ventricular myocytes in a dose-dependent manner; with IC_{50} of 30 ± 4.0 μM (Zhang and Hancox, 2000). These studies suggest that the pharmacological effects of gadolinium are complex, potentially involving SACs, LTCC, and NCX.

4.1.3 Aims

The aim of this chapter is to investigate action potential properties of the rat PV myocardium under stretch. Furthermore, this study examines the effect of NA on stretch-induced electrical activity. The experiments in this chapter were designed to examine how the electrical characteristics of PV cardiomyocytes are affected by five different pharmacological agents. Gadolinium (SAC blocker), ORM-10103 (selective Na^+/Ca^{2+} exchanger inhibitor; NCX inhibitor), verapamil (Ca^{2+} channel blocker), prazosin (α-adrenergic blocker), and propranolol (β-adrenergic blocker), were investigated under the combination of stretch and adrenergic stimulation.

4.2 Methods

4.2.1 Animals, dissection, and, preparation of the rat PVs

Rat PVs were isolated as described earlier in section 2.2.1. After removing the lung from animal, the left and the posterior right of lung were dissected. The PVs were carefully excised and placed in ice cold HEPES solution (composition(mM); NaCl 150, KCl 5.4, HEPES 10, glucose 10, $MgCl_2$ 1.2, and $CaCl_2$ 1.8 (pH adjusted to 7.4 with 1 M NaOH) , gassed with O_2.

The electrophysiological studies were performed using the techniques described in section Experiment protocols). Action potentials were evoked by stimulating the PVs at a frequency of 0.1 Hz, with twice the threshold voltage and 2 ms pulse duration.

4.2.2 Experiment protocols

4.2.2.1 Microelectrode studies

The recording chamber was placed on the stage of a wild M20 microscope (Wild Heerbrugg, Switzerland). The tissues were visualised with a 20x objective lens using Hoffman modulation contrast optics (Modulation Optics, Greenvale, NY, USA). To reduce artefacts from mechanical vibration and electrical noise, the chamber and micromanipulator were positioned on an air table (model AVT 701, Wentworth Laboratories LTD, Bedford, UK) enclosed inside a Faraday cage (Figure 4-1A).

A

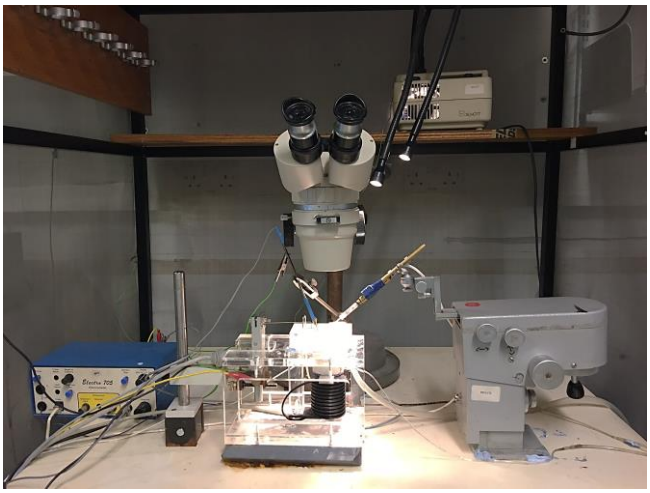

B

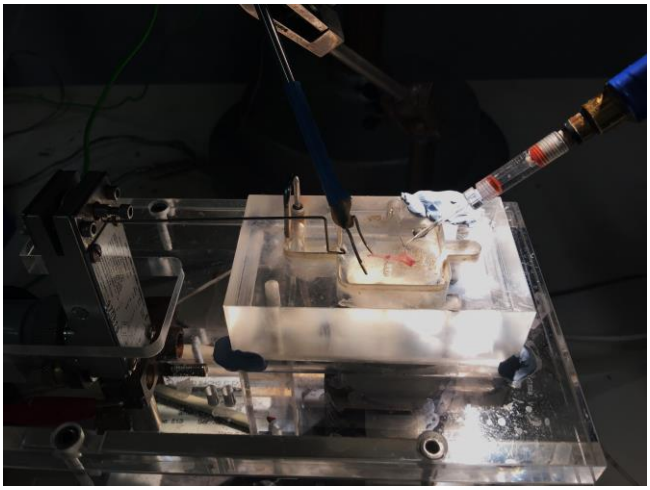

Figure 4-1 Photographs illustrating the experimental set-up used for intracellular recordings under stretch. (A) The potential difference between the recording microelectrode in the cell and the reference electrode is measured by the Electro 705 electrometer, amplified by the CED 1902 amplifier and recorded onto the hard disk. **(B)** The tissue is shown pinned out in the recording chamber under stretching condition. A pair of bipolar platinum electrodes (shown on the left of the tissue sample) was inserted across the PV. The recording electrode (shown on right) was inserted into the PV.

The tissue preparation was pinned horizontally onto a Sylgard® 184 (Dow Corning, USA) coated recording chamber (Figure 4-1B). For recording the action potentials, one end of the preparation was pinned to the bottom of the tissue bath and the other end was connected to the Grass FT03C force transducer (Grass Instruments, Quincy, Massachusetts, USA) with silk thread. All experiments were carried out at twice the threshold voltage and pulse duration of 2 ms, with a stimulation frequency at 0.1 Hz.

The tissue was perfused at a constant rate (10 ml/min) with Tyrode solution with the following composition (in mM): NaCl 118, KCl 2.7, $CaCl_2$ 1.2, $MgCl_2$ 1.2, $NaHCO_3$ 25, NaH_2PO_4 2.2, and glucose 11. This solution has previously been used in a stretch-induced arrhythmia model of the rat PV (Kuz'min and Rozenshtraukh, 2012a, 2012b). The solution was continuously gassed with 95% O_2 and 5% CO_2, pH 7.35± 0.05. The temperature was maintained constant at 37°C using a temperature regulator (HSE Temperature Regulator, Type 319, Hugo Sachs, Germany).

Action potentials were recorded using the conventional microelectrode technique. Recording pipettes were pulled from borosilicate glass capillaries (1.5 mm outer diameter, 0.86 inner diameter; Warner Instruments, USA). These were shaped with a vertical micropipette puller (model P-30, Sutter Instrument Co., Novato, USA) and filled with 3M KCl to produce electrodes with a resistance of 20-50 MΩ. To position the microelectrode a mechanical micromanipulator was used prior to inserting into the cardiomyocytes during the experiment (Leitz, Wetzlar, Germany).

A silver/silver chloride bead type reference electrode was positioned in the recording chamber. The potential difference between the reference electrode and the recording

microelectrode in the cell was measured by a unitary gain high input impedance electrometer (model Electro 705, World Precision Instruments, Hertfordshire, UK).

Electrical signals were amplified using a CED 1902 amplifier (Cambridge Electronic Design LTD, Cambridge, UK), sampled at 20 kHz by a computer controlled data acquisition system (National Instruments PCI-6221 data acquisition board) connected to the computer using a custom BNC interface. The amplified signals were displayed using WinEDR electrophysiology software (Version 3.6.9, Dr. John Dempster, University of Strathclyde) and simultaneously stored on computer hard disk for analysis.

Platinum electrodes, placed at least 1 cm from the recording electrode (to minimise artefacts), were used to electrically stimulate the tissue. Rectangular voltage pulses were supplied by a Grass S44 stimulator via a stimulus isolation unit (model SIU 5A, Grass Instrument Co., USA). Following impalement of the cell, stimulation voltage was decreased in 5 V steps until the threshold voltage capable of eliciting an action potential was reached. All experiments were carried out at twice the threshold voltage and a pulse duration of 2 ms, with a stimulation.

Action potentials were recorded using WinEDR software and exported to WinWCP software (Version 5.1.6 Dr. John Dempster, University of Strathclyde) for analysis. The following action potential parameters were measured (Figure 4-2):

- Peak Amplitude – The peak action potential amplitude measured relative to the resting membrane potential
- Rise time –The time taken for the action potential to rise from 10% to 90% of the peak amplitude

- T_{50} – The time taken for the action potential to fall from peak amplitude to 50% of peak amplitude
- T_{90} – The time taken for the action potential to fall from peak amplitude to 10% of peak amplitude
- APD_{90} – The action potential duration at 90% repolarisation

These propertied were measured from the average of 4-6 consecutive action potentials for each experimental observation.

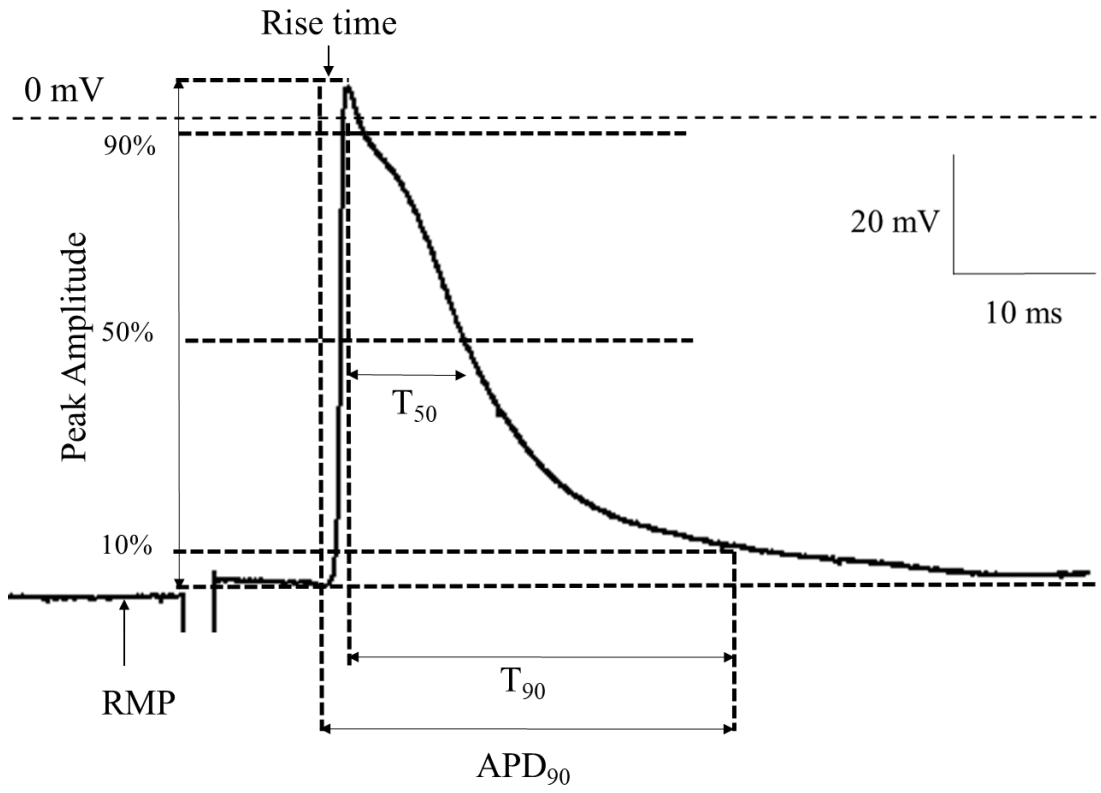

Figure 4-2 Illustration of electrically evoked action potential in PV cardiomyocyte

The action potential parameters i.e. the resting membrane potential (RMP), rise time, peak amplitude, the time taken for 50% and 90% repolarisation (T_{50} and T_{90}) and the duration of action potential measured at 90% repolarisation (APD_{90})

4.2.2.2 Effect of stretch-induced spontaneous activity in the rat PV cardiomyocytes

To record the effect of different tensions on rat PV cardiomyocytes, a standard protocol was used to obtain the recordings of the RMP and action potential. Action potentials were recorded before (0g or resting condition) and after successive stretches of 0.5g and then 1 g. These were recorded during a 1-minute period in each condition, immediately after inserting the electrode into the cardiomyocytes.

4.2.2.3 Effect of NA on the stretch-induced activity in the rat PV cardiomyocytes

The PV preparation was incubated in Tyrode's solution under resting then 0.5 g and 1 g stretch. NA (10 µM) was perfused into the chamber for 5 minutes at a rate of 10 ml/min to induce ectopic activity under resting and stretching conditions (0g, 0.5g and 1 g stretch). After NA perfusion, action potentials were recorded for 1 minute at each tension.

4.2.3.4 Effect of non-cumulative concentrations of NA on stretch-induced activity in the rat PV cardiomyocytes

With previous experiments, stretch 1 g significantly increased the incidence of spontaneous activity in the rat PVs. As a consequence, in this experiment the PV preparation was incubated in the Tyrode's solution under 1 g stretch. The effect of NA on activity in the PV cardiomyocytes was tested by adding non-cumulative concentrations of NA (10 µM, 30 µM and 100 µM, respectively) into the recording chamber for 5 minutes at each concentration. After NA perfusion, action potentials

were recorded at steady state for 1 minute before proceeding to subsequent concentrations.

4.2.3.5 Effects of the pharmacological agents on combined stretch and NA induced ectopic activity of the rat PV cardiomyocytes

PV preparations were equilibrated in the tissue chamber perfusion with Tyrode's solution under 1 g stretch, which followed the result from the experiment 4.2.2.2. In control, NA 100 µM was perfused into the tissue chamber for 5 minutes at a rate 10 ml/min to generate ectopic activity. The ectopic action potentials from PV cardiomyocytes in this control situation were recorded for a period of 1 minute. Different drugs (see list below) were then perfused into the recording chamber for 5 minutes and their effect on stretch and NA induced ectopic activity of PV cardiomyocytes was also recorded for a 1-minute period.

The following pharmacological agents were examined in this experimental protocol: gadolinium (80 µM), a stretch-activated ion channel blocker; verapamil (1 µM), a Ca^{2+} channel blocker; ORM-10103 (1 µM), a novel specific inhibitor of the Na^{+}/Ca^{2+} exchanger; prazosin (1 µM), a selective α_1-adrenergic receptor antagonist; and propranolol (1 µM), a non-cardioselective beta-adrenergic antagonist.

4.2.3 Statistics

Graphs were produced using Graph Prism (version 6.01, Graph PAD Software Inc., San Diego, CA, USA). Data are reported as mean ± sem. with values obtained from n different preparations. Prism was also used to determine any differences between groups with one-way analysis of variance (ANOVA) followed by Tukey's post-hoc test.

4.3 Results

4.3.1 Stretch-induced spontaneous activity in the rat PV cardiomyocytes

Under the resting condition (0g), no ectopic action potentials were observed, as illustrated in Figure 4-3A. The incidence of spontaneous activity in PVs under stretch (0.5 g and 1 g) increased force dependently. Figure 4-3B and C show examples of stretch-induced spontaneous activity during different tensions (n=6).

Increasing tension up to 1 g significantly increased the frequency of ectopic action potentials (0.2 ± 0.03 Hz) when compared with the PV under resting condition (0.1 ± 0.002 Hz, n=6, $p<0.05$); however, the frequency of ectopic action potentials was not significantly different between 0.5g stretch (0.1 ± 0.01 Hz) and the control group as illustrated in Figure 4-4D.

Detailed analysis of action potentials demonstrated that RMP, peak amplitude, rise time, $T_{50,}$ $T_{90,}$ and APD_{90} were not affected by increasing tension from 0g to 1g, as seen in Figure 4-4A, B, C, E, F, and G, and Table 4-1. Additionally, the contraction of ectopic activity in the rat PVs was not significantly different from the control group (0g) (Figure 4-4H).

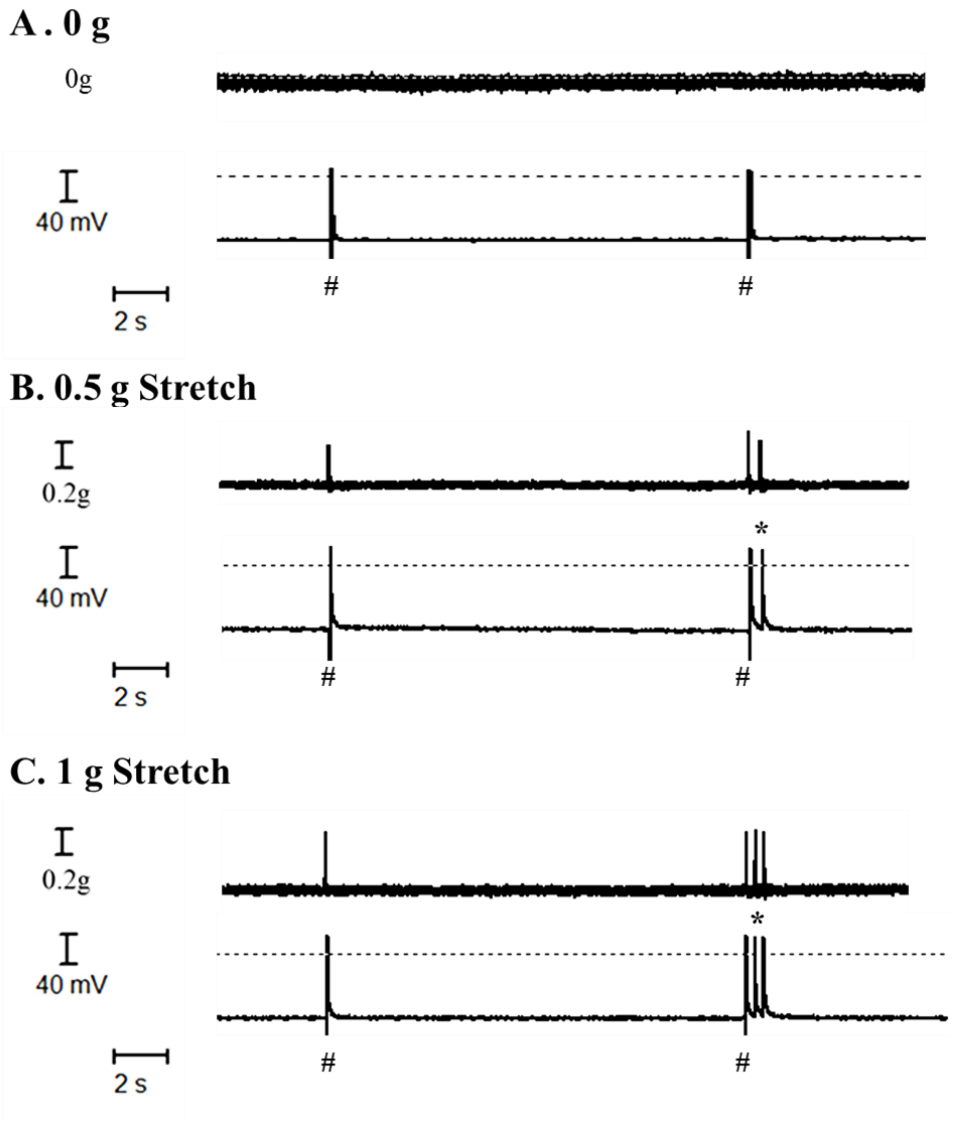

Figure 4-3 Simultaneous twitch tension and action potential recordings in the rat PV cardiomyocytes at different tensions. (A) Unstretch (0 g), (B) 0.5 g stretch and (C) 1 g stretch. # indicates electric stimulation (ES) at 0.1 Hz, and * indicates spontaneous activity (n=6).

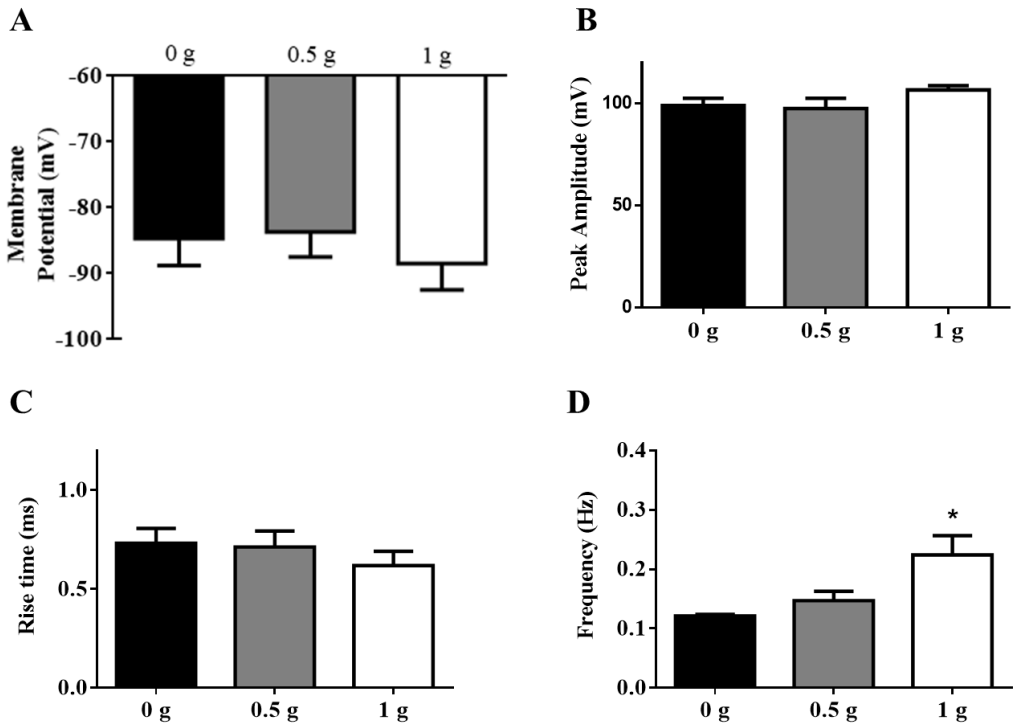

Figure 4-4 The action potential properties and contractile activity of the rat PV cardiomyocytes before (0 g) and after stretch (0.5 g, and 1 g). (A) Resting membrane potential (B) Peak amplitude (C) Rise time of action potential, and (D) Frequency of action potential. All data are presented as mean ± s.e.m., *$p<0.05$ vs Control group (0g), and n=6.

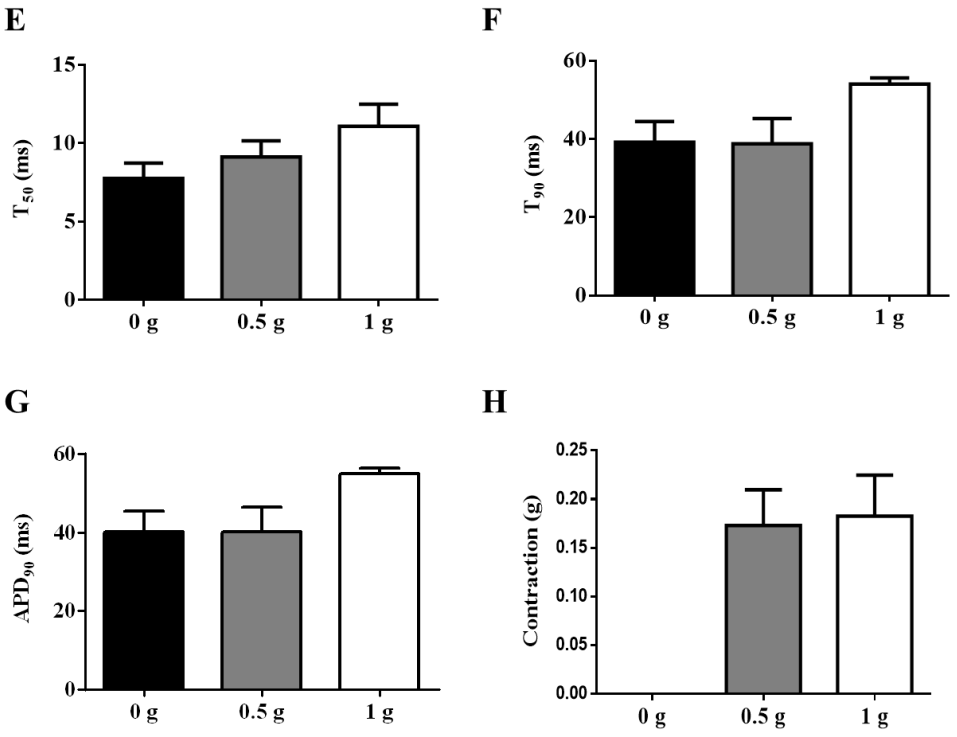

Figure 4-4 (Cont.) (E) Time taken for 50% repolarisation (T_{50}), (F) Time taken for 90% repolarisation (T_{90}), (G) The duration at 90% repolarisation (APD_{90}) of action potentials, and (H) Contraction amplitude. All data are presented as mean ± s.e.m., and n=6.

Table 4-1 Action potential parameters illustrating the effects of stretch on electrical activity of the rat PV cardiomyocytes

Action potential parameters	0 g	0.5 g	1 g
Resting membrane potential (mV)	-84.7 ± 4.1	-83.7 ± 3.8	-88.5 ± 4.0
Peak amplitude (mV)	99.0±3.5	97.6 ± 4.9	106.7 ± 2.1
Rise time (ms)	0.7 ± 0.1	0.7 ± 0.1	0.6 ± 0.1
Frequency (Hz)	0.1 ± 0.003	0.1 ± 0.01	0.2 ± 0.03*
T_{50} (ms)	7.8 ± 1.0	9.1 ± 1.0	11.1 ± 1.4
T_{90} (ms)	39.2 ± 5.3	38.8 ± 6.5	54.0 ± 1.6
APD_{90} (ms)	40.2 ± 5.3	40.3 ± 6.3	54.9 ± 1.6
Contraction amplitude (g)	0	0.2±0.03	0.2±0.04

All data are presented as mean ± s.e.m., and n=6**.**

*$p<0.05$ vs 0 g.

4.3.2 Effect of NA on stretch-induced spontaneous activity in the rat PV cardiomyocytes

Under resting conditions (0g) there was no ectopic action potentials in the presence of NA, as illustrated in Figure 4-5A. The application NA induced ectopic action potential in the rat PVs, which increased firing rates depending on the stretch force (0.5g and 1g) (Figure 4-5B and C).

The combined 1 g stretch and NA significantly increased the frequency of ectopic action potentials (1.4 ± 0.4 Hz, n=6, $p<0.05$), but not in the 0.5 g stretch condition (0.6 ± 0.1 Hz, n=6) compared with the control (0.2 ± 0.01 Hz, Figure 4-6D). However, the stretch plus NA 10 μM was not significantly different in RMP, peak amplitude, rise time, T50, T90 and APD90 of action potential as shown in Figure 4-6A, B, C, E, F, and G and Table 4-2. In addition, no statistically significant change was detected in the contraction parameter (Figure 4-6H).

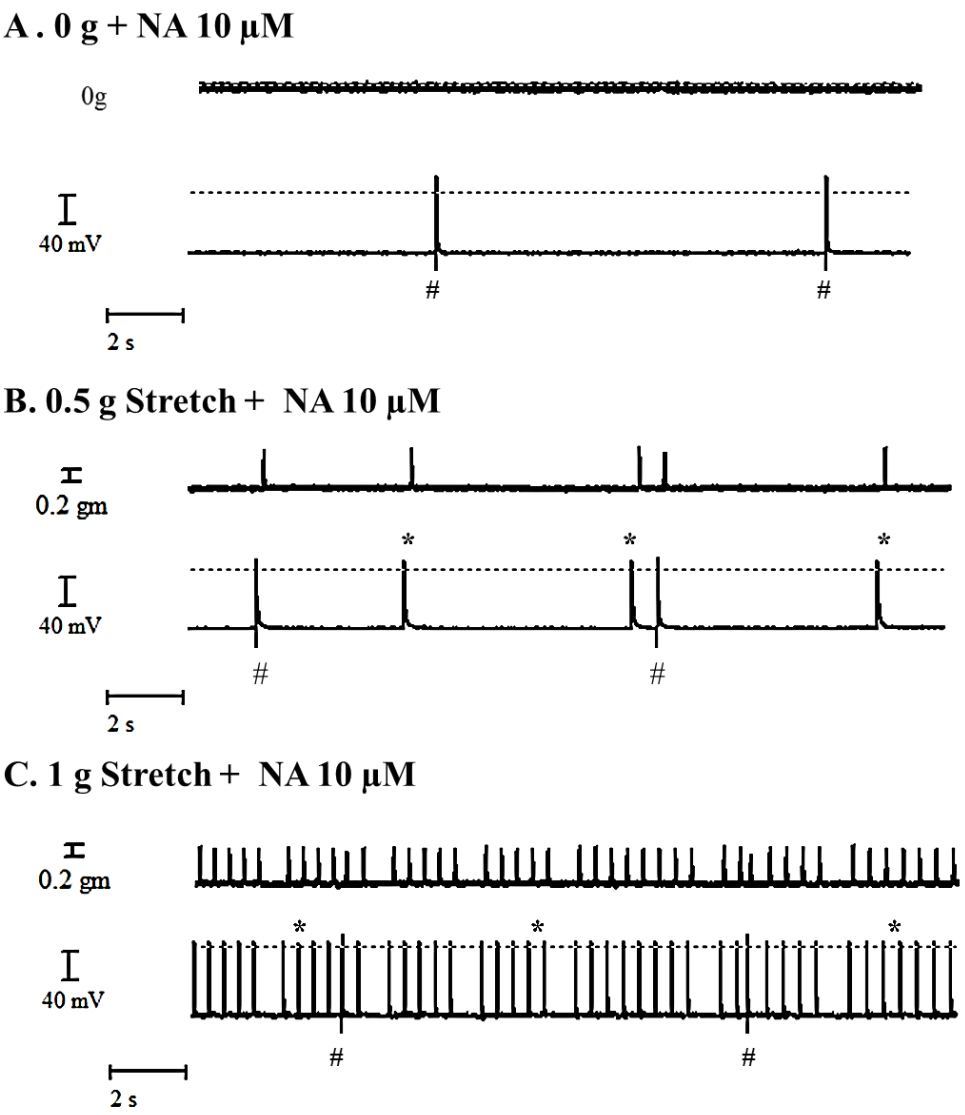

Figure 4-5 Simultaneous twitch tension and action potential recordings in the rat PV cardiomyocytes at different tensions in the presence of NA 10 µM. (A) Under resting (0 g) and (B) 0.5 g stretch and (C) 1 g stretch. # indicates electric stimulation (ES) at 0.1 Hz, * indicates NA-induced automaticity, n=6.

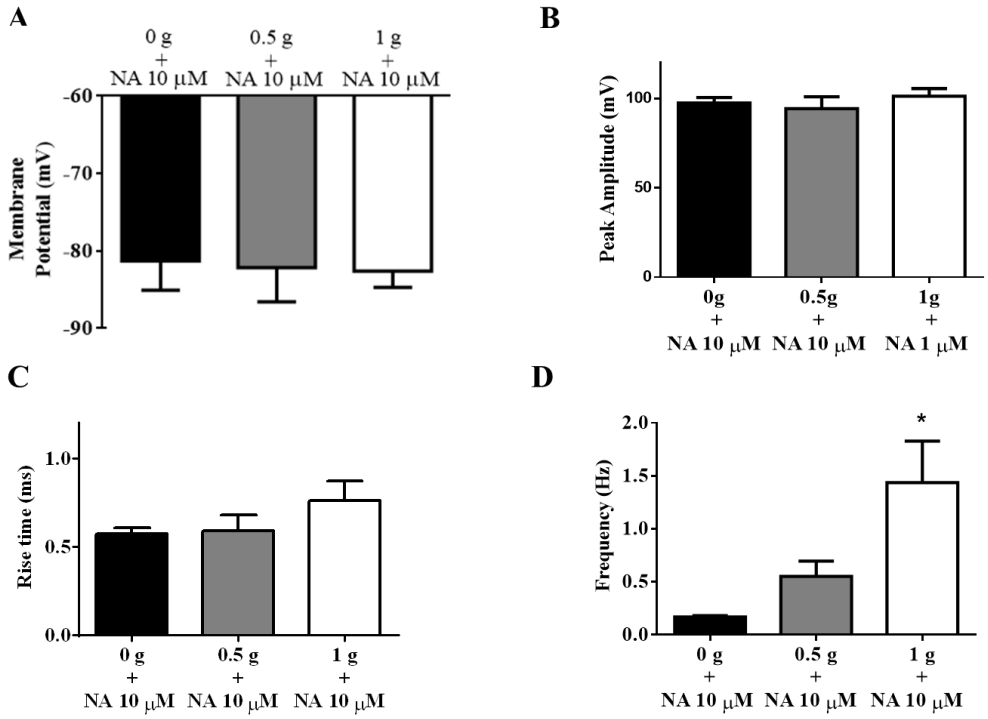

Figure 4-6 The action potential properties and contractile response during combined stretch and NA in the rat PV cardiomyocytes. A) Resting membrane potential (B) Peak amplitude (C) Rise time of action potential, and (D) Frequency of action potential. All data are presented as mean ± s.e.m., *$p<0.05$ vs Control group (0g), and n=6.

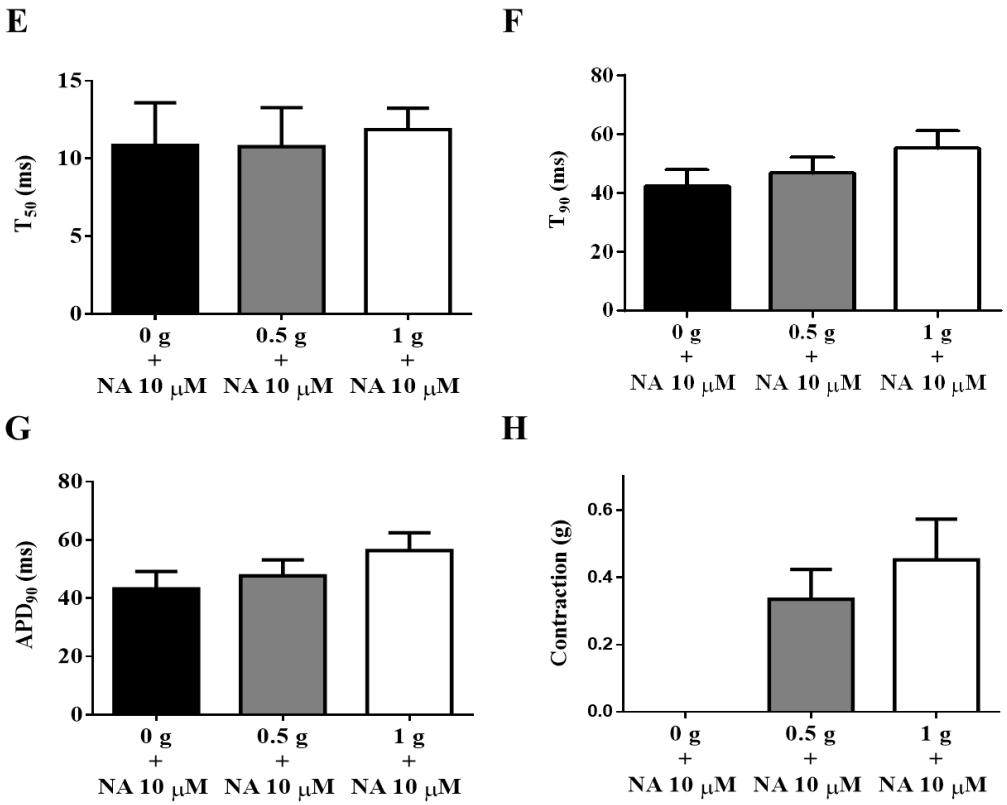

Figure 4-6 (Cont.) ((E) Time taken for 50% repolarisation (T_{50}), (F) Time taken for 90% repolarisation (T_{90}), (G) the duration at 90% repolarisation (APD_{90}) of action potentials, and (H) Contraction amplitude. All data are presented as mean ± s.e.m., and n=6.

Table 4-2 Action potential parameters during combined stretch and NA in the rat PV cardiomyocytes

Action potential parameters	0 g + NA 10 µM	0.5 g + NA 10 µM	1 g +NA 10 µM
Resting membrane potential (mV)	-81.3 ± 3.8	-82.2 ± 4.4	-82.6 ± 2.1
Peak amplitude (mV)	97.5 ± 3.0	94.3 ± 6.6	101.2 ± 4.3
Rise time (ms)	0.7 ± 0.1	0.6 ± 0.1	0.8 ± 0.1
Frequency (Hz)	0.2 ± 0.01	0.6 ±0.1	1.4 ± 0.4*
T_{50} (ms)	10.9 ± 2.7	10.8 ± 2.5	11.9 ± 1.3
T_{90} (ms)	42.2 ± 5.9	46.7 ± 5.5	55.1 ± 6.1
APD_{90} (ms)	43.2 ± 5.9	47.7 ± 5.5	56.4 ± 3.2
Contraction amplitude (g)	0	0.3±0.1	0.5±0.1

All data are presented as mean ± s.e.m., and n=6**.**

*$p<0.05$ vs 0 g + NA 10 µM.

4.3.3 Effect of non-cumulative administration of NA on stretch-induced activity in the rat PV cardiomyocytes

In control, rat PV cardiomyocytes showed some spontaneous activity during 1 g stretch. The data shows that NA at concentrations of 10 µM, 30 µM and 100 µM generated ectopic action potentials under 1 g stretch (Figure 4-7).

NA 10, 30, and 100 µM increased the frequency of ectopic action potentials in a concentration-dependent manner;1.4 ± 0.2 Hz, 1.5 ± 0.4 Hz and 3.6 ± 0.8 Hz, respectively, when compared with the control group (0.1 ± 0.004 Hz, n=4, $p<0.05$) as shown in Figure 4-9D. In addition, NA 10, 30, and 100 µM significantly increased T_{90} (51.8 ± 2.7 ms, 53.9 ± 6.3 ms, and 56.7 ± 5.2 ms) and APD_{90} (53.0 ± 2.8 ms, 54.7 ± 6.2 ms, and 57.5 ± 5.1 ms) of action potentials in rat PV cardiomyocytes when compared with control PVs (T_{90} 31.3 ± 2.3 ms and APD_{90} 32.2 ± 2.2 ms, n=4, $p<0.05$), as shown in Figure 4-9F-G.

However, increasing the concentration of NA up to 100 µM had no effect on the RMP, peak amplitude, rise time and T_{50}, in the PV cardiomyocytes under stretch, as illustrated in Figure 4-9A, B, C, E, and H, and Table 4-3.

Additionally, since NA was shown to induce arrhythmogenic activity in the form of ectopic action potentials in the PV, the ability of NA to induce automaticity and EADs was also examined. The occurrence of EADs was observed in the rat PV preparations; Figure 4-8 shows examples in which NA changed action potential characteristics and the induction of EADs in PV cardiomyocytes under stretch.

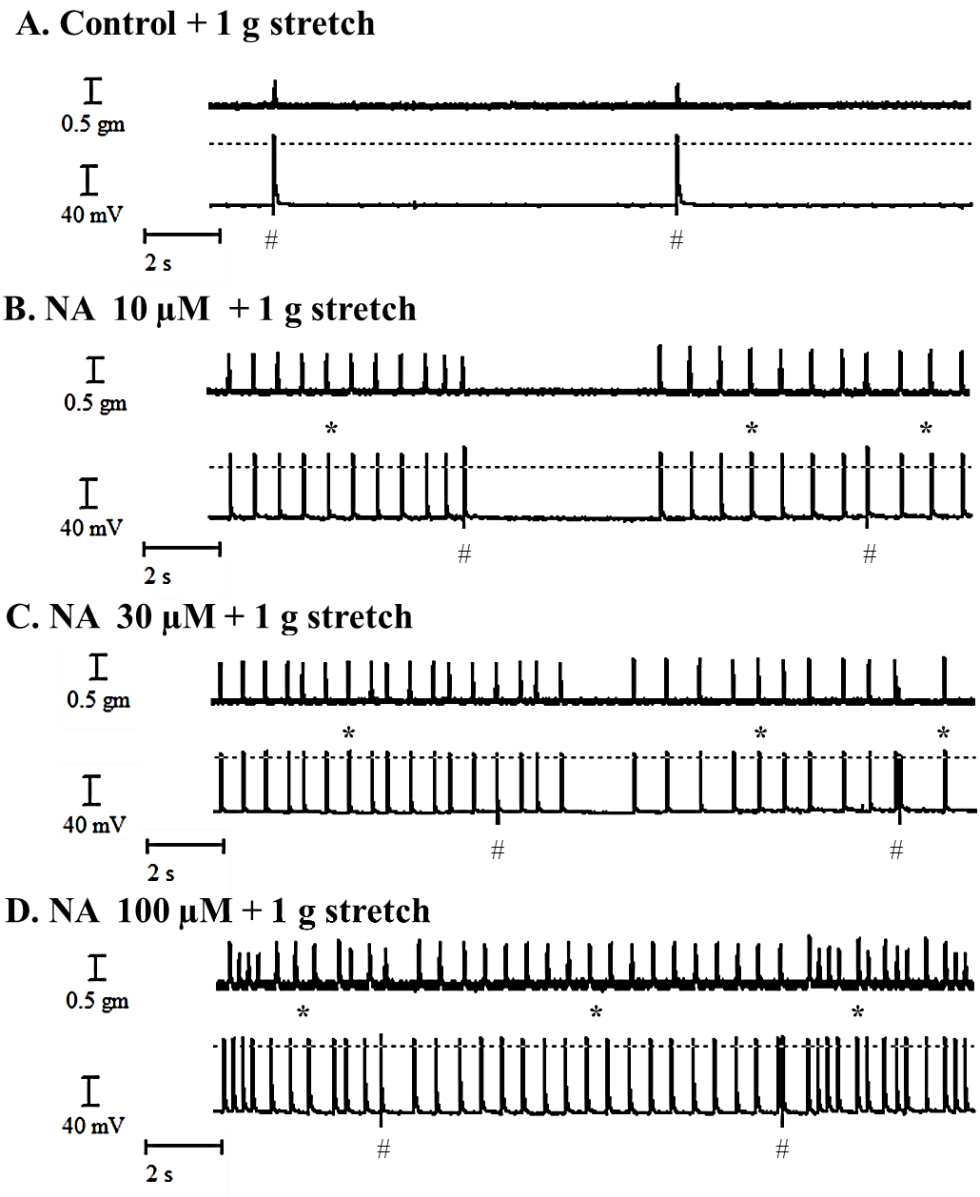

Figure 4-7 Simultaneous twitch tension and action potential recordings following non-cumulative administration of NA in the rat PV cardiomyocytes under 1 g stretch.(A), Control, (B) NA 10 µM, (C) NA 30 µM and (D) NA 100µM. # Electric stimulation (ES) at 0.1 Hz and * NA-induced automaticity, (n = 4).

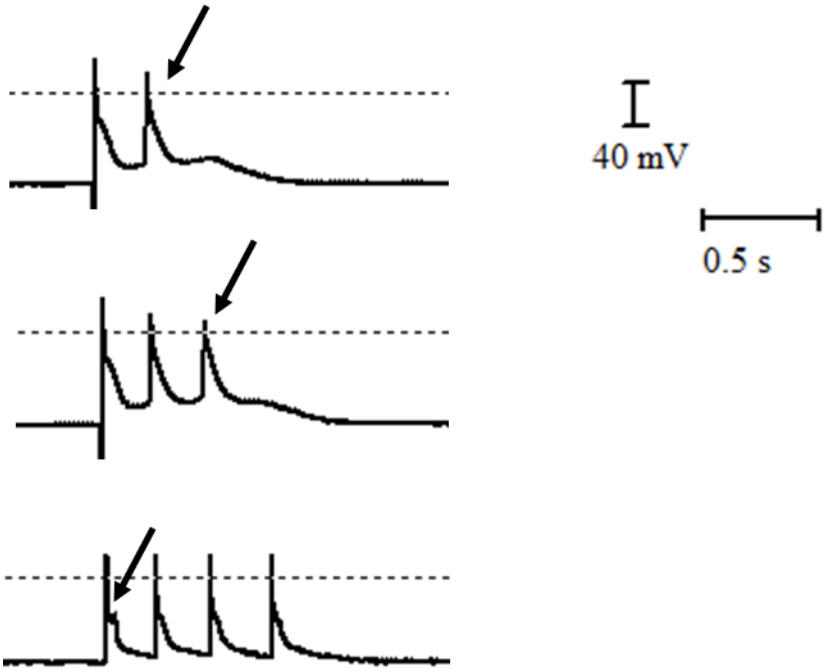

Figure 4-8 Examples showing the application of NA 100 μM induced the genesis of early after-depolarisations (EADs) in the rat PV cardiomyocytes under 1 g stretch.The arrow indicates EADs.

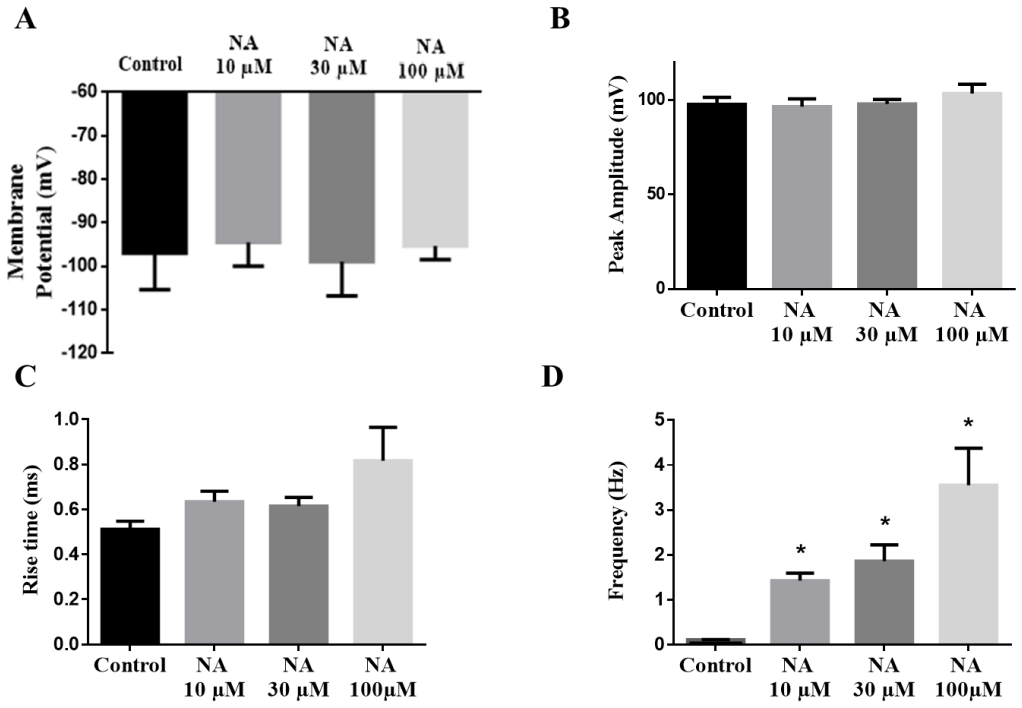

Figure 4-9 The action potential properties and contraction activity of non-cumulative administration of NA in the rat PV cardiomyocytes under 1g stretch

(A) Resting membrane potential (B) Peak amplitude (C) Rise time of action potential, and (D) Frequency of action potential. All data are presented as mean ± s.e.m., *$p<0.05$ vs Control group (0g), and n=4.

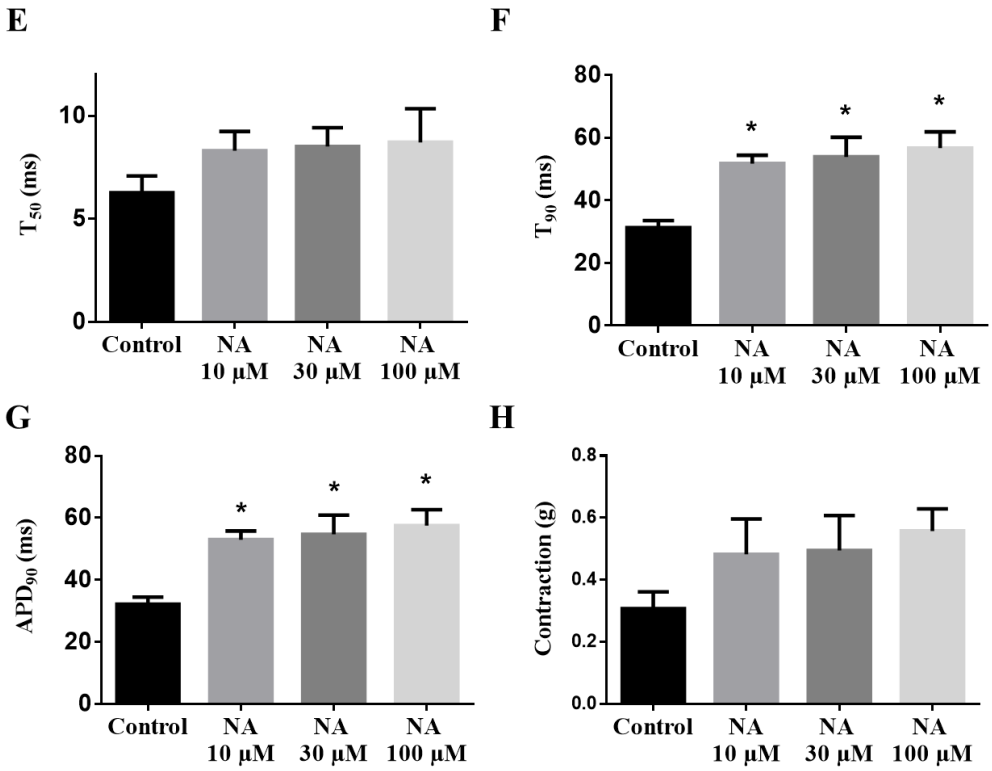

Figure 4-9 (Cont.) (E) Time taken for 50% repolarisation (T_{50}), (F) Time taken for 90% repolarisation (T_{90}), (G) The duration at 90% repolarisation (APD_{90}) of action potentials, and (H) Contraction amplitude. All data are presented as mean ± s.e.m., and n=4.

Table 4-3 Effect of non-cumulative administration of NA on action potentials in the rat PV cardiomyocytes under stretch

Action potential parameters	Control	NA 10 μM	NA 30 μM	NA 100 μM
Resting membrane potential (mV)	-96.9 ± 8.4	-94.5 ± 5.5	-98.9 ± 7.9	-95.3 ± 3.1
Peak amplitude (mV)	97.9 ± 3.7	96.6 ± 4.1	98.1 ± 2.3	103.6 ± 4.9
Rise time (ms)	0.5 ± 0.04	0.6 ± 0.1	0.6 ± 0.04	0.8 ± 0.1
Frequency (Hz)	0.1 ± 0.004	1.4 ± 0.2*	1.9 ± 0.4*	3.6 ± 0.8*
T_{50} (ms)	6.3 ± 0.8	8.3 ± 0.9	8.5 ± 0.9	8.7 ± 1.6
T_{90} (ms)	31.3 ± 2.3	51.8 ± 2.7*	53.9 ± 6.3*	56.7 ± 5.2*
APD_{90} (ms)	32.2 ± 2.2	53.0 ± 2.8*	54.7 ± 6.2*	57.5 ± 5.1*
Contraction amplitude (g)	0.3±0.1	0.5±0.1	0.5±0.1	0.6±0.7

All data are presented as mean ± s.e.m., and n=4**.**

*p<0.05 vs Control group (0g).

4.3.4 Effect of gadolinium on the combined stretch and NA induced ectopic activity of the rat PV cardiomyocytes

The rat PV cardiomyocytes displayed incidence of ectopic activity under 1 g stretch combined with NA 100 μM (Figure 4-10A). The presence of gadolinium 80 μM inhibits stretch-induced changes in electrical activity and contraction in rat atrial myocytes (Tavi et al., 1996). Figure 4-10B shows that gadolinium 80 μM inhibited the ectopic action potentials induced by the combination of stretch and NA. Figure 4-11D shows that gadolinium significantly decreased the frequency of NA-induced automaticity under 1g stretch from 3.7 ± 0.6 Hz to 1.0 ± 0.3 Hz ($n=6$, $p<0.05$).

The presence of gadolinium 80 μM had no effect on RMP (Figure 4-11A), nor peak amplitude of the action potential in rat PV cardiomyocytes (Figure 4-11B). Treatment with gadolinium caused no statistically significant changes in rise time, T50, T90 and APD90 of action potentials compared with the control, as shown in Figure 4-11F, and Table 4-4. In addition, no statistically significant change was detected in the contraction parameter (Figure 4-11E).

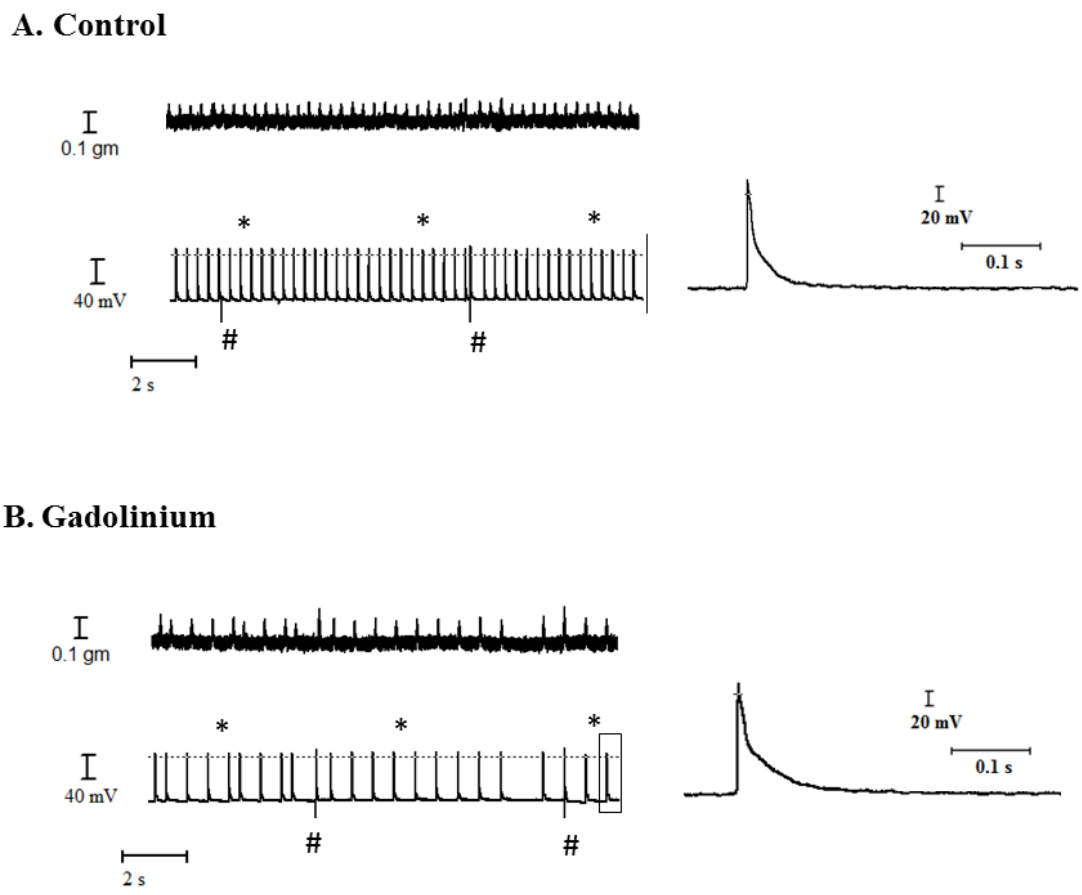

Figure 4-10 Effect of gadolinium on the combination of stretch and NA induced ectopic activity in the rat PV cardiomyocytes. (A) Representative recordings of twitch tension and action potential in absence of gadolinium (control; the combination of stretch and NA 100 µM) (B) Representative recordings of twitch tension and action potential in presence of gadolinium 80 µM. The expanded segments present the pre-post gadolinium. # indicates electrical stimulation, * indicates NA induced ectopic action potential and n=6.

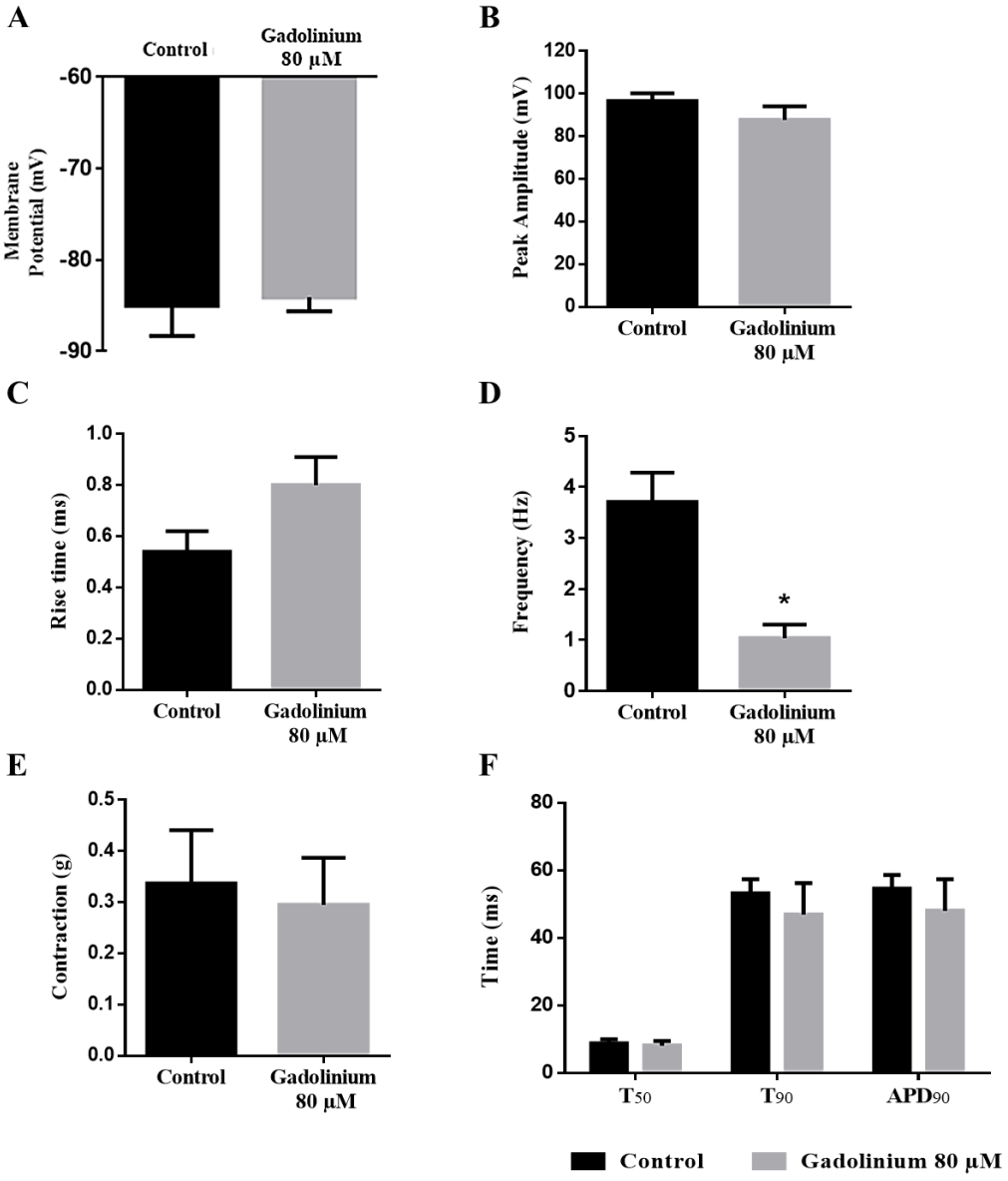

Figure 4-11 Effect of gadolinium on the action potential parameters of the PVs with the combination of stretch and NA. Control; the combination of stretch and NA 100 µM, Gadolinium 80 µM (A) Resting membrane potential (B) Peak amplitude (C) Rise time of action potential, (D) Frequency of action potential (E) Contraction amplitude (F) Time taken for 50% repolarisation (T_{50}), Time taken for 90% repolarisation (T_{90}), and the duration at 90% repolarisation (APD_{90}) of action potentials. All data are presented as mean ± s.e.m., * $p < 0.05$ vs control and n=6.

Table 4-4 The effect of gadolinium on action potential parameters of ectopic activity induced by combined stretch and NA in the rat PV cardiomyocytes

Action potential parameters	Control	Gadolinium 80 μM
Resting membrane potential (mV)	-85.0 ± 3.3	-84.1 ± 1.5
Peak amplitude (mV)	96.6 ± 3.7	87.8 ± 6.3
Rise time (ms)	0.5 ± 0.1	0.8 ± 0.1
Frequency (Hz)	3.7 ± 0.6	1.0 ± 0.3*
T_{50} (ms)	8.8 ± 1.2	8.1 ± 1.3
T_{90} (ms)	53.2 ± 4.2	46.9 ± 9.4
APD_{90} (ms)	54.6 ± 4.0	48.0 ± 9.4
Contraction amplitude (g)	0.3±0.1	0.3±0.1

All data are presented as mean ± s.e.m., and n=6**.**

*p<0.05 vs control group (0g).

4.3.5 Effect of verapamil on the combined stretch and NA induced ectopic activity of the rat PV cardiomyocytes

In control, the combination of stretch and NA 100 µM induced ectopic action potentials in the rat PV myocardium (Figure 4-12A). The application of Ca^{2+} channel blocker; verapamil 1 µM reversed the stretch activated increase in intracellular Ca^{2+} in isolated guinea pig ventricular myocytes (Gannier et al., 1996). The effect of verapamil on the combination of stretch and NA induced ectopic activity of the rat PV cardiomyocytes is illustrated in Figure 4-12B.

Treatment with verapamil significantly decreased the frequency of NA-induced automaticity under the stretch condition from 3.6 ± 0.7 Hz to 0.5 ± 0.1 Hz (n=6, $p<0.05$, Figure 4-13D). However, verapamil had no effect on RMP (Figure 4-13A) or action potential peak amplitude (Figure 4-13B).

Moreover, the rise time, T50, T90 and APD90 of action potentials were not significantly altered in the presence of verapamil when compared with control group (Figure 4-13F). Verapamil also had no effect on the contraction amplitude of the rat PV (0.3 ± 0.1g) when compared with the PV control (0.3 ± 0.1g) as illustrated in Figure 4-13E, and Table 4-5.

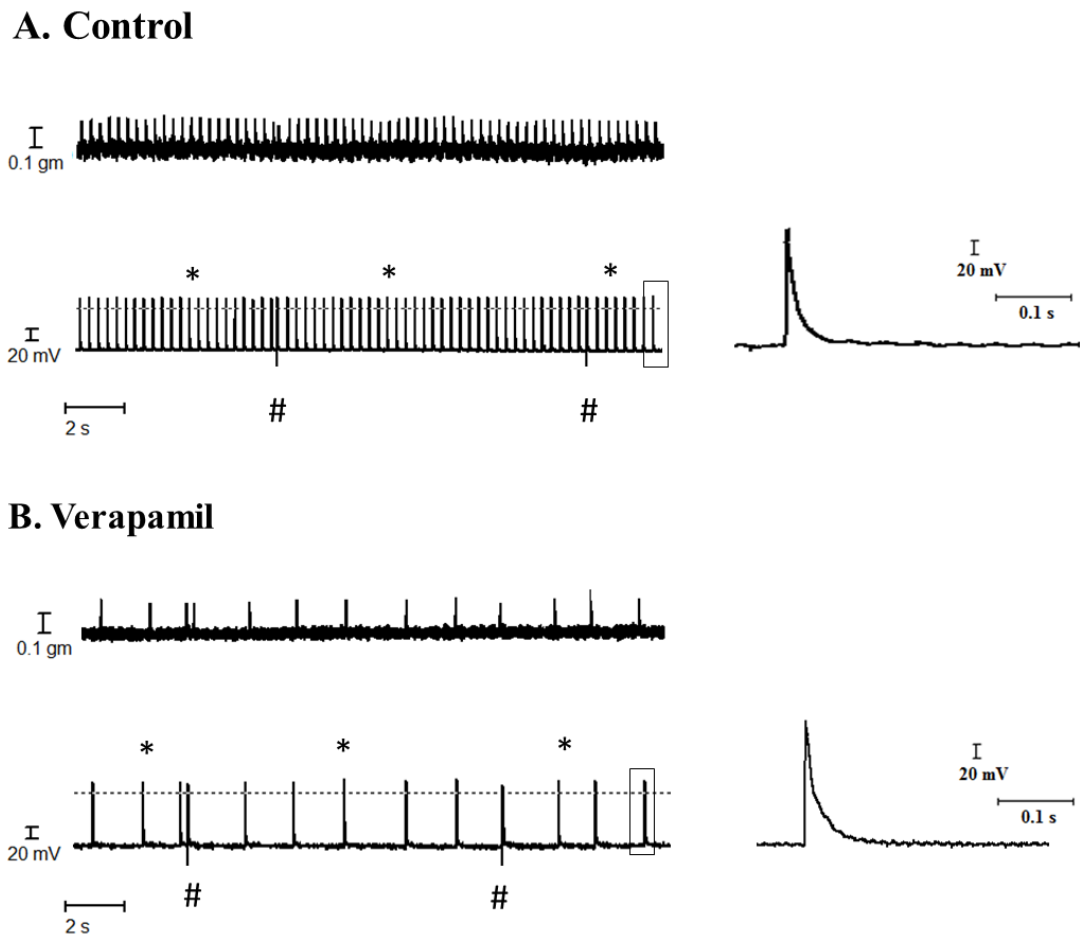

Figure 4-12 Effect of verapamil on the combination of stretch and NA induced ectopic activity of the rat PV cardiomyocytes. (A) Representative recordings of twitch tension and action potential in absence of verapamil, (control; the combination of stretch and NA 100 µM) (B) Representative recordings of twitch tension and action potential in presence of verapamil 1 µM. The expanded segments present the pre-post verapamil, # Electrical stimulation, * NA induced ectopic action potential and (n=6).

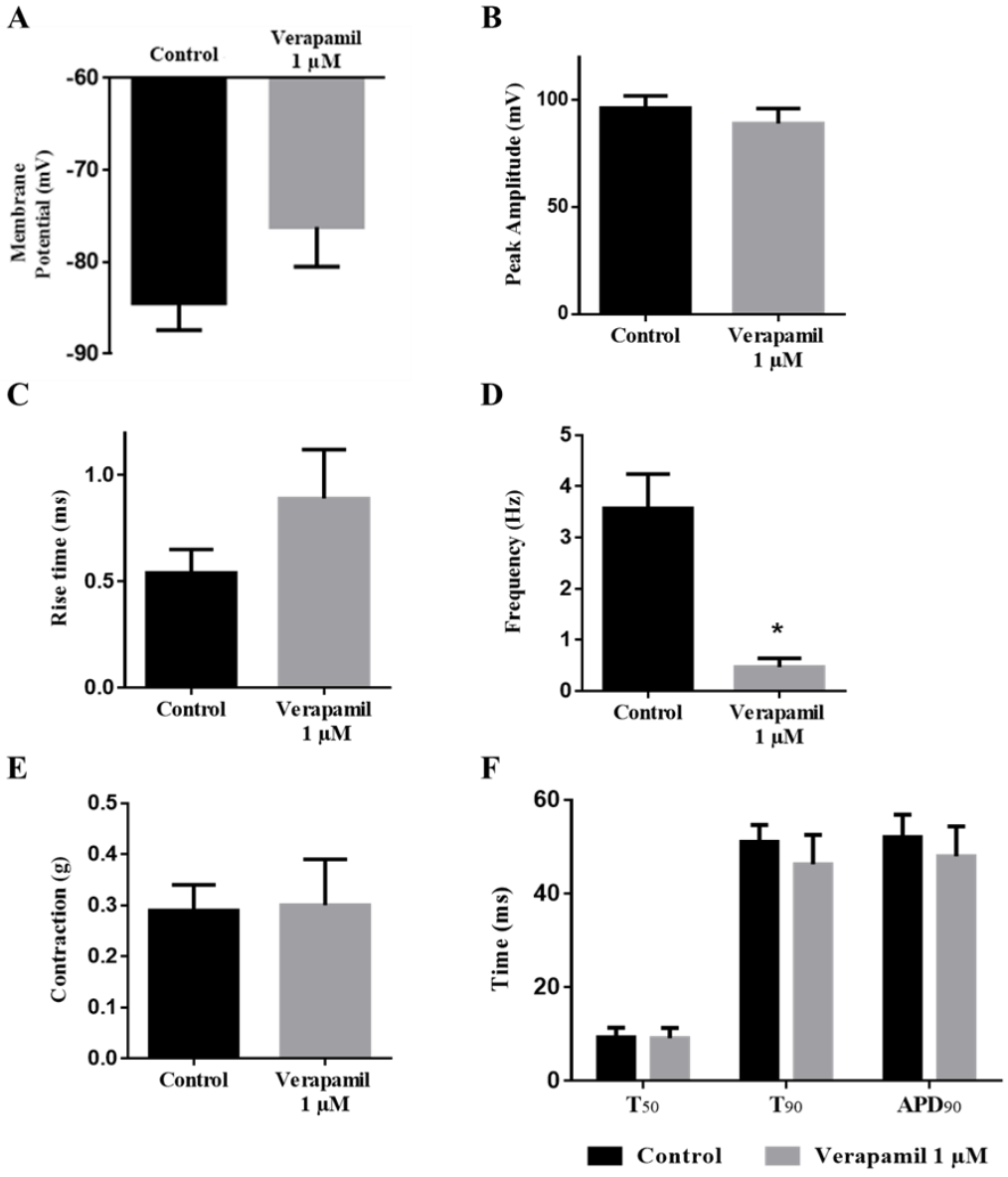

Figure 4-13 Effect of verapamil on the action potential parameters of the PVs with the combination of stretch and NA. Control; the combination of stretch and NA 100 µM, Verapamil 1 µM (A) Resting membrane potential (B) Peak amplitude (C) Rise time of action potential, (D) Frequency of action potential (E) Contraction amplitude (F) Time taken for 50% repolarisation (T_{50}), Time taken for 90% repolarisation (T_{90}), and the duration at 90% repolarisation (APD_{90}) of action potentials. All data are presented as mean ± s.e.m., * $p < 0.05$ vs control and n=6.

Table 4-5 The effect of verapamil on action potential parameters of ectopic activity induced by combined stretch and NA in the rat PV cardiomyocytes

Action potential parameters	Control	Verapamil 1 μM
Resting membrane potential (mV)	-85.0 ± 2.9	-76.2 ± 4.3
Peak amplitude (mV)	96.2 ± 5.8	89.0 ± 7.04
Rise time (ms)	0.5 ± 0.1	0.9 ± 0.2
Frequency (Hz)	3.6 ± 0.7	0.5 ± 0.2*
T_{50} (ms)	9.3 ± 2.1	9.1 ± 2.2
T_{90} (ms)	51.1 ± 3.6	46.3 ± 6.4
APD_{90} (ms)	52.1 ± 4.8	48.0 ± 6.4
Contraction amplitude (g)	0.3±0.1	0.3±0.1

All data are presented as mean ± s.e.m., and n=6**.**

*p<0.05 vs Control group (0g).

4.3.6 Effect of ORM-10103 on the combined stretch and NA induced ectopic activity of the rat PV cardiomyocytes

The presence of ORM 10103 ranging from 0.1 to 10 μM reduced both the outward and the inward NCX currents in a concentration-dependent manner in canine ventricular myocytes (Jost et al., 2013). The present study shows that the combination of stretch and NA as a control group induced ectopic action potentials in the rat PV cardiomyocytes (Figure 4-14A). The representative recording in Figure 4-14B shows ORM-10103 1 μM reduced the ectopic action potentials in the rat PV cardiomyocytes.

ORM-10103 had no effect on the RMP and peak amplitude of ectopic action potentials in the rat PV myocardium compared with the control group, as seen in Figure 4-15A and B (n=6). The action potential rise time was not significantly changed by ORM-10103 (Figure 4-15C). Treatment with ORM-10103 significantly reduced the frequency of NA-induced automaticity under stretch from 3.6 ± 0.5 Hz to 1.1 ± 0.2 Hz (n=6, $p<0.05$, Figure 4-15D). However, ORM-10103 did not significantly alter rise time, T50, T90 and APD90 of action potentials (Figure 4-15F) as well as ectopic contraction in the rat PVs as shown in Figure 4-15E and Table 4-6).

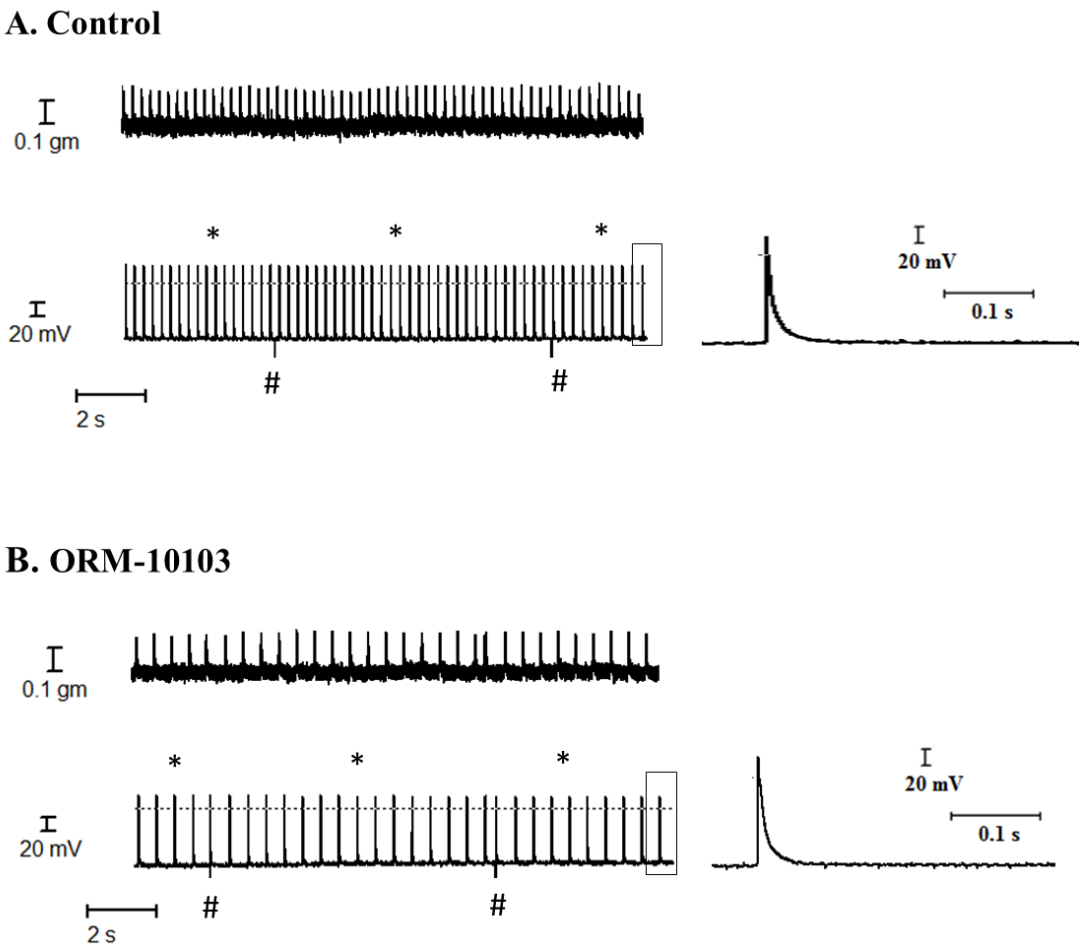

Figure 4-14 Effect of ORM-10103 on the combination of stretch and NA induced ectopic activity in the rat PV cardiomyocytes. (A) Representative recordings of twitch tension and action potential in absence of ORM-10103, (control; the combination of stretch and NA 100 µM) (B) Representative recordings of twitch tension and action potential in presence of ORM-10103 1 µM. The expanded segments present the pre-post verapamil, # Electrical stimulation, * NA induced ectopic action potential and (n=6).

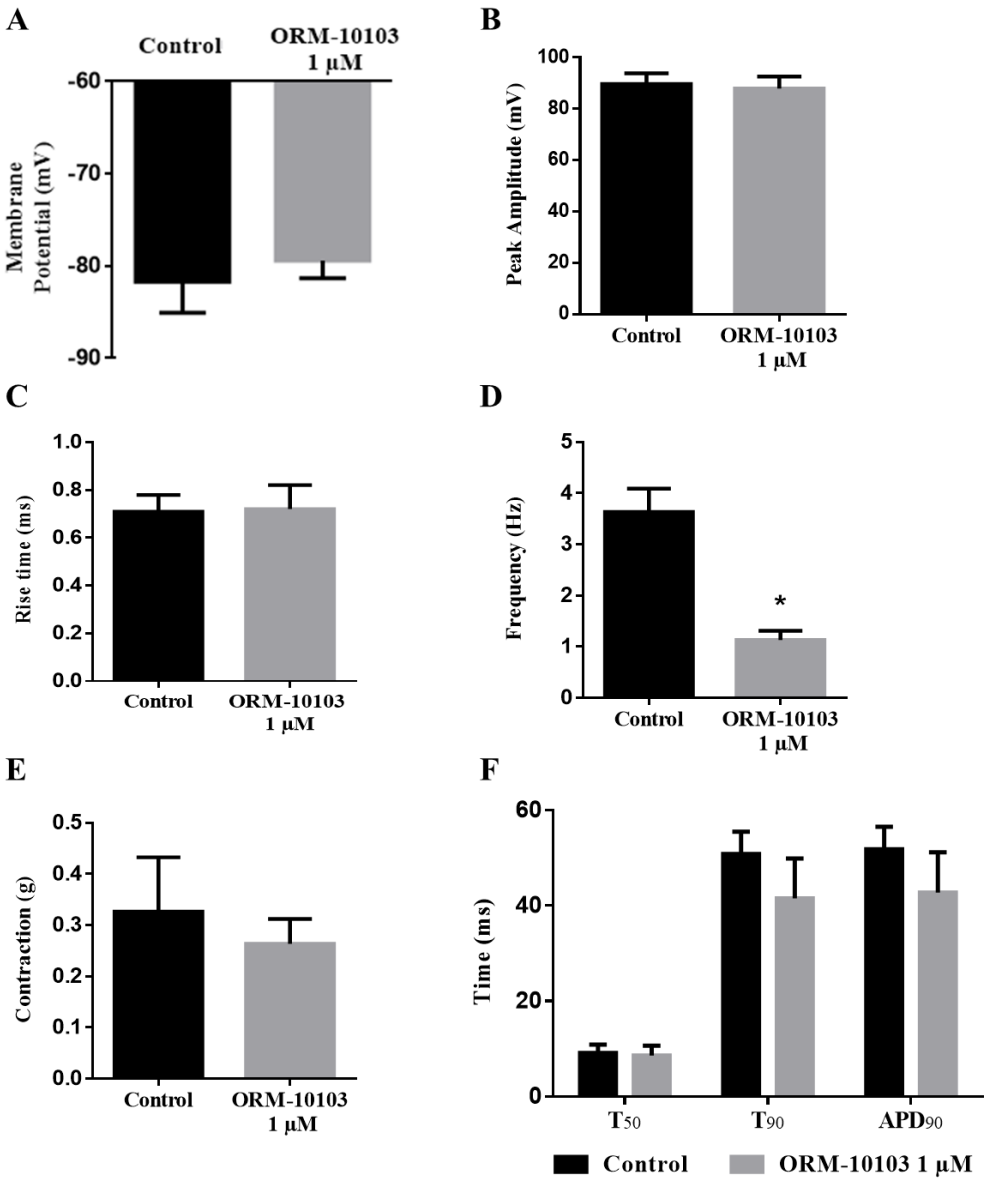

Figure 4-15 Effect of ORM-10103 on the action potential parameters of the PVs with the combination of stretch and NA. Control; the combination of stretch and NA 100 µM, ORM-10103 1 µM (A) Resting membrane potential (B) Peak amplitude (C) Rise time of action potential, (D) Frequency of action potential (E) Contraction amplitude (F) Time taken for 50% repolarisation (T_{50}), Time taken for 90% repolarisation (T_{90}), and the duration at 90% repolarisation (APD_{90}) of action potentials. All data are presented as mean ± s.e.m., * $p < 0.05$ vs control and n=6.

Table 4-6 The effect of ORM-10103 on action potential parameters of ectopic activity induced by combined stretch and NA in the rat PV cardiomyocytes

Action potential parameters	Control	ORM-10103 1 μM
Resting membrane potential (mV)	-81.7 ± 3.4	-79.4 ± 1.9
Peak amplitude (mV)	89.7 ± 4.2	88.0 ± 4.6
Rise time (ms)	0.7 ± 0.1	0.7 ± 0.1
Frequency (Hz)	3.6 ± 0.5	1.1 ± 0.2*
T_{50} (ms)	9.1 ± 1.7	8.6 ± 2.1
T_{90} (ms)	50.8 ± 4.6	41.5 ± 8.3
APD_{90} (ms)	51.9 ± 4.7	42.7 ± 8.5
Contraction amplitude (g)	0.3±0.1	0.3±0.04

All data are presented as mean ± s.e.m., and n=6**.**

*p<0.05 vs Control group (0g).

4.3.7 Effect of prazosin on the combination of stretch and NA induced ectopic activity of the rat PV cardiomyocytes

Prazosin; an α_1- adrenoceptor antagonist (1 μM) inhibited ectopic activity induced by NA in the rat PVs (Maupoil et al., 2007, Doisne et al., 2009). Therefore, to observe any effects of α-adrenergic blockade on the combination of stretch and NA induced ectopic activity of the rat PV cardiomyocytes, prazosin was added to the preparation (Figure 4-16).

Treatment with prazosin had no effect on the RMP (Figure 4-17A) or action potential peak amplitude of ectopic action potentials in the rat PV myocardium (n=6, Figure 4-17B). However, prazosin did significantly reduce the frequency of spontaneous action potentials in rat PV cardiomyocytes under the combination of stretch and NA from 3.6 ± 0.5 to 0.4 ± 0.1 Hz (n=6, $p<0.05$, Figure 4 17D).

There were no statistically significant changes in rise time, T50, T90 or APD90 of action potentials compared with the PV control, as seen in Figure 4-17F. As summarised in Table 4-7, the presence of prazosin did not significantly decrease the amplitude of ectopic contraction in the PV (Figure 4-17E).

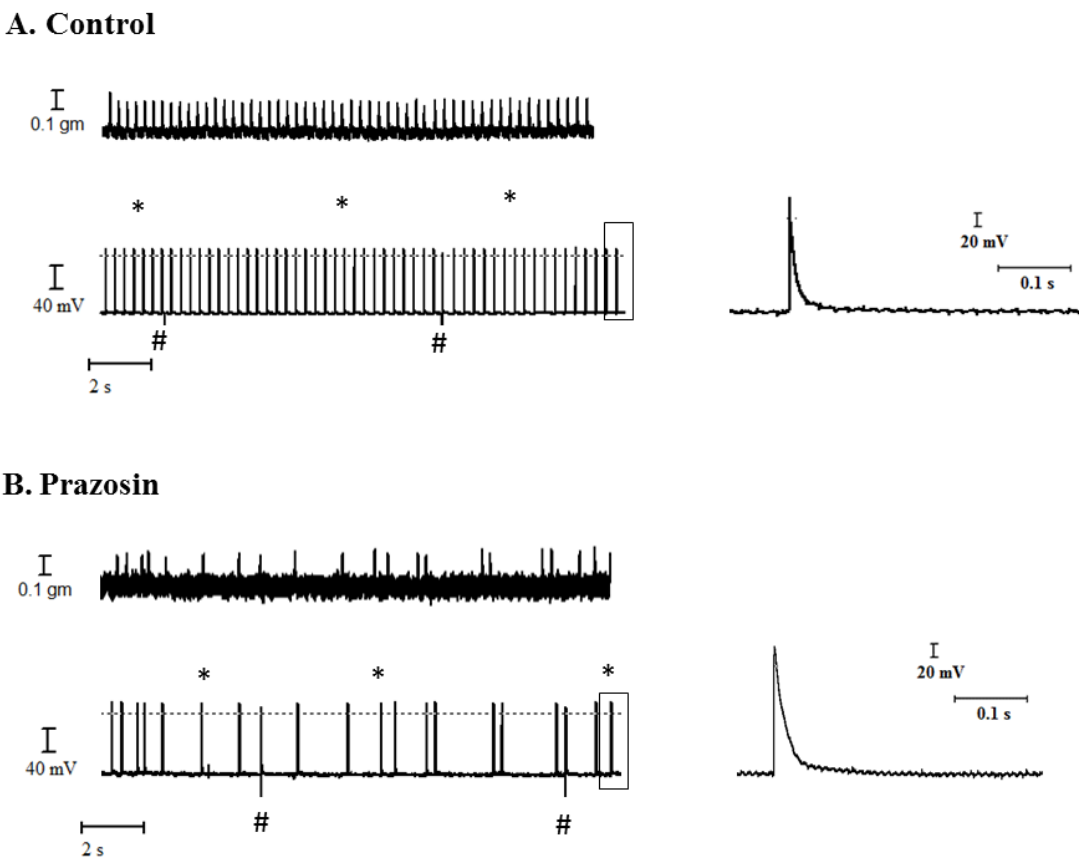

Figure 4-16 Effect of prazosin on the combination of stretch and NA induced ectopic activity in the rat PV cardiomyocytes. (Control; the combination of stretch and NA 100 µM) (A) Representative recordings of twitch tension and action potential in absence of prazosin, (B) Representative recordings of twitch tension and action potential in presence of prazosin 1 µM. The expanded segments present the pre-post prazosin, # Electrical stimulation, * NA induced ectopic action potential and (n=6).

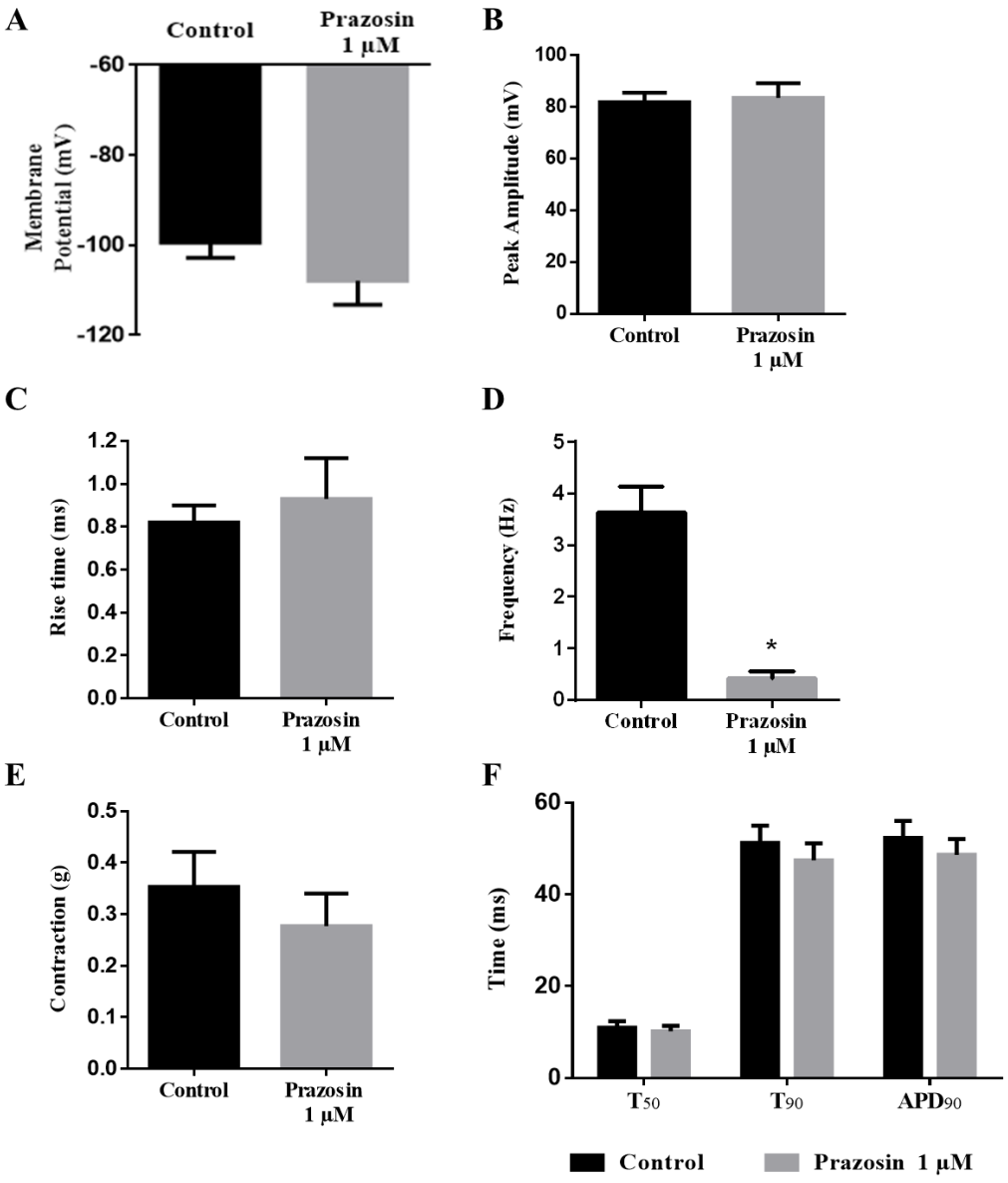

Figure 4-17 Effect of prazosin on the action potential parameters of the PVs with the combination of stretch and NA. Control; the combination of stretch and NA 100 µM, Prazosin1 µM (A) Resting membrane potential (B) Peak amplitude (C) Rise time of action potential, (D) Frequency of action potential (E) Contraction amplitude (F) Time taken for 50% repolarisation (T_{50}), Time taken for 90% repolarisation (T_{90}), and the duration at 90% repolarisation (APD_{90}) of action potentials. All data are presented as mean ± s.e.m., * $p < 0.05$ vs control and n=6.

Table 4-7 The effect of prazosin on action potential parameters of ectopic activity induced by combined stretch and NA in the rat PV cardiomyocytes

Action potential parameters	Control	Prazosin 1 μM
Resting membrane potential (mV)	-81.1 ± 2.0	-77.3 ± 2.6
Peak amplitude (mV)	81.9 ± 3.7	83.6 ± 5.7
Rise time (ms)	0.8 ± 0.1	0.9 ± 0.2
Frequency (Hz)	3.6 ± 0.1	0.4 ± 0.1*
T_{50} (ms)	11.0 ± 1.4	10.2 ± 1.2
T_{90} (ms)	51.21 ± 3.74	47.44 ± 3.68
APD_{90} (ms)	52.34 ± 3.71	48.64 ± 3.44
Contraction amplitude (g)	0.4 ± 0.1	0.3 ± 0.03

All data are presented as mean ± s.e.m., and n=6**.**

*p<0.05 vs Control group (0g).

4.3.8 Effect of propranolol on the combination of stretch and NA induced ectopic activity of the rat PV cardiomyocytes

The presence of propranolol 1 μM inhibited the responses to electrical stimulation in the rat LA (Doggrell, 1990). The present study shows that NA 100 μM combined with 1g stretch was applied to generate spontaneous activity in rat PV cardiomyocytes as the control condition (Figure 4-18A). The effect of β-adrenoceptor blockade was studied by perfusing with propranolol (Figure 4-18B).

Microelectrode studies demonstrated that propranolol had no effect on the RMP or the peak amplitude of ectopic action potentials, as shown in Figure 4-19A and B. However, the frequency of NA-induced automaticity under stretch was significantly reduced by propranolol from 3.6 ± 0.6 to 0.2 ± 0.04 Hz ($n=6$, $p<0.05$, Figure 4-19D).

Detailed examination of the ectopic action potentials revealed that the presence of propranolol 1 μM did not alter the combination of stretch and NA induced changes in the rise time, T50, T90 and APD90 of action potentials compared with the control group, as seen in Figure 4-19C and F. Moreover, the amplitude of contraction was not significantly different after applying propranolol to the rat PV preparations (Figure 4-19E, and Table 4-8).

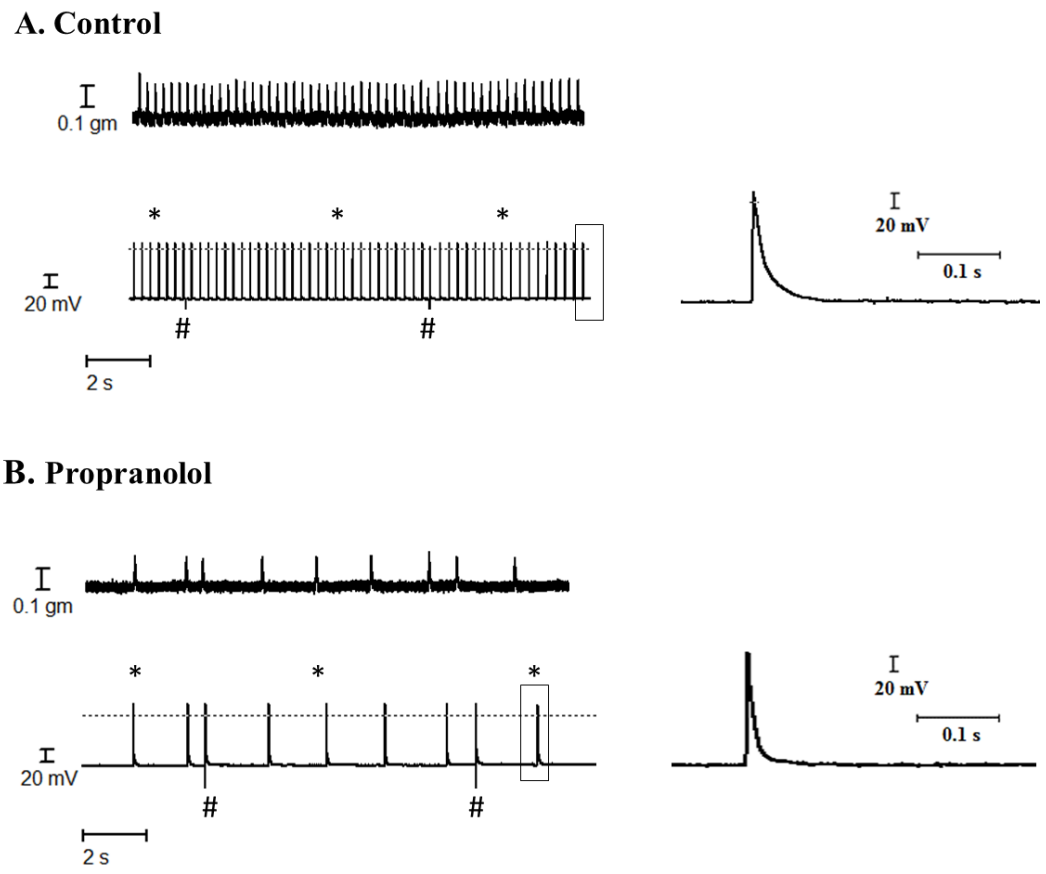

Figure 4-18 Effect of propranolol on the combination of stretch and NA induced ectopic activity of the rat PV cardiomyocytes. (Control; the combination of stretch and NA 100 µM) (A) Representative recordings of twitch tension and action potential in absence of propranolol (B) Representative recordings of twitch tension and action potential in presence of propranolol 1 µM. The expanded segments present the pre-post propranolol, # Electrical stimulation, * NA induced ectopic action potentials and (n=6).

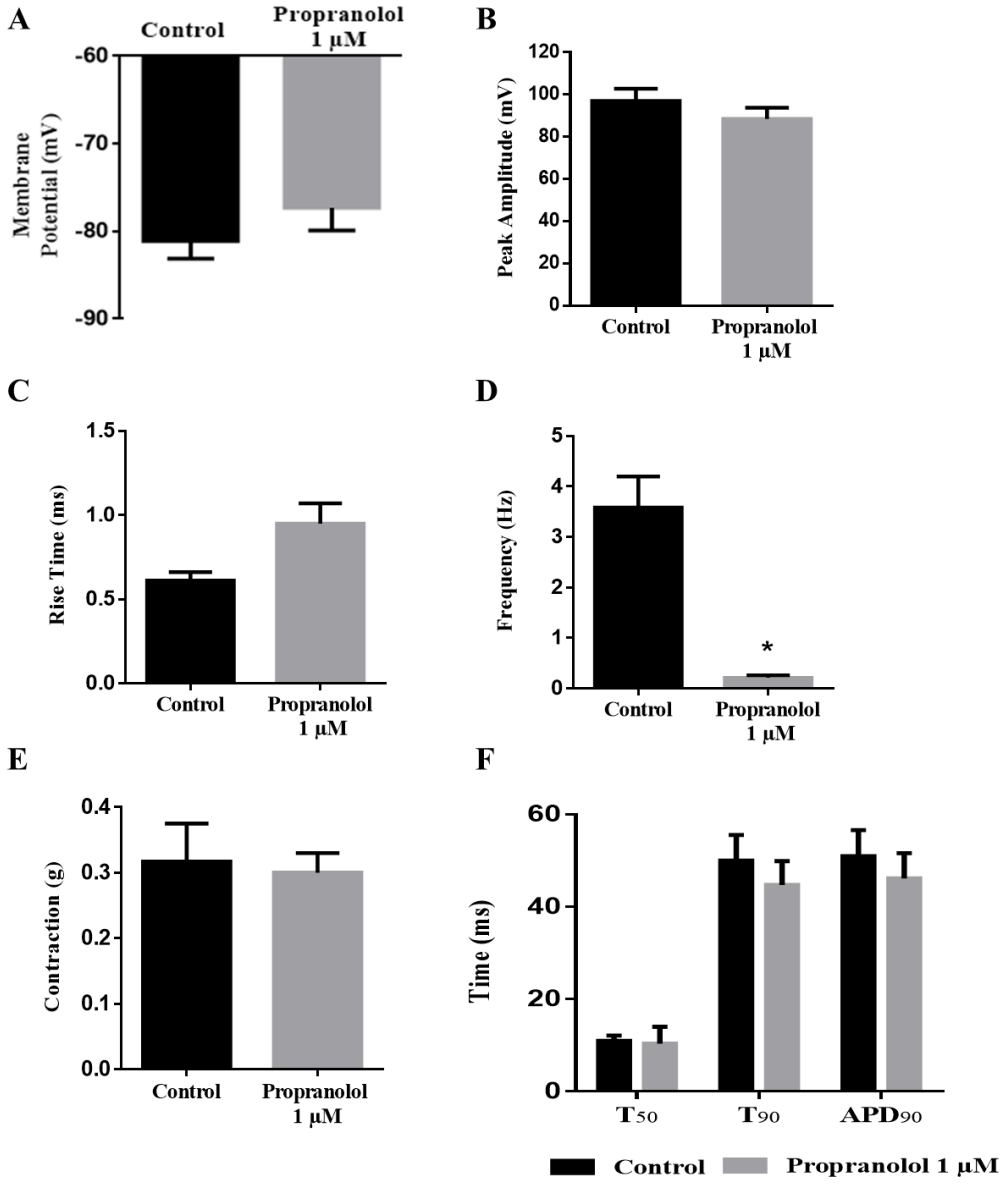

Figure 4-19 Effect of propranolol on the action potential parameters of the PVs with the combination of stretch and NA. Control; the combination of stretch and NA 100 µM, Propranolol 1 µM (A) Resting membrane potential (B) Peak amplitude (C) Rise time of action potential, (D) Frequency of action potential (E) Contraction amplitude (F) Time taken for 50% repolarisation (T_{50}), Time taken for 90% repolarisation (T_{90}), and the duration at 90% repolarisation (APD_{90}) of action potentials. All data are presented as mean ± s.e.m., * $p < 0.05$ vs control and n=6.

Table 4-8 The effect of propranolol on action potential parameters of ectopic activity induced by combined stretch and NA in the rat PV cardiomyocytes

Action potential parameters	Control	Propranolol 1 μM
Resting membrane potential (mV)	-83.3 ± 2.2	-81.2 ± 3.7
Peak amplitude (mV)	96.9 ± 5.9	88.4 ± 5.4
Rise time (ms)	0.6 ± 0.1	1.0 ± 0.1
Frequency (Hz)	3.6 ± 0.6	0.2 ± 0.04*
T_{50} (ms)	11.0 ± 1.1	10.4 ± 3.7
T_{90} (ms)	50.0 ± 5.6	44.7 ± 5.2
APD_{90} (ms)	51.0 ± 5.7	46.2 ± 5.4
Contraction amplitude (g)	0.3±0.1	0.3±0.03

All data are presented as mean ± s.e.m., and n=6**.**

*p<0.05 vs Control group (0g)

4.4 Discussion

4.4.1 Effect of stretch-induced spontaneous activity in the rat PV cardiomyocytes

In the present study stretch increased the incidence of spontaneous electrical and mechanical activity but had no noticeable effect on action potential characteristics in rat PV cardiomyocytes. This is consistent with Hamaguchi et al. (2016), who reported that mechanical stretch increases the firing rate of spontaneous electrical activity but does not action potential parameters in guinea pig PV myocardium. In contrast, Chang et al. (2007) showed that stretch changed the electrophysiological properties, shortened APD and increased the incidence of spontaneous activity in rabbit PV cardiomyocytes.

Previous studies have shown that mechanoelectrical feedback leads to changes in the electrical activity of the heart (Nazir, 1996a, Chang et al., 2007). This mechanoelectrical feedback is induced by the activation of SACs, which can affect both the inward and outward ionic currents, resulting in the change of APD and increasing automaticity (Ruknudin et al., 1993, Ravelli and Allessie, 1997, Patterson et al., 2006). These results suggest that stretch is an important factor in electrical activity of the PVs, although its specific effect on action potentials is debated. It is fair to hypothesise that stretch-induced arrhythmogenic activity of the PVs may be involved in the genesis of AF.

4.4.2 Effect of NA on stretch-induced spontaneous activity in rat PV cardiomyocytes

This study has also shown that application of NA increases the generation of ectopic action potentials, prolongs APD and induces EADs in rat PV cardiomyocytes under 1 g stretch. This observation is consistent with earlier studies of the PVs described above. In addition, it has been shown that NA and isoproterenol prolong the terminal phase of repolarisations (EADs), which is enhanced by increasing Ca^{2+} transient and NCX currents in canine hearts (Patterson et al., 2006). Tsuneoka et al. (2012) demonstrated that NA induces automaticity activity and EADs in mouse PV myocardium. Likewise, a study in isolated ventricular myocytes from patients with heart failure showed prolonged APD and induced EADs in the presence of NA (Veldkamp et al., 2001).

The sympathetic and parasympathetic nervous systems play important roles in autonomic activity, which generate and sustain AF (Namekata et al., 2010). Previous studies in rabbit, guinea pig, rat, and mouse PV cardiomyocytes have shown that NA, stimulating both α and β adrenoceptors, induces automatic electrical activity (Doisne et al., 2009, Namekata et al., 2010, Takahara et al., 2011, Tsuneoka et al., 2012).

The application of NA also induces EADs, which are generated at the end of the action potential plateau phase, resulting in prolonged APD. EADs relate to increased inward I_{CaL} (January et al., 1991) or activation of the NCX channels in response to Ca^{2+} release from the SR, which causes Ca^{2+} overload and action potential prolongation (Szabo et al., 1994, Nattel and Dobrev, 2012). The PVs might be a particular point of initiation of automatic electrical activity. Hocini et al. (2000) demonstrated the predominant

source of ectopic activity initiating AF was located in individual human PVs. Tan et al. (2008) also showed that the ectopic foci responsible for initiating AF have high densities of sympathetic nerves and PAS-positive specialized conduction cells in PVs of the dog. Some studies have shown ganglionated plexi at the PV-LA junction where adrenergic neurotransmitters induce excess Ca^{2+} intracellularly leading to Ca^{2+} overload and generating EADs in PV cells (Scherlag et al., 2006, Tan et al., 2006). This may suggest that NA-induced action potential prolongation and EADs in rat PV cardiomyocytes could be related to the induction of AF via the sympathetic nervous system.

4.4.3 Effect of pharmacological agents on stretch-induced spontaneous activity in rat PV cardiomyocytes

In the present study, gadolinium (80 μM) decreased the incidence of spontaneous electrical activity in rat PV cardiomyocytes caused by combining stretch and NA. This is in agreement with previous reports in rabbit atrial cardiomyocytes (Bode et al., 2000), rabbit PV myocardium (Chang et al., 2007, Seol et al., 2008) and guinea pig PV cardiomyocytes (Hamaguchi et al., 2016). Gadolinium, a SAC blocker, has been shown to inhibit the effect of stretch-induced changes in the action potential and EADs/DADs in rat and rabbit cardiac cells (Tavi et al., 1996, Bode et al., 2000, Seol et al., 2008). The mechanical stretch-induced increase in spontaneous activity in guinea pig PV cardiomyocytes was decreased by gadolinium (Hamaguchi et al., 2016). Previous studies have also shown that gadolinium can inhibit stretch-induced automaticity in rabbit PV myocardium in a dose-dependent manner (Chang et al.,

2007). Similarly, Seol et al. (2008) demonstrated that gadolinium suppresses the swelling-induced stretch-activated nonselective cationic currents and mechanical stretch-activated nonselective cationic currents in cardiomyocytes isolated from rabbit PVs. In addition, a study in isolated ventricular myocytes has shown that gadolinium inhibits cardiac I_{CaL}, at a concentration of 10 μM (Lacampagne et al., 1994), and NCX currents, at a concentration of 100 μM (Zhang and Hancox, 2000). Thus, this finding suggests that gadolinium at concentration 80 μM may have antiarrhythmic potential, which would indicate a non-specific action, involving the SAC, LTCC and NCX.

In the present study, verapamil (1 μM), a specific LTCC-blocker, significantly decreased the occurrence of ectopic action potentials in the rat PV myocardium under the stretch plus NA condition. This may be in agreement with previous reports by (Gannier et al., 1996) , which demonstrated that the stretch-induced increase in intracellular Ca^{2+} in isolated guinea pig ventricular myocytes can be reversed by verapamil. Similarly, verapamil has been shown to slightly decreased the incidence of spontaneous activity in rabbit PV cardiomyocytes during stretch (Chang et al., 2007). Previous studies have shown stretch can increase I_{CaL} through LTCC (Kamkin et al., 2003a), which prolonged APD in mouse ventricular myocytes. Matsuda et al. (1996) also reported that stretch increased I_{CaL} in rabbit atrial myocytes and sinoatrial node cells. In contrast, Eckardt et al. (2000) reported verapamil (1 μM) had no effect on stretch-induced changes in repolarisation and stretch-induced arrhythmias in isolated rabbit ventricles. In addition, verapamil did not inhibit AF induction during acute dilatation in rabbit hearts (Bode et al., 2000). Therefore, these apparently conflicting reports may suggest that verapamil, rather than having a direct effect on SACs, acts on LTCC in PV cardiomyocytes.

The present study also investigated the effects of ORM 10103, an NCX inhibitor, on stretch plus NA induced ectopic action potentials. ORM 10103 was found to decrease the number of ectopic events. Previous studies in human, mouse, and rat cardiomyocytes have shown that mechanical stretch increases intracellular Na^+ concentrations via SACs, activating NCX, which enhances Ca^{2+} influx through the cell membrane (Tavi et al., 1998, Alvarez et al., 1999, Baartscheer et al., 2003a, Isenberg et al., 2003). Considering the action of ORM-10103, it may be suggested that this effect is caused by inhibiting the NCX process, limiting Ca^{2+} influx into the cell, therefore preventing PV cardiomyocytes from generating rapid ectopic events.

This study demonstrated that the application of prazosin (1 μM) and propranolol (1 μM) decreased the number of ectopic events in the rat PV myocardium during stretch in the presence of NA, which is consistent with previous reports in mouse and rat PVs by Okamoto et al. (2012), which demonstrated prazosin and propranolol block NA-induced automaticity in rat PV cardiomyocytes. It has also been shown that prazosin, a selective α_1-adrenergic receptor antagonist, and atenolol, a selective β_1-receptor antagonist, have an inhibitory effect on catecholamine-induced autonomic activity in the rat PV (Doisne et al., 2009). In addition, propranolol, a β-adrenoceptor blocker, inhibits the effect of NA-induced automatic electrical activity in the mouse PV myocardium (Tsuneoka et al., 2012).

In rat atrial myocytes, automaticity activity induced by stretch is enhanced by isoproterenol. Isoproterenol, which produces β-adrenergic stimulation, can therefore modulate the effects of stretch (Wagner et al., 2004). Kuz'min and Rozenshtraukh (2012a) also demonstrated that isoproterenol induces changes in electrical activity and

excitability of the rat PV myocardium. Studies in rat, mouse and guinea pig myocardium have all shown that NA induces automaticity in PV preparations (Doisne et al., 2009, Takahara et al., 2011, Tsuneoka et al., 2012).

In conclusion, this study has shown that stretch induces ectopic action potentials in rat PV cardiomyocytes, which is enhanced by the application of NA. Stretch-activated ion channels are thought to contribute largely to this abnormal electrical activity. Application of NA increases this effect via the sympathetic nervous system, α-β adrenoceptor stimulation, and increasing Ca^{2+} influx into cardiac muscle cells. Additionally, the combination of stretch and NA may increase intracellular Ca^{2+} via the activation of NCX in reverse mode. Overall, these findings indicate that stretch-induced arrhythmogenic activity may be involved in the generation of AF.

Mechanical stretch may affect cardiomyocytes via opening of SACs that leads to Na^{+} and Ca^{2+} entry into the cells (Reed et al., 2014, Hamaguchi et al., 2016). As a consequence of increasing permeability to Na^{+}, increased intracellular Na^{+} leads to the activation of the NCX and intracellular influx of Ca^{2+} (Tavi et al., 1998). Stretch also alters intracellular Ca^{2+} concentration by the entry of Ca^{2+} via LTCC; as reviewed by Calaghan et al. (2003) and Lammerding et al. (2004). Gadolinium (SACs blocker), ORM-10103 (a selective inhibitor of the NCX current), and verapamil (Ca^{2+}channel blocker) reduce the incidence of stretch-induced ectopic action potentials enhanced by NA in the rat PV myocardium. Considering prior knowledge of these drugs, we may suggest that gadolinium inhibits stretch-induced electrical changes by blocking SACs; ORM-10103 inhibits ectopic action potentials by blocking the NCX currents; and verapamil reverses these stretch and NA induced changes by blocking Ca^{2+} influx

through LTCC during stretch. Furthermore, prazosin (α_1-blocker) and propranolol (non-selective β -blocker) also decreased the frequency of NA-induced automaticity under 1 g stretch. These findings suggest a complex interaction of cellular mechanisms including physical stretch and adrenergic stimulation induce arrhythmogenic activity, which may provide a substrate to initiate and sustain AF.

Chapter 5. General Discussion

5.1 Characteristics of cardiomyocytes in the rat PV and atria

Chapter 2 the characteristics of cardiomyocytes found in the rat PV and atria were revealed using Masson's trichrome staining. The PV sections showed that cardiomyocytes are located outside of the adventitial layer, separated from smooth muscle. Longitudinal sections of the rat PV showed myocardial sleeves extending from LA into the PVs. This study revealed a non-uniform alignment of myocardial fibres within sleeves. Moreover, transverse sections showed the circumferential fibre arrangement surrounding the lumen of the PVs. Higher magnification of the PV sections showed the rectangular and striated appearance of the cardiac muscle fibres, which are similar to the cardiomyocytes found in the LA. The LA and PV staining sections also revealed that cardiomyocytes contain one or two nuclei, which are located centrally within the cells. Additionally, intercalated discs were found at the end-to-end junctions of cardiomyocytes in both sections. Nathan and Eliakim (1966) demonstrated the presence of myocardial sleeves extending over human PVs. Cheung (1981a) demonstrated that action potentials and automaticity were recorded at the distal end of the PVs, which could be generated within these myocardial sleeves. Moreover, Haissaguerre et al. (1998) reported that myocardial sleeves within the PVs were a source of ectopic beats possibly involved in the initiation of AF. Therefore, the present studies confirm that cardiomyocytes extend from LA into the PV, which forms a myocardial sleeve, in agreement with previous findings in humans and other mammals (Calkins et al., 2008, Namekata et al., 2010, Takahara et al., 2011, Tsuneoka et al., 2012), and may be associated with the occurrence of AF.

5.2 Identification of the SAN and the expression HCN4 channel of the rat PV and atria

In the present study, the SAN was identified using Masson's trichrome staining in the rat RA. The location of the rat SAN is positioned between the SVC and the roof of the RA, near to the sinus node artery. Under a light microscope, the SAN cells are observed as small, ovoid, pale staining and poorly striated in appearance, which are different from atrial muscle cells. However, in this study using Masson's trichrome staining, node cells were not observed in any area of the rat PV section.

It has been reported that the SAN is the pacemaker of the heart (Satoh, 2003). In humans and rodents, the SAN is located in the posterior wall of the RA, extending from the superior vena cava. (Satoh, 2003, Liu et al., 2007, Ferreira et al., 2011, Wen and Li, 2015, Huang et al., 2016). These nodal cells exhibit a clear, structureless and pale appearance (Waller et al., 1993, Satoh, 2003).

In this study using light microscopy did not reveal node-like cells in any area of the rat PV section. Saito et al. (2000) and Perez-Lugones et al. (2003) also found no evidence of node-like cells in normal human PV preparations under light microscopy. However, Masani (1986) demonstrated that node-like cells are present in the myocardial sleeve of the rat PVs with the electron microscope. The electron microscope technique generally produces much higher resolution images than light microscopy, which may account for this considering the characteristics of node-like cells. They are reported to have appeared with the typical clear structure, either individually or in small groups, among the ordinary myocardium. Using periodic acid-Schiff (PAS) staining for glycogen, which is contained in node cells, Chou et al. (2005)

showed positive findings for node-like cells in the canine PV under a light microscope. Perez-Lugones et al. (2003) also identified myocardial cells with pale cytoplasm in the PV of humans with AF by light microscopy and electron microscopy. Therefore, to identify node-like cells in the PV, the electron microscope technique may be considered for closer examination of the tissue staining. Moreover, the overall pathological conditions of the heart, with or without exhibiting AF, may relate to the presence of node-like cells in the PV preparation and our ability to identify these using different imaging techniques.

To further investigate the differences between SAN and atrial muscle cells, immunohistochemistry was used to identify the expression of HCN4, a specific maker for node cells, responsible for the pacemaker current (I_f) in the heart (Bois et al., 2011). The RA section showed the expression of HCN4 in SAN cells but not in atrial muscle cell area. In the rat PV section, no significant expression of HCN4 protein was observed. This is in agreement with previous studies in rats, which showed that HCN4 is highly expressed in the SAN, but not in PVs (Yamamoto et al., 2006, Xiao et al., 2016). However, the recent study by Li et al. (2014) showed high expression levels of HCN4 channel mRNA and proteins in the atria and PVs of aged dogs; this may relate to the overall pathological condition of the dogs' hearts. Therefore, immunohistochemistry can be used to identify HCN4, a marker of SAN cells, in the RA but not in the PVs. The source of arrhythmogenic activity involved in the initiation of AF may not have an influence on node-like cells in the normal PVs. However, pathological conditions encountered in aging, e.g. heart failure, may be associated with the ectopic beats originating in the myocardial sleeves of the PVs.

5.3 NA induced ectopic activity in the rat PVs

Chapter 3 findings showed that NA, a non-selective adrenoceptor agonist, induces ectopic activity in the rat PV at 37°C. This ectopic activity was decreased by reducing the temperature to 25°C. Increasing extracellular Ca^{2+} also changed ectopic contraction characteristics, specifically increasing the frequency and the duration of ectopic contractions in the rat PVs. Prazosin (α_1-blocker), propranolol (β-blocker), carbachol (cholinergic agonist), and verapamil (Ca^{2+} channel blocker) decreased the number of ectopic events generated by NA.

This study shows ectopic activity recorded from cardiomyocytes in the PV. The autonomic nervous system has two divisions; sympathetic nervous system and parasympathetic nervous system, which are both known to influence the automaticity of the PV myocardium (Namekata et al., 2013). Increasing catecholaminergic activity is an important stimulator of enhanced automaticity in PV cardiomyocytes (Mahida et al., 2015). The stimulation of adrenergic and cholinergic activity regulates multiple cardiac ion currents (e.g. Na^+, K^+ and Ca^{2+}), which has an influence on the generation and maintenance of AF (Workman, 2010). Maupoil et al. (2007) demonstrated that ectopic activity in the PV requires activation of both α and β adrenoceptors. Likewise, studies in PV myocardium have shown that NA induces automatic electrical activity in guinea pig, rat and mouse PV cardiomyocytes (Cheung, 1981a, Doisne et al., 2009, Namekata et al., 2010, Takahara et al., 2011, Tsuneoka et al., 2012). As noted, ectopic activity in the rat PV may relate to the α-adrenergic receptor signalling pathway, which activates phospholipase C (PLC), and the β-adrenergic receptor signalling pathway, which stimulates protein kinase A (PKA). These pathways cause increased Ca^{2+} entry

into the cells via LTCC and enhanced release of Ca^{2+} from the sarcoplasmic reticulum in the heart. Therefore, PVs receive both sympathetic and parasympathetic innervations, which are considered to play important roles in the generation of AF through their effects on the PV cardiomyocytes.

Furthermore, temperature plays a key role in the modulation of contractile and electrophysiological activity of cardiomyocytes. In isolated rat PVs, ectopic activity increased in response to stimulations by NA at 37°C but not at the lower temperature of 25°C. This is consistent with previous reports in rabbit PV by Chen et al. (2003), isolated rabbit atria by Beaulnes and Day (1957), and in dog hearts by Patterson et al. (2006), where increasing temperature increases the isometric tension, duration of force development, and duration of action potentials. Chen et al. (2003) also showed PV cardiomyocytes have larger transient inward currents at high temperature compared with low temperature. Thus, temperature may have an influence on electrophysiological properties and the genesis of arrhythmogenic activity in PV cardiomyocytes.

Overall, results obtained from the rat PV indicate that the sympathetic neuronal influence on the PV myocardium leads to the generation of automatic activity through activation of both α- and β-adrenergic receptors. These mechanisms may be involved in the generation and maintenance of AF, with the PV acting as an origin under the autonomic nervous control.

5.4 Stretch induced changes in PV cardiomyocytes

Chapter 4 showed that stretch increased the incidence of spontaneous activity but had no effect on the action potential characteristics in rat PV cardiomyocytes. This study also shows that application of NA increases the incidence of ectopic action potentials, prolongs APD and induces EADs in rat PV cardiomyocytes under 1 g stretch.

Previous studies have shown that mechanical stretch increases the firing rate of spontaneous electrical activity in the PV myocardial layer (Ravelli, 2003, Chang et al., 2007). Stretch also induces activation of SACs, which increases intracellular Na^+ and Ca^{2+} and results in changes of APD and increasing automaticity (Seol et al., 2008, Seol et al., 2011). In addition, application of NA to cardiomyocytes induces changes in electrical activity followed by the generation of automaticity activity in guinea pig, rat and mouse PV myocardium (Namekata et al., 2010, Doisne et al., 2009, Tsuneoka et al., 2012).

In addition, EADs occur during the action potential plateau or during late repolarisation (Gaztañaga et al., 2012, Nattel and Dobrev, 2012). Stretch can trigger arrhythmias caused by EADs and DADs of the membrane potential (Tavi et al., 1996). The mechanism suggested to be responsible for these arrhythmias is the Ca^{2+} overload caused by stretch (Lab, 1996, Chang et al., 2007, Seol et al., 2011). During the stretch-induced Ca^{2+} overload, the Ca^{2+}-induced inactivation of the I_{CaL} opens a time window in which the increased NCX current can trigger EADs (Tavi et al., 1998). Moreover, NA can generate EADs by increasing inward I_{CaL}, resulting in increased intracellular Ca^{2+} and subsequently activating Ca^{2+} release from the sarcoplasmic reticulum. Spontaneous Ca^{2+} release from the sarcoplasmic reticulum leads to reverse-mode

activation of the NCX, causing Ca^{2+} overload and subsequently generating EADs (January et al., 1991, Vassalle and Lin, 2004, Nattel and Dobrev, 2012, Tse et al., 2016).

Therefore, this study suggested that stretch changed electrophysiological activity in the rat PVs, which enhanced the automatic activity induced by the application of NA. In addition, the combination of stretch and NA may induce Ca^{2+} overload generated EADs, resulting in prolonged APD, which occurred during phase 2 of the action potential.

Gadolinium is known as a potent SAC blocker, and has been widely used in atrial ventricular myocytes and PV myocardium (Tavi et al., 1996, Bode et al., 2000, Hansen et al., 1991, Zeng et al., 2000, Chang et al., 2007, Seol et al., 2008, Hamaguchi et al., 2016). It has also been reported that gadolinium blocks Ca^{2+} channels by inhibiting I_{CaL} in a dose-dependent manner (Lacampagne et al., 1994). Another study also showed that gadolinium inhibits NCX currents in isolated guinea pig ventricular myocytes (Zhang and Hancox, 2000). Finding that gadolinium inhibits changes induced by stretch plus NA may demonstrate the antiarrhythmic potential of blocking SACs; however, contributions from Ca^{2+} and NCX must also be considered.

Treatment with ORM-10103 (NCX inhibitor) can be used as inward and outward NCX current inhibitors (Terracciano and Hancox, 2013). In this study, ORM-10103 also suppressed the ectopic action potentials in the rat PVs, suggesting that the NCX is involved in the combination of stretch and NA mediated arrhythmogenic activity. Stretch-induced SAC opening leads to Na^{+} influx to the cells, subsequently rising intracellular Na^{+}, which favours Ca^{2+} entry via reverse mode of the NCX (Rice and

Bers, 2011). Thus, ORM-10103 may inhibit the NCX process, limiting Ca^{2+} influx into the cell, therefore preventing PV cardiomyocytes from generating ectopic events.

Furthermore, prazosin (α_1-blocker) and propranolol (non-selective β-blocker) also decreased the frequency of NA-induced automaticity under stretch. In rat atrial myocytes, stretch-induced automaticity is enhanced by isoproterenol (β-adrenergic stimulation) (Wagner et al., 2004). Moreover, NA induces automaticity in PV preparations from rat, mouse and guinea pig myocardium (Doisne et al., 2009, Namekata et al., 2010, Takahara et al., 2011, Tsuneoka et al., 2012). These results may suggest that the sympathetic nervous system influences the PV myocardium leading to the generation of automaticity through activation of both α- and β-adrenergic receptors.

Stretch may be the precipitating factor in changing the electrophysiological properties of the PVs, which can be reversed by SAC, NCX, and calcium channel blockers. NA enhances the arrhythmogenic activity of PVs, which was inhibited by the effect of both α_1 and β adrenoceptor blockers. These findings suggest that stretch and catecholamines may be linked to AF originating in the PVs.

5.5 Summary

To summarise, this study has shown that histological techniques in rats confirm that cardiomyocytes extend from the LA into the PV, which forms a myocardial sleeve, in agreement with previous findings in humans and other mammals. This histological study also identified the SAN located in the RA. SAN cells are observed as small, ovoid, pale staining and poorly striated in appearance, which are clearly different from atrial muscle cells viewed under a light microscope. However, the node-like cells were not observed in any area of the rat PV section. Further using immunohistochemistry, HCN4, a marker of pacemaker cells, was found in SAN cells but not in atrial muscle cells. In addition, the expression of HCN4 protein was not detected in any area of the rat PVs. Therefore, the present study indicates that cardiomyocytes extend from LA into the PV, which forms a myocardial sleeve that may be associated with the occurrence of AF; although in this physiological 'normal' preparation node-like cells were not seen in the PV. Considering that node-like cells were not observed in the PV sections, it is plausible to suggest that AF triggered by the PV may not involve these cell types.

NA-induced ectopic activity in rat PVs was mediated via α-β-adrenergic receptors, indicating that increased catecholaminergic activity is an important mediator of enhanced automaticity in rat PV cardiomyocytes. Furthermore, mechanical stretch also induced changes in electrical characteristics and induced ectopic action potentials in the rat PVs. SACs may be an important link between stretch and ectopic activity in PV, potentially acting as a main factor in the development of AF. Thus, stretching of the PVs may be considered as an influence on AF.

In this thesis, we used tissues obtained from healthy animals to investigate the anatomical and physiological properties of PVs, which may be considered the primary limitation of this study. To confirm these findings and further our understanding of the mechanism of AF in the PV, pathophysiological tissue samples from humans with AF may be used in future studies. Moreover, the examination of arrhythmogenic properties of the PV has revealed that Ca^{2+} may be associated with ectopic activity and EADs under stretching conditions. Further investigation with Ca^{2+} imaging techniques using the Ca^{2+} sensitive fluorescent indicator, fluo-4, could be implemented to monitor intracellular Ca^{2+} on stretch-induced activity in rat PV cardiomyocytes. Better knowledge of factors regulating arrhythmias generated in the PV will lead to the discovery and development of novel therapeutic strategies and pharmacological agents for treatment of AF.

References

ABERNETHY , D. R. & SCHWARTZ , J. B. 1999. Calcium-Antagonist Drugs. *New England Journal of Medicine,* 341**,** 1447-1457.

AIMOND, F., RAUZIER, J.-M., BONY, C. & VASSORT, G. 2000. Simultaneous activation of p38 MAPK and p42/44 MAPK by ATP stimulates the K+ current ITREK in cardiomyocytes. *Journal of Biological Chemistry,* 275**,** 39110-39116.

ALDHOON, B. & KAUTZNER, J. 2012. Complications of catheter ablation for atrial fibrillation. *Cor et Vasa,* 54**,** e414-e420.

ALTOMARE, C., TERRAGNI, B., BRIOSCHI, C., MILANESI, R., PAGLIUCA, C., VISCOMI, C., MORONI, A., BARUSCOTTI, M. & DIFRANCESCO, D. 2003. Heteromeric HCN1–HCN4 Channels: A Comparison with Native Pacemaker Channels from the Rabbit Sinoatrial Node. *The Journal of Physiology,* 549**,** 347-359.

ALVAREZ, B. V., PÉREZ, N. G., ENNIS, I. L., DE HURTADO, M. C. C. & CINGOLANI, H. E. 1999. Mechanisms Underlying the Increase in Force and Ca2+ Transient That Follow Stretch of Cardiac Muscle A Possible Explanation of the Anrep Effect. *Circulation research,* 85**,** 716-722.

ANDERSON, J. L. & PRYSTOWSKY, E. N. 1999. Sotalol: An important new antiarrhythmic. *American Heart Journal,* 137**,** 388-409.

ARMOUR, J. A., MURPHY, D. A., YUAN, B.-X., MACDONALD, S. & HOPKINS, D. A. 1997. Gross and microscopic anatomy of the human intrinsic cardiac nervous system. *The Anatomical Record,* 247**,** 289-298.

ÁRNADÓTTIR, J. & CHALFIE, M. 2010. Eukaryotic Mechanosensitive Channels. *Annual Review of Biophysics,* 39**,** 111-137.

ARORA, R. & KODURI, H. K. 2014. Mechanisms of Atrial Fibrillation. *In:* KIBOS, A. S., KNIGHT, B. P., ESSEBAG, V., FISHBERGER, S. B., SLEVIN, M. & ȚINTOIU, I. C. (eds.) *Cardiac Arrhythmias: From Basic Mechanism to State-of-the-Art Management.* London: Springer London.

ARORA, R., NG, J., ULPHANI, J., MYLONAS, I., SUBACIUS, H., SHADE, G., GORDON, D., MORRIS, A., HE, X., LU, Y., BELIN, R., GOLDBERGER, J. J. & KADISH, A. H. 2007. Unique Autonomic Profile of the Pulmonary Veins and Posterior Left Atrium. *Journal of the American College of Cardiology,* 49**,** 1340-1348.

ARORA, R., ULPHANI, J. S., VILLUENDAS, R., NG, J., HARVEY, L., THORDSON, S., INDERYAS, F., LU, Y., GORDON, D., DENES, P., GREENE, R., CRAWFORD, S., DECKER, R., MORRIS, A., GOLDBERGER, J. & KADISH, A. H. 2008. Neural substrate for atrial fibrillation: implications for targeted parasympathetic blockade in the posterior

left atrium. *American Journal of Physiology - Heart and Circulatory Physiology,* 294**,** H134-H144.

BAARTSCHEER, A., SCHUMACHER, C., VAN BORREN, M., BELTERMAN, C., CORONEL, R. & FIOLET, J. 2003a. Increased Na^+/H^+-exchange activity is the cause of increased $[Na^+]$ i and underlies disturbed calcium handling in the rabbit pressure and volume overload heart failure model. *Cardiovascular research,* 57**,** 1015-1024.

BAARTSCHEER, A., SCHUMACHER, C. A., BELTERMAN, C. N. W., CORONEL, R. & FIOLET, J. W. T. 2003b. [Na+]i and the driving force of the Na+/Ca2+-exchanger in heart failure. *Cardiovascular Research,* 57**,** 986-995.

BARANCHUK, A., MORILLO, C. A., THOENES, M., VENTURA, R. & CONNOLLY, S. J. 2008. Current role of medical therapy for prevention or termination of atrial fibrillation. *Atrial Fibrillation.* Springer.

BAUMGARTEN, C. M. 2013. *Origin of mechanotransduction: stretch-activated ion channels* [Online]. Available: https://www.ncbi.nlm.nih.gov/books/NBK6374/.

BEAULNES, A. & DAY, M. 1957. Effect of temperature on arrhythmia in isolated rabbit atria. *The Journal of Physiology,* 137**,** 86-94.

BELUS, A. & WHITE, E. 2003. Streptomycin and intracellular calcium modulate the response of single guinea- pig ventricular myocytes to axial stretch. *The Journal of physiology,* 546**,** 501-509.

BENJAMIN, E. J., LEVY, D., VAZIRI, S. M., D'AGOSTINO, R. B., BELANGER, A. J. & WOLF, P. A. 1994. Independent risk factors for atrial fibrillation in a population-based cohort: The framingham heart study. *JAMA,* 271**,** 840-844.

BERDAJS, D., PATONAY, L. & TURINA, M. I. 2003. The clinical anatomy of the sinus node artery. *The Annals of Thoracic Surgery,* 76**,** 732-735.

BERLIN, J., CANNELL, M. & LEDERER, W. J. 1989. Cellular origins of the transient inward current in cardiac myocytes. Role of fluctuations and waves of elevated intracellular calcium. *Circulation Research,* 65**,** 115-126.

BETT, G. & SACHS, F. 2000. Whole-cell mechanosensitive currents in rat ventricular myocytes activated by direct stimulation. *The Journal of membrane biology,* 173**,** 255-263.

BISHOP, S. P. & COLE, C. R. 1967. Morphology of the specialized conducting tissue in the atria of the equine heart. *The Anatomical Record,* 158**,** 401-415.

BJØRNSTAD, H., TANDE, P. M., LATHROP, D. A. & REFSUM, H. 1993. Effects of temperature on cycle length dependent changes and restitution of action

potential duration in guinea pig ventricular muscle. *Cardiovascular Research,* 27**,** 946-950.

BODE, F., KATCHMAN, A., WOOSLEY, R. L. & FRANZ, M. R. 2000. Gadolinium decreases stretch-induced vulnerability to atrial fibrillation. *Circulation,* 101**,** 2200-2205.

BODE, F., SACHS, F. & FRANZ, M. R. 2001. Tarantula peptide inhibits atrial fibrillation. *Nature,* 409**,** 35-36.

BOIS, P., CHATELIER, A., BESCOND, J. & FAIVRE, J.-F. 2011. Pharmacology of hyperpolarization-activated cyclic nucleotide-gated (HCN) channels. *Ion Channels and Their Inhibitors.* Springer.

BOLTER, C. P. & ATKINSON, K. J. 1988. Influence of temperature and adrenergic stimulation on rat sinoatrial frequency. *American Journal of Physiology - Regulatory, Integrative and Comparative Physiology,* 254**,** R840-R844.

BOWMAN, C. L., GOTTLIEB, P. A., SUCHYNA, T. M., MURPHY, Y. K. & SACHS, F. 2007. Mechanosensitive Ion Channels and the Peptide Inhibitor GsMTx-4: History, Properties, Mechanisms and Pharmacology. *Toxicon : official journal of the International Society on Toxinology,* 49**,** 249-270.

BOYDEN, P. A., TILLEY, L. P., ALBALA, A., LIU, S. K., FENOGLIO, J. J. & WIT, A. L. 1984. Mechanisms for atrial arrhythmias associated with cardiomyopathy: a study of feline hearts with primary myocardial disease. *Circulation,* 69**,** 1036-1047.

BOYETT, M. R., HONJO, H. & KODAMA, I. 2000. The sinoatrial node, a heterogeneous pacemaker structure. *Cardiovascular Research,* 47**,** 658-687.

BREZDEN, B. L., GARDNER, D. R. & MORRIS, C. E. 1986. A Potassium-Selective Channel in Isolated Lymnaea Stagnalis Heart Muscle Cells. *Journal of Experimental Biology,* 123**,** 175.

BRIOSCHI, C., MICHELONI, S., TELLEZ, J. O., PISONI, G., LONGHI, R., MORONI, P., BILLETER, R., BARBUTI, A., DOBRZYNSKI, H. & BOYETT, M. R. 2009. Distribution of the pacemaker HCN4 channel mRNA and protein in the rabbit sinoatrial node. *Journal of molecular and cellular cardiology,* 47**,** 221-227.

BUSH, E. W., HOOD, D. B., PAPST, P. J., CHAPO, J. A., MINOBE, W., BRISTOW, M. R., OLSON, E. N. & MCKINSEY, T. A. 2006. Canonical transient receptor potential channels promote cardiomyocyte hypertrophy through activation of calcineurin signaling. *Journal of Biological Chemistry,* 281**,** 33487-33496.

CALAGHAN, S. & WHITE, E. 1999. The role of calcium in the response of cardiac muscle to stretch. *Progress in biophysics and molecular biology,* 71**,** 59-90.

CALAGHAN, S. C., BELUS, A. & WHITE, E. 2003. Do stretch-induced changes in intracellular calcium modify the electrical activity of cardiac muscle? *Progress in Biophysics and Molecular Biology,* 82**,** 81-95.

CALKINS, H., HO, S. Y., ANGEL CABRERA, J., DELLA BELLA, P., FARRE, J., KAUTZNER, J. & TCHOU, P. 2008. Anatomy of the left atrium and pulmonary veins. *International Journal of Cardiology, Blackwell, USA,* 1-10.

CAVALIÉ, A., MCDONALD, T. F., PELZER, D. & TRAUTWEIN, W. 1985. Temperature-induced transitory and steady-state changes in the calcium current of guinea pig ventricular myocytes. *Pflügers Archiv,* 405**,** 294-296.

CHAMBERLAIN, P., JENNINGS, K., PAUL, F., CORDELL, J., BERRY, A., HOLMES, S., PARK, J., CHAMBERS, J., SENNITT, M. & STOCK, M. 1999. The tissue distribution of the human β3-adrenoceptor studied using a monoclonal antibody: Direct evidence of the β3-adrenoceptor in human adipose tissue, atrium and skeletal muscle. *International journal of obesity,* 23**,** 1057-1065.

CHANDLER, N. J., GREENER, I. D., TELLEZ, J. O., INADA, S., MUSA, H., MOLENAAR, P., DIFRANCESCO, D., BARUSCOTTI, M., LONGHI, R., ANDERSON, R. H., BILLETER, R., SHARMA, V., SIGG, D. C., BOYETT, M. R. & DOBRZYNSKI, H. 2009. Molecular Architecture of the Human Sinus Node. *Insights Into the Function of the Cardiac Pacemaker,* 119**,** 1562-1575.

CHANG, S.-L., CHEN, Y.-C., CHEN, Y.-J., WANGCHAROEN, W., LEE, S.-H., LIN, C.-I. & CHEN, S.-A. 2007. Mechanoelectrical feedback regulates the arrhythmogenic activity of pulmonary veins. *Heart,* 93**,** 82-88.

CHANG, S. L., CHEN, Y.C., CHEN, Y.J. 2007. Mechanoelectrical feedback regulates the arrhythmogenic activity of pulmonary veins. *Heart* 93**,** 82–88.

CHARD, M. & TABRIZCHI, R. 2009. The role of pulmonary veins in atrial fibrillation: a complex yet simple story. *Pharmacology & therapeutics,* 124**,** 207-218.

CHEN, P.-S. & TAN, A. Y. 2007. Autonomic nerve activity and atrial fibrillation. *Heart rhythm : the official journal of the Heart Rhythm Society,* 4**,** S61-S64.

CHEN, S.-A., HSIEH, M.-H., TAI, C.-T., TSAI, C.-F., PRAKASH, V., YU, W.-C., HSU, T.-L., DING, Y.-A. & CHANG, M.-S. 1999. Initiation of atrial fibrillation by ectopic beats originating from the pulmonary veins electrophysiological characteristics, pharmacological responses, and effects of radiofrequency ablation. *Circulation,* 100**,** 1879-1886.

CHEN, Y.-C., CHEN, S.-A., CHEN, Y.-J., CHANG, M.-S., CHAN, P. & LIN, C.-I. 2002a. Effects of thyroid hormone on the arrhythmogenic activity of pulmonary vein cardiomyocytes. *Journal of the American College of Cardiology,* 39**,** 366-372.

CHEN, Y.-J., CHEN, S.-A., CHANG, M.-S. & LIN, C.-I. 2000. Arrhythmogenic activity of cardiac muscle in pulmonary veins of the dog: implication for the genesis of atrial fibrillation. *Cardiovascular research,* 48**,** 265-273.

CHEN, Y.-J., CHEN, S.-A., CHEN, Y.-C., YEH, H.-I., CHAN, P., CHANG, M.-S. & LIN, C.-I. 2001. Effects of rapid atrial pacing on the arrhythmogenic activity of single cardiomyocytes from pulmonary veins implication in initiation of atrial fibrillation. *Circulation,* 104**,** 2849-2854.

CHEN, Y.-J., CHEN, S.-A., CHEN, Y.-C., YEH, H.-I., CHANG, M.-S. & LIN, C.-I. 2002b. Electrophysiology of single cardiomyocytes isolated from rabbit pulmonary veins: implication in initiation of focal atrial fibrillation. *Basic research in cardiology,* 97**,** 26-34.

CHEN, Y.-J., CHEN, Y.-C., CHAN, P., LIN, C.-I. & CHEN, S.-A. 2003. Temperature regulates the arrhythmogenic activity of pulmonary vein cardiomyocytes. *Journal of biomedical science,* 10**,** 535-543.

CHEN, Y. J. & CHEN, S. A. 2006. Electrophysiology of pulmonary veins. *Journal of cardiovascular electrophysiology,* 17**,** 220-224.

CHEN, Y. J., CHEN, Y. C., WONGCHAROEN, W., LIN, C. I. & CHEN, S. A. 2008. Effect of K201, a novel antiarrhythmic drug on calcium handling and arrhythmogenic activity of pulmonary vein cardiomyocytes. *British Journal of Pharmacology,* 153**,** 915-925.

CHEUNG, D. 1981a. Electrical activity of the pulmonary vein and its interaction with the right atrium in the guinea-pig. *The Journal of Physiology,* 314**,** 445.

CHEUNG, D. 1981b. Pulmonary vein as an ectopic focus in digitalis-induced arrhythmia.

CHEVALIER, P., TABIB, A., MEYRONNET, D., CHALABREYSSE, L., RESTIER, L., LUDMAN, V., ALIÈS, A., ADELEINE, P., THIVOLET, F., BURRI, H., LOIRE, R., FRANÇOIS, L. & FANTON, L. 2005. Quantitative study of nerves of the human left atrium. *Heart Rhythm,* 2**,** 518-522.

CHOU, C.-C., NIHEI, M., ZHOU, S., TAN, A., KAWASE, A., MACIAS, E. S., FISHBEIN, M. C., LIN, S.-F. & CHEN, P.-S. 2005. Intracellular Calcium Dynamics and Anisotropic Reentry in Isolated Canine Pulmonary Veins and Left Atrium. *Circulation,* 111**,** 2889-2897.

CORLEY, S. D., EPSTEIN, A. E., DIMARCO, J. P., DOMANSKI, M. J., GELLER, N., GREENE, H. L., JOSEPHSON, R. A., KELLEN, J. C., KLEIN, R. C., KRAHN, A. D., MICKEL, M., MITCHELL, L. B., NELSON, J. D., ROSENBERG, Y., SCHRON, E., SHEMANSKI, L., WALDO, A. L. & WYSE, D. G. 2004. Relationships Between Sinus Rhythm, Treatment, and Survival in the Atrial Fibrillation Follow-Up Investigation of Rhythm Management (AFFIRM) Study. *Circulation,* 109**,** 1509-1513.

CRAELIUS, W., CHEN, V. & EL-SHERIF, N. 1988. Stretch activated ion channels in ventricular myocytes. *Bioscience Reports,* 8**,** 407-414.

CULLINGTON, D., YASSIN, A. & CLELAND, J. 2008. Beta-blockers in the treatment of cardiovascular disease. *Prescriber,* 19**,** 31-39.

DANG, D., ARIMIE, R. & HAYWOOD, L. J. 2002. A review of atrial fibrillation. *Journal of the National Medical Association,* 94**,** 1036.

DAVIES, M. J. & ANDERSON, R. H. 1983. *The conduction system of the heart,* Butterworth-Heinemann.

DE JONG, A. M., MAASS, A. H., OBERDORF-MAASS, S. U., VAN VELDHUISEN, D. J., VAN GILST, W. H. & VAN GELDER, I. C. 2011. Mechanisms of atrial structural changes caused by stretch occurring before and during early atrial fibrillation. *Cardiovascular Research,* 89**,** 754-765.

DEROUBAIX, E., FOLLIGUET, T., RÜCKER-MARTIN, C., DINANIAN, S., BOIXEL, C., VALIDIRE, P., DANIEL, P., CAPDEROU, A. & HATEM, S. N. 2004. Moderate and chronic hemodynamic overload of sheep atria induces reversible cellular electrophysiologic abnormalities and atrial vulnerability. *Journal of the American College of Cardiology,* 44**,** 1918-1926.

DHEIN, S., ENGLERT, C., RIETHDORF, S., KOSTELKA, M., DOHMEN, P. M. & MOHR, F.-W. 2014. Arrhythmogenic effects by local left ventricular stretch: effects of flecainide and streptomycin. *Naunyn-Schmiedeberg's Archives of Pharmacology,* 387**,** 763-775.

DIFRANCESCO, D. 1993. Pacemaker mechanisms in cardiac tissue. *Annual review of physiology,* 55**,** 455-472.

DOBREV, D., VOIGT, N. & WEHRENS, X. H. T. 2011. The ryanodine receptor channel as a molecular motif in atrial fibrillation: pathophysiological and therapeutic implications. *Cardiovascular Research,* 89**,** 734-743.

DOBRZYNSKI, H., BOYETT, M. R. & ANDERSON, R. H. 2007. New Insights Into Pacemaker Activity. *Promoting Understanding of Sick Sinus Syndrome,* 115**,** 1921-1932.

DOGGRELL, S. A. 1990. The membrane stabilizing and β1-adrenoceptor blocking activity of (+)-and (−)-propranolol on the rat left atria. *General Pharmacology: The Vascular System,* 21**,** 677-680.

DOISNE, N., MAUPOIL, V., COSNAY, P. & FINDLAY, I. 2009. Catecholaminergic automatic activity in the rat pulmonary vein: electrophysiological differences between cardiac muscle in the left atrium and pulmonary vein. *American Journal of Physiology-Heart and Circulatory Physiology,* 297**,** H102-H108.

DROUAL, R. 2015. *Physiology 101* [Online]. Available: http://droualb.faculty.mjc.edu/Course%20Materials/Physiology%20101/Chapter%20Notes/Fall%202011/chapter_5%20Fall%202011.htm.

ECKARDT, L., KIRCHHOF, P., MÖNNIG, G., BREITHARDT, G., BORGGREFE, M. & HAVERKAMP, W. 2000. Modification of Stretch-Induced Shortening of Repolarization by Streptomycin in the Isolated Rabbit Heart. *Journal of Cardiovascular Pharmacology*, 36**,** 711-721.

EHRLICH, J. R., CHA, T. J., ZHANG, L., CHARTIER, D., MELNYK, P. & HOHNLOSER, S. H. 2003. Cellular electrophysiology of canine pulmonary vein cardiomyocytes: action potential and ionic current properties. *The Journal of Physiology*, 551**,** 801-813.

FARIA, D. M., VIVIANE, A. G., GALVÃO, K. M., CARICATI-NETO, A. & GODOY, C. M. G. 2009. Influence of age on inducibility and cholinergic modulation of arrhythmia in isolated rat right atria. *Age*, 31**,** 51-58.

FERREIRA, A. J., MORAES, P. L., FOUREAUX, G., ANDRADE, A. B., SANTOS, R. A. S. & ALMEIDA, A. P. 2011. The Angiotensin-(1-7)/Mas Receptor Axis Is Expressed in Sinoatrial Node Cells of Rats. *Journal of Histochemistry and Cytochemistry*, 59**,** 761-768.

FINCH, A. M., SARRAMEGNA, V. & GRAHAM, R. M. 2006. Ligand Binding, Activation, and Agonist Trafficking. *In:* PEREZ, D. M. (ed.) *The Adrenergic Receptors: In the 21st Century*. Totowa, NJ: Humana Press.

FRANK, O. 1895. *Zur Dynamik des Herzmuskels*, Druck v. R. Oldenbourg.

FRANZ, M. R., BURKHOFF, D., T YUE, D. & SAGAWA, K. 1989. Mechanically induced action potential changes and arrhythmia in isolated and in situ canine hearts. *Cardiovascular research*, 23**,** 213-223.

FRANZ, M. R., CIMA, R., WANG, D., PROFITT, D. & KURZ, R. 1992. Electrophysiological effects of myocardial stretch and mechanical determinants of stretch-activated arrhythmias. *Circulation*, 86**,** 968-78.

FYNN, S. P. & KALMAN, J. M. 2004. Pulmonary Veins. *Pacing and Clinical Electrophysiology*, 27**,** 1547-1559.

GANNIER, F., WHITE, E., GARNIER, D. & LE GUENNEC, J.-Y. 1996. A possible mechanism for large stretch-induced increase in [Ca2+] i in isolated guinea-pig ventricular myocytes. *Cardiovascular research*, 32**,** 158-167.

GANNIER, F., WHITE, E., LACAMPAGNE, A., GARNIER, D. & GUENNEC, J.-Y. L. 1994. Streptomycin reverses a large stretch induced increases in $[Ca^{2+}]i$ in isolated guinea pig ventricular myocytes. *Cardiovascular Research*, 28**,** 1193-1198.

GARTNER, L. P. H., ORIZAGA, J. L., GARTNER, L. P. H., GARTNER, J. L. L. P., HIATT, J. L., GARTNER, L. P. H., RENARD, J. L. S., DE ROBERTIS, E., SAEZ, E. & FRANCISCO, A. 2002. *Texto atlas de histología,* McGraw-Hill Interamericana.

GAZTAÑAGA, L., MARCHLINSKI, F. E. & BETENSKY, B. P. 2012. Mechanisms of Cardiac Arrhythmias. *Revista Española de Cardiología (English Edition),* 65**,** 174-185.

GERILECHAOGETU, F. H., GOLDEN HB, NIZAMUTDINOV D, DOSTAL JD, ET AL. 2014. Current Concepts in the Role of Mechanosensing in the Regulation of Cardiac Contractile Function. *Austin J Clin Med. 2014;1(3): 1015,* 1**,** 1-15.

GERMANN, W. & STANFIELD, C. 2005. Principles of human physiology. 2 ed.: San Francisco: Benjamin Cummings. xxix.

GHAZI, S. R., TADJALLI, M. & BANIABBAS, A. 1998. Anatomy of the Sinus Node of Domestic Cats (Felis catus). *Journal of Applied Animal Research,* 14**,** 57-64.

GOONETILLEKE, L. & QUAYLE, J. 2012. TREK-1 K+ Channels in the Cardiovascular System: Their Significance and Potential as a Therapeutic Target. *Cardiovascular Therapeutics,* 30**,** e23-e29.

GUHARAY, F. & SACHS, F. 1984. Stretch-activated single ion channel currents in tissue-cultured embryonic chick skeletal muscle. *The Journal of physiology,* 352**,** 685.

HAGIWARA, N., MASUDA, H., SHODA, M. & IRISAWA, H. 1992. Stretch-activated anion currents of rabbit cardiac myocytes. *The Journal of Physiology,* 456**,** 285.

HAISSAGUERRE, M., JAÏS, P., SHAH, D. C., TAKAHASHI, A., HOCINI, M., QUINIOU, G., GARRIGUE, S., LE MOUROUX, A., LE MÉTAYER, P. & CLÉMENTY, J. 1998. Spontaneous initiation of atrial fibrillation by ectopic beats originating in the pulmonary veins. *New England Journal of Medicine,* 339**,** 659-666.

HAMAGUCHI, S., HIKITA, K., TANAKA, Y., TSUNEOKA, Y., NAMEKATA, I. & TANAKA, H. 2016. Enhancement of Automaticity by Mechanical Stretch of the Isolated Guinea Pig Pulmonary Vein Myocardium. *Biological and Pharmaceutical Bulletin,* 39**,** 1216-1219.

HAMILL, O. P. & MCBRIDE, D. W. 1996. The pharmacology of mechanogated membrane ion channels. *Pharmacological Reviews,* 48**,** 231-252.

HANSEN, D. E., BORGANELLI, M., STACY, G. & TAYLOR, L. K. 1991. Dose-dependent inhibition of stretch-induced arrhythmias by gadolinium in isolated

canine ventricles. Evidence for a unique mode of antiarrhythmic action. *Circulation Research,* 69**,** 820-831.

HARADA, M., LUO, X., QI, X. Y., TADEVOSYAN, A., MAGUY, A., ORDOG, B., LEDOUX, J., KATO, T., NAUD, P., VOIGT, N., SHI, Y., KAMIYA, K., MUROHARA, T., KODAMA, I., TARDIF, J.-C., SCHOTTEN, U., VAN WAGONER, D. R., DOBREV, D. & NATTEL, S. 2012. Transient Receptor Potential Canonical-3 Channel–Dependent Fibroblast Regulation in Atrial Fibrillation. *Circulation,* 126**,** 2051-2064.

HASSINK, R. J., ARETZ, H. T., RUSKIN, J. & KEANE, D. 2003. Morphology of atrial myocardium in human pulmonary veins: a postmortem analysis in patients with and without atrial fibrillation. *Journal of the American College of Cardiology,* 42**,** 1108-1114.

HEDBERG, A., KEMPF, F., JOSEPHSON, M. E. & MOLINOFF, P. B. 1985. Coexistence of beta-1 and beta-2 adrenergic receptors in the human heart: effects of treatment with receptor antagonists or calcium entry blockers. *Journal of Pharmacology and Experimental Therapeutics,* 234**,** 561-568.

HEIJMAN, J., VOIGT, N., NATTEL, S. & DOBREV, D. 2014. Cellular and Molecular Electrophysiology of Atrial Fibrillation Initiation, Maintenance, and Progression. *Circulation Research,* 114**,** 1483-1499.

HENRY, W. L., MORGANROTH, J., PEARLMAN, A. S., CLARK, C. E., REDWOOD, D. R., ITSCOITZ, S. B. & EPSTEIN, S. E. 1976. Relation between echocardiographically determined left atrial size and atrial fibrillation. *Circulation,* 53**,** 273-279.

HO, S., CABRERA, J., TRAN, V., FARRE, J., ANDERSON, R. & SANCHEZ-QUINTANA, D. 2001. Architecture of the pulmonary veins: relevance to radiofrequency ablation. *Heart,* 86**,** 265-270.

HO, S. Y., ANDERSON, R. H. & SÁNCHEZ-QUINTANA, D. 2002. Atrial structure and fibres: morphologic bases of atrial conduction. *Cardiovascular Research,* 54**,** 325-336.

HO, S. Y., SANCHEZ-QUINTANA, D., CABRERA, J. A. & ANDERSON, R. H. 1999. Anatomy of the left atrium: implications for radiofrequency ablation of atrial fibrillation. *Journal of cardiovascular electrophysiology,* 10**,** 1525-1533.

HOCINI, M., HAÏSSAGUERRE, M., SHAH, D., JAÏS, P., PENG, J. T., YAMANE, T., DEISENHOFER, I., GARRIGUE, S., FUIMAONO, K., PIKE, R. O. B. & CLÉMENTY, J. 2000. Multiple Sources Initiating Atrial Fibrillation from a Single Pulmonary Vein Identified by a Circumferential Catheter. *Pacing and Clinical Electrophysiology,* 23**,** 1828-1831.

HOCINI, M., HO, S. Y., KAWARA, T., LINNENBANK, A. C., POTSE, M., SHAH, D., JAÏS, P., JANSE, M. J., HAÏSSAGUERRE, M. & DE BAKKER, J. M.

2002. Electrical conduction in canine pulmonary veins electrophysiological and anatomic correlation. *Circulation,* 105**,** 2442-2448.

HONGO, K., WHITE, E., LE GUENNEC, J. Y. & ORCHARD, C. H. 1996. Changes in [Ca2+]i, [Na+]i and Ca2+ current in isolated rat ventricular myocytes following an increase in cell length. *The Journal of Physiology,* 491**,** 609-619.

HONJO, H., BOYETT, M. R., NIWA, R., INADA, S., YAMAMOTO, M., MITSUI, K., HORIUCHI, T., SHIBATA, N., KAMIYA, K. & KODAMA, I. 2003. Pacing-induced spontaneous activity in myocardial sleeves of pulmonary veins after treatment with ryanodine. *Circulation,* 107**,** 1937-1943.

HU, H. & SACHS, F. 1996. Mechanically activated currents in chick heart cells. *The Journal of membrane biology,* 154**,** 205-216.

HU, H. & SACHS, F. 1997. Stretch-activated ion channels in the heart. *Journal of molecular and cellular cardiology,* 29**,** 1511-1523.

HUANG, C. X., HU, C. L. & LI, Y. B. 2006. Atrial fibrillation may be a vascular disease: The role of the pulmonary vein. *Medical Hypotheses,* 68**,** 629-634.

HUANG, H., WANG, W., LIU, P., JIANG, Y., ZHAO, Y., WEI, H. & NIU, W. 2009. TRPC1 expression and distribution in rat hearts. *European journal of histochemistry: EJH,* 53**,** 217.

HUANG, X., YANG, P., YANG, Z., ZHANG, H. & MA, A. 2016. Age-associated expression of HCN channel isoforms in rat sinoatrial node. *Experimental Biology and Medicine,* 241**,** 331-339.

INOUE, R., YUBIN, D., YAOPENG, H. & ICHIKAWA, J. 2012. *The Pathophysiological Implications of TRP Channels in Cardiac Arrhythmia*, INTECH Open Access Publisher.

IRIBE, G. & KOHL, P. 2008. Axial stretch enhances sarcoplasmic reticulum Ca2+ leak and cellular Ca2+ reuptake in guinea pig ventricular myocytes: Experiments and models. *Progress in Biophysics and Molecular Biology,* 97**,** 298-311.

ISENBERG, G., KAZANSKI, V., KONDRATEV, D., GALLITELLI, M. F., KISELEVA, I. & KAMKIN, A. 2003. Differential effects of stretch and compression on membrane currents and [Na+] c in ventricular myocytes. *Progress in biophysics and molecular biology,* 82**,** 43-56.

IWASAKI, Y.-K., NISHIDA, K., KATO, T. & NATTEL, S. 2011. Atrial Fibrillation Pathophysiology. *Implications for Management,* 124**,** 2264-2274.

JAMES, T., N., SHERF, L., FINE, G. & MORALES, A., R. 1966. Comparative Ultrastructure of the Sinus Node in Man and Dog. *Circulation,* 34**,** 139-163.

JAMES, T. N. 1962. Anatomy of the sinus node of the dog. *The Anatomical Record,* 143**,** 251-265.

JAMES, T. N. 1967. Anatomy of the Cardiac Conduction System in the Rabbit. *Circulation Research,* 20**,** 638-648.

JAMES, T. N. 1970. Cardiac conduction system: Fetal and postnatal development. *American Journal of Cardiology,* 25**,** 213-226.

JANUARY, C. T., CHAU, V. & MAKIELSKI, J. C. 1991. Triggered activity in the heart: cellular mechanisms of early after-depolarizations. *European Heart Journal,* 12**,** 4-9.

JENSEN, B. C., O'CONNELL, T. D. & SIMPSON, P. C. 2011. Alpha-1-adrenergic receptors: targets for agonist drugs to treat heart failure. *Journal of molecular and cellular cardiology,* 51**,** 518-528.

JOST, N., NAGY, N., CORICI, C., KOHAJDA, Z., HORVÁTH, A., ACSAI, K., BILICZKI, P., LEVIJOKI, J., POLLESELLO, P. & KOSKELAINEN, T. 2013. ORM- 10103, a novel specific inhibitor of the Na^+/Ca^{2+} exchanger, decreases early and delayed afterdepolarizations in the canine heart. *British journal of pharmacology,* 170**,** 768-778.

JU, Y.-K., CHU, Y., CHAULET, H., LAI, D., GERVASIO, O. L., GRAHAM, R. M., CANNELL, M. B. & ALLEN, D. G. 2007. Store-Operated Ca2+ Influx and Expression of TRPC Genes in Mouse Sinoatrial Node. *Circulation Research,* 100**,** 1605-1614.

KAMKIN, A., KISELEVA, I. & ISENBERG, G. 2000. Stretch-activated currents in ventricular myocytes: amplitude and arrhythmogenic effects increase with hypertrophy. *Cardiovascular Research,* 48**,** 409-420.

KAMKIN, A., KISELEVA, I. & ISENBERG, G. 2003a. Ion selectivity of stretch-activated cation currents in mouse ventricular myocytes. *Pflügers Archiv,* 446**,** 220-231.

KAMKIN, A., KISELEVA, I., WAGNER, K.-D., BOHM, J., THERES, H., GÜNTHER, J. & SCHOLZ, H. 2003b. Characterization of stretch-activated ion currents in isolated atrial myocytes from human hearts. *Pflügers Archiv,* 446**,** 339-346.

KAWASHIMA, T. 2005. The autonomic nervous system of the human heart with special reference to its origin, course, and peripheral distribution. *Anatomy and Embryology,* 209**,** 425-438.

KELLY, D., MACKENZIE, L., HUNTER, P., SMAILL, B. & SAINT, D. A. 2006. Gene expression of stretch-activated channels and mechanoelectric feedback in the heart. *Clinical and Experimental Pharmacology and Physiology,* 33**,** 642-648.

KHAN, R. 2004. Identifying and understanding the role of pulmonary vein activity in atrial fibrillation. *Cardiovascular Research,* 64**,** 387-394.

KIM, D. 1992. A mechanosensitive K^+ channel in heart cells. Activation by arachidonic acid. *The Journal of General Physiology,* 100**,** 1021-1040.

KIM, D. 1993. Novel cation-selective mechanosensitive ion channel in the atrial cell membrane. *Circulation Research,* 72**,** 225-231.

KISELEVA, I., KAMKIN, A., WAGNER, K.-D., THERES, H., LADHOFF, A., SCHOLZ, H., GÜNTHER, J. & LAB, M. J. 2000. Mechanoelectric feedback after left ventricular infarction in rats. *Cardiovascular Research,* 45**,** 370-378.

KISTLER, P. M., SANDERS, P., DODIC, M., SPENCE, S. J., SAMUEL, C. S., ZHAO, C., CHARLES, J. A., EDWARDS, G. A. & KALMAN, J. M. 2006. Atrial electrical and structural abnormalities in an ovine model of chronic blood pressure elevation after prenatal corticosteroid exposure: implications for development of atrial fibrillation. *European Heart Journal,* 27**,** 3045-3056.

KLABUNDE, R. 2011. *Cardiovascular physiology concepts,* Lippincott Williams & Wilkins.

KLAVINS, J. V. 1963. Demonstration of striated muscle in the pulmonary veins of the rat. *Journal of Anatomy,* 97**,** 239-241.

KOHL, P., BOLLENSDORFF, C. & GARNY, A. 2006. Effects of mechanosensitive ion channels on ventricular electrophysiology: experimental and theoretical models. *Experimental physiology,* 91**,** 307-321.

KRACKLAUER, M. P., FENG, H. Z., JIANG, W., LIN, J. L. C., LIN, J. J. C. & JIN, J. P. 2013. Discontinuous thoracic venous cardiomyocytes and heart exhibit synchronized developmental switch of troponin isoforms. *FEBS Journal,* 280**,** 880-891.

KUMAGAI, K., YASUDA, T., TOJO, H., NOGUCHI, H., MATSUMOTO, N., NAKASHIMA, H., GONDO, N. & SAKU, K. 2000. Role of Rapid Focal Activation in the Maintenance of Atrial Fibrillation Originating from the Pulmonary Veins. *Pacing and Clinical Electrophysiology,* 23**,** 1823-1827.

KUWAHARA, K., WANG, Y., MCANALLY, J., RICHARDSON, J. A., BASSEL-DUBY, R., HILL, J. A. & OLSON, E. N. 2006. TRPC6 fulfills a calcineurin signaling circuit during pathologic cardiac remodeling. *The Journal of clinical investigation,* 116**,** 3114-3126.

KUZ'MIN, V. & ROZENSHTRAUKH, L. Changes in the excitability of the rat pulmonary vein myocardium induced by adrenergic stimulation. Doklady Biological Sciences, 2012a. Springer, 71-74.

KUZ'MIN, V. S. & ROZENSHTRAUKH, L. V. 2012b. The effects of isoproterenol and barium on automatic activity in the myocardium of the rat pulmonary veins. *Doklady Biological Sciences,* 444**,** 153-156.

LAB, M. 1996. Mechanoelectric feedback (transduction) in heart: concepts and implications. *Cardiovascular research,* 32**,** 3-14.

LACAMPAGNE, A., GANNIER, F., ARGIBAY, J., GARNIER, D. & LE GUENNEC, J.-Y. 1994. The stretch-activated ion channel blocker gadolinium also blocks L-type calcium channels in isolated ventricular myocytes of the guinea-pig. *Biochimica et Biophysica Acta (BBA) - Biomembranes,* 1191**,** 205-208.

LAMMERDING, J., KAMM, R. D. & LEE, R. T. 2004. Mechanotransduction in cardiac myocytes. *Annals of the New York Academy of Sciences,* 1015**,** 53-70.

LAU, D. H., MACKENZIE, L., KELLY, D. J., PSALTIS, P. J., BROOKS, A. G., WORTHINGTON, M., RAJENDRAM, A., KELLY, D. R., ZHANG, Y., KUKLIK, P., NELSON, A. J., WONG, C. X., WORTHLEY, S. G., RAO, M., FAULL, R. J., EDWARDS, J., SAINT, D. A. & SANDERS, P. 2010a. Hypertension and atrial fibrillation: Evidence of progressive atrial remodeling with electrostructural correlate in a conscious chronically instrumented ovine model. *Heart Rhythm,* 7**,** 1282-1290.

LAU, D. H., MACKENZIE, L., KELLY, D. J., PSALTIS, P. J., WORTHINGTON, M., RAJENDRAM, A., KELLY, D. R., NELSON, A. J., ZHANG, Y., KUKLIK, P., BROOKS, A. G., WORTHLEY, S. G., FAULL, R. J., RAO, M., EDWARDS, J., SAINT, D. A. & SANDERS, P. 2010b. Short-term hypertension is associated with the development of atrial fibrillation substrate: A study in an ovine hypertensive model. *Heart Rhythm,* 7**,** 396-404.

LEITCH, S. P. & BROWN, H. F. 1999. Effect of raised extracellular calcium on characteristics of the guinea-pig ventricular action potential. *Journal of Molecular and Cellular Cardiology,* 28**,** 541-551.

LEMOLA, K., CHARTIER, D., YEH, Y.-H., DUBUC, M., CARTIER, R., ARMOUR, A., TING, M., SAKABE, M., SHIROSHITA-TAKESHITA, A., COMTOIS, P. & NATTEL, S. 2008. Pulmonary Vein Region Ablation in Experimental Vagal Atrial Fibrillation. *Role of Pulmonary Veins Versus Autonomic Ganglia,* 117**,** 470-477.

LÉVY, S., CAMM, A. J., SAKSENA, S., ALIOT, E., BREITHARDT, G., CRIJNS, H., DAVIES, W., KAY, N., PRYSTOWSKY, E., SUTTON, R., WALDO, A. & WYSE, D. G. 2003. International consensus on nomenclature and classification of atrial fibrillation. *A collaborative project of the Working Group on Arrhythmias and the Working Group on Cardiac Pacing of the European Society of Cardiology and the North American Society of Pacing and Electrophysiology,* 5**,** 119-122.

LI, N., CSEPE, T. A., HANSEN, B. J., DOBRZYNSKI, H., HIGGINS, R. S., KILIC, A., MOHLER, P. J., JANSSEN, P. M., ROSEN, M. R. & BIESIADECKI, B. J. 2015. Molecular mapping of sinoatrial node HCN channel expression in the human heart. *Circulation: Arrhythmia and Electrophysiology,* 8**,** 1219-1227.

LI, X. T., DYACHENKO, V., ZUZARTE, M., PUTZKE, C., PREISIG-MÜLLER, R., ISENBERG, G. & DAUT, J. 2006. The stretch-activated potassium channel TREK-1 in rat cardiac ventricular muscle. *Cardiovascular research,* 69**,** 86-97.

LI, Y.-D., HONG, Y.-F., ZHANG, Y., ZHOU, X.-H., JI, Y.-T., LI, H.-L., XU, G.-J., LI, J.-X., SUN, L., ZHANG, J.-H., XIN, Q., YUSUFUAJI, Y., XIONG, J. & TANG, B.-P. 2014. Association between Reversal in the Expression of Hyperpolarization-Activated Cyclic Nucleotide-Gated (HCN) Channel and Age-Related Atrial Fibrillation. *Medical Science Monitor : International Medical Journal of Experimental and Clinical Research,* 20**,** 2292-2297.

LIANG, L., PAN, Q., LIU, Y., CHEN, H., LI, J., BRUGADA, R., BRUGADA, P., HONG, K., PEREZ, G. J., ZHAO, C., QI, J., ZHANG, Y., PENG, L., LI, L. & CHEN, Y.-H. 2008. High sensitivity of the sheep pulmonary vein antrum to acetylcholine stimulation. *Journal of Applied Physiology,* 105**,** 293-298.

LIN, H.-J., WOLF, P. A., KELLY-HAYES, M., BEISER, A. S., KASE, C. S., BENJAMIN, E. J. & D'AGOSTINO, R. B. 1996. Stroke Severity in Atrial Fibrillation. *The Framingham Study,* 27**,** 1760-1764.

LIN, Y.-K., LIN, F.-Z., CHEN, Y.-C., CHENG, C.-C., LIN, C.-I., CHEN, Y.-J. & CHEN, S.-A. 2010. Oxidative Stress on Pulmonary Vein and Left Atrium Arrhythmogenesis. *Circulation Journal,* 74**,** 1547-1556.

LIU, J., DOBRZYNSKI, H., YANNI, J., BOYETT, M. R. & LEI, M. 2007. Organisation of the mouse sinoatrial node: structure and expression of HCN channels. *Cardiovascular Research,* 73**,** 729-738.

LIU, L. & NATTEL, S. 1997. Differing sympathetic and vagal effects on atrial fibrillation in dogs: role of refractoriness heterogeneity. *American Journal of Physiology - Heart and Circulatory Physiology,* 273**,** H805-H816.

LUDATSCHER, R. M. 1968. Fine structure of the muscular wall of rat pulmonary veins. *Journal of Anatomy,* 103**,** 345-357.

LUDWIG, A., ZONG, X., JEGLITSCH, M., HOFMANN, F. & BIEL, M. 1998. A family of hyperpolarization-activated mammalian cation channels. *Nature,* 393**,** 587-591.

LUGENBIEL, P., WENZ, F., SYREN, P., GESCHWILL, P., GOVOROV, K., SEYLER, C., FRANK, D., SCHWEIZER, P. A., FRANKE, J., WEIS, T., BRUEHL, C., SCHMACK, B., RUHPARWAR, A., KARCK, M., FREY, N., KATUS, H. A. & THOMAS, D. 2016. TREK-1 (K2P2.1) K+ channels are

suppressed in patients with atrial fibrillation and heart failure and provide therapeutic targets for rhythm control. *Basic Research in Cardiology,* 112**,** 8.

LUK, H.-N., LO, C.-P., TIEN, H.-C., LEE, D., CHEN, Z.-L., WANG, F., HSIN, S.-T. & DAY, Y.-J. 2008. Mechanical Characterization of Rabbit Pulmonary Vein Sleeves in In Vitro Intact Ring Preparation. *Journal of the Chinese Medical Association,* 71**,** 610-618.

MACLEOD, D. P. & HUNTER, E. G. 1967. The pharmacology of the cardiac muscle of the great veins of the rat. *Canadian Journal of Physiology and Pharmacology,* 45**,** 463-473.

MACLEOD, K. 1986. Adrenergic-cholinergic interactions in left atria: interaction of carbachol with alpha-and beta-adrenoceptor agonists. *Canadian journal of physiology and pharmacology,* 64**,** 597-601.

MAHIDA, S., SACHER, F., DERVAL, N., BERTE, B., YAMASHITA, S., HOOKS, D., DENIS, A., AMRAOUI, S., HOCINI, M., HAISSAGUERRE, M. & JAIS, P. 2015. Science Linking Pulmonary Veins and Atrial Fibrillation. *Arrhythmia & Electrophysiology Review,* 4**,** 40-43.

MARKIDES, V. & SCHILLING, R. J. 2003. Atrial fibrillation: classification, pathophysiology, mechanisms and drug treatment. *Heart,* 89**,** 939-943.

MAROTO, R., RASO, A., WOOD, T. G., KUROSKY, A., MARTINAC, B. & HAMILL, O. P. 2005. TRPC1 forms the stretch-activated cation channel in vertebrate cells. *Nat Cell Biol,* 7**,** 179-185.

MARTIN, C., PALOMO, M. A. & MCMAHON, E. G. 1996. Comparison of bidisomide, flecainide and dofetilide on action potential duration in isolated canine atria: effect of isoproterenol. *Journal of Pharmacology and Experimental Therapeutics,* 278**,** 154-162.

MASANI, F. 1986. Node-like cells in the myocardial layer of the pulmonary vein of rats: an ultrastructural study. *Journal of Anatomy,* 145**,** 133-142.

MATSUDA, N., HAGIWARA, N., SHODA, M., KASANUKI, H. & HOSODA, S. 1996. Enhancement of the L-Type Ca^{2+} Current by Mechanical Stimulation in Single Rabbit Cardiac Myocytes. *Circulation Research,* 78**,** 650-659.

MAUPOIL, V., BRONQUARD, C., FRESLON, J. L., COSNAY, P. & FINDLAY, I. 2007. Ectopic activity in the rat pulmonary vein can arise from simultaneous activation of α1- and β1-adrenoceptors. *British Journal of Pharmacology,* 150**,** 899-905.

MELNYK, P., EHRLICH, J. R., POURRIER, M., VILLENEUVE, L., CHA, T.-J. & NATTEL, S. 2005. Comparison of ion channel distribution and expression in cardiomyocytes of canine pulmonary veins versus left atrium. *Cardiovascular Research,* 65**,** 104-116.

MISCHKE, K., ZARSE, M., KNACKSTEDT, C. & SCHAUERTE, P. 2011. Rate Control in Atrial Fibrillation by Cooling: Effect of Temperature on Dromotropy in Perfused Rabbit Hearts. *Cardiology Research and Practice,* 2011**,** 4.

MOHRMAN, D. E. & HELLER, L. J. 2002. Cardiovascular physiology.

MONFREDI, O., DOBRZYNSKI, H., MONDAL, T., BOYETT, M. R. & MORRIS, G. M. 2010. The Anatomy and Physiology of the Sinoatrial Node—A Contemporary Review. *Pacing and Clinical Electrophysiology,* 33**,** 1392-1406.

MOUBARAK, J. B., ROZWADOWSKI, J. V., STRZALKA, C. T., BUCK, W. R., TAN, W. S., KISH, G. F., KISIEL, T., FRONC, H. C. & MALONEY, J. D. 2000. Pulmonary Veins- Left Atrial Junction: Anatomic and Histological Study. *Pacing and Clinical Electrophysiology,* 23**,** 1836-1838.

MUELLER-HOECKER, J., BEITINGER, F., FERNANDEZ, B., BAHLMANN, O., ASSMANN, G., TROIDL, C., DIMOMELETIS, I., KAAB, S. & DEINDL, E. 2008. Of rodents and humans: a light microscopic and ultrastructural study on cardiomyocytes in pulmonary veins. *Int J Med Sci,* 5**,** 152-158.

MUGELLI, A., CERBAI, E., AMERINI, S. & VISENTIN, S. 1986. The role of temperature on the development of oscillatory afterpotentials and triggered activity. *Journal of Molecular and Cellular Cardiology,* 18**,** 1313-1316.

MURAKAMI, S. & KURACHI, Y. 2008. Mechanisms of Action of Antiarrhythmic Drugs. *In:* GUSSAK, I., ANTZELEVITCH, C., WILDE, A. A. M., FRIEDMAN, P. A., ACKERMAN, M. J. & SHEN, W.-K. (eds.) *Electrical Diseases of the Heart: Genetics, Mechanisms, Treatment, Prevention.* London: Springer London.

MYAGMAR, B.-E., FLYNN, J. M., COWLEY, P. M., SWIGART, P. M., MONTGOMERY, M. D., THAI, K., NAIR, D., GUPTA, R., DENG, D. X., HOSODA, C., MELOV, S., BAKER, A. J. & SIMPSON, P. C. 2017. Adrenergic Receptors in Individual Ventricular MyocytesNovelty and Significance. *The Beta-1 and Alpha-1B Are in All Cells, the Alpha-1A Is in a Subpopulation, and the Beta-2 and Beta-3 Are Mostly Absent,* 120**,** 1103-1115.

NABIPOUR, A. 2012. Comparative histological structure of the sinus node in mammals. *Turkish Journal of Veterinary and Animal Sciences,* 36**,** 463-469.

NAMDAR, M., TERES, C. & SHAH, D. 2014. Atrial fibrillation–novel insights from pathophysiology.

NAMEKATA, I., TSUNEOKA, Y., AKIBA, A., NAKAMURA, H., SHIMADA, H., TAKAHARA, A. & TANAKA, H. 2010. Intracellular calcium and membrane

potential oscillations in the guinea pig and rat pulmonary vein myocardium. *bioimages,* 18**,** 11-22.

NAMEKATA, I., TSUNEOKA, Y. & TANAKA, H. 2013. Electrophysiological and Pharmacological Properties of the Pulmonary Vein Myocardium. *Biological and Pharmaceutical Bulletin,* 36**,** 2-7.

NATHAN, H. & ELIAKIM, M. 1966. The Junction Between the Left Atrium and the Pulmonary Veins. *Circulation,* 34**,** 412.

NATHAN, H. & GLOOBE, H. 1970. Myocardial atrio-venous junctions and extensions (sleeves) over the pulmonary and caval veins: Anatomical observations in various mammals. *Thorax,* 25**,** 317-324.

NATTEL, S. 2003. Atrial electrophysiology and mechanisms of atrial fibrillation. *Journal of cardiovascular pharmacology and therapeutics,* 8**,** S5-S11.

NATTEL, S. 2005. Combined parasympathetic-sympathetic nerve discharge and pulmonary vein afterdepolarizations: A new unifying concept with basic and clinical relevance. *Heart Rhythm,* 2**,** 632-633.

NATTEL, S., BURSTEIN, B. & DOBREV, D. 2008. Atrial Remodeling and Atrial Fibrillation. *Mechanisms and Implications,* 1**,** 62-73.

NATTEL, S. & DOBREV, D. 2012. The multidimensional role of calcium in atrial fibrillation pathophysiology: mechanistic insights and therapeutic opportunities. *European Heart Journal,* 33**,** 1870-1877.

NATTEL, S. & HARADA, M. 2014. Atrial Remodeling and Atrial Fibrillation: Recent Advances and Translational Perspectives. *Journal of the American College of Cardiology,* 63**,** 2335-2345.

NAZIR, S. A. 1996a. Mechanoelectric feedback and atrial arrhythmias. *Cardiovascular Research,* 32**,** 52-61.

NAZIR, S. A. 1996b. Mechanoelectric feedback in the atrium of the isolated guinea-pig heart. *Cardiovascular research,* 32**,** 112-119.

NGUYEN, B. L., FISHBEIN, M. C., CHEN, L. S., CHEN, P.-S. & MASROOR, S. 2009. Histopathological substrate for chronic atrial fibrillation in humans. *Heart Rhythm,* 6**,** 454-460.

NIKOLOVA-KRSTEVSKI, V., WAGNER, S., BOWMAN, I., FRIEDRICH, O. & FATKIN, D. 2013. TRPC6 (transient receptor potential Ca2+ channel 6) activity in the atrial endocardium exposed to increased mechanical stress is determined by the duration of the mechanical stretch stimuli. *Heart, Lung and Circulation,* 22**,** S5-S6.

NISHIDA, K., MICHAEL, G., DOBREV, D. & NATTEL, S. 2010. Animal models for atrial fibrillation: clinical insights and scientific opportunities. *Europace,* 12**,** 160-172.

NIU, W. & SACHS, F. 2003. Dynamic properties of stretch-activated K+ channels in adult rat atrial myocytes. *Progress in biophysics and molecular biology,* 82**,** 121-135.

NOF, E., ANTZELEVITCH, C. & GLIKSON, M. 2010. The Contribution of HCN4 to Normal Sinus Node Function in Humans and Animal Models. *Pacing and Clinical Electrophysiology,* 33**,** 100-106.

O'CONNELL, T. D., JENSEN, B. C., BAKER, A. J. & SIMPSON, P. C. 2014. Cardiac Alpha1-Adrenergic Receptors: Novel Aspects of Expression, Signaling Mechanisms, Physiologic Function, and Clinical Importance. *Pharmacological Reviews,* 66**,** 308-333.

OHBA, T., WATANABE, H., MURAKAMI, M., TAKAHASHI, Y., IINO, K., KUROMITSU, S., MORI, Y., ONO, K., IIJIMA, T. & ITO, H. 2007. Upregulation of TRPC1 in the development of cardiac hypertrophy. *Journal of Molecular and Cellular Cardiology,* 42**,** 498-507.

OKAMOTO, Y., TAKANO, M., OHBA, T. & ONO, K. 2012. Arrhythmogenic coupling between the Na^+–Ca^{2+} exchanger and inositol 1,4,5-triphosphate receptor in rat pulmonary vein cardiomyocytes. *Journal of Molecular and Cellular Cardiology,* 52**,** 988-997.

PARMLEY, W. W. & CHUCK, L. 1973. Length-dependent changes in myocardial contractile state. *American Journal of Physiology--Legacy Content,* 224**,** 1195-1199.

PATTERSON, E., LAZZARA, R., SZABO, B., LIU, H., TANG, D., LI, Y.-H., SCHERLAG, B. J. & PO, S. S. 2006. Sodium-calcium exchange initiated by the Ca^{2+} transient: an arrhythmia trigger within pulmonary veins. *Journal of the American College of Cardiology,* 47**,** 1196-1206.

PATTERSON, S. W. & STARLING, E. H. 1914. On the mechanical factors which determine the output of the ventricles. *The Journal of Physiology,* 48**,** 357-379.

PAUZA, D. H., SKRIPKA, V., PAUZIENE, N. & STROPUS, R. 2000. Morphology, distribution, and variability of the epicardiac neural ganglionated subplexuses in the human heart. *The Anatomical Record,* 259**,** 353-382.

PERDE, F., YANNI, J., DERMENGIU, D. & DOBRZYNSKI, H. 2015. Funny current and sudden cardiac death. *Rom J Leg Med,* 23**,** 95-100.

PEREZ-LUGONES, A., MCMAHON, J. T., RATLIFF, N. B., SALIBA, W. I., SCHWEIKERT, R. A., MARROUCHE, N. F., SAAD, E. B., NAVIA, J. L., MCCARTHY, P. M., TCHOU, P., GILLINOV, A. M. & NATALE, A. 2003.

Evidence of Specialized Conduction Cells in Human Pulmonary Veins of Patients with Atrial Fibrillation. *Journal of Cardiovascular Electrophysiology,* 14**,** 803-809.

PÉREZ, N. G., DE HURTADO, M. C. C. & CINGOLANI, H. E. 2001. Reverse Mode of the Na+-Ca2+ Exchange After Myocardial Stretch. *Underlying Mechanism of the Slow Force Response,* 88**,** 376-382.

PEYRONNET, R., NERBONNE, J. M. & KOHL, P. 2016. Cardiac Mechano-Gated Ion Channels and Arrhythmias. *Circulation research,* 118**,** 311-329.

PO, S. S., LI, Y., TANG, D., LIU, H., GENG, N., JACKMAN, W. M., SCHERLAG, B., LAZZARA, R. & PATTERSON, E. 2005. Rapid and Stable Re-Entry Within the Pulmonary Vein as a Mechanism Initiating Paroxysmal Atrial Fibrillation. *Journal of the American College of Cardiology,* 45**,** 1871-1877.

RANG, H. P., RITTER, J. M., FLOWER, R. J. & HENDERSON, G. 2014. *Rang & Dale's Pharmacology: With student consult online access,* Elsevier Health Sciences.

RAVELLI, F. 2003. Mechano-electric feedback and atrial fibrillation. *Progress in biophysics and molecular biology,* 82**,** 137-149.

RAVELLI, F. & ALLESSIE, M. 1997. Effects of atrial dilatation on refractory period and vulnerability to atrial fibrillation in the isolated Langendorff-perfused rabbit heart. *Circulation,* 96**,** 1686-1695.

RAVELLI, F., MASÈ, M., DEL GRECO, M., MARINI, M. & DISERTORI, M. 2011. Acute Atrial Dilatation Slows Conduction and Increases AF Vulnerability in the Human Atrium. *Journal of Cardiovascular Electrophysiology,* 22**,** 394-401.

RAVENS, U. & ZIEGLER, A. 1980. Effects of carbachol on contractile force and action potentials of isolated atria at different rates of stimulation. *Journal of cardiovascular pharmacology,* 2**,** 881-892.

REED, A., KOHL, P. & PEYRONNET, R. 2014. Molecular candidates for cardiac stretch-activated ion channels. *Global Cardiology Science and Practice***,** 19.

REMES, J., VAN BRAKEL, T. J., BOLOTIN, G., GARBER, C., DE JONG, M. M., VAN DER VEEN, F. H. & MAESSEN, J. G. Persistent atrial fibrillation in a goat model of chronic left atrial overload. *The Journal of Thoracic and Cardiovascular Surgery,* 136**,** 1005-1011.

RHODIN, J. A. 1975. Atlas of histology.

RICE, J. J. & BERS, D. M. 2011. The response of cardiac muscle to stretch: calcium and force. *Cardiac Mechano-Electric Coupling and Arrhythmias***,** 74.

ROSEN, M., ANYUKHOVSKY, E. & STEINBERG, S. 1991. Alpha-Adrenergic Modulation of Cardiac Rhythm. *Physiology,* 6**,** 134-138.

ROUX, N., HAVET, E. & MERTL, P. 2004. The myocardial sleeves of the pulmonary veins: potential implications for atrial fibrillation. *Surgical and Radiologic Anatomy,* 26**,** 285-289.

RUFF, C. T. 2012. Stroke Prevention in Atrial Fibrillation. *Circulation,* 125**,** e588-e590.

RUKNUDIN, A., SACHS, F. & BUSTAMANTE, J. O. 1993. Stretch-activated ion channels in tissue-cultured chick heart. *American Journal of Physiology-Heart and Circulatory Physiology,* 264**,** H960-H972.

SAINT, D. A. 2002. Stretch- activated channels in the heart: Their role in arrhythmias and potential as antiarrhythmic drug targets. *Drug development research,* 55**,** 53-58.

SAINT, D. A., MACKENZIE, L. & KELLY, D. 2014. Mechanoelectric feedback does not contribute to the Frank-Starling relation in the rat and guinea pig heart. *AIMS Biophysics,* 1**,** 16-30.

SAITO, T., WAKI, K. & BECKER, A. E. 2000. Left Atrial Myocardial Extension onto Pulmonary Veins in Humans. *Journal of Cardiovascular Electrophysiology,* 11**,** 888-894.

SALMON, A. H. J., MAYS, J. L., R. DALTON, G., JONES, J. V. & LEVI, A. J. 1997. Effect of streptomycin on wall-stress-induced arrhythmias in the working rat heart. *Cardiovascular Research,* 34**,** 493-503.

SÁNCHEZ-QUINTANA, D., LÓPEZ-MÍNGUEZ, J. R., PIZARRO, G., MURILLO, M. & CABRERA, J. A. 2012. Triggers and Anatomical Substrates in the Genesis and Perpetuation of Atrial Fibrillation. *Current Cardiology Reviews,* 8**,** 310-326.

SARANTOS-LASKA, C., MCCULLOCH, M. W., RAND, M. J. & LASKA, F. J. 1984. THE POSITIVE INOTROPIC ACTION OF ISOPRENALINE IS ASSOCIATED WITH THE RELEASE OF NORADRENALINE FROM RABBIT, GUINEA-PIG AND RAT ATRIA. *Journal of Autonomic Pharmacology,* 4**,** 175-185.

SASAKI, N., MITSUIYE, T. & NOMA, A. 1992. Effects of Mechanical Stretch on Membrane Currents of Single Ventricular Myocytes of Guinea-Pig Heart. *The Japanese Journal of Physiology,* 42**,** 957-970.

SATOH, H. 2003. Sino-Atrial Nodal Cells of Mammalian Hearts: Ionic Currents and Gene Expression of Pacemaker Ionic Channels. *Journal of Smooth Muscle Research,* 39**,** 175-193.

SAVELIEVA, I. & JOHN CAMM, A. 2003. Atrial fibrillation and heart failure: natural history and pharmacological treatment. *Europace,* 5**,** S5-S19.

SCHERLAG, B. J., PATTERSON, E. & PO, S. S. 2006. The neural basis of atrial fibrillation. *Journal of Electrocardiology,* 39**,** S180-S183.

SCHMIDT, C., KISSELBACH, J., SCHWEIZER, P. A., KATUS, H. A. & THOMAS, D. 2011. The pathology and treatment of cardiac arrhythmias: focus on atrial fibrillation. *Vascular Health and Risk Management,* 7**,** 193-202.

SCHMIDT, C., WIEDMANN, F., TRISTRAM, F., ANAND, P., WENZEL, W., LUGENBIEL, P., SCHWEIZER, P. A., KATUS, H. A. & THOMAS, D. 2014. Cardiac expression and atrial fibrillation-associated remodeling of K2P2.1 (TREK-1) K+ channels in a porcine model. *Life Sciences,* 97**,** 107-115.

SCHOTTEN, U., NEUBERGER, H.-R. & ALLESSIE, M. A. 2003. The role of atrial dilatation in the domestication of atrial fibrillation. *Progress in Biophysics and Molecular Biology,* 82**,** 151-162.

SCICCHITANO, P., CARBONARA, S., RICCI, G., MANDURINO, C., LOCOROTONDO, M., BULZIS, G., GESUALDO, M., ZITO, A., CARBONARA, R., DENTAMARO, I., RICCIONI, G. & CICCONE, M. M. 2012. HCN Channels and Heart Rate. *Molecules,* 17**,** 4225.

SEO, K., RAINER, P. P., SHALKEY HAHN, V., LEE, D.-I., JO, S.-H., ANDERSEN, A., LIU, T., XU, X., WILLETTE, R. N., LEPORE, J. J., MARINO, J. P., BIRNBAUMER, L., SCHNACKENBERG, C. G. & KASS, D. A. 2014. Combined TRPC3 and TRPC6 blockade by selective small-molecule or genetic deletion inhibits pathological cardiac hypertrophy. *Proceedings of the National Academy of Sciences,* 111**,** 1551-1556.

SEOL, C. A., KIM, W. T., HA, J. M., CHOE, H., JANG, Y. J., YOUM, J. B., EARM, Y. E. & LEEM, C. H. 2008. Stretch-activated currents in cardiomyocytes isolated from rabbit pulmonary veins. *Prog Biophys Mol Biol,* 97**,** 217-31.

SEOL, C. A., KIM, W. T., YOUM, J. B., EARM, Y. E. & LEEM, C. H. 2011. *Mechano-sensitivity of pulmonary vein cells: implications for atrial arrhythmogenesis*.

SETH, M., ZHANG, Z.-S., MAO, L., GRAHAM, V., BURCH, J., STIBER, J., TSIOKAS, L., WINN, M., ABRAMOWITZ, J., ROCKMAN, H. A., BIRNBAUMER, L. & ROSENBERG, P. 2009. TRPC1 channels are critical for hypertrophic signaling in the heart. *Circulation research,* 105**,** 1023-1030.

SHI, W., WYMORE, R., YU, H., WU, J., WYMORE, R. T., PAN, Z., ROBINSON, R. B., DIXON, J. E., MCKINNON, D. & COHEN, I. S. 1999. Distribution and Prevalence of Hyperpolarization-Activated Cation Channel (HCN) mRNA Expression in Cardiac Tissues. *Circulation Research,* 85**,** e1-e6.

SIGURDSON, W., RUKNUDIN, A. & SACHS, F. 1992. Calcium imaging of mechanically induced fluxes in tissue-cultured chick heart: role of stretch-activated ion channels. *American Journal of Physiology-Heart and Circulatory Physiology,* 262**,** H1110-H1115.

SINGAL, P. K., GUPTA, M. & PRASAD, K. 1985. Effects of increase in extracellular calcium on frequency-dependent inotropism in cardiac muscle. *The Canadian journal of cardiology,* 1**,** 294-297.

SOBOTTA, J. & HAMMERSEN, F. 1980. *Histology: Color Atlas of Cytology, Histology and Microscopic Anatomy,* Urban & Schwarzenberg.

SOLTI, F., VECSEY, T., KEKESI, V. & JUHASZ-NAGY, A. 1989. The effect of atrial dilatation on the genesis of atrial arrhythmias. *Cardiovascular Research,* 23**,** 882-886.

SOMERVILLE, W. 1960. The effect of hypothermia on atrial fibrillation and other arrhythmias. *British Heart Journal,* 22**,** 515-521.

SOUTHAN, C., SHARMAN, J. L., BENSON, H. E., FACCENDA, E., PAWSON, A. J., ALEXANDER, S. P., BUNEMAN, O. P., DAVENPORT, A. P., MCGRATH, J. C. & PETERS, J. A. 2015. The IUPHAR/BPS Guide to PHARMACOLOGY in 2016: towards curated quantitative interactions between 1300 protein targets and 6000 ligands. *Nucleic acids research,* 44**,** D1054-D1068.

SPASSOVA, M. A., XU, W. & GILL, D. 2006. TRPC6 is a stretch-activated ion channel inhibited by tarantula toxin GsMTx-4. *The FASEB Journal,* 20**,** LB19.

STACY JR, G. P., JOBE, R., TAYLOR, L. K. & HANSEN, D. E. 1992. Stretch-induced depolarizations as a trigger of arrhythmias in isolated canine left ventricles. *The American journal of physiology,* 263**,** H613-21.

STEINER, I., HÁJKOVÁ, P., KVASNIČKA, J. & KHOLOVÁ, I. 2006. Myocardial sleeves of pulmonary veins and atrial fibrillation: a postmortem histopathological study of 100 subjects. *Virchows Archiv,* 449**,** 88-95.

STEWART, S., HART, C., HOLE, D. & MCMURRAY, J. 2001. Population prevalence, incidence, and predictors of atrial fibrillation in the Renfrew/Paisley study. *Heart,* 86**,** 516-521.

SUCHYNA, T. M., JOHNSON, J. H., HAMER, K., LEYKAM, J. F., GAGE, D. A., CLEMO, H. F., BAUMGARTEN, C. M. & SACHS, F. 2000. Identification of a peptide toxin from Grammostola spatulata spider venom that blocks cation-selective stretch-activated channels. *The Journal of general physiology,* 115**,** 583-598.

SUCKOW, M. A., WEISBROTH, S. H. & FRANKLIN, C. L. 2005. *The laboratory rat,* Academic Press.

SUDLOW, M., THOMSON, R., THWAITES, B., RODGERS, H. & KENNY, R. A. 1998. Prevalence of atrial fibrillation and eligibility for anticoagulants in the community. *The Lancet,* 352**,** 1167-1171.

SULKE, N., SAYERS, F. & LIP, G. Y. H. 2007. Rhythm control and cardioversion. *Heart,* 93**,** 29-34.

SWEENEY, C. M., JONES, J. F. & BUND, S. J. 2007. Adrenoceptor and cholinoceptor modulation of rat pulmonary vein cardiac muscle contractility. *Vascular pharmacology,* 46**,** 166-170.

SZABO, B., SWEIDAN, R., RAJAGOPALAN, C. V. & LAZZARA, R. 1994. Role of Na^+: Ca^{2+} Exchange Current in Cs+- Induced Early Afterdepolarizations in Purkinje Fibers. *Journal of cardiovascular electrophysiology,* 5**,** 933-944.

TAKAHARA, A., SUGIMOTO, T., KITAMURA, T., TAKEDA, K., TSUNEOKA, Y., NAMEKATA, I. & TANAKA, H. 2011. Electrophysiological and pharmacological characteristics of triggered activity elicited in guinea-pig pulmonary vein myocardium. *Journal of pharmacological sciences,* 115**,** 176-181.

TAKAHASHI, K., MATSUDA, Y. & NARUSE, K. 2016. Mechanosensitive ion channels. *AIMS Biophys*.

TAKAHASHI, Y., IESAKA, Y., TAKAHASHI, A., GOYA, M., KOBAYASHI, K., FUJIWARA, H. & HIRAOKA, M. 2003. Reentrant Tachycardia in Pulmonary Veins of Patients with Paroxysmal Atrial Fibrillation. *Journal of Cardiovascular Electrophysiology,* 14**,** 927-932.

TAN, A. Y., CHEN, P.-S., CHEN, L. S. & FISHBEIN, M. C. 2007. Autonomic nerves in pulmonary veins. *Heart rhythm : the official journal of the Heart Rhythm Society,* 4**,** S57-S60.

TAN, A. Y., LI, H., WACHSMANN-HOGIU, S., CHEN, L. S., CHEN, P.-S. & FISHBEIN, M. C. 2006. Autonomic Innervation and Segmental Muscular Disconnections at the Human Pulmonary Vein-Atrial JunctionImplications for Catheter Ablation of Atrial-Pulmonary Vein Junction. *Journal of the American College of Cardiology,* 48**,** 132-143.

TAN, A. Y., ZHOU, S., JUNG, B. C., OGAWA, M., CHEN, L. S., FISHBEIN, M. C. & CHEN, P.-S. 2008. Ectopic atrial arrhythmias arising from canine thoracic veins during in vivo stellate ganglia stimulation. *American Journal of Physiology - Heart and Circulatory Physiology,* 295**,** H691-H698.

TAN, J. H. C., LIU, W. & SAINT, D. A. 2002. Trek-like Potassium Channels in Rat Cardiac Ventricular Myocytes Are Activated by Intracellular ATP. *The Journal of Membrane Biology,* 185**,** 201-207.

TANAKA, H., MASUMIYA, H., SEKINE, T., SIJUKU, T., SUGAHARA, M., TANIGUCHI, H., TERADA, M., SAITO, W. & SHIGENOBU, K. 1996. Myocardial and vascular effects of efonidipine in vitro as compared with nifedipine, verapamil and diltiazem. *General Pharmacology: The Vascular System*, 27**,** 451-454.

TASAKI, H. 1969. Electrophysiological study of the striated muscle cells of extrapulmonary vein of guinea-pig. *Japanese circulation journal,* 33**,** 1087-1098.

TAVI, P., HAN, C. & WECKSTRÖM, M. 1998. Mechanisms of Stretch-Induced Changes in $[Ca^{2+}]$ i in Rat Atrial Myocytes Role of Increased Troponin C Affinity and Stretch-Activated Ion Channels. *Circulation Research,* 83**,** 1165-1177.

TAVI, P., LAINE, M. & WECKSTRÖM, M. 1996. Effect of gadolinium on stretch-induced changes in contraction and intracellularly recorded action- and afterpotentials of rat isolated atrium. *British journal of pharmacology,* 118**,** 407-413.

TERRACCIANO, C. & HANCOX, J. 2013. ORM- 10103: a significant advance in sodium- calcium exchanger pharmacology? *British journal of pharmacology,* 170**,** 765-767.

TERRENOIRE, C., LAURITZEN, I., LESAGE, F., ROMEY, G. & LAZDUNSKI, M. 2001. A TREK-1–Like Potassium Channel in Atrial Cells Inhibited by β-Adrenergic Stimulation and Activated by Volatile Anesthetics. *Circulation Research,* 89**,** 336-342.

TOPS, L. F., SCHALIJ, M. J. & BAX, J. J. 2010. Imaging and atrial fibrillation: the role of multimodality imaging in patient evaluation and management of atrial fibrillation. *European Heart Journal,* 31**,** 542-551.

TREUTING, P. M. & DINTZIS, S. M. 2011. *Comparative Anatomy and Histology: A Mouse and Human Atlas (Expert Consult)*, Academic Press.

TSE, G., LAI, E. T. H., LEE, A. P. W., YAN, B. P. & WONG, S. H. 2016. Electrophysiological Mechanisms of Gastrointestinal Arrhythmogenesis: Lessons from the Heart. *Frontiers in Physiology*, 7.

TSUNEOKA, Y., KOBAYASHI, Y., HONDA, Y., NAMEKATA, I. & TANAKA, H. 2012. Electrical activity of the mouse pulmonary vein myocardium. *Journal of pharmacological sciences,* 119**,** 287-292.

VAITKEVICIUS, R., SABURKINA, I., ZALIUNAS, R., PAUZIENE, N., VAITKEVICIENE, I., SCHAUERTE, P. & PAUZA, D. H. 2008. Innervation of pulmonary veins: Morphologic pattern and pathways of nerves in the human fetus. *Annals of Anatomy - Anatomischer Anzeiger*, 190**,** 158-166.

VAN DER HEYDEN, M. A. G., WIJNHOVEN, T. J. M. & OPTHOF, T. 2005. Molecular aspects of adrenergic modulation of cardiac L-type Ca^{2+} channels. *Cardiovascular Research,* 65**,** 28-39.

VAN WAGONER, D. R. 1993. Mechanosensitive gating of atrial ATP-sensitive potassium channels. *Circulation Research,* 72**,** 973-983.

VASSALLE, M. & LIN, C.-I. 2004. Calcium overload and cardiac function. *Journal of Biomedical Science,* 11**,** 542-565.

VELDKAMP, M., VERKERK, A., VAN GINNEKEN, A., BAARTSCHEER, A., SCHUMACHER, C., DE JONGE, N., DE BAKKER, J. & OPTHOF, T. 2001. Norepinephrine induces action potential prolongation and early afterdepolarizations in ventricular myocytes isolated from human end-stage failing hearts. *European heart journal,* 22**,** 955-963.

VERHEULE, S., WILSON, E., EVERETT, T., SHANBHAG, S., GOLDEN, C. & OLGIN, J. 2003. Alterations in Atrial Electrophysiology and Tissue Structure in a Canine Model of Chronic Atrial Dilatation Due to Mitral Regurgitation. *Circulation,* 107**,** 2615-2622.

VERHEULE, S., WILSON, E. E., ARORA, R., ENGLE, S. K., SCOTT, L. R. & OLGIN, J. E. 2002. Tissue structure and connexin expression of canine pulmonary veins. *Cardiovascular Research,* 55**,** 727-738.

WAGNER, M. B., KUMAR, R., JOYNER, R. W. & WANG, Y. 2004. Induced automaticity in isolated rat atrial cells by incorporation of a stretch-activated conductance. *Pflügers Archiv,* 447**,** 819-829.

WAKILI, R., VOIGT, N., KÄÄB, S., DOBREV, D. & NATTEL, S. 2011. Recent advances in the molecular pathophysiology of atrial fibrillation. *The Journal of Clinical Investigation,* 121**,** 2955-2968.

WAKTARE, J., HNATKOVA, K., SOPHER, S., MURGATROYD, F., GUO, X., CAMM, A. & MALIK, M. 2001. The role of atrial ectopics in initiating paroxysmal atrial fibrillation. *European heart journal,* 22**,** 333-339.

WALLENTIN, L., YUSUF, S., EZEKOWITZ, M. D., ALINGS, M., FLATHER, M., FRANZOSI, M. G., PAIS, P., DANS, A., EIKELBOOM, J., OLDGREN, J., POGUE, J., REILLY, P. A., YANG, S. & CONNOLLY, S. J. 2010. Efficacy and safety of dabigatran compared with warfarin at different levels of international normalised ratio control for stroke prevention in atrial fibrillation: an analysis of the RE-LY trial. *The Lancet,* 376**,** 975-983.

WALLER, B. F., GERING, L. E., SLACK, J. D. & BRANYAS, N. A. 1993. Anatomy, histology, and pathology of the cardiac conduction system: Part I. *Clinical Cardiology,* 16**,** 249-252.

WALLUKAT, G. 2002. The β-Adrenergic Receptors. *Herz,* 27**,** 683-690.

WANGEMANN, T., GIESSLER, C., WILLMY-MATTHES, P., SILBER, R.-E. & BRODDE, O.-E. 2003. The indirect negative inotropic effect of carbachol in β1-adrenoceptor antagonist-treated human right atria. *European Journal of Pharmacology,* 458**,** 163-170.

WARD, M.-L. & ALLEN, D. G. 2010. Stretch-activated channels in the heart: contribution to cardiac performance. *Mechanosensitivity of the Heart.* Springer.

WARD, M.-L., WILLIAMS, I. A., CHU, Y., COOPER, P. J., JU, Y.-K. & ALLEN, D. G. 2008. Stretch-activated channels in the heart: Contributions to length-dependence and to cardiomyopathy. *Progress in Biophysics and Molecular Biology,* 97**,** 232-249.

WATANABE, H., MURAKAMI, M., OHBA, T., ONO, K. & ITO, H. 2009. The pathological role of transient receptor potential channels in heart disease. *Circulation Journal,* 73**,** 419-427.

WEN, Y. & LI, B. 2015. Morphology of mouse sinoatrial node and its expression of NF-160 and HCN4. *International Journal of Clinical and Experimental Medicine,* 8**,** 13383-13387.

WHITE, E. 2006. Mechanosensitive channels: therapeutic targets in the myocardium? *Current pharmaceutical design,* 12**,** 3645-3663.

WHITE, E. 2011. Mechano-sensitive channel blockers: a new class of antiarrhythmic drugs? *Cardiac Mechano-Electric Coupling and Arrhythmias***,** 462.

WHITE, E., BOYETT, M. & ORCHARD, C. 1995. The effects of mechanical loading and changes of length on single guinea-pig ventricular myocytes. *The Journal of Physiology,* 482**,** 93.

WILLIAMS, E. M. V. 1984. A Classification of Antiarrhythmic Actions Reassessed After a Decade of New Drugs. *The Journal of Clinical Pharmacology,* 24**,** 129-147.

WORKMAN, A. J. 2010. Cardiac adrenergic control and atrial fibrillation. *Naunyn-Schmiedeberg's Archives of Pharmacology,* 381**,** 235-249.

WYSE, D. G., WALDO, A. L., DIMARCO, J. P., DOMANSKI, M. J., ROSENBERG, Y., SCHRON, E. B., KELLEN, J. C., GREENE, H. L., MICKEL, M. C., DALQUIST, J. E. & CORLEY, S. D. 2002. A Comparison of Rate Control and Rhythm Control in Patients with Atrial Fibrillation. *New England Journal of Medicine,* 347**,** 1825-1833.

XIAO, Y., CAI, X., ATKINSON, A., LOGANTHA, S., HART, G., BOYETT, M., SHUI, Z. & DOBRZYNSKI, H. Histological and immunohistochemical study of the myocardial sleeves of the extensive pulmonary vein network of the rat. Proceedings of The Physiological Society, 2013. The Physiological Society.

XIAO, Y., CAI, X., ATKINSON, A., LOGANTHA, S. J., BOYETT, M. & DOBRZYNSKI, H. 2016. Expression of connexin 43, ion channels and Ca2+-handling proteins in rat pulmonary vein cardiomyocytes. *Experimental and Therapeutic Medicine,* 12**,** 3233-3241.

YAMAMOTO, M., DOBRZYNSKI, H., TELLEZ, J., NIWA, R., BILLETER, R., HONJO, H., KODAMA, I. & BOYETT, M. R. 2006. Extended atrial conduction system characterised by the expression of the HCN4 channel and connexin45. *Cardiovascular research,* 72**,** 271-281.

YANG, X. & SACHS, F. 1989. Block of stretch-activated ion channels in Xenopus oocytes by gadolinium and calcium ions. *Science,* 243**,** 1068-1071.

YANNI, J., TELLEZ, J., SUTYAGIN, P., BOYETT, M. & DOBRZYNSKI, H. 2010. Structural remodelling of the sinoatrial node in obese old rats. *Journal of molecular and cellular cardiology,* 48**,** 653-662.

YILDIZ, O., GUL, H. & SEYREK, M. 2013. *Pharmacology of arterial grafts for coronary artery bypass surgery*, INTECH Open Access Publisher.

YOSHIDA, K. & AONUMA, K. 2012. Catheter ablation of atrial fibrillation: Past, present, and future directions. *Journal of Arrhythmia,* 28**,** 83-90.

YOUM, J. B., HAN, J., KIM, N., ZHANG, Y.-H., KIM, E., JOO, H., LEEM, C. H., KIM, S. J., CHA, K. A. & EARM, Y. E. 2006. Role of stretch-activated channels on the stretch-induced changes of rat atrial myocytes. *Progress in biophysics and molecular biology,* 90**,** 186-206.

YOUM, J. B., HAN, J., KIM, N., ZHANG, Y.-H., KIM, E., LEEM, C. H., KIM, S. J. & EARM, Y. E. 2005. Role of stretch-activated channels in the heart: action potential and Ca2+ transients.

YOUNG, B., WOODFORD, P. & O'DOWD, G. 2013. *Wheater's functional histology: a text and colour atlas*, Elsevier Health Sciences.

YUE, Z., XIE, J., YU, A. S., STOCK, J., DU, J. & YUE, L. 2015. Role of TRP channels in the cardiovascular system. *American Journal of Physiology - Heart and Circulatory Physiology,* 308**,** H157-H182.

ZENG, T., BETT, G. C. & SACHS, F. 2000. Stretch-activated whole cell currents in adult rat cardiac myocytes. *American Journal of Physiology-Heart and Circulatory Physiology,* 278**,** H548-H557.

ZHANG, K., QIU, F., YANG, Q., XIAO, G.-S., LI, G.-R. & WANG, Y. 2016. Abstract 14601: TRPC1 Channel Is Upregulated in Atria of Patients With Atrial Fibrillation. *Circulation,* 134**,** A14601-A14601.

ZHANG, Y. & HANCOX, J. 2000. Gadolinium inhibits Na^{+}- Ca^{2+} exchanger current in guinea- pig isolated ventricular myocytes. *British journal of pharmacology,* 130**,** 485-488.

ZHANG, Y. H., YOUM, J. B., SUNG, H. K., LEE, S. H., RYU, S. Y., LEE, S. H., HO, W. K. & EARM, Y. E. 2000. Stretch- activated and background non-selective cation channels in rat atrial myocytes. *The Journal of physiology,* 523**,** 607-619.

ZHAO, L.-N., FU, L., GAO, Q.-P., XIE, R.-S. & CAO, J.-X. 2011. Regional Differential Expression of TREK-1 at Left Ventricle in Myocardial Infarction. *Canadian Journal of Cardiology,* 27**,** 826-833.

ZIMETBAUM, P. 2012. Antiarrhythmic Drug Therapy for Atrial Fibrillation. *Circulation,* 125**,** 381-389.

ZIMMER, H.-G. 2002. Who Discovered the Frank-Starling Mechanism? *Physiology,* 17**,** 181-184.

ZIPES, D. P., MIHALICJ, M. J. & ROBBINS, G. T. 1974. Effects of selective vagal and stellate ganglion stimulation on atrial refractoriness. *Cardiovascular Research,* 8**,** 647-655.

ZONTA, F., D'AGOSTINO, G. & GRANA, E. 1986. The influence of verapamil and papaverine on the calcium- and epinephrine-induced responses of isolated guinea-pig atria. *Pharmacological Research Communications,* 18**,** 1031-1041.